Precast Concrete Elements for Accelerated Bridge Construction

Volume 1-1. Laboratory Testing of Precast Substructure Components: Boone County Bridge

Volume 1-2. Laboratory Testing of Full-Depth Precast, Prestressed Concrete Deck Panels: Boone County Bridge

Volume 1-3. Field Testing of a Precast Concrete Bridge: Boone County Bridge

Final Report
January 2009

Sponsored by
the Iowa Highway Research Board (IHRB Project TR-561),
the Iowa Department of Transportation (CTRE Project 06-262),
and
Boone County, Iowa, through the Federal Highway Administration's
Innovative Bridge Research and Construction Program

ctre
Center for Transportation Research and Education

IOWA STATE UNIVERSITY

About the Bridge Engineering Center

The mission of the Bridge Engineering Center is to conduct research on bridge technologies to help bridge designers/owners design, build, and maintain long-lasting bridges.

Disclaimer Notice

The contents of this report reflect the views of the authors, who are responsible for the facts and the accuracy of the information presented herein. The opinions, findings and conclusions expressed in this publication are those of the authors and not necessarily those of the sponsors.

The sponsors assume no liability for the contents or use of the information contained in this document. This report does not constitute a standard, specification, or regulation.

The sponsors do not endorse products or manufacturers. Trademarks or manufacturers' names appear in this report only because they are considered essential to the objective of the document.

Nondiscrimination Statement

Iowa State University does not discriminate on the basis of race, color, age, religion, national origin, sexual orientation, gender identity, sex, marital status, disability, or status as a U.S. veteran. Inquiries can be directed to the Director of Equal Opportunity and Diversity, (515) 294-7612.

GENERAL ABSTRACT

Precast Concrete Elements for Accelerated Bridge Construction

Precast concrete elements and accelerated bridge construction techniques have the potential to improve the health of the U.S. highway system. In precast bridge construction, the individual components are manufactured off-site and assembled on-site. This method usually increases the components' durability, reduces on-site work and construction time, minimizes traffic disruption, and lowers life-cycle costs. Before widespread implementation, however, the benefits of precast elements and accelerated bridge construction must be verified in the laboratory and field.

For this project, precast bridge elements and accelerated bridge construction techniques were investigated in the laboratory and at three bridge projects in Iowa: in Boone County, Madison County, and Black Hawk County. The objectives were to evaluate the precast bridge elements, monitor the long-term performance of the completed bridges, and evaluate accelerated bridge construction techniques.

The results of these investigations are presented in three volumes, as described below; this volume is Volume 1.

Vol. 1-1. Laboratory Testing of Precast Substructure Components: Boone County Bridge

1-2. Laboratory Testing of Full-Depth Precast, Prestressed Concrete Deck Panels: Boone County Bridge

1-3. Field Testing of a Precast Concrete Bridge: Boone County Bridge

In 2006, a continuous four-girder, three-span bridge was constructed that included precast abutments, pier cap elements, prestressed beams, and precast full-depth deck panels. All of the precast elements performed well during strength testing and were set quickly and smoothly during construction, and the completed bridge experienced very small displacements and strains when subjected to live loads.

Vol. 2. Laboratory Testing, Field Testing, and Evaluation of a Precast Concrete Bridge: Madison County Bridge

In 2007, a two-lane single-span bridge was constructed that had precast box girders with precast abutments. The elements performed well during laboratory load transfer and strength testing, and the completed bridge performed well in terms of maximum deflections and differential displacements between longitudinal girder joints.

Vol. 3. Laboratory Testing, Field Testing, and Evaluation of a Precast Concrete Bridge: Black Hawk County

In 2007, two precast modified beam-in-slab bridge (PMBISB) systems were constructed, each of which included precast abutment caps, backwalls, and deck panels. Various deck panel configurations transferred load effectively during laboratory testing, and all precast elements met expectations. The completed bridges experienced very low induced stresses and met AASHTO deflection criteria, while the PMBSIB system effectively transferred load transversely.

Volume 1-1. Laboratory Testing of Precast Substructure Components: Boone County Bridge

Technical Report Documentation Page

1. Report No. IHRB Project TR-561	2. Government Accession No.	3. Recipient's Catalog No.	
4. Title and Subtitle Precast Concrete Elements for Accelerated Bridge Construction: Laboratory Testing of Precast Substructure Components, Boone County Bridge		5. Report Date January 2009 6. Performing Organization Code	
7. Author(s) Terry J. Wipf, F. Wayne Klaiber, and Samantha Hockerman		8. Performing Organization Report No. CTRE Project 06-262	
9. Performing Organization Name and Address Bridge Engineering Center Iowa State University 2711 South Loop Drive, Suite 4700 Ames, IA 50010-8664		10. Work Unit No. (TRAIS) 11. Contract or Grant No.	
12. Sponsoring Organization Name and Address Iowa Highway Research Board Iowa Department of Transportation 800 Lincoln Way Ames, IA 50010		13. Type of Report and Period Covered Final Report 14. Sponsoring Agency Code	
15. Supplementary Notes Visit www.ctre.iastate.edu for color PDF files of this and other research reports.			

16. Abstract

In July 2006, construction began on an accelerated bridge project in Boone County, Iowa that was composed of precast substructure elements and an innovative, precast deck panel system. The superstructure system consisted of full-depth deck panels that were prestressed in the transverse direction, and after installation on the prestressed concrete girders, post-tensioned in the longitudinal direction.

Prior to construction, laboratory tests were completed on the precast abutment and pier cap elements. The substructure testing was to determine the punching shear strength of the elements. Post-tensioning testing and verification of the precast deck system was performed in the field. The forces in the tendons provided by the contractor were verified and losses due to the post-tensioning operation were measured. The stress (strain) distribution in the deck panels due to the post-tensioning was also measured and analyzed.

The entire construction process for this bridge system was documented. Representatives from the Boone County Engineers Office, the prime contractor, precast fabricator, and researchers from Iowa State University provided feedback and suggestions for improving the constructability of this design.

17. Key Words	18. Distribution Statement		
accelerated bridge construction—Boone County, Iowa—field testing—laboratory strength testing—precast concrete abutments, pier caps, deck panels—prestressed concrete girders	No restrictions.		
19. Security Classification (of this report)	**20. Security Classification (of this page)**	**21. No. of Pages**	**22. Price**
Unclassified.	Unclassified.	200	NA

PRECAST CONCRETE ELEMENTS FOR ACCELERATED BRIDGE CONSTRUCTION:
LABORATORY TESTING OF PRECAST SUBSTRUCTURE COMPONENTS, BOONE COUNTY BRIDGE

Final Report
January 2009

Co-Principal Investigators
Terry J. Wipf, Director, Bridge Engineering Center
Center for Transportation Research and Education, Iowa State University

Brent M. Phares, Associate Director, Bridge Engineering Center
Center for Transportation Research and Education, Iowa State University

F. Wayne Klaiber, Professor, Department of Civil, Construction, and Environmental Engineering
Iowa State University

Research Assistant
Samantha Hockerman

Authors
Terry J. Wipf, F. Wayne Klaiber, and Samantha Hockerman

Sponsored by
the Iowa Highway Research Board (IHRB Project TR-561)
and Boone County, Iowa,
through the Federal Highway Administration's
Innovative Bridge Research and Construction Program

Preparation of this report was financed in part
through funds provided by the Iowa Department of Transportation
through its research management agreement with the
Center for Transportation Research and Education (CTRE Project 06-262).

Center for Transportation Research and Education
Iowa State University
2711 South Loop Drive, Suite 4700
Ames, IA 50010-8664
Phone: 515-294-8103
Fax: 515-294-0467
www.ctre.iastate.edu

TABLE OF CONTENTS

LIST OF FIGURES

LIST OF TABLES

ACKNOWLEDGEMENTS

The authors would like to thank the Iowa Highway Research Board, the Iowa Department of Transportation, Boone County and the Federal Highway Administration for providing funding, design expertise, and research collaboration for this project. Special recognition is give to the following individuals for their significant contributions to the research: Ahmad Abu-Hawash, Jim Nelson, Stuart Nielsen, and many other staff from the Office of Bridges and Structures at the Iowa Department of Transportation; Curtis Monk, Iowa Division, Federal Highway Administration; Dave Anthoney (recently retired), Bob Kieffer and Scott Kruse, Boone County; and Doug Wood, Iowa State University along with numerous other graduate and undergraduate students.

EXECUTIVE SUMMARY

In July 2006, construction began on an accelerated bridge project in Boone County, Iowa that was composed of precast substructure elements and an innovative, precast deck panel system. The superstructure system consisted of full-depth deck panels that were prestressed in the transverse direction, and after installation on the prestressed concrete girders, post-tensioned in the longitudinal direction.

Prior to construction, laboratory tests were completed on the precast abutment and pier cap elements. The substructure testing was to determine the punching shear strength of the elements.

Post-tensioning testing and verification of the precast deck system was performed in the field. The forces in the tendons provided by the contractor were verified and losses due to the post-tensioning operation were measured. The stress (strain) distribution in the deck panels due to the post-tensioning was also measured and analyzed.

The entire construction process for this bridge system was documented. Representatives from the Boone County Engineers Office, the prime contractor, precast fabricator, and researchers from Iowa State University provided feedback and suggestions for improving the constructability of this design.

All of these areas are included in this first section of Volume 1.

1. INTRODUCTION

1.1 Background

Constructing and rehabilitating bridges with minimal impact to traffic has become a transportation priority as traffic volumes nationwide increase. Renewal of the infrastructure in the United States (U.S.) is necessary for several reasons, including increases in population, projected increase in vehicle miles traveled, obsolete or deficient structures, impact of road construction, and injuries and fatalities related to work zones (NCHRP, 2003).

Rapid construction has several advantages over traditional construction methods. The six main goals of rapid construction technology include:

- Minimize traffic disruption
- Improve work zone safety
- Minimize environmental impact
- Improve constructability
- Increase quality
- Lower life-cycle cost (NCHRP, 2003)

There are several different types of rapid construction technologies currently used in the U.S. One technology uses precast concrete bridge components. The precast components are fabricated off-site, allowed to cure, and then transported to the construction site for installation. This technology allows bridges to be constructed faster than traditional construction methods, reducing the amount of time the bridge and/or associated roads are closed to the public, and reducing the total construction time. Since construction time above waterways can be reduced, the amount of debris that falls from the construction site is reduced, therefore reducing the environmental impact.

The importance of rapid construction technologies has been recognized by the Federal Highway Administration (FHWA) and the Iowa Department of Transportation (DOT) Office of Bridges and Structures. This report is based on the construction of a new accelerated construction precast bridge system located in Boone County, Iowa and evaluation of bridge components tested in the laboratory. Funding for the design, construction, and evaluation of this project was provided by the FHWA-sponsored Innovative Bridge Research and Construction (IBRC) Program. Funding for the laboratory testing was provided by the Iowa DOT and the Iowa Highway Research Board; funding for the documentation and the post-tensioning monitoring and verification was provided by the FHWA and Boone County.

This research focused on the bridge constructed on 120th Street in Boone County over Squaw Creek; the bridge replaced an existing Marsh Arch bridge at the site, which can be seen in Figure 1. The new bridge is a continuous, four-girder, three-span bridge with a full-depth, precast deck and can be seen in Figure 2. Bridge dimensions are 151 feet and 4 inches long and 33 feet and 2 inches wide. Deck panels were 8-inches thick, half the width of the bridge, and prestressed in

the transverse direction. Each panel had two full-depth channels, located over the prestressed girders, for post-tensioning. Once the panels were erected, the entire bridge deck was post-tensioned in the longitudinal direction, after which the post-tensioning channels were grouted. Precast pier caps and precast abutments were also used in the bridge substructure. Although this exact design had not been previously constructed, a similar partial-depth deck system has been constructed and tested in Nebraska (Badie *et al.*, 1998).

Figure 1. Marsh Arch bridge previously on 120th Street

Figure 2. Completed replacement bridge on 120th Street

1.2 Research Objectives

The objectives of this project were determined based on input from the Iowa DOT, the Boone County engineer, the Federal Highway Administration (FHWA), and the faculty at Iowa State University (ISU) involved with the project. This research project focused on the following objectives:

- Determine the actual strength of the connection between the precast abutment cap and the piles
- Document the construction process, particularly any problems or difficulties that occurred

- Install instrumentation to allow for long-term monitoring of the bridge deck
- Monitor and evaluate the deck panels and post-tensioning strand forces during the post-tensioning operation

These objectives were met through various tests performed on test specimens in the laboratory and through field testing during the post-tensioning operation. Additional laboratory testing was performed under the same project funding, but was not the responsibility of the author and thus not reported in this thesis.

1.3 Scope of Research

The first task for this project was to complete a literature review related to the project. First, literature on accelerated bridge technologies, along with precast, prestressed, and post-tensioned concrete bridge components was reviewed. Since the bridge deck system and substructure had never been constructed in the state of Iowa, the focus of the literature review was on full-depth, precast concrete deck panels, partial-depth precast concrete deck panels, hybrid deck panels such as NUDECK (Badie *et al.*, 1998) and on precast substructures. Several papers on the shear strength of deep beams were also reviewed because of concerns regarding the shear capacity of the abutment caps and pier caps. A summary of the literature reviewed for this project is presented in Chapter 2.

After completion of the literature review, the next task in the project was the laboratory testing. Three different laboratory tests were performed: a single pile abutment cap test, a double pile abutment cap test, and a single pile pier cap test. Each of these tests and the fabrication of the test specimens are further described in Chapter 3.

In Chapter 4, results of the laboratory tests as well as a complete discussion of the results are presented. The connection between the pile and the abutment was analyzed and compared to the laboratory results and the design strength as calculated by the Iowa DOT.

The next task included the post-tensioning testing and verification. During the post-tensioning operation, field measurements were recorded and later analyzed. A description of the field testing associated with the post-tensioning operation, a summary of the tests results from the field verification, and a comparison of the results obtained by the contractor and those of the research team are presented in Chapter 5.

The final task for this project was documentation of the construction process. This task involved taking pictures in the field as construction progressed and getting feedback from the contractor, subcontractor and the construction inspector. Documentation of the construction process was performed to evaluate the time savings of the precast system and to determine where improvements could be made. Representatives from the Boone County Engineer's Office, from the prime contractor, from the precast fabricator, and researchers from Iowa State University submitted feedback on the project. Construction documentation is described in Chapter 6.

Chapter 7 contains a summary and conclusions based on the completed research and documentation, and in Chapter 8 recommendations for additional research are presented.

2. LITERATURE REVIEW

2.1 General

Constructing and rehabilitating bridges with minimal impact to traffic has become a priority with the increase in traffic volume. In April 2004, an 11-person team from the U.S. took a tour of Japan, the Netherlands, Belgium, Germany, and France to observe rapid construction bridge technologies being used in these countries and to identify technologies that may be implemented in the U.S. (Russell *et al.*, 2005). Renewal of the infrastructure in the U.S. is necessary for several reasons, including increases in population, projected increase in vehicle miles traveled, obsolete or deficient structures, impact of road construction, and injuries and fatalities related to work zones (NCHRP, 2003).

Rapid construction has several advantages over traditional construction methods. The six main goals of rapid construction technology include: minimize traffic disruption, improve work zone safety, minimize environmental impact, improve constructability, increase quality, and lower life-cycle cost (NCHRP, 2003).

The disadvantages of rapid construction include an increase in construction cost, size and weight limitations of precast members, availability, and contractor familiarity (Russell *et al.*, 2005). These disadvantages need to be considered when determining if using rapid construction technologies are appropriate for a given project.

2.1.1 Precast Concrete

There are many advantages for using precast concrete elements in a bridge project. Elements can be fabricated off-site and stock piled before construction begins. Once construction has progressed, the precast elements can be transported to the bridge site and set in place immediately. At a precast plant, formwork is reused for standardized elements, and no formwork is required in the field, which reduces material costs and results in time and labor savings (VanGeem, 2006).

Most rapid construction technologies are focused around using precast elements in the super- and sub-structure. Disadvantages in using precast elements include increased cost, finding a qualified fabricator, and also stock piling and transportation issues. Fortunately, many of the costs associated with these disadvantages can be reduced by standardization of the precast elements used. For low- to moderate-volume bridges, transportation and storage of the elements does not pose a problem. To reduce quality control problems or issues with an inexperienced contractor, the Precast/Prestressed Concrete Institute (PCI) certifies precast manufacturers (Arditi *et al.*, 2000).

Precast concrete also has the advantage of being prestressed or post-tensioned. The concept behind prestressing and post-tensioning is to put the concrete element under permanent compression, which increases the performance and durability of the member since concrete

performs well under compression but has low tensile strength. The permanent compressive forces are designed to offset the forces induced by the self weight of the member and external loading (Naaman, 2004).

There are several different methods of prestressing and post-tensioning, however the most common technique is to use high strength steel bars or strands to apply compressive force to the concrete element. Typically, a hydraulic jack is used to tension the bar or strand to a pre-determined stress before it is anchored. The force in the steel is usually measured by hydraulic pump pressure and checked by measuring the elongation of the bar or strand. When the pump pressure and required minimum elongation has been met, the desired force has been obtained in the bar (Naaman, 2004). There are additional methods of prestressing, such as electrothermal methods or self-expanding cement, but these are not typically used in the United States and therefore will not be discussed.

The main difference between prestressing and post-tensioning is the time when the compressive force is applied to the concrete. For prestressing, the tendons are stressed before the concrete is cast. Bonds between the tendons and the concrete resist the force from the strands trying to shorten, putting a compressive force on the concrete (Naaman, 2004).

In contrast, post-tensioning is performed after the concrete element has reached strength and typically after it has been cast or erected at the construction site. Before the concrete is cast, post-tensioning ducts are installed in the forms; after the precast element has been placed in the field, post-tensioning tendons or bars are threaded through the element. After the post-tensioning has been completed, the ducts may be grouted or other measures taken to prevent corrosion (Naaman, 2004).

2.1.2 Prestressed Concrete

There are many benefits to using precast, prestressed elements, especially in low-volume bridge replacements such as the bridge replacement in Boone County. Low-volume roads are good candidates for precast, prestressed bridges because of the typical simple layout and the requirement for short- to medium-span lengths of the bridges. The use of standard precast elements, along with the elimination of falsework, forms, tying steel and finishing concrete in the field, can reduce cost, which is always a factor in construction projects (Tokerud, 1979).

Prestressed concrete beams and slab elements are typically cast in long beds, allowing more than one element to be cast at a time. Before the concrete is placed, the wires or stands are threaded through the formwork and then stressed. The stressed tendons are anchored to bulkheads located outside the concrete forms. After the concrete is cast and has reached an appropriate strength, the wires or strands are cut, compressing the concrete. A bulkhead located on a precasting bed can be seen in Figure 3.

One of the most significant benefits of prestressed concrete is the quality control during fabrication and regulation of the design and construction processes. There are several different

regulatory manuals including *AASHTO LRFD Bridge Design Specifications (1998)*, the *ACI 318-05 Building Code (2005)*, and *PCI Design Handbook (2004)* which provide guidelines for strength, serviceability, and durability of precast concrete products. The aforementioned manuals also provide guidelines for estimating short- and long-term losses in prestressed elements. Calculating exact values for prestressing losses can be difficult since there are different factors that attribute to losses such as: elastic shortening of concrete, creep of concrete, shrinkage of concrete, relaxation of the tendons, and seating losses (ACI 318-05, 2005).

Figure 3. Bulkhead in a prestressed concrete casting bed

Durability of a prestressed element is directly related to the quality of fabrication. High strength concrete is used to decrease the permeability of the concrete and to decrease the time required for the concrete to reach the desired strength. The prestressing tendons may not be released and the concrete element may not be moved until the concrete has reached the strength specified by the designer. After the concrete has reached strength, the tendons can be released and the element can be moved without risk of cracking the concrete. Stress guidelines provided by bridge specifications and/or building codes ensure precast concrete does not crack under self weight or service loads (Hale and Russell, 2006).

2.1.3 Post-tensioned Concrete

The process of post-tensioning concrete is similar to prestressing concrete and applies the same design principles. One advantage of post-tensioning concrete is several concrete elements may be post-tensioned together to act continuously. Primarily, there are two post-tensioning schemes: one uses bonded tendons and the other uses unbonded tendons. For bonded tendons, the post-tensioning ducts are filled with grout after the tendons are stressed and anchored; after the grout cures, the force along the length of the tendon is distributed to the adjacent concrete. In contrast, unbonded tendons are coated with grease or bitumen, covered with waterproof material, and

threaded through the ducts. Since no grout is used, the force in the tendons essentially applied at the anchorage zones (Naaman, 2004).

There are several different types of proprietary post-tensioning anchors that can be used, depending on the strand or bar being post-tensioned. The type of anchorage used also depends on the size and strength of the concrete element, the number of strands used, and other design constraints. Several common post-tensioning anchors are shown in Figure 4.

a) DSI bonded multi-strand anchorage

b) DSI bonded multi-strand flat anchorage

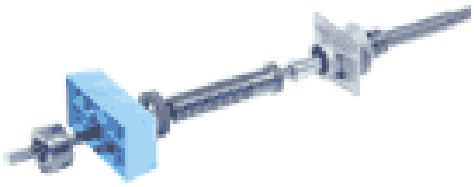

c) VSL mono-strand anchorage

d) VSL threaded bar anchorage

Figure 4. Common post-tensioning anchorages (Bonded Strand Post-Tensioning System, 2007) (VSL Post-Tensioning Systems, 2007)

Anchorage zones in post-tensioned concrete are an area of concrete subjected to high levels of stress. Anchorage zones can be congested and difficult to design and construct due to the size of the anchorages and the amount of mild reinforcing required. To prevent cracking and bursting of concrete in the anchorage zone, secondary reinforcement such as spirals and closed stirrups can be used, and recently fiber-reinforced concrete has been used to reduce congestion (Haroon *et al.*, 2006). The Boone County project did not require abnormally high amounts of post-tensioning strand, but the end panels with the anchorage plates were still congested. Fabrication of one of the end panels is shown in Figure 5a while one of the completed end panels is shown in Figure 5b.

a) end panel reinforcement

b) complete end panel in the field

Figure 5. Boone County anchorage zone reinforcement

One material commonly used for post-tensioning ducts is galvanized steel. This material is highly susceptible to corrosion and research has shown that tendons corrode at a faster rate if the galvanized duct is also corroded (Salas *et al.*, 2004). Plastic ducts are now being used to prevent early onset of corrosion, but even with plastic ducts, there are areas where tendons are still susceptible to corrosion. Joints between concrete elements and high- and low-profile points in the tendons are at the highest risk (Cooper and Pearson-Kirk, 2006).

Issues with corrosion have forced improvements in grouting practices for post-tensioned bridges. One way to ensure the ducts are completely grouted is by using high-pressure grouting. In this method, the duct is typically grouted from one location, either the center or from one end. The high pressure forces the grout through the ducts, until grout can be seen at the farthest end of the duct (Schokker *et al.*, 1999). Even if the duct is completely filled with grout, this does not guarantee corrosion protection. If the grout cracks, moisture can still reach the tendons. For the best corrosion protection, high performance, low-shrinkage grouts are recommended (Hamilton *et al.*, 2000). High performance grouts with the use of silica fume have low permeability which slows chloride penetration and corrosion (Khayat *et al.*, 1999).

Post-tensioning channels used in the Boone County project avoided the corrosion protection issues related to the type of post-tensioning ducts and the presence of air voids in the ducts by eliminating the ducts all together. Open channels allowed the strands to be inspected as grout was placed and prevented the formation of air voids around the tendons. The channels in one of the deck panels can be seen in Figure 6.

A specialty concrete, designed to have low-permeability and low shrinkage to further prevent cracks near the tendons, was used in the channels. Details of the specialty concrete mix can be found in Chapter 3.

Figure 6. Boone County replacement bridge deck panel

2.2 Bridge Deck Systems

The most common bridge superstructure in the U.S. consists of erecting steel, reinforced concrete, or prestressed concrete girders, and using formwork to place a cast-in-place (CIP) concrete deck. Eliminating the deck formwork reduces construction time and lane closure time, and improves worker safety (Russell *et al.*, 2005). There are several different types of deck systems that are used in rapid construction projects. In the following section, three different types of bridge deck systems are discussed: full-depth precast deck panels, partial-depth precast deck panels, and hybrid deck panels.

2.2.1 Full-Depth Concrete Deck Panels

A typical precast deck panel system consists of precast concrete panels, placed adjacent to each other, perpendicular to the bridge girders. Most recent systems use prestressing as reinforcement in the transverse direction. Longitudinal post-tensioning is used to place the joints between panels in compression, which promotes monolithic behavior and improves durability. Grouted shear keys are used at the transverse joints. The panels are connected to the bridge girders using shear pocket connectors which ensure composite action between the deck and girders (Hieber *et al.*, 2005).

Typically, the panels are approximately eight inches thick, span the width of the bridge, and are approximately ten feet long. A wearing course is not required, but is often included to improve the riding surface of the finished panels.

There are several key issues to consider with a full-depth deck system. The first is the bearing between the panels and the girders. Differential camber and fabrication variations can affect the bearing between the deck and the girders. An uneven bearing surface can cause spalling at the transverse joints and an uneven riding surface. One solution to this potential problem is to grout between the panel and the girder, thus creating a continuous bearing surface. However, often times the gap between the panel and girder is too small to grout. Another solution is to

temporarily support the panels above the girders to create a haunch region. The haunch can be grouted and the supports removed after the grout cures. Leveling bolts and shims are typically used in this application (Hieber *et al.*, 2005).

Another key issue to consider is the connection of the panels to the bridge girders. Proper connection ensures a composite action between the panels and girders. Insufficient connections can allow the panels to lift off the bridge, which causes fatigue and vibration problems. Insufficient connections may also cause cracking in the panels and at the joints. There are several different types of connections, all of which included a mechanical connection and a grouted region (Hieber *et al.*, 2005).

Typically, full-depth concrete deck panels are post-tensioned together. The amount of post-tensioning force required for the bridge deck is a critical issue. If insufficient force is applied, the connection between the panels may crack, which can cause maintenance issues and shorten the lifespan of the bridge. The amount of post-tensioning force required varies depending on the bridge properties and the type of support. Continuously-supported bridges require higher post-tensioning force to prevent joint cracking than simply-supported bridges (Issa *et al.*, 1998). There are two options for post-tensioning the deck panels together: full bridge post-tensioning and staged post-tensioning. For full bridge post-tensioning, the deck panels are all stressed after every panel is in place. In staged post-tensioning, each panel is post-tensioned once in place next to the previously placed panel. This may be temporary or permanent, but the design details for staged post-tensioning are more involved than full bridge post-tensioning because of the multiple post-tensioning operations required (Yamane *et al.*, 1998).

A third issue to consider is the joints between the panels. These joints must be able to transfer shear and axial forces between adjacent panels, and prevent leakage through the deck. Often, water that leaks through the deck contains chlorides, which accelerates deck, girder, and reinforcement deterioration. Typically, 'female-to-female' shear keys have been used because of superior performance over 'female-to-male' shear keys. Problems with joints usually arise because of low-quality joint material, poor joint details, inconsistent/inadequate construction procedures, or the lack of routine maintenance. Joints that have a larger area and easy flow path often perform better because there is more room for the grout to flow. Grout with high-early strength is the most commonly recommended material. This allows post-tensioning to be completed shortly after the joint has been grouted, so construction can proceed (Harrison and LeBlanc, 2005).

Another issue with full-depth deck panels is the transverse prestressing in each panel. Prestressing allows thinner panels, provides better crack controls, and helps with the durability of the panel during transportation and erection. One drawback to prestressed panels is the development of the strands in the section of the panels that overhangs the exterior girder. This problem can be solved by adding mild reinforcing steel to that area (Hieber *et al.*, 2005).

The last key issue to consider is the wearing surface of the deck. Full-depth panels typically have a rough surface due to the grouted joints and shear pockets. Typically, a wearing surface is added for rider satisfaction and safety, and improved durability (Hieber *et al.*, 2005). Another

option is to fabricate the panels one quarter inch thicker and then grind the surface of the deck when construction is finished.

2.2.2 Partial-Depth Concrete Deck Panel

Partial depth precast panels are thin reinforced/prestressed concrete deck panels that are used to span in between girders and serve as stay-in-place formwork for the CIP deck. Panels are designed to span between each girder, are typically about eight feet in the longitudinal direction and about 3.5-inches thick. The panels are typically prestressed in the transverse direction and the prestressing strands serve as the reinforcement in the bottom of the bridge deck. Panels are then placed adjacent to each to each other, but not connected at the adjacent transverse joints. Deck overhangs have to be formed with removable formwork. A layer of reinforcing steel is placed on top of the panels, and then the CIP deck is placed (Hieber *et al.*, 2005).

The biggest advantage to partial depth precast panels is the elimination of deck formwork. However, since CIP concrete is still used for the deck and formwork is still required for the deck overhangs, the time-savings for partial deck panels is not as great as the time-savings for full-depth concrete panels. Reflective cracking over the transverse joints can be a problem. This is attributed to the discontinuity between precast panels which leads to a decrease in deck stiffness (Badie *et al.*, 1998).

There are several key issues to consider when using partial-depth precast panels. First is issue of panel thickness; because the panels are so thin, they are susceptible to damaged during handling and construction. Damage to the panels can be avoided by limiting the number of times the panels must be moved and placing the lifting hardware at locations in the panels to minimize stresses (Hieber *et al.*, 2005).

Another issue of concern is the bearing of the panels on the supporting girders. Cracks can form in the concrete deck if a solid, uniform bearing region is not provided. Cracked concrete can prevent the deck from acting continuously over the girders. As a result, the CIP deck may delaminate from the panels at the joints. Current practices use grout or concrete to fill the bearing area which provides proper bearing (Hieber *et al.*, 2005).

The third issue with partial-depth deck panels is the development of prestressing within the panels. Because the partial-depth panels span in between the girders, there is a short distance to develop the prestressing strands in the panels. It is important to make sure other factors, such as dirty prestressing strands or sudden de-tensioning by the fabricator, don't increase the required development length. However, decreasing the development length too much can create problems as well. Panels with small development lengths have a greater potential for splitting (Hieber *et al.*, 2005).

The last issue of concern with partial-depth is ensuring composite action between the CIP deck and the precast panels. A common way to increase the composite action is to roughen the surface of the precast panels during fabrication. Precast panels should also be clean and free of

debris and contaminants to ensure complete bond is achieved between the CIP deck and precast panels.

There are limitations on the size of partial-depth panels. According to AASHTO LRFD Section 9.7.4.3.1 (1998) the precast panels should not be greater than 55 percent of the total deck depth nor less than 3.5 inches. These limitations help to reduce cracks in the CIP deck over the panel joints and also to help develop composite action.

2.2.3 Hybrid Deck Systems

The NUDECK system is a stay-in-place precast, prestressed system developed to solve the problems in the existing stay-in-place (SIP) systems. This system uses partial-depth panels with a CIP composite deck. NUDECK can be constructed significantly faster than CIP systems and slightly faster than other SIP systems. Shown in Figure 7 is a section view of a typical NUDECK panel; the panel is symmetric about the bridge's longitudinal centerline (Badie *et al.*, 1998).

Several changes were made to previous SIP systems in the development of the NUDECK system. The first problem addressed was reducing the number of panels needed; the NUDECK system spans the entire width of the bridge, thus reducing the required number of panels needed by two. Eliminating the need for forming the overhangs was the second issue. To accomplish this, the NUDECK panels extend over the outside girders providing SIP formwork for the overhangs. Third, the issue of the transverse prestressing being not fully developed in the panels was addressed. In the NUDECK system, the prestressing is continuous over the girders, allowing the prestressing to fully develop (Fallaha *et al.*, 2004).

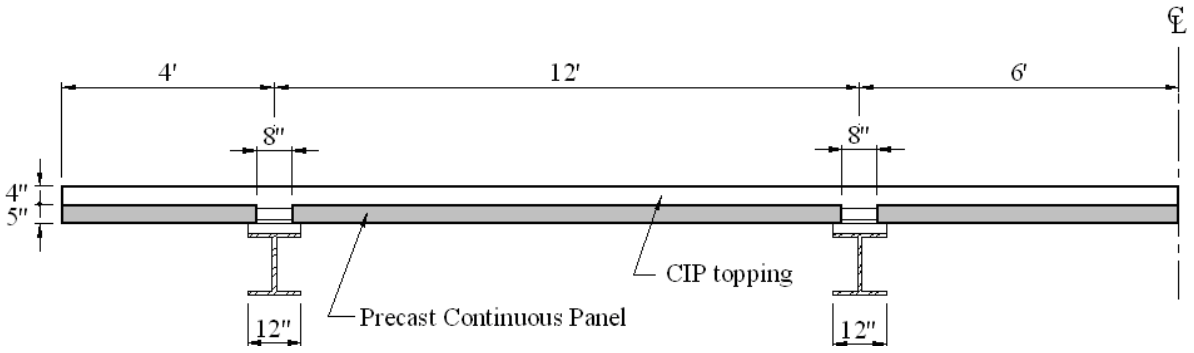

Figure 7. Typical cross-section of the NUDECK panel

Another issue was transverse cracking. In the NUDECK system, the entire bridge is post-tensioned, providing continuous longitudinal support. Next, the issue of supporting finishing machines without the need for additional brackets was addresses. NUDECK panels were designed to support the weight of the finishing machines, the CIP concrete surface, and the panel self-weight without additional support. The last issue was longitudinal cracking over girder lines

caused by creep in the individual SIP panels. In the NUDECK system, the panels are continuous over the girder lines, thus eliminating creep issues (Badie *et al.*, 1998).

There are several block outs in each panel, located longitudinally over the each beam line. Block outs serve as post-tensioning channels, are positioned to avoid interference with the shear studs, and also simplify the post-tensioning process (Fallaha *et al.*, 2004).

In order to provide adequate shear connection between precast panels in the longitudinal directions, shear keys and reinforced pockets were used. A simple leveling device was used to level the panels on the girders. After post tensioning, the block outs in the panels were grouted using a flowable mortar to connect the panels to the girders. The CIP surface was placed once the mortar reached a specified compressive strength (Badie *et al.*, 2005).

All of the precast deck panel systems discussed use grouted joints to connect the panels. However, grouted joints are a major issue of concern because of difficulty in achieving high-strength grout in the field. Panels are typically grouted together using a variety of different grouting materials such as cememtitious grout, epoxy mortar, or polymer concrete. Because the transverse joint acts as a structural member, it must resist vertical shear and bending caused by vehicle loading. Effects of shrinkage of the grout and vertical shortening of the panels induce direct tension on the joint as well (Issa *et al.*, 2003).

Strength and quality of joint material is very important to the durability of the bridge. If the grouting material is not strong enough to resist the service loads, the joint will crack, resulting in leakage. Cracked joints can be expensive to repair and maintain (Issa *et al.*, 2003).

2.3 Bridge Substructure Systems

2.3.1 Precast Abutments

Precast abutments can be beneficial to rapid construction projects. One drawback to using precast abutments is connecting the abutment to the deck. If the abutment is entirely precast, an expansion joint has to be placed between the deck and the abutment. Expansion joints tend to reduce the lifespan of bridges, and integral abutments are typically preferred. Even if an integral abutment is used, precast elements can still be used for the wingwalls to reduce the amount of formwork and CIP concrete (Tokerud, 1979). A closure pour between the precast elements and the abutment will be required to achieve an integral abutment.

2.3.2 Precast Concrete Piers

Precast concrete pier systems use precast piles and a precast pier cap to create a pier. Precast piers are compatible with a number of different foundation and substructure types. For larger bridges, precast pier caps, also called bent caps or cap-beams, may be necessary. A picture of a bridge in Nebraska using precast girders and precast pier caps is shown in Figure 8. Pier caps allow twin-span bridges to use the same piers for foundations. Precast, prestressed or post-

tensioned caps can significantly reduce the cap size, which reduces the weight of the substructure. For extremely large bridges, pier caps may be fabricated and transported in two pieces and post-tensioned together on site (Billington *et al.*, 1999).

Figure 8. Bridge pier cap located Lincoln, Nebraska

Individual components of the pier are connected with mild reinforcing steel splices or post-tensioning. Two types of connections are typically used: grouted joints and match-cast joints. Match-casting uses the joint face of a previously cast component as part of the formwork for the adjacent component. This results in a "perfect" fit between the two components and reduced on-site construction time, when the elements are delivered in the correct order. The drawback to this procedure is that the fabrication process is often more time and labor intensive, which can be more expensive and if the elements are placed in a different order than which they were fabricated, the segments may not fit (Hieber *et al.*, 2005).

There are several advantage to using precast concrete piers besides the time and labor savings in the field. As with all precast elements, fabrication of all the elements is done off-site, which allows the precast elements to be fabricated before construction at the bridge site begins. Elements can then be stockpiled until they are needed in the field. Because precast elements are typically fabricated in a climate-controlled environment, the quality control for the material and construction of precast elements is higher than the quality control that can be maintained though all kinds of weather in the field. This results in higher durability of the precast elements (Billington *et al.*, 2001).

Precast elements also have the advantage of using high performance concrete, which typically increases the strength and durability of precast elements. The use of high-performance concrete also results in more slender substructure designs, as can be seen in Figure 9, which also results in significant material savings for a project (Billington *et al.*, 2001).

There are several key issues to consider with precast concrete piers. The first issue is the connection between the footing and the column, which will depend on the type of footing, precast or cast-in-place. There are several different types of connections available, however, the most appropriate connection will depend on project-specific conditions (Hieber *et al.*, 2005).

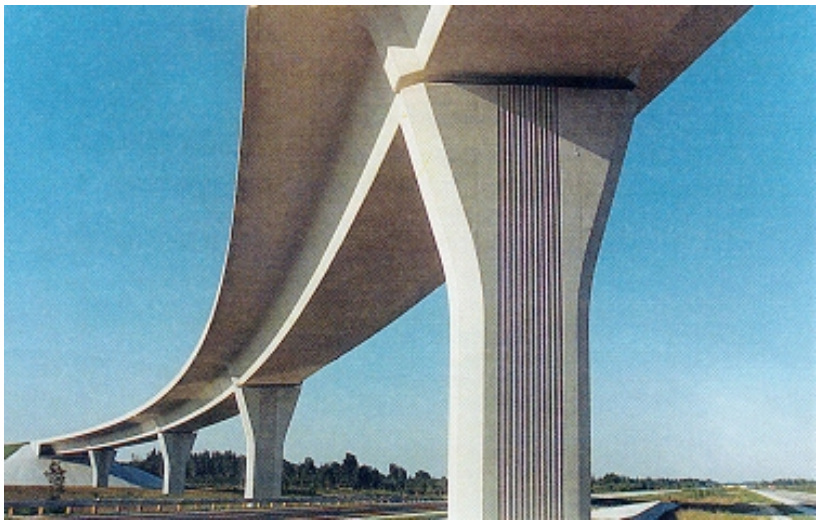

Figure 9. Slender pier design of the Florida Turnpike in Miami, Florida

The next issue is the connection between the column elements. Match-cast joints are typically preferred because of problems that may occur with grouted joints. Grouted joints may lack a uniform bearing surface, which can cause edge crushing. Poor grout placement or grout quality may result in partially filled joints, stress concentrations, cracking, and corrosion of the reinforcing steel. Shear keys can be added to increase the shear capacity of the joint. The epoxy used in the joint may also provide extra shear capacity, but typically is not designed to do so (Hieber *et al.*, 2005).

Another issue to consider with precast pier systems is the connection between the column and pier cap or abutment. There are two types of connections used: post-tensioning bars or strands, or mild reinforcing bars in grouted ducts. A drawback to the grouted duct connection is the ducts takes up twice as much room as a normal reinforcing bar. The connection region in the column and pier cap is already congested, so fitting the ducts in can be a problem (Hieber *et al.*, 2005).

A fourth issue to consider is the connection between the pier cap elements. If the pier cap has to be fabricated and transported in several segments, the segments will have to be connected with grouted, cast-in-place concrete or match-cast connections. The last issue to consider in precast pier systems is the weight and size that can be transported, either of which can govern the size of the precast segment. Local limitations should be researched and considered during design (Hieber *et al.*, 2005).

As with most accelerated construction technologies, there is an increased cost to precast substructures. Part of the cost is related to the experience of the contractor and precast concrete

fabricator. Some of the cost of precast substructures will reduce as standardized substructures are developed and the contractors involved gain experience (Billington *et al.*, 2005).

Another precast pier system currently under investigation for use in the United States is the Sumitomo system. The Sumitomo precast structure for resisting earthquakes and for rapid construction (SPER) system uses stay-in-place precast concrete panels as formwork and as structural elements. For shorter piers, the segments are stacked on top of each other, epoxied together, and then filled with CIP concrete, creating a solid pier. For taller piers, inner and outer panels are used to create a hollow pier. For both types of piers, cross ties and couplers are used to provide transverse reinforcement. High strength bars are typically used for the transverse reinforcement to reduce congestion between the panels. CIP concrete is typically used to connect the piers to the superstructure (*Russell et al.*, 2005).

3. LABORATORY CONSTRUCTION AND TESTING

3.1 Laboratory Specimen Fabrication

The substructure specimens tested in the laboratory were designed and fabricated based on the project plans for these elements in the Boone County bridge replacement project. In other words, the laboratory specimen were built to replicate the actual bridge elements. A total of nine full-scale specimens were fabricated in the laboratory, seven abutment specimens and two pier cap specimens. A description of the various test elements and their designations are presented in Table 1.

Table 1. Laboratory specimens and designations

Specimen	Description
Abutment 1	ASC1
Abutment 2	ASC2
Abutment 3	ASO1
Abutment 4	ASC3
Abutment 5	ASO2
Abutment 6	ADC1
Abutment 7	ADC2
Pier Cap 1	PSC1
Pier Cap 2	PSC2

Where:

A = Abutment specimen
P = Pier cap specimen
S = Single pile
D = Double pile
C = Centered pile
O = Offset pile

Specimens were fabricated and tested three at a time to optimize the space required in the laboratory for storing materials, building formwork, and casting concrete.

3.1.1 Single Pile Abutment Cap Construction

The abutment system consisted of a precast abutment cap that used corrugated metal pipe (CMP) as a ‘block out’ for the piles. During construction, the abutment cap was placed over H-piles already driven in the field after which a special concrete mix was used to fill the void and thus connect the piles and the abutment. Specimens were designed to represent the worst-case load condition on the actual abutments. Tests were performed using the prestressed girder spacing around the center pile; this provided the maximum moment to which the abutment would be

subjected. The side view of the entire abutment, along with the sections of the abutment used in the various test specimens, can be seen in Figure 10. In this figure, the four precast girders and five piles can be seen.

During fabrication and testing, the abutment specimens were inverted. This provided the safest, most stable configuration for testing, and also made grouting the piles in place easier. The external details of the abutment test specimen are presented in Figure 11. There were two different single pile abutment tests specimen fabricated: one test with the pile centered in the CMP (i.e. the "C" designation in Table 1) and one with the pile offset the maximum distance in the CMP (i.e. the "O" designation in Table 1), designated by dimension "A" in Figure 11. Actual values for "A" and a top view of the centered and offset pile are shown in Figure 12.

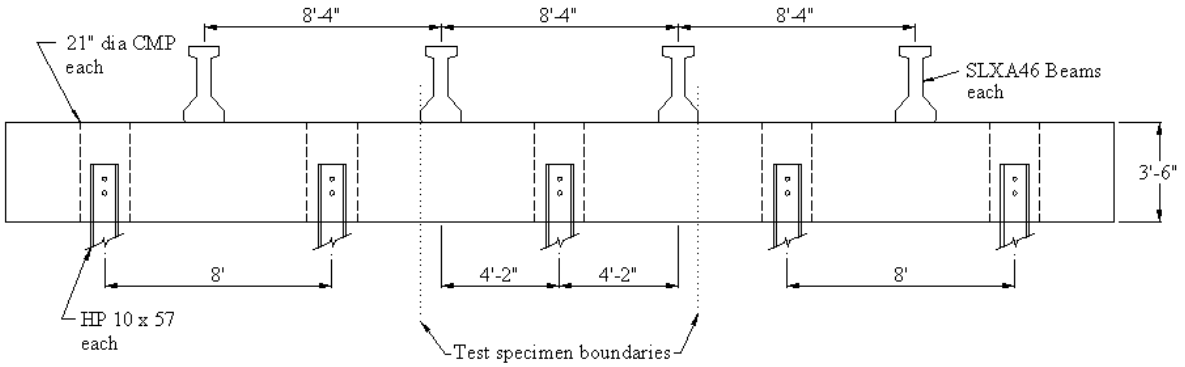

Figure 10. Side view of the Boone County replacement bridge abutment

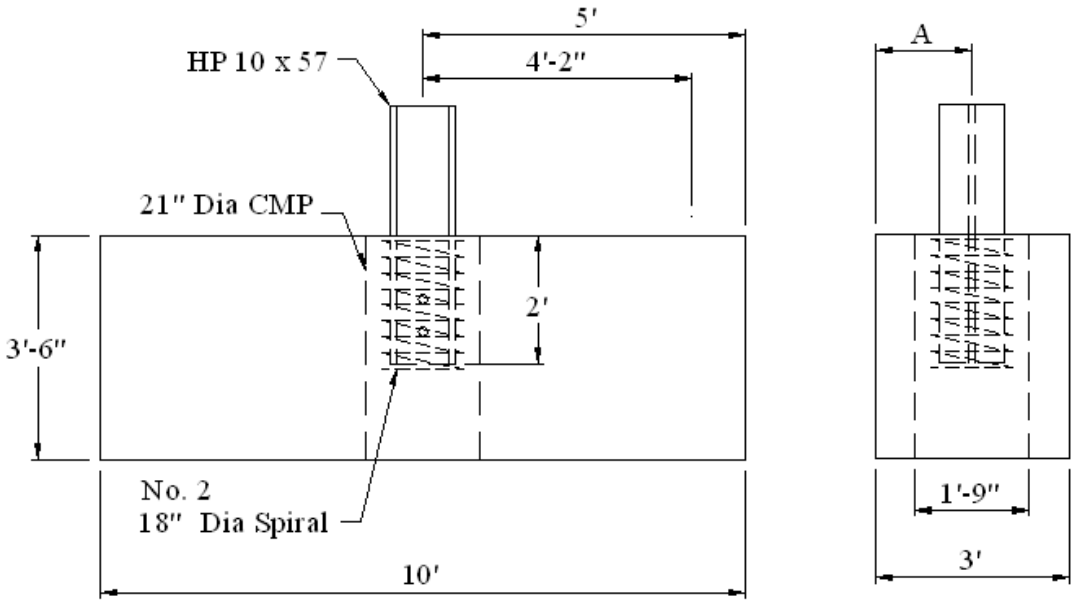

Figure 11. Single pile abutment test specimen

Test specimens replicated the actual abutment cross-section used in the field, including the dimensions and reinforcement. Both test specimens were ten feet in length, with the CMP

centered in the specimen. The reinforcement (size and spacing) in the test specimens was taken from the project plans and adapted for a ten-foot long section of the abutment. In the abutment, the No. 8 longitudinal bars were continuous; bars were lap spliced where necessary. In the test specimens, the longitudinal bars were limited to nine-feet and ten-inches in length, to provide one inch cover at the end of the bars; this provided sufficient bar length to ensure full development. A top view of the specimen, as well as an end view, showing the reinforcement is presented in Figure 13.

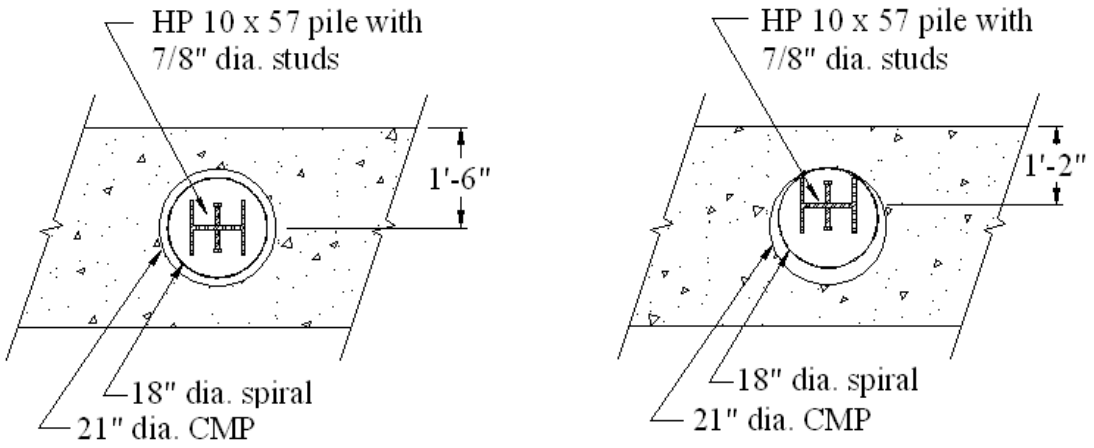

a) centered pile location **b) offset pile location**

Figure 12. Abutment pile locations

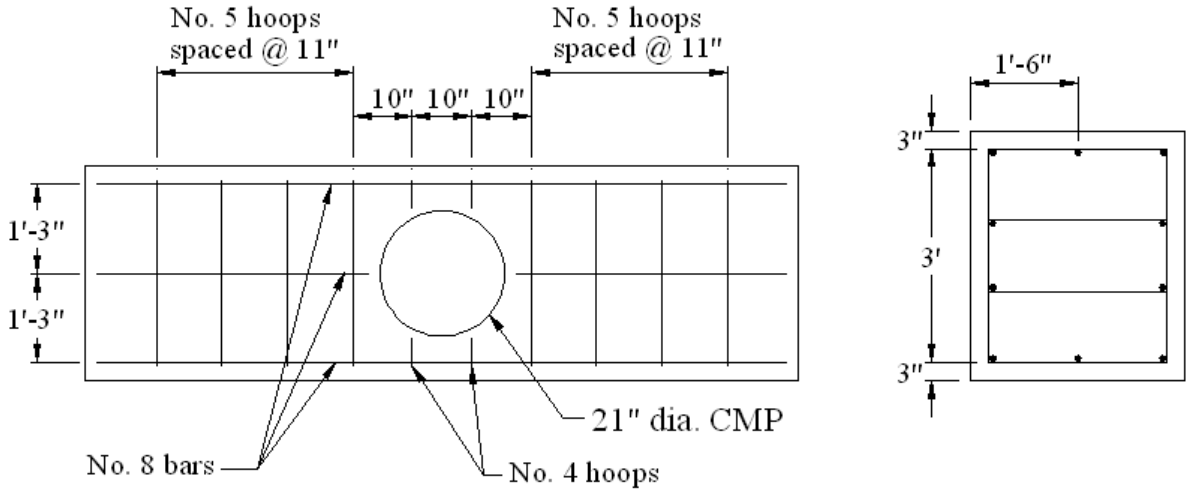

a) top view **b) end view**

Figure 13. Single pile abutment reinforcement

Each H-pile in the abutment specimens had four 7/8-inch diameter studs, five inches in length, welded to the pile web six inches apart, two of which can be seen in Figure 14. A No. 2 bar, bent in an 18-inch diameter spiral with a 3-inch pitch was designated in the bridge plans to complete

the connection between the abutment and the pile. A portion of the CMP, spiral, and pile section with the studs is shown in Figure 15.

All of the reinforcing steel used was ordered through a local contractor's supply store and was pre-cut and bent to the appropriate dimensions except for the No. 4 ties, which were cut and bent in the laboratory. The reinforcement was assembled in the laboratory and placed in the partially assembled formwork, which had been previously coated with a release agent. One of the reinforcement cages in the formwork before the last side of the forms was attached is shown in Figure 16.

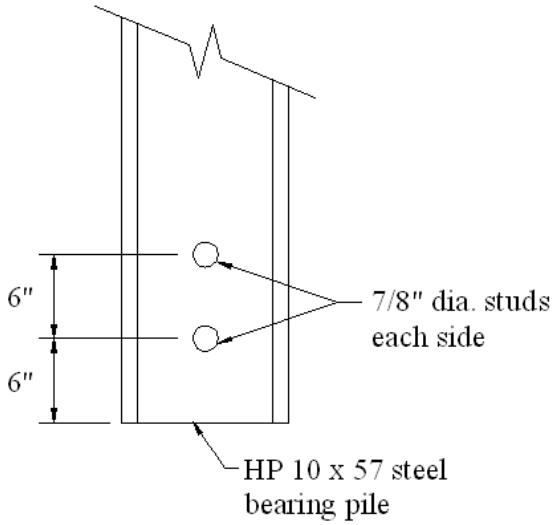

Figure 14. H-pile stud connection detail

Figure 15. H-pile connection in test specimen before concrete was placed

Figure 16. Single pile abutment specimen reinforcement placed in the formwork

Metal chairs were used under the cages to ensure proper cover for the reinforcement. Wooden blocks were used between the ends of the formwork and the reinforcement cages to obtain the desired cover when necessary. The blocks were removed during concrete placement, after enough concrete was placed to keep the reinforcement from moving.

After the formwork was partially assembled, the CMP was placed in the reinforcement cage and secured with wire ties, after which the formwork was completed. To give the forms more stability during concrete placement, internal and external steel straps were used. Internal straps were placed at three of the joints in the formwork, one foot from the bottom of the forms. Two external straps were used on top of the formwork. The CMP, external straps, and the completed formwork for one test specimen are shown in Figure 17.

The estimated weight of each individual specimen was 7.8 ton. To facilitate lifting and moving the specimens, four lifting hooks were embedded in each specimen. Lifting hooks were attached to wooden "two-by-fours" with bolts and positioned to provide at least two inches of concrete cover for the top of the hooks. Each bolt was greased before the concrete was placed so after the concrete had cured, the bolts and two-by-fours could be easily removed. Styrofoam was used to cover each CMP to keep concrete out during the casting of the abutment specimens. A view of the lifting hooks attached to the formwork and the Styrofoam is presented in Figure 18.

After all of the formwork for the first three specimen was completed, as specified in the Iowa DOT bridge replacement plans, a C4 precast concrete bridge mix in compliance with AASHTO Standard Specification for Highway Bridges (1996) with a four-inch slump and a minimum 28-day compressive strength of 5,000 psi was ordered from Iowa State Ready Mix and placed. This was the same concrete mix specified in the Boone County plans for the precast substructure elements.

Before concrete was actually placed, slump tests were performed to ensure the concrete had the minimum desired slump of three inches. If the concrete slump was less than three inches, water was added until the desired slump was obtained. Slump tests were performed whenever concrete was placed. The laboratory concrete bucket and overhead crane were used for placing the concrete. Several electric concrete vibrators were used throughout the pour to consolidate the concrete, especially in the area surrounding the CMP. Concrete was placed in approximately four lifts and vibrated between each lift; placement in one of the specimen is shown in Figure 19. While the concrete was being placed, twelve control cylinders were made using the concrete from a particular truck.

Figure 17. Completed formwork with the CMP for the first abutment test specimen

Figure 18. Lifting hooks and Styrofoam cover before placing concrete

A screed was used to strike off the concrete even with the formwork, after which trowels were used to hand-float the surface. The first finished series of test specimens can be seen in Figure

20. In total, thirteen cubic yards of concrete were required to fabricate the three specimen and control cylinders. Once the concrete reached initial set, the surface was covered with wet burlap and plastic sheets for curing. Each specimen remained covered with the plastic and wet burlap, which was removed after seven days and the formwork was 'stripped'.

The H-piles were grouted into place one week after the concrete in the precast portion of the abutment specimen was placed. For grouting the piles into place, the plans called for a special high-strength concrete mix (minimum compressive strength of 6,000 psi) with 1/2-inch aggregate and a high-range water reducer (HRWR) to improve the long- term workability of the concrete. In the laboratory, the concrete mix did not have the HRWR, but was otherwise the same mix specified in the bridge plans. Since the quantity placed in the laboratory was less than two cubic yards, the long-term workability was not an issue.

Each H-pile was to be placed in the CMP with a minimum two foot embedment length, as specified on the bridge plans. As previously described, the test specimens were inverted from the field orientation; therefore, the piles were grouted in at the top of the specimens. To obtain the desired embedment length, the piles were attached to steel angles using C-clamps, which in turn were supported by the CMP. One of the piles offset in the CMP, before the special concrete mix was placed, is shown in Figure 21.

Figure 19. Concrete being placed in the first series of abutment specimen

Figure 20. Hand-finished specimen before initial set

Placing concrete in the CMP was challenging. The opening was too small to use the concrete bucket without wasting large amounts of concrete. Thus the concrete was placed by hand using shovels and buckets; a student can be seen placing concrete around the H-pile in Figure 22. Vibrators were again used to ensure adequate compaction, and to eliminate voids under the ends of the piles and around the shear studs. Fifteen control cylinders were made using the grout concrete mix.

Grouted concrete was finished by hand, however, because of the small space between the CMP and piles, a straight edge or trowel could not be used. A pile grouted in place can be seen in Figure 23. After the grouted concrete reached initial set, since each CMP was approximately one half inch longer than the depth of the added grout, water was ponded on top of the grout for curing. After 24 hours, the C-clamps and angles previously described were removed. Water was kept on the surface of the grouted concrete for seven days.

Figure 21. H-pile in place before placing grout

Figure 22. Concrete being placed in the CMP around the H-pile

Figure 23. H-pile after being grouted in place

3.1.2 Single Pile Pier Cap Construction

The pier cap design was similar to the precast abutment cap design. Instead of using H-piles, the piers were supported by concrete-filled pipe piles. During construction, the pier caps were supported by falsework until the concrete connecting the piles to the pier had reached sufficient strength. In the single pier cap test specimen, the pipe pile was centered in the CMP. Each test specimen replicated the pier cap used in the field, including the dimensions and reinforcement. Similar to the abutment specimens, the pier cap specimens were inverted during fabrication and testing. External details of the pier cap specimens are shown in Figure 24.

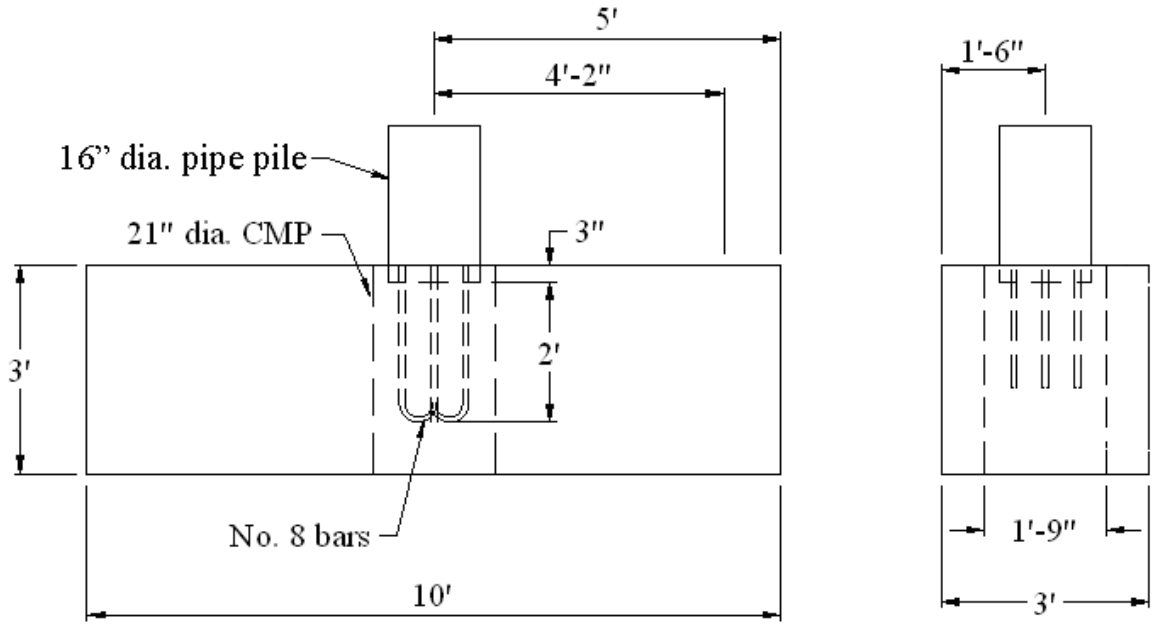

a) side view **b) end view**

Figure 24. Single pile pier cap test specimen

The reinforcement in the specimens was the same as that specified the project plans (size and spacing), which was adapted for a ten-foot long section of the pier cap. As previously described for the abutment, the pier cap longitudinal bars were continuous, lap spliced where needed and cut to provide one inch of cover for the ends of the No. 8 bars. A top view and cross-section of the pier cap reinforcement can be seen in Figure 25.

The reinforcement connection between the pipe pile and the pier cap consisted of four No. 8 bars, two straight bars and two bars with 180° hooks, shown in Figure 26. Additional No. 4 hoops, 10-inches in diameter, were also used in the connection. As the concrete in the pipe piles was placed, the reinforcement connection was embedded in the fresh concrete.

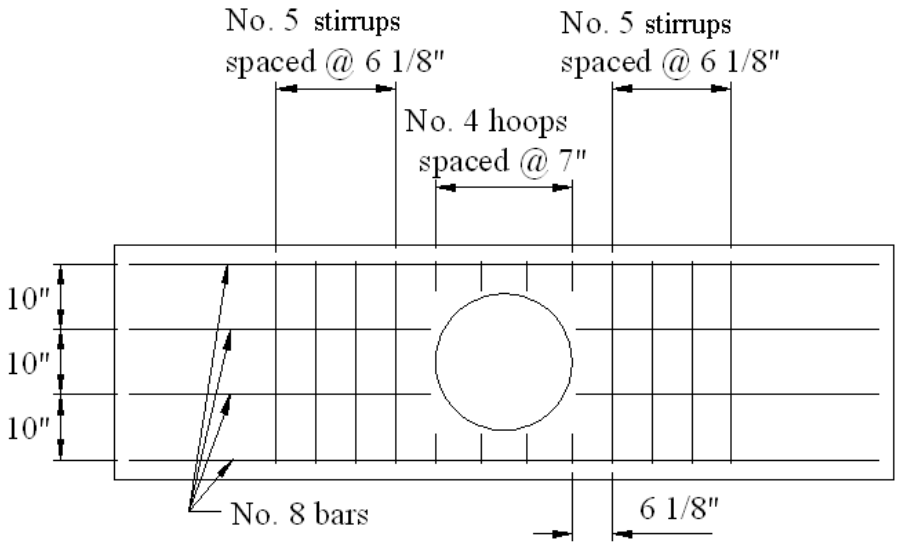

a) Top view of pier cap reinforcement

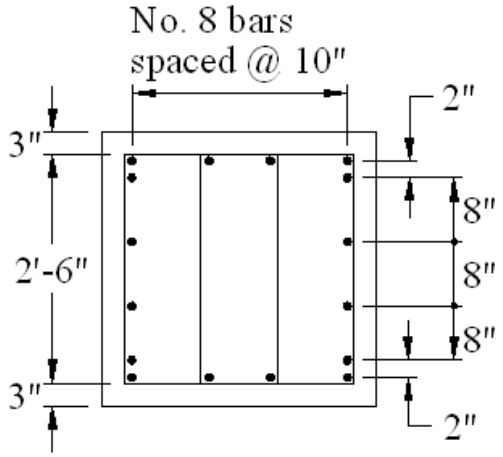

b) Cross-section view of pier cap reinforcement

Figure 25. Pier cap reinforcement

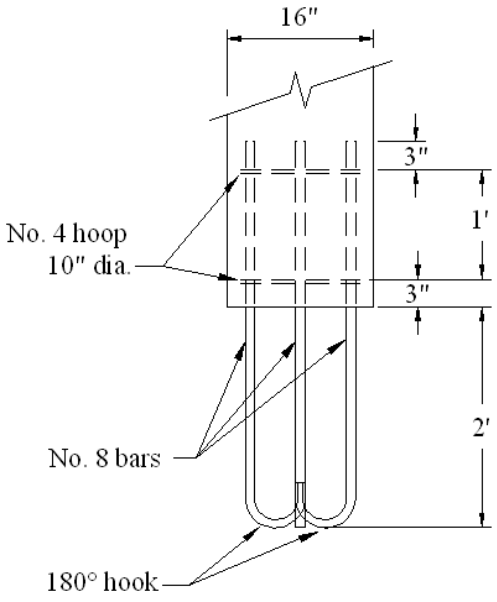

Figure 26. Pipe pile connection detail

The same formwork used for casting the abutment specimens were used in the pier specimens. After the formwork was partially assembled and a release agent applied, the reinforcement cages were placed in the formwork on metal chairs, and the CMP was placed in the reinforcement and secured. Since the abutment specimens and pier cap specimens were the same size, the same lifting hooks and internal and external strap arrangements were used. One of the finished pier cap forms, with the CMP, reinforcement, and external straps is shown in Figure 27.

The pipe pile connection before and after placing concrete is shown in Figure 28. A wooden shim was used to hold the reinforcing steel in place at the correct embedment length. Another wooden shim was used inside the pipe to obtain the desired cover for the No. 4 hoop. Shims were removed after sufficient concrete was placed to keep the reinforcement stable.

Figure 27. Pier cap reinforcement

Pier cap specimen PSC1 was constructed with the second set of single pile specimens, (ASC3 and ASO2); PSC2 was fabricated and placed with the third series of specimens. The last two series were fabricated, finished, and cured in the same manner as the first series, which has been previously described in some detail. Twelve control cylinders for each truck were also placed for each series of specimens. Concrete on the inside of the pipe piles was placed at the same time as the corresponding series of specimen, and thus had the same strength. Concrete in the pipe was also cured with wet burlap and plastic, in the same manner as the concrete in the test specimen.

Pipe piles were grouted into place seven days after the specimen and pipe pile concrete was placed. The pipe pile was grouted in using the same method as was described for grouting the H-piles into place. Steel angles were bolted to the side of the pipe pile, which in turn was supported by the CMP to provide the desired embedment length for the pile; a pipe pile grouted in place can be seen in Figure 29.

a) Pipe pile before placing concrete

b) Pipe pile after placing concrete

Figure 28. Pipe pile connection before and after placing concrete

Figure 29. Pipe pile after being grouted in place in PSC1

3.1.3 Double Pile Abutment Specimen Construction

For the abutment section, a double pile test was also performed. Connection details in the double pile test varied slightly from the single pile tests due to changes made in the actual field connection. The single pile test specimens were constructed according to the project plans and tested before construction of the substructure in the field. However, during field construction, the spiral reinforcement was omitted. Thus, the spiral reinforcing was eliminated in the double pile test to better represent field conditions.

Another change was made to the double pile connection detail. Based on the results from the single pile tests, the depth of concrete inside the CMP was decreased to reduce the capacity of the connection, which should lead to failure at a lower applied force. In order to decrease the depth of concrete in the pipe while keeping the pile connection intact, 12 inches of insulation board was placed in the bottom of the CMP. This resulted in a concrete depth of two and a half feet. As with the single pile abutment specimens and pier cap specimens, the double pile abutment specimens were inverted during fabrication and testing. The external details of the double pile specimens are presented in Figure 30.

Specimen size was limited to twelve feet for handling and constructability purposes. The reinforcing cages used in the double pile specimens were adapted from the bridge plans and thus had reinforcement similar to that used in the single pile abutment specimens. However, the reinforcement was designed and constructed to fit two CMP in the formwork; all other construction details remained the same. The top and end views of the reinforcement are presented in Figure 31.

H-piles used in the double pile specimen had the same welded studs on the pile web as shown in Figure 14. Internal straps were increased from three straps for the single pile specimens to four straps for the double pile specimens; external straps were also increased from two straps for the single pile specimens to three straps for the double pile specimens. Lifting hooks used in the double pile specimens were the same number and layout as were used in the single pile specimens. The reinforcement in the formwork for a double pile test specimen, along with the external straps and lifting hooks, can be seen in Figure 32.

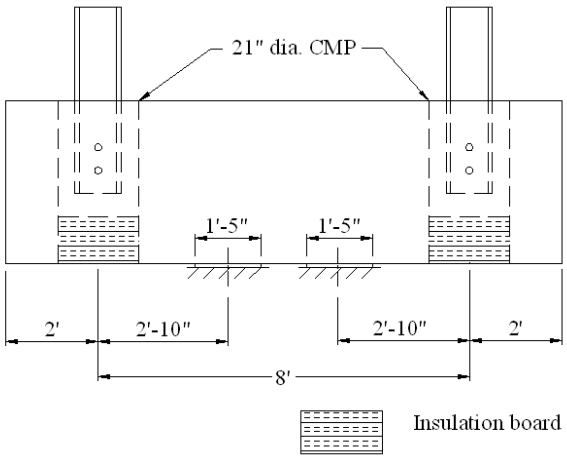

a) Top view

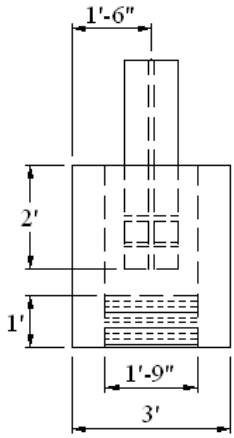

b) End view

Figure 30. Double pile abutment test specimen

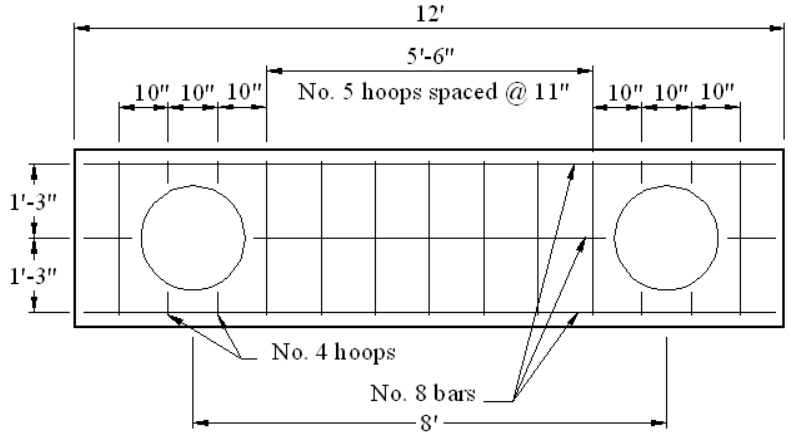

a) Top view

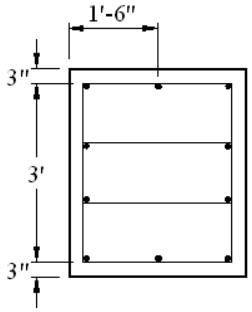

b) End view

Figure 31. Double pile abutment specimen reinforcement

Concrete used in the double pile abutment specimens was the same mix used in the single pile abutment and pier cap specimens. As with the previous specimens, Styrofoam was used to cover the CMP to keep concrete out of the void. Concrete was placed using the overhead crane and concrete bucket, vibrated, and finished by hand. A finished double pile specimen before initial set was reached is shown in Figure 33.

While the concrete was being placed, twelve control cylinders from the concrete in each truck were made. Once the concrete reached initial set, the surface was covered with wet burlap and plastic sheets for curing. The specimen remained covered for seven days, after which the covering was removed and the formwork 'stripped'.

Figure 32. Finished reinforcement and formwork for ADC1

Figure 33. Abutment 6 after hand-finishing

Before the H-piles were grouted into place, as previously noted, twelve inches of insulation board were placed at the bottom of the CMP, leaving six inches of concrete cover below the tip of the H-piles. Steel angles and C-clamps were used to support the H-piles, which in turn were supported by the CMP during concrete placement. One of the H-piles being held in the desired position before placing concrete was complete is shown in Figure 34. Note the absence of the spiral reinforcement in the CMP.

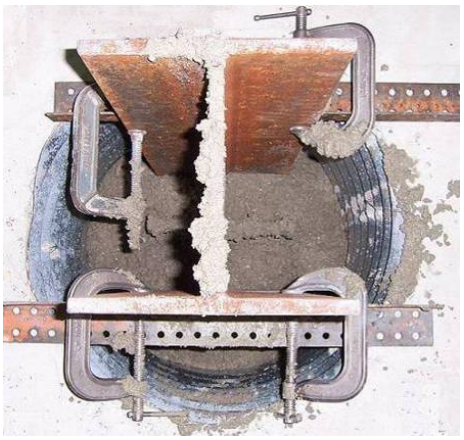

Figure 34. Double pile abutment specimen H-pile before being fully grouted

The concrete inside the CMP was hand finished because of previously described space constraints. After the grout concrete reached initial set, the height of the CMP allowed water to be ponded on top of the grout concrete for curing. After twenty-four hours, the C-clamps and steel angles were removed, however, water was kept on the surface of the grouted concrete for seven days. As before, a total of twelve control cylinders were made for the grout concrete mix.

The last construction task was to use a grinder to smooth and level the surface of the pile. This was to ensure even loading during testing and to prevent localized failure in one of the pile flanges.

3.2 Laboratory Testing

The main concern with the substructure elements was the possibility of the grouted concrete shearing from the CMP and 'punching' through the precast section of the abutment and pier caps. For the abutment sections, there also was a concern that the pile may punch through the concrete in the CMP; this was not a concern for the pier cap due to the large surface area of the concrete-filled pipe pile.

Test were performed on three different substructure specimens: single pile abutment and pier cap tests were performed to determine the capacity of the specimen when subjected to a combination of shear and negative moment; double pile abutment tests were performed to determine the positive moment capacity of the abutment section. After the double pile specimens were tested, punching shear tests were performed on each individual pile to determine the punching shear capacity of the H-pile connection.

3.2.1 Single Pile Test – Abutments and Pier Cap

The single pile abutment and pier cap tests had two simulated beams spaced on eight-feet, four-inch centers, according to the bridge plans. This beam spacing provided the maximum negative moment in the substructure sections at the pile location. Beam spacing and support dimensions are presented in Figure 35.

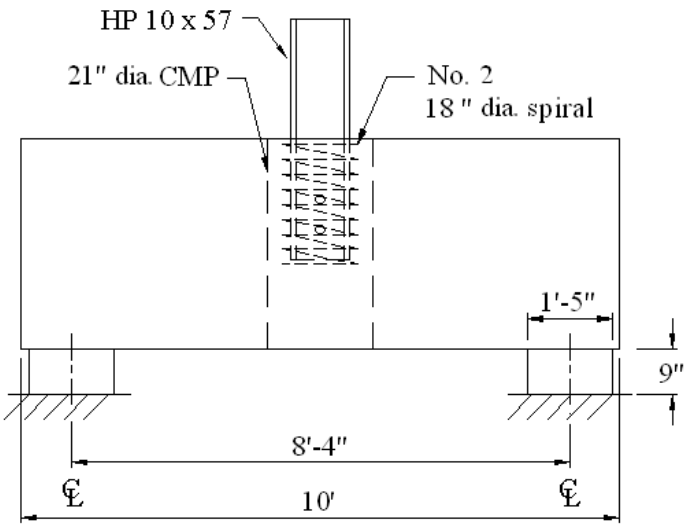

Figure 35. Single pile abutment test support details

The pier cap specimens were tested using the same arrangement as the abutment test shown. Each specimen was instrumented with linear variable deflection transducers (LVDT) and strain gages. Transducers were placed on the top and bottom faces of the specimen to measure differential deflection between the precast concrete and the grouted concrete in the CMP, and total deflections during testing. A total of nine deflection transducers were used: four on the top surface of the specimen and five on the bottom surface. On the bottom surface of the specimen, one deflection transducer was placed adjacent to the support to measure the deflection due to the compression of the neoprene pads so that the actual deflection of the test specimen could be determined.

Strain gages were used on the pile flanges to determine if there was uniform loading. Each H-pile was instrumented with four strain gages, one gage on each flange of the pile; each pipe pile had two gages placed opposite each other. The concrete was also instrumented with four strain gages. Each of the transverse sides of the specimen had two strain gages attached, one at the top and one at the bottom. Placement of the gages varied slightly for each specimen, depending on the quality of the concrete surface. The instrumentation plan for the single pile specimens is presented in Figure 36 (spirals and pipe pile steel not shown for clarity); instrumentation used on the pier cap specimens was the same as that was used on the single pile abutment specimens, with the exception that only two strain gages were used on the pipe piles.

The variable dimensions for the deflection transducers and strain gages are labeled with letters in Figure 36; deflection instrumentation dimensions for each specimen are given in Table 2 and strain gage location dimensions are given in Table 3. Some of the instrumentation on ASC1 can be seen in Figure 37.

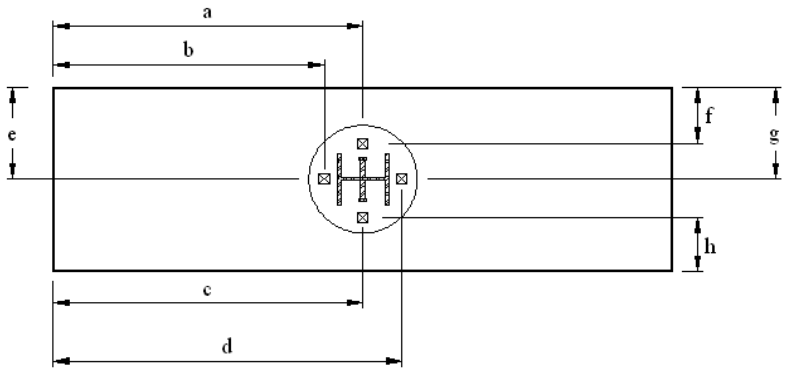

a) Location of the deflection transducers used in the single H-pile and pipe pile tests, top view

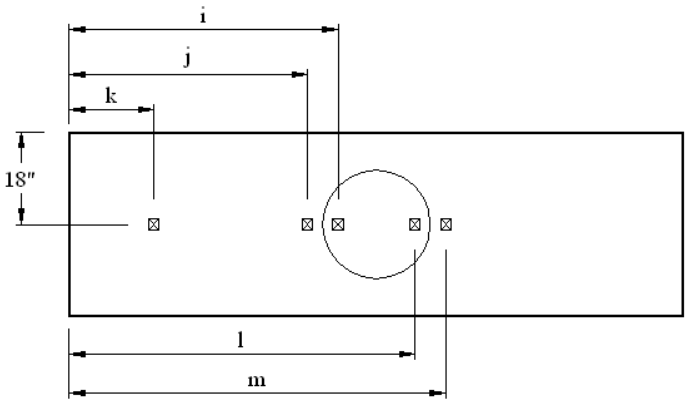

b) Location of the deflection transducers used in the single H-pile and pipe pile tests, bottom view

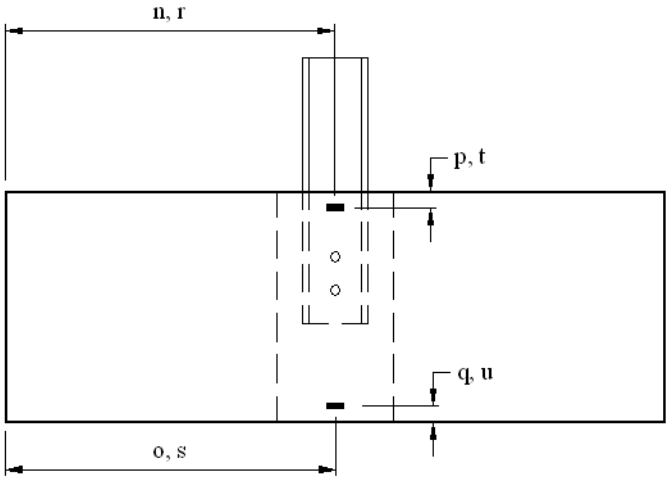

c) Location of the strain gages used in the single pile tests (north face, south face)

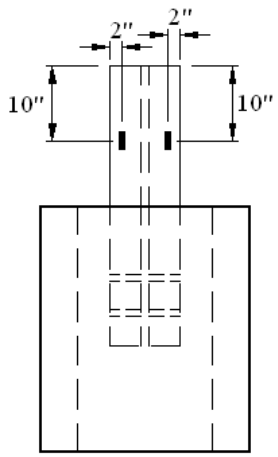

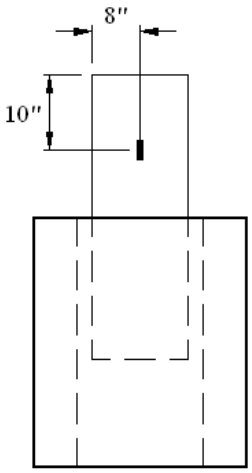

d) Location of H-pile strain gages **e) Location of pipe pile strain gages**

Figure 36. Single pile abutment test instrumentation plan

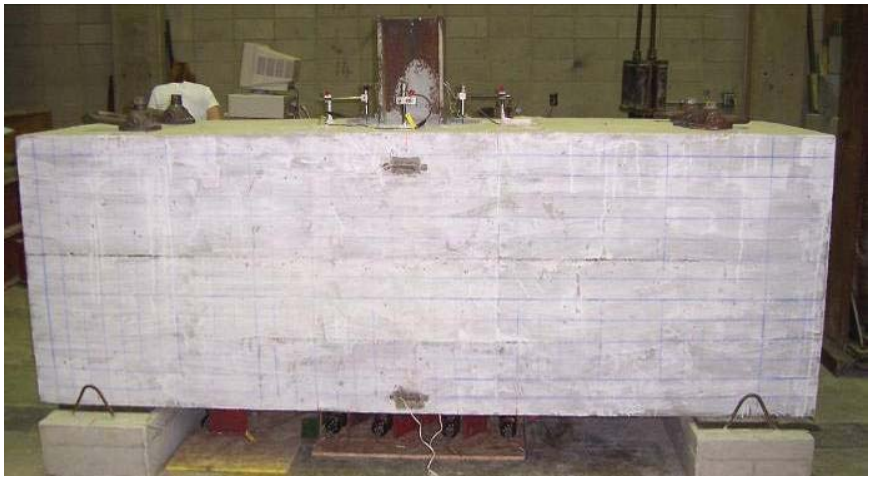

Figure 37. Instrumentation on ASC1 prior to testing

Table 2. Location of deflection instrumentation on the single pile specimens

Specimen	Top Deflection Dimensions (in.)								Bottom Deflection Dimensions (in.)				
	a	b	c	d	e	f	g	h	i	j	k	l	m
ASC1	58	50.5	57.5	66.5	19	10.5	16	26	54	45	24	66	75
ASC2	59.75	51.5	59.75	67.75	17.5	9.5	18	10.75	53.5	45.75	22	65.5	75.25
ASC3	62	62.5	60	67.5	18.5	10	20	10	54.5	43.5	20	65	74
ASO1	61.5	52.25	59.25	68	17.25	10.75	15.75	10	54	45.25	21.5	65.5	75
ASO2	60	44.5	59.75	70.5	17.5	4.75	18.25	6	55.75	47.25	21	67.75	66.25
PSC1	57.5	51	58.5	68.5	18	8.25	51.5	9	53.75	45	21.75	68	77.5

Table 3. Location of strain gage instrumentation on the single pile specimens

Specimen	North Face Dimensions (in.)				South Face Dimensions (in.)			
	n	o	p	q	r	s	t	u
ASC1	59	59	4.5	2.75	58.25	58.5	1.5	4
ASC2	60	60	3.25	2.25	60	60	5.25	2
ASC3	57.5	60	2.25	3.5	60.25	58.25	2.5	1
ASO1	60.5	60.5	3.75	2.25	60.25	60.25	3.25	7
ASO2	62.5	62	4	1	63.5	62.75	3	2
PSC1	59	59	1	0.75	57.5	59.5	3	2.5

As previously noted, the specimens were inverted for testing due to stability concerns. The simulated beams rested on the floor, the specimens were placed on neoprene pads on top of the beams, and the protruding pile was then loaded. An actual test arrangement for one of the abutment specimen is shown in Figure 38.

Abutment and pier cap specimens were tested seven days after the grouted concrete was placed, or as soon as the grouted concrete reached the appropriate strength, if strength was not met in seven days. Specimens were initially loaded to a proof load of 160 kip, twice the unfactored design load. This proof load was held for 15 minutes before loading continued. The load cell used for testing had a maximum capacity of 300 kips (±10 pounds) while the hydraulic pump and Load Frame 1 each had capacities of 400 kips. Therefore, each specimen was loaded to 300 kips after which the load cell was removed, and loading continued to the maximum capacity of the test specimen. While the load cell was in use, strain and deflection measurements were taken at approximately 10 kip increments.

Figure 38. Laboratory test arrangement for ASC1

After the load cell was removed, loading continued and measurements were taken at approximately eight kip increments, as measured using the gage reading of the hydraulic pump. Each specimen was loaded until failure or until the safety of the load frame became a concern. Periodically during testing, loading was paused to mark the crack pattern on the specimen; the crack pattern was also marked at the final load.

3.2.2 Double Pile Positive Moment Test

Double pile abutment specimens were tested to measure the effects of the combination of shear and positive moment on the abutment and to determine if this loading condition could produce a

punching shear failure between the precast concrete and the concrete in the CMP. Support conditions were adjusted from the plans to produce a maximum positive moment in the abutment section between the piles. In the field, the abutment section can never be subjected to the same loads as in the laboratory tests because of the support conditions (i.e. continuous spans); the loads in the laboratory (i.e. simple spans) were more severe than actual field conditions. Double pile specimens were inverted and tested in the same manner as the single pile specimens; the support conditions for the double pile specimens are presented in Figure 39.

Each test specimen was instrumented using twelve strain gages on the concrete, eight strain gages on the H-pile, four deflection transducers at each pile connection (eight LVDTs total), and six deflection transducers along the bottom of the specimen. Deflection transducers were placed on the top and bottom faces of the specimen to measure total deflection and differential deflection during testing; the eight LVDTs on the top surface of the specimen were used for differential deflection measurements while the six transducers on the sides of the specimen were used for measuring total deflections.

Strain gages were used on the H-piles to ensure even loading. Each H-pile was instrumented with four strain gages, one on each flange of the pile. The concrete section was also instrumented with a total of twelve strain gages. Strain gages were placed at the top and bottom of the transverse sides at both pile locations and at the center of each specimen; the exact location of the strain gages varied slightly for each specimen depending on the surface of the concrete.

The instrumentation plan for the double pile specimens is presented in **Error! Reference source not found.** (the insulation board is not shown for clarity). Variable dimensions for the location of the top deflection transducers, the bottom deflection transducers, the strain gages on the north face of the specimens, and the strain gages on the south face of the specimens are presented in Table 4, Table 5, Table 6, and Table 7, respectively.

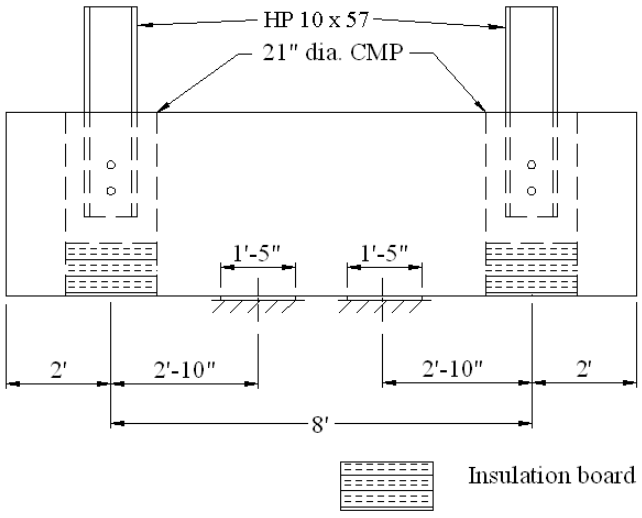

Figure 39. Double pile abutment test support details

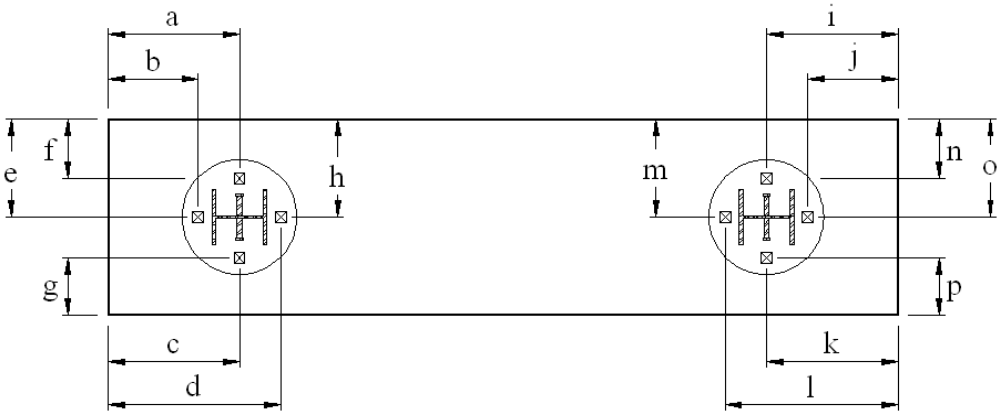

a) Location of deflection transducers (top view)

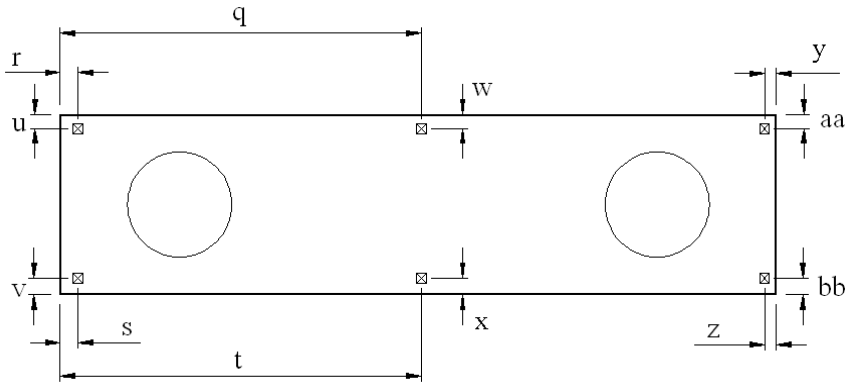

b) Location of deflection transducers (bottom view)

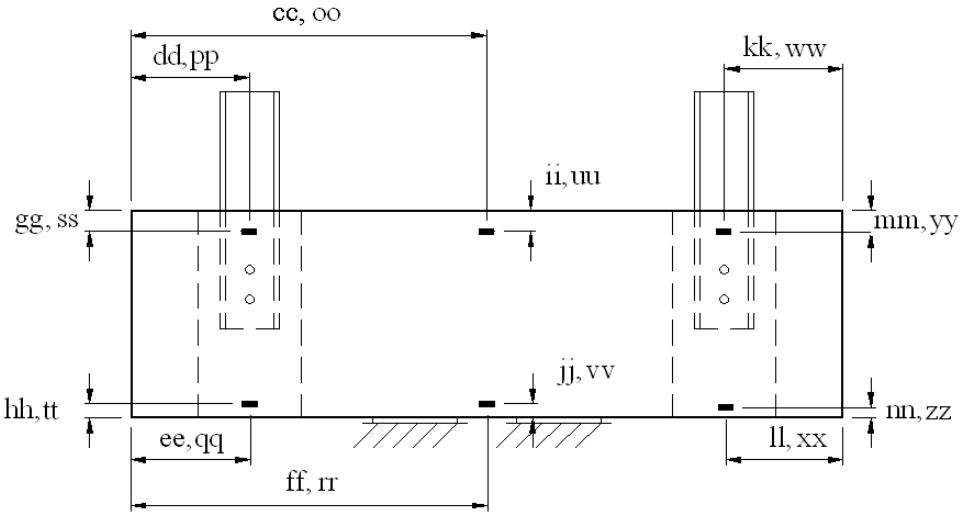

c) Locations of the strain gages (north and south face)

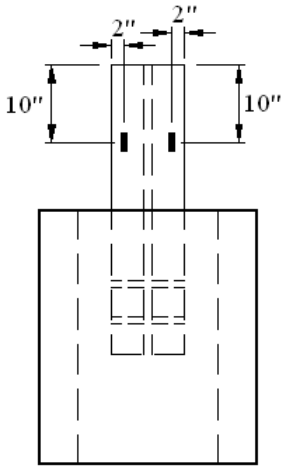

d) Location of the strain gages on the H-piles

Figure 40. Double pile abutment test instrumentation plan

Complete instrumentation on the north face of ADC1 can be seen in Figure 41 prior to testing. Laboratory testing arrangements were similar to that used in the single pile specimen tests, however, the double pile test required two load frames so that both piles could be loaded simultaneously; Load Frame 2 had a capacity of 150 kips. The laboratory testing arrangement for ADC2 is shown in Figure 42.

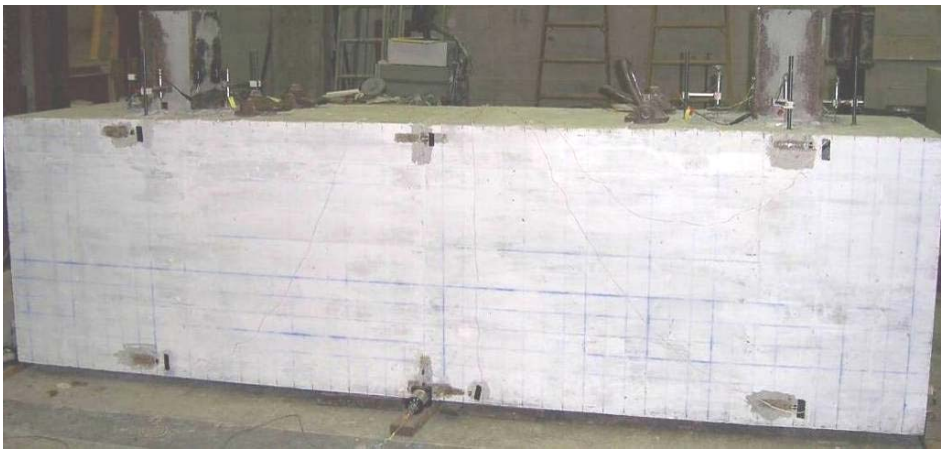

Figure 41. Instrumentation on an ADC1 prior to testing

Table 4. Double pile specimens: location of top deflection instrumentation.

Specimen	Top Deflection Dimensions (in.)															
	a	b	c	d	e	f	g	h	i	j	k	l	m	n	o	p
ADC1	21.5	15.3	23	35.5	19	11.5	11.3	17.8	21	13.5	19.5	29	21	13.5	17.8	11.5
ADC2	22.5	17.5	23.3	38	18.5	9.5	13.3	18.8	21.3	11.3	21	35.5	17.8	10.5	18	11.5

Table 5. Double pile specimens: locations of bottom deflection instrumentation.

Specimen	Bottom Deflection Dimensions (in.)											
	q	r	s	t	u	v	w	x	y	z	aa	bb
ADC1	72.75	0.5	0.5	78	0.5	0.5	0.5	0.5	0.5	0.5	0.5	0.5
ADC2	72.5	0.5	0.5	76.5	0.5	0.5	0.5	0.5	0.5	0.5	0.5	0.5

Table 6. Double pile specimens: locations of strain gages, north face.

Specimen	North Face Strain Dimensions (in.)											
	cc	dd	ee	ff	gg	hh	ii	jj	kk	ll	mm	nn
ADC1	68	21.25	20.25	69.25	2.5	3.25	3	3.25	19.25	18.5	2.75	4
ADC2	68.5	21.5	24.3	67.5	2	2.5	2.75	3	20.5	20.75	1.75	2.75

Table 7. Double pile specimens: location of strain gages, south face.

Specimen	South Face Strain Dimensions (in.)											
	oo	pp	qq	rr	ss	tt	uu	vv	ww	xx	yy	zz
ADC1	66.5	19.5	20	75.5	2.75	3	2	2.5	21	21.25	3.25	1.75
ADC2	75.5	20.5	21.25	74	2.25	2.5	2	1.75	21.5	23	2.5	1.75

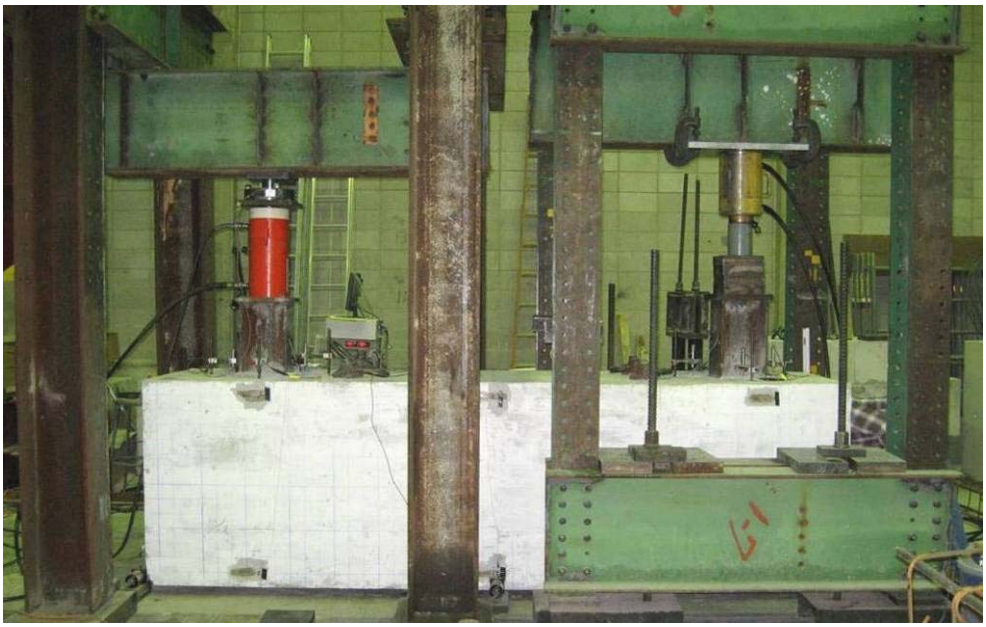

Figure 42. Laboratory test arrangement for ADC2

The double pile abutment specimens were tested seven days after the grouted concrete was placed, or as soon as the grouted concrete reached the appropriate strength, if strength was not met in seven days. Specimen were tested by simultaneously loading both of the H-piles at approximately the same rate up to 140 kips (ADC1) or 150 kips (ADC2). Deflection and strain measurements were taken at approximately 10 kip intervals. Loading was stopped at 140 or 150 kips due to concerns with the safety of the load frames. Periodically during testing and at the final load, loading was paused to mark the crack pattern on the sides and top surface of the specimen.

3.2.3 Shear Test

After the combination shear and positive moment tests were complete, the double pile abutment specimen had not completely failed. The area of concrete around the CMP had not cracked, so additional tests were performed on the specimen. Each abutment was adjusted to center one of the piles under the larger load frame. Support conditions were moved so there were two supports located adjacent to the CMP around the pile being tested. A third support was placed under the opposite end of the abutment for stability. The load frame and test arrangement for one of the pile shear test can be seen in Figure 43.

Since the abutments were already instrumented, the same instrumentation was used in the shear test. The bottom deflection gages were omitted since the bottom of the concrete in the CMP could not be instrumented for comparison; also the four strain gages on the concrete located at the center of the specimen were omitted since the center gages were beyond the area of interest. Thus in the shear tests, data measured by the four strain gages on the concrete at the pile location, the four strain gages on the H-pile being tested, and the four LVDTs located adjacent to the pile were recorded.

Each pile was loaded to 400 kips, measurements being recorded approximately every 10 kips with the load cell in place (up to 300 kips), and every eight kips after the load cell was removed. The differential deflections were monitored and the specimen was checked for cracks throughout the loading. Since there were no cracks on the specimens visible to the naked eye, none were marked.

Figure 43. Double pile abutment shear Test 1

4. LABORATORY TEST RESULTS

4.1 Single Pile Abutment Test Results

The results from the abutment and pier cap tests described in Chapter 3 are presented in this chapter. During the test of PSC2 there was a premature localized failure over one of the supports. Since the failure that occurred was independent of the CMP and pile connection, the results for PSC2 are not presented. Each pile in the actual abutment in the field was designed by the Iowa DOT to support a service load of 80 kip; the piles in the pier cap were designed to support a service load of 72 kip each.

To simplify the comparison of results, the instrumentation numbering for the single pile specimens was kept consistent. The following instrumentation labels and locations apply to all of the single pile tests. Labels and locations for the strain gages applied to the concrete are shown in Figure 44. As previously noted, the location dimensions for all of the gages which vary on each specimen can be found in Table 2 and Table 3.

The only difference in instrumentation labeling for all of the single pile specimens was for the pier cap test; only two strain gages were used, G5 and G7, which were directly each other on the pipe pile. Locations of the strain gages on the H-pile for the abutments are shown in Figure 45a, the locations for the top deflection transducers are shown in Figure 45b, locations of the strain gages on the pipe pile are shown in Figure 45c and the locations for the bottom deflection transducers are shown in Figure 45d. This instrumentation labeling will be used throughout the results section.

Control cylinders for the precast concrete and the grouted concrete were broken at seven days and twenty-eight days, corresponding to when the concrete was placed. Separate cylinders were also made from the precast concrete and the grouted concrete for each specimen and were broken on the day each respective test was performed. All of the concrete cylinders were broken according to ASTM C39; concrete strengths on test day and at 28-days are listed in Table 8.

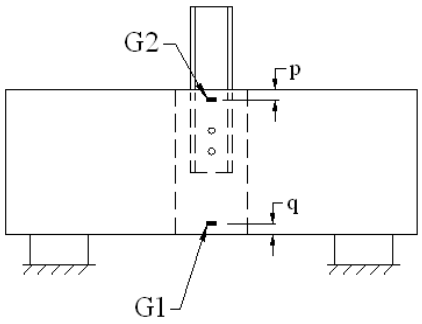

a) Strain gage locations on the north face

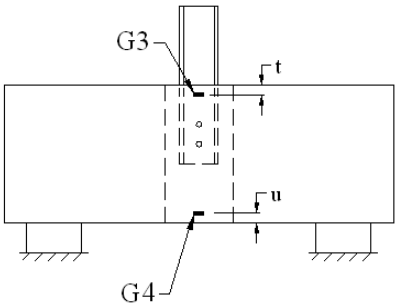

b) Strain gage locations on the south face

Figure 44. Single pile specimens: locations of strain gages on concrete.

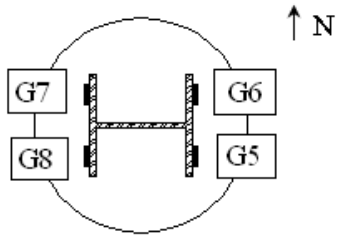

a) Strain gage locations on H-pile

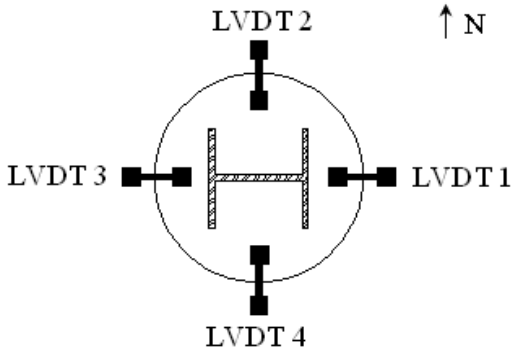

b) Location of top deflection transducers

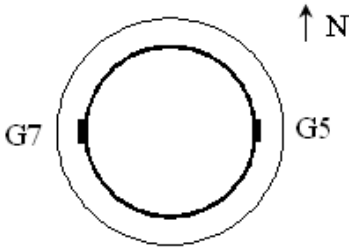

c) Strain gage locations on pipe pile

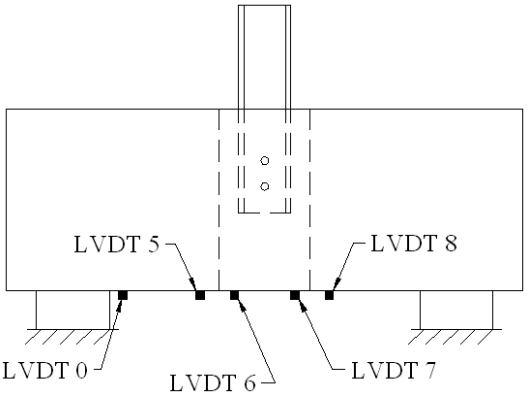

d) Location of bottom deflection transducers

Figure 45. Single pile specimen instrumentation locations

Table 8. Test day and 28-day concrete strengths for each test

Specimen	Precast Concrete Strength (psi)		Grouted Concrete Strength (psi)	
	Test Day	28-Day	Test Day	28-Day
ASC1	5020	6230	5220	6955
ASC2	4945	6230	5300	6955
ASO1	4340	5505	5520	6955
ASC3	5185	5315	4000	4280
ASO2	5685	5855	3115	4280
ADC1	6490*	5745	5540	5975
ADC2	6515*	5650	4010	5525
PSC1	5270	5315	3500	4280

* Test was performed after the precast concrete 28-day strength was measured.

Results from the slump tests were also recorded. All of the concrete met the minimum slump requirement of three inches before the concrete was placed. The maximum slump recorded was 4.5 inches; complete results from the slump test can be found in Appendix A.

4.1.1 Centered Pile Results

There were three single pile abutment specimens tested with centered piles, all of which displayed similar strain and deflection behavior, and had similar crack patterns under the applied load. The results for ASC3 are presented and discussed in the following pages; complete results for ASC1 and ASC2 are presented in Appendix A.

During testing, four parameters were measured: strains in the steel pile, concrete strains, differential movement between the concrete in the CMP and the precast concrete, and the total deflection of the specimen (see **Error! Reference source not found.** for location of instrumentation). Strains in the steel pile were examined first to ensure the pile was loaded uniformly. Steel pile strains measured during the testing of ASC3 are presented in Figure 46. The behavior of the H-piles is represented by the measured strain data. Stress data for the pile will not be presented since the stress-strain relationship remains linear throughout testing (i.e. the piles did not yield). For this report, compressive strains and stresses are negative, tensile strains and stresses are positive.

As may be seen in the figure, the strains measured in the flanges of the pile were not equal, however, the strains in the two flanges did increase at approximately the same rate; this indicates an eccentricity of the applied load. For example, during the ASC3 test, for an applied load of 276 kip, the difference between the north strains and south strains was approximately 175 μ-strain; actual strains and stresses in the four gages are listed in Table 9 (stresses were calculated using Hooke's Law and 29,000 ksi for the modulus of elasticity for the pile).

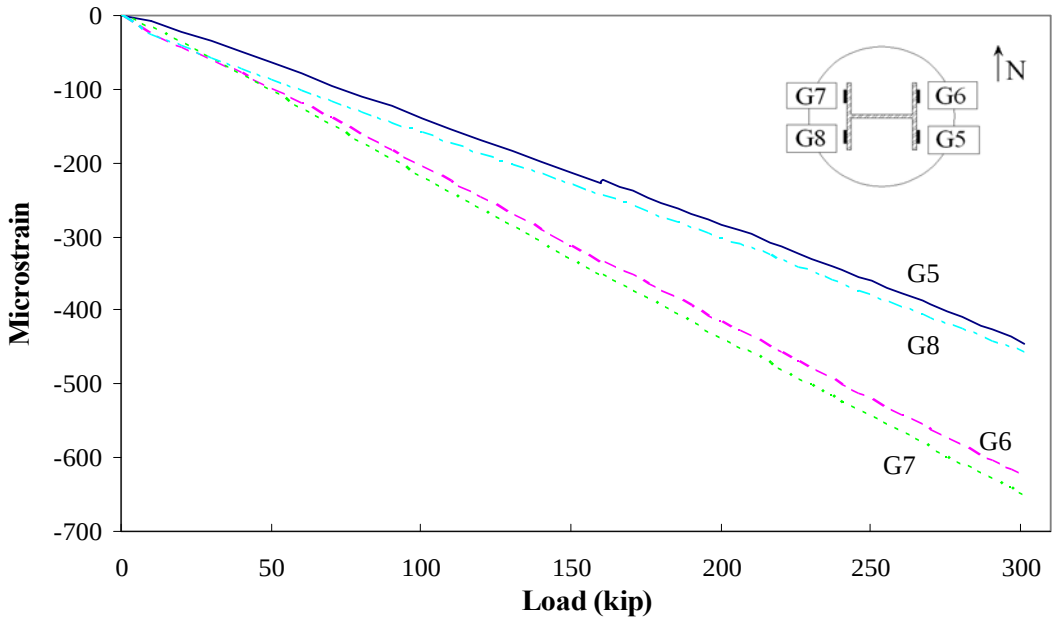

Figure 46. Steel strains for ASC3

Table 9. Strains and stresses in ASC3 at applied load of 276 kip.

Gage	Strain (10-6)	Stress (ksi)	Stress Difference (%)
G5	401	11.6	-
G6	574	16.6	43
G7	598	17.4	49
G8	418	12.1	4

Strains measured are due to the axial load applied to the pile and the load eccentricity. A system of equations, using the known strains, gage locations, and pile properties, was used to calculate the load eccentricity. Based on the strains given in Table 9, the axial load on the pile was offset 0.35 inches to the north and 0.07 inches to the west, which caused a stress difference of approximately 50% in the pile at this load.

The maximum strain difference measured in all of the piles was approximately 180 μ-strains in ADC2, which corresponds to a maximum eccentricity of 0.14 inches to the south and 0.86 inches to the west. Inadvertent eccentricity of the applied load was noted in all of the tests, the largest eccentricity calculated was less than one inch. Concrete stresses were examined to see if the eccentricity affected the specimen behavior, however, no clear trend relating the eccentricities to the stresses emerged.

All of the specimens tested were classified as deep beams based on the ACI Building Code (2005) criteria stating a deep beam is a beam under point load where the clear span is less than four times the beam depth. Since the clear span in all tests was eight-feet, four-inches and the depth was three-feet, six-inches the specimens met the deep beam criteria.

Strains in the concrete were examined to see how the pile connection affected the specimen behavior. Concrete strains were converted to estimated stresses using the modulus of elasticity of the concrete and Hooke's Law. The modulus of elasticity was calculated according to Section 5.4.2.4 of the AASHTO LRFD Bridge Design Specifications (1996). Concrete tensile strength was estimated based on the assumption that tensile strength is approximately 8-10% of the compressive strength. Concrete compressive strength, a range of the tensile strength, and the modulus of elasticity for each centered single pile abutment specimen are presented in Table 10. Concrete stresses in ASC3 are presented in Figure 47. Locations of the stresses (strains) in the figure were presented in Figure 44.

There are two distinct trends in the top and bottom specimen stresses that can be seen in Figure 47. At the bottom of the specimen, G1 and G4 indicate only tensile forces in the concrete at that location for all loads applied. The gages at the top of the specimen, G2 and G3, indicate the concrete is initially in compression, which agrees with simple beam theory. At a load of approximately 160 kip, ASC3 reached the cracking moment capacity of the section and the initial cracks in the sides of the specimen were noticed.

Table 10. Strength properties for centered, single pile abutment specimens

Test	Concrete Compressive Strength (psi)	Concrete Tensile Strength (psi)	Modulus of Elasticity (ksi)
ASC1	5020	400-500	4295
ASC2	4945	395-495	4265
ASC3	5180	415-520	4365

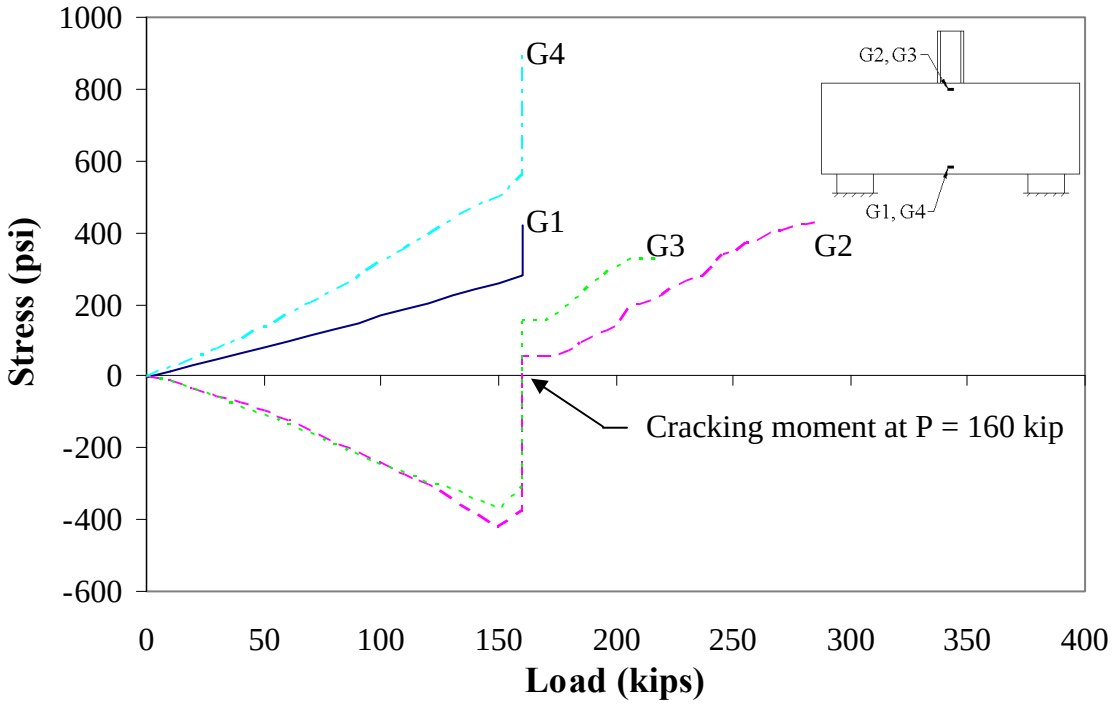

Figure 47. Concrete stresses in ASC3

As presented in Table 10, the tensile capacity of ASC3 was between 415 psi and 520 psi. Before the cracking moment was reached, the tensile stresses at the bottom of the concrete were less than 520 psi. During testing, cracks in the concrete propagated through several of the strain gages, which made them inoperable.

Stresses in the concrete at the top of the specimen changed when the cracking moment was reached; stresses changed from compressive to tensile. However, the concrete at the top of the specimen did not crack since the tensile stresses were less than 520 psi. The expected behavior of the section was the uncracked concrete at the top of the specimen should have been in compression. Since the concrete at the top of the specimen had tensile stresses immediately after the cracking moment was reached, it is apparent the pile connection and CMP affected the behavior of the specimen. This will be discussed in some detail in Section 4.4 of this chapter.

The ultimate goal of the laboratory testing was to determine if a pile would shear through the concrete, or cause the concrete in the CMP to 'punch' through the specimen. During testing, none of the H-piles punched through the concrete and none of the connections failed in shear. To determine if there was any differential movement between the precast concrete and the concrete in the CMP, the differential deflection measurements taken from the top of the specimen were analyzed. The transducers did measure small amounts of movement between the concrete in the CMP and the precast abutment (LVDT precision was 0.0005 inches); differential deflections measured during the testing of ASC3 are presented in Figure 48. Note for the LVDTs, negative movement was downward movement. The maximum differential deflection measured on top of ASC3 was -0.0033 inches at the east transducer and slightly less at the north transducer. The transducers at the west and south locations measured -0.001 inches or less.

Deflections on the bottom of the specimen were found by subtracting the compression of the neoprene bearing pads, measured by the transducer located adjacent to the support (LVDT 0) from the four deflections measured near the center of the specimen. As shown in Figure 49, the largest deflections measured during testing were from LVDT 6 and LVDT 7, the two transducers located closest to the center of the specimen. Deflections measured by LVDT 5 and 8 were further from the center of the specimen and as would be expected, were also smaller than the deflections measured LVDT 6 and 7. As shown in the two figures, there is a large difference in the magnitude between the differential deflections (Figure 48) and the total deflections (Figure 49). Based on the small magnitude of the measured differential deflection and possible experimental error, shear failure between the precast concrete and the concrete in the CMP was not detected.

As shown in Figure 49, the total deflection was linear before the cracking moment was reached. The deflection continued to increase essentially linearly up to an applied load of 340 kip, when the deflection behavior changed. After 340 kip, deflections increased rapidly under a small change in applied load, most likely due to yielding of the tension reinforcement in the specimen.

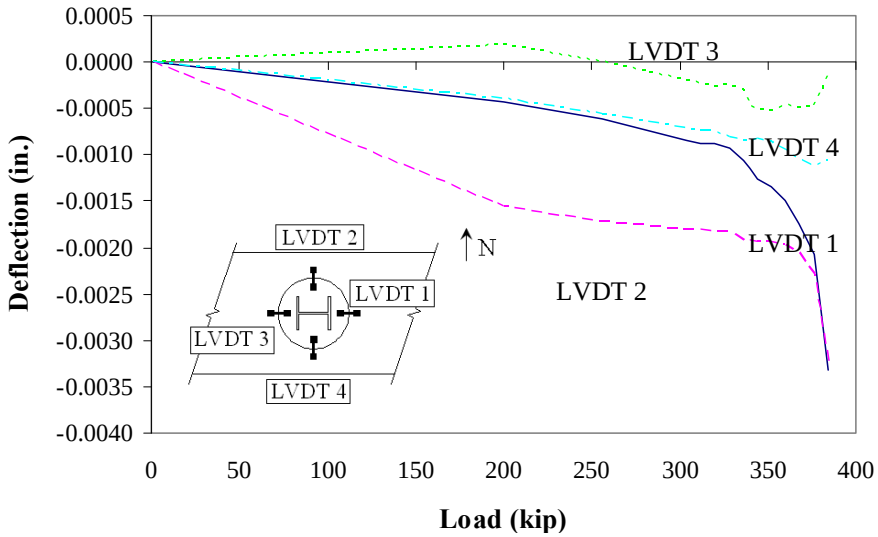

Figure 48. Differential deflection for ASC3

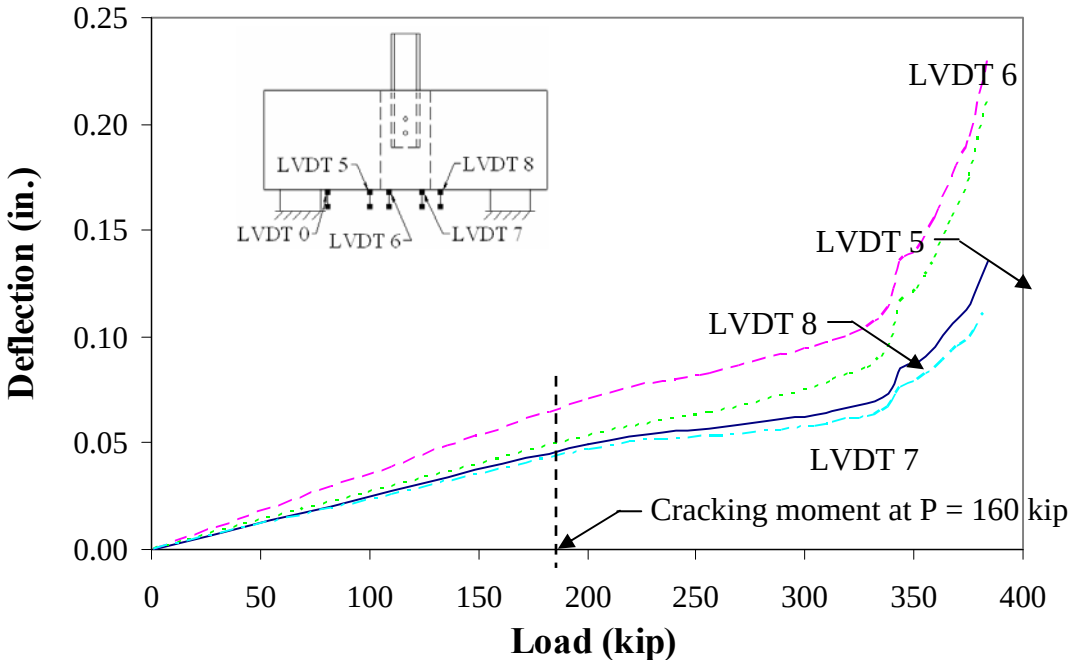

Figure 49. Bottom deflection for ASC3

In comparison, the stiffness of the uncracked specimen was approximately 3830 kip/inch, while at failure the stiffness was approximately 400 kip/inch. Based on the criteria that failure occurs when the specimen stiffness decreases by 50% or more, ASC3 failed at the applied load of 384 kip. The specimen failed in flexure, not due to punching shear at the pile connection, which was expected. However, since the specimen was a deep beam, the total deflection was caused by a combination of flexure and shear.

Each pile in the actual abutments was designed by the Iowa DOT to support an unfactored service load of 80 kip. Test specimens were loaded to at least four and a half times this magnitude before flexural-shear failure in the precast concrete occurred. The maximum applied load, the load to produce the cracking moment, and the experimental cracking moment for the centered, single-pile abutment tests are presented in Table 11.

As can be seen, laboratory testing for the centered, single pile abutment test show that the actual strength of the section is at least four and a half times the required strength of 80 kip. The minimum cracking moment for the centered, single pile specimens was reached at 250 kip-feet, or a pile load of approximately 120 kip; the average calculated cracking moment was 280 kip-feet, or when an average load of 135 kip was applied.

Table 11. Test results for centered-pile abutment tests

Specimen	Maximum Applied Load (kip)	Applied Load at Cracking Moment (kip)	Experimental Cracking Moment (kip-feet)
ASC1	360	120	250
ASC2	396	125	260
ASC3	384	160	330

Due to the fact the laboratory specimens were simply supported and the abutments in the field are continuously supported, the loading conditions in the laboratory are more severe than actual conditions. Loading conditions (including self-weight) and moment diagrams for the laboratory specimens and the actual abutments are shown in Figure 50 and Figure 51, respectively. For comparison, the load and moment diagrams were based on a load of 80 kip and the self-weight of the abutment. As shown, the maximum moment resulting from an 80 kip load in the field was only eighty percent of the maximum moment induced by an 80 kip load in the laboratory. Note: moment diagrams are plotted on the compression side.

a) Load diagram **b) Moment diagram**

Figure 50. Load and moment diagrams for laboratory tests

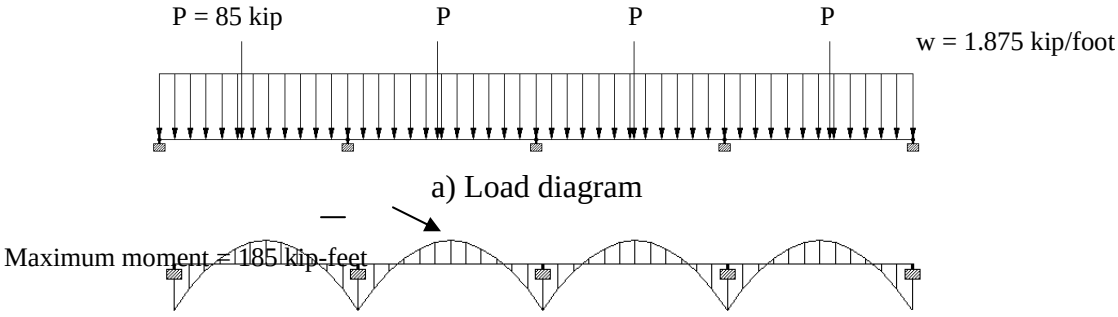

a) Load diagram

b) Moment diagram

Figure 51. Load and moment diagrams for actual abutment

4.1.2 Offset Pile Results

Two offset, single pile abutment specimens were tested, ASO1 and ASO2. Each pile was offset approximately four inches, the maximum offset to allow the spirals to fit. Both of the specimens

exhibited similar strain and deflection behavior and similar crack patterns under load. Since the offset specimens behaved in the same manner, only the results for ASO2 are presented and discussed; complete results for ASO1 are presented in Appendix A.

For the offset pile abutments, the steel strain data were analyzed first to ensure even loading; the strains in the steel pile for ASO2 are shown in Figure 52. The difference in strains was less than 100 μ-strains. As previously discussed, the difference in measured strains was due to a slight eccentricity in the axial loading applied to the pile.

Hooke's Law was again used to convert concrete strains to stresses while the tensile strength of the concrete as before was assumed to be eight to ten percent of the compressive strength of the concrete. The concrete compressive strength, range of concrete tensile strength, and the calculated modulus of elasticity for each of the offset, single pile abutment tests are presented in Table 11. Concrete stresses for ASO2 are shown in Figure 53.

As can be seen in Figure 53, the stress behavior in the concrete for the offset single pile abutment is similar to the stress behavior in the centered pile specimen previously discussed. A difference in behavior can be seen between the top and the bottom of the specimen. In specimen ASO2, the cracking moment was reached at an applied load of approximately 150 kip. After the cracking moment was reached, the concrete at the top of the specimen displayed tensile stresses, the same as in the centered, single pile abutment.

Differential movements between the precast concrete and the concrete in the CMP were measured using the top deflection transducers in ASO2 and are presented in Figure 54. The maximum differential deflection measured was -0.0018 inches at the south transducer (the concrete in the CMP moved down) and slightly less at the east transducer; the north and west transducers measured less than -0.001 inches of differential movement. The total deflections were calculated using the same procedure as was used in the centered, single pile abutment deflections and are shown in Figure 55.

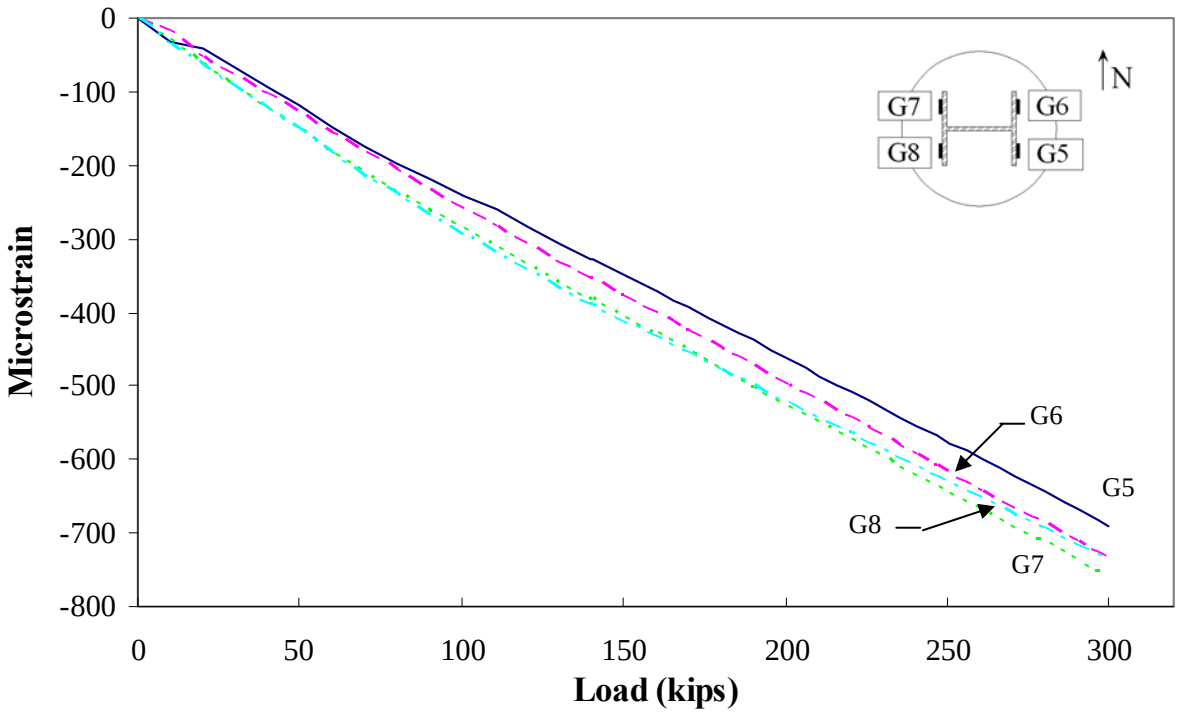

Figure 52. Steel strain for ASO2

Table 11. Strength properties for offset, single pile abutments

Specimen	Concrete Compressive Strength (psi)	Concrete Tensile Strength (psi)	Modulus of Elasticity (ksi)
ASO1	4340	350-435	3995
ASO2	5685	455-570	4570

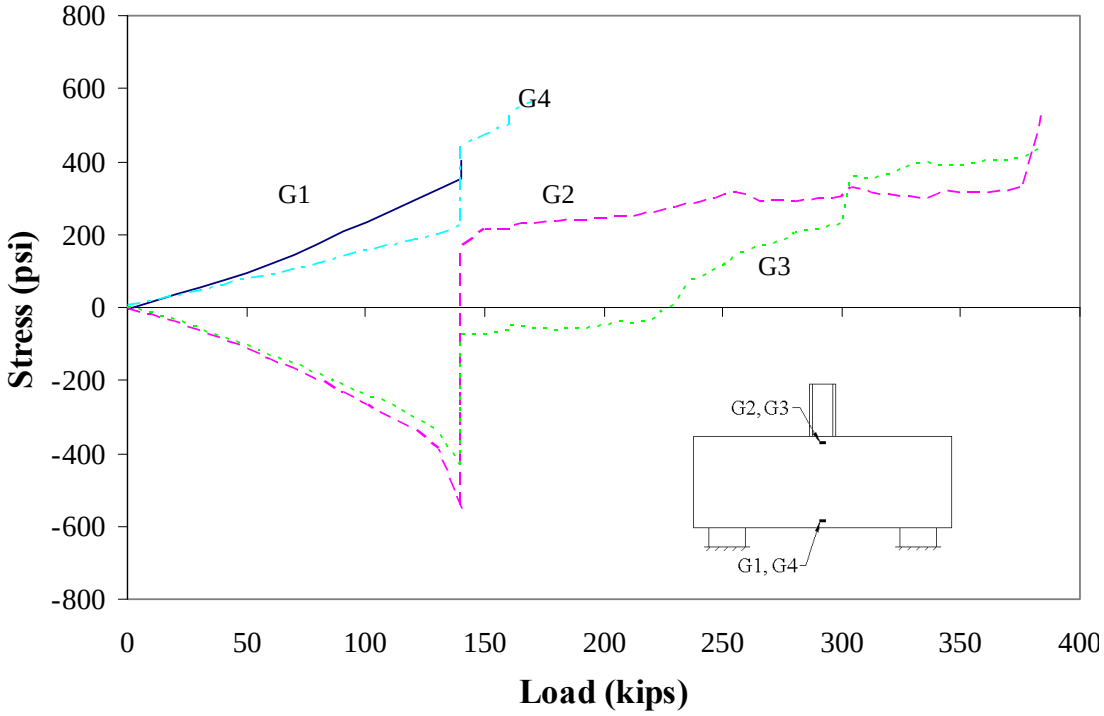

Figure 53. Concrete stresses in ASO2

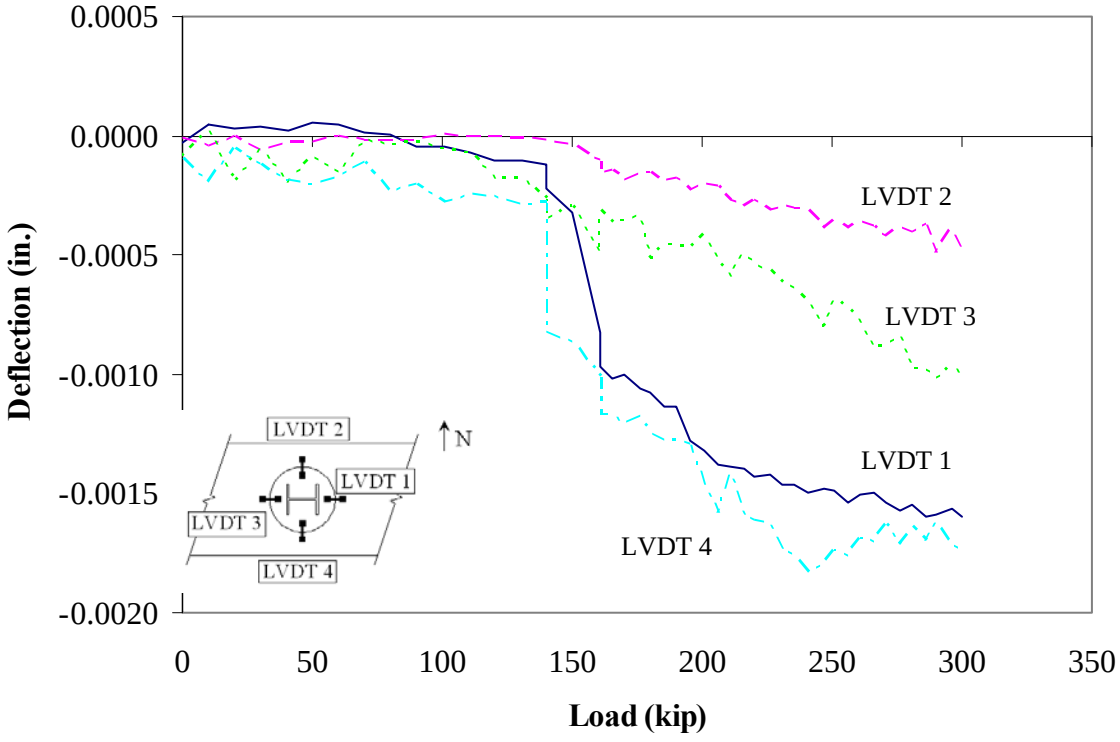

Figure 54. Differential deflection for ASO2

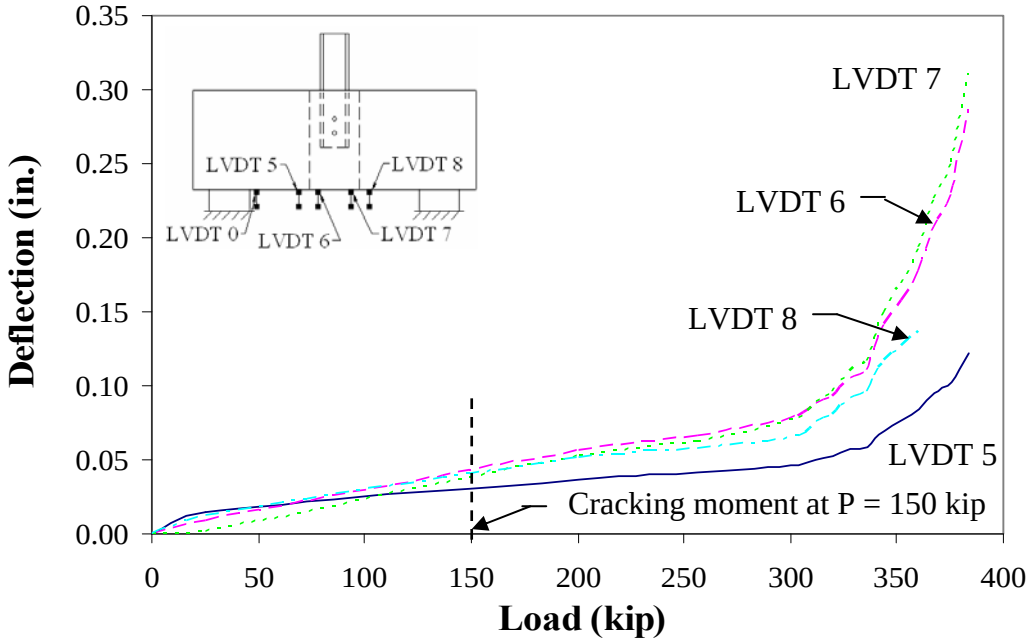

Figure 55. Total deflection for ASO2

As shown in Figure 55, the total deflection was linear prior to the cracking moment. The linear behavior continued until the applied load approximately reached 300 kip. After this point, the deflections increased rapidly with a slight increase in the load, similar to the deflection behavior discussed for the centered, single pile specimen. Based on the failure criteria discussed earlier, ASO2 failed at the final load of 384 kip. As with the centered pile specimen, total deflection was due to a combination of flexure and shear.

The offset, single pile abutment specimens were designed for the same load as the centered abutment specimen. Each of the offset abutments were loaded to 4.8 times the unfactored design load without significant differential movement between the precast concrete and the concrete in the CMP. Maximum load, load to produce the cracking moment, and cracking moment determined through testing are presented in Table 12.

Stress, strain and deflection behavior for the offset abutments was very similar to the behavior of the centered, single pile abutments. Laboratory testing for the offset, single pile abutment test has shown the strength of the section is at almost five times the required unfactored design load of 80 kip. At approximately 150 kip, the cracking moment for each section was reached. No significant difference in strength or behavior of the specimen was determined due to the offset locations of the piles. As previously discussed, the loading conditions for the offset pile specimens were more severe than the loading condition on the actual abutments.

Table 12. Test results from offset-pile abutment tests.

Specimen	Maximum Load (kip)	Applied Load at Cracking Moment (kip)	Experimental Cracking Moment (kip-feet)
ASO1	384	160	330
ASO2	384	150	315

4.2 Pier Cap Test Results

In addition to the abutment testing, two single pile pier caps were tested to determine if the concrete in the CMP would fail in shear and punch through the precast section of the pier cap. Because of the surface area of the concrete-filed pipe pile, there was not the same concern for the pile punching through the concrete. The cross-section of the H-pile was 16.8 square inches, compared to the 201.1 square inch cross-section of the pipe pile.

There were two pier cap sections initially tested; however, as previously mentioned, PSC2 failed prematurely due to a localized failure at one of the supports. Failure occurred over the support, however, the pile connection did not exhibit any signs of distress or failure. Therefore, the results for PSC2 will not be presented. The results for PSC1 are presented and discussed in this section.

Strain gages were applied to the pipe pile to measure strains during loading; G5 was located on the east side of the pile and G7 was located on the west side of the pile (see Figure 45c); steel strains measured during the testing of PSC1 are shown in Figure 56. Since strain gage G7 was not working properly during the test, only the results from G5 are presented in the figure. Because results from G7 were invalid, strains were recorded from only one gage, and therefore load eccentricity could not be determined.

When compared to the steel strains measured in the abutment specimen, the pipe pile strains are significantly less. This is due to the fact that in the abutment tests, the entire applied load was transferred solely through the H-pile. In contrast, for the pier cap testing the pipe pile was filled with concrete. Load was transferred through the concrete and steel, and over a much larger surface area. The larger bearing area for the same load will produce smaller stress.

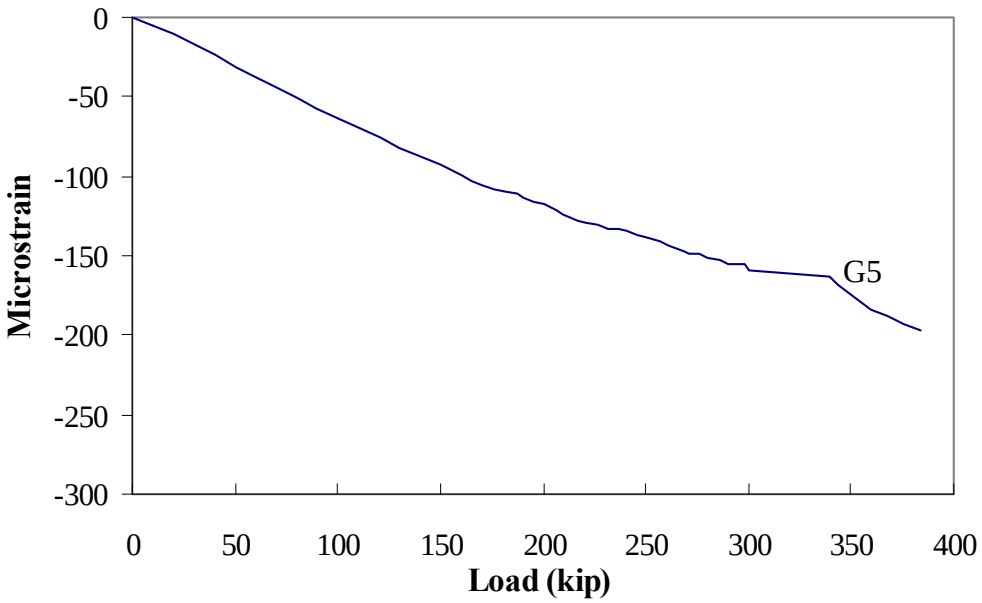

Figure 56. Steel strains for PSC1

Concrete strains in the pier cap were measured at the same locations as the abutment specimen, shown in Figure 44. Hooke's Law was used to convert concrete strains into stresses. Tensile strength was approximated as eight to ten percent of the compressive strength. The compressive strength, a range of the tensile strength and modulus of elasticity are presented in Table 13 and the concrete stresses are presented in Figure 57.

As with the abutment sections, the pier cap exhibited two distinctly different stress patterns in the concrete at the top of the specimen and at the bottom of the specimen. However, there is a noticeable difference in the behavior of the pier cap compared to the abutments. As with the abutments during initial loading, the stress at the top of the concrete is in compression and the bottom of the concrete is in tension. After the cracking moment is reached, the concrete at the top of the pier cap remains in compression and the concrete at the bottom remains in tension, following the expected behavior of the specimen. In comparison, the concrete at the top of the abutment specimen was subjected to tensile stresses immediately after the cracking moment was reached. This indicates the CMP and pile connection had a different effect on the behavior of the section.

During loading, the concrete in the CMP did not punch through specimen and there was no movement between the precast concrete and the concrete in the CMP that was noticeable. Deflection transducers on top of the specimen were used to measure any differential movement that may not have been visible; these differential deflections are presented in Figure 58.

Table 13. Strength properties for PSC1

Specimen	Concrete Compressive Strength (psi)	Concrete Tensile Strength (psi)	Modulus of Elasticity (ksi)
PSC1	5270	420-530	4400

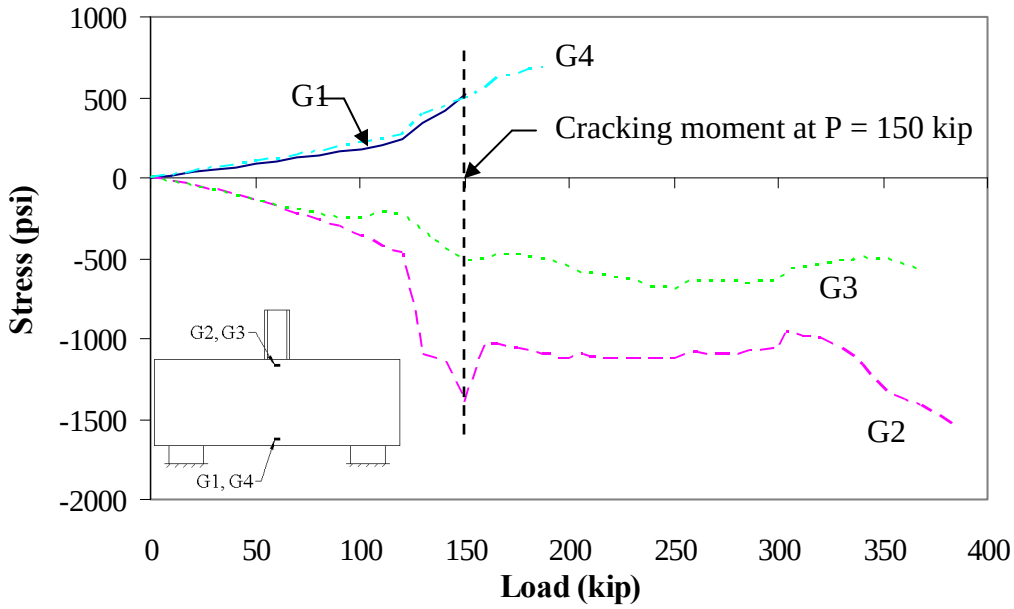

Figure 57. Concrete stresses in PSC1

The differential deflection measured in the pier cap was similar to the differential deflection measured for the abutments. A maximum deflection of -0.003 inches was measured by the west transducer and was slightly less at the north transducer; the south and east transducers measured less than 0.0005 inches of total movement, which is the LVDT precision and therefore most likely noise.

Total deflections were also measured and are presented in Figure 59. To obtain the total deflection of the specimen, the deflection of the neoprene pad was subtracted from the original deflection data taken at the center of the specimen. As Figure 58 and Figure 59 have shown, the differential movement was several orders of magnitude smaller than the total deflections measured.

As shown in Figure 59, the total deflection of PSC1 was relatively small before the cracking moment was reached. After the specimen cracked, the deflection was linear until the maximum load was applied, indicating the reinforcing bars did not yield. The difference in deflections between the abutments and the pier caps will be discussed later in this chapter.

The pier cap was designed by the Iowa DOT to support a unfactored load of 72 kip. PSC1 was loaded to 384 kip, which is close to 5.3 times the unfactored design load specified. Under the ultimate load, no appreciable differential movement was detected between the precast concrete and the concrete in the CMP, and the reinforcement did not yield. The maximum load, the theoretical cracking moment, and the experimental cracking moment for PSC1 are presented in Table 14.

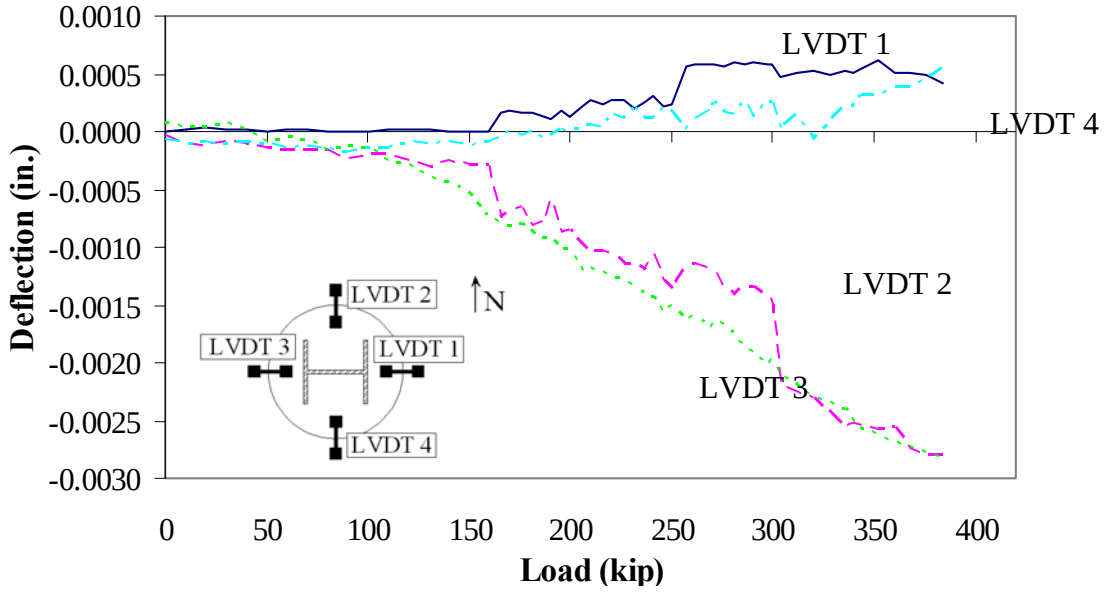

Figure 58. Differential deflection in PSC1

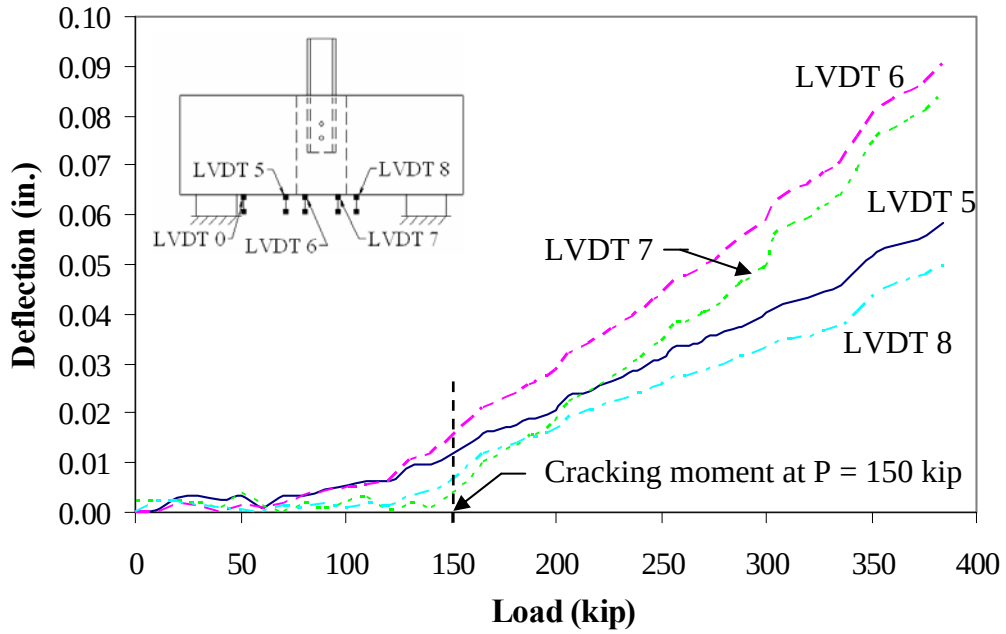

Figure 59. Total deflection in PSC1

Table 14. Pier cap test results

Specimen	Maximum Load (kip)	Applied Load at Cracking Moment (kip)	Experimental Cracking Moment (kip-feet)
PSC1	384	150	312

Laboratory testing for the pier cap has shown the strength of the pier cap is over five times the required design load of 72 kip. First cracks were noticed at an applied load of approximately 150 kip, which is equivalent to a cracking moment of approximately 312 kip-feet; 2.1 times greater than the maximum load the pier cap was designed to support. As previously discussed, the loading conditions in the laboratory were more severe than the actual loading conditions.

4.3 Double Pile Abutment Test Results

Results from the double pile tests described in Chapter 3 are presented in this section. There were two different tests performed on the double pile specimen: combination shear and negative moment tests on the entire specimens and shear tests on t individual pile.

4.3.1 Negative Moment Test Results

Instrumentation was increased for the double pile abutment specimen, requiring a change to the labeling system previously used in the single pile tests. The labels and locations of the strain gages on the concrete are shown in Figure 60. As previously noted, the dimensions for the concrete gages varied slightly based on the quality of the surface of the concrete; those dimensions are presented in Table 6 and Table 7.

Both piles were instrumented with strain gages, and the pile connection was instrumented with LVDTs to measure differential movement between the precast concrete and the concrete in the CMP. The labels and location of the strain gages on the H-pile and deflection transducers are shown in Figure 61 and Figure 62, respectively. Based on the testing system and support conditions, the total deflection transducers were placed on the bottom outside perimeter of the test specimens. The labels and locations of the total deflection transducers are shown in Figure 63.

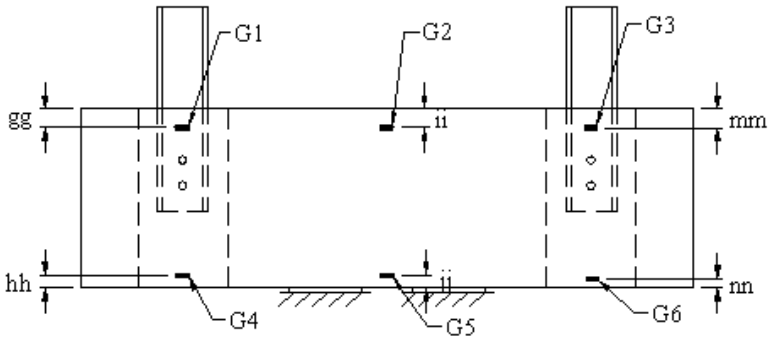

a) North face strain gage locations

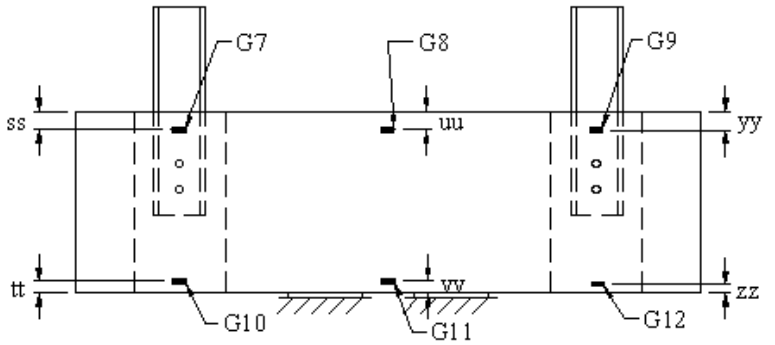

b) South face strain gage locations

Figure 60. Double pile specimen strain gage instrumentation plan

Figure 61. Double pile specimens: identification and location of pile strain gages

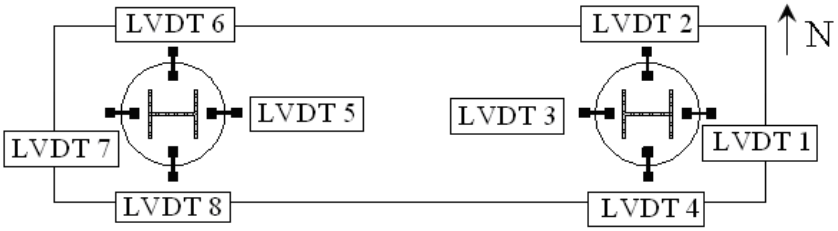

Figure 62. Double pile specimens: identification and location of top deflection transducers

Figure 63. Double pile abutment specimens: identification and location of bottom deflection transducers

The negative moment tests were performed first. Similar stress and deflection behavior, and similar crack patterns were exhibited in each specimen. For this reason, the results from ADC1 are presented and discussed in this chapter; results for ADC2 are presented in Appendix A.

One of the difficulties encountered with the double pile test was using two different hydraulic jacks to load the piles at the same rate. The measured strains in the H-piles were analyzed first to ensure even loading between the piles and even load distribution through each pile. Results from the steel pile strain gages for ADC1 are presented in Figure 64 and Figure 65, respectively.

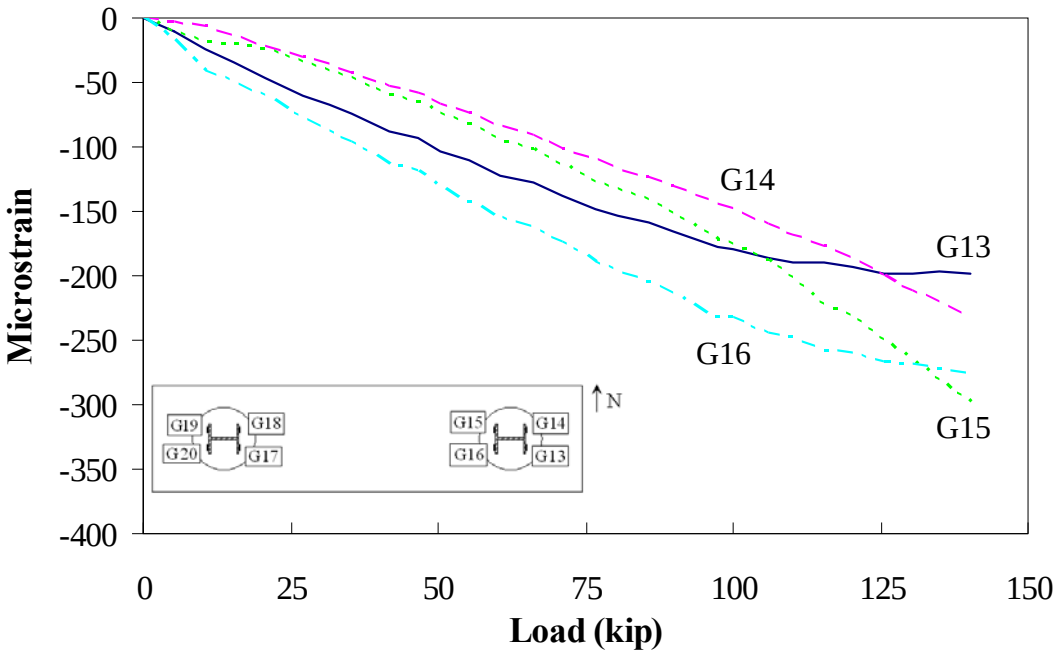

Figure 64. East pile steel strains in ADC1

When compared, magnitudes of the strains in the H-piles are relatively similar. The west pile had slightly lower strains, indicating a lower load than the east pile. This agrees with the recorded loads; the east pile had a maximum load of 140 kip and the west pile had a maximum load of 138 kip. The difference in strains in each pile was also analyzed. As previously discussed, the difference in strains was caused by an eccentricity in the pile load.

Pile load eccentricities were less than 0.9 inches, and as previously discussed, eccentricities did not correlate to concrete stress behavior. Next, strains measured at the concrete face were converted to stresses. Before the stresses were calculated, the modulus of elasticity was calculated. Concrete compressive strength, a range for the concrete tensile strength, and the calculated modulus of elasticity are presented in Table 15.

Stresses measured in the concrete were examined at three different locations: the center of the specimen, the east pile connection, and the west pile connection. Since both piles were loaded simultaneously, the maximum moment in the abutment occurred between the supports at the center of the specimen; obviously the maximum stresses occurred at this location as well. Concrete stresses at the center of the specimen are shown in Figure 66.

As would be expected, the stress data show the concrete at the bottom of the specimen was subjected to compressive stress and the concrete at the top of the specimen was under tensile stress. However, at the center of the specimen, there was no pile connection or CMP, which was the connection and area of interest. Stresses at the east and west piles were examined next and are shown in Figure 67 and Figure 68; see Figure 60 for the strain gage locations applied to the concrete.

When comparing the stresses measured at the center of the specimen to the stresses measured at the pile locations, there is one noticeable difference. The levels of stress measured at the pile locations are at least ten times less than the stresses measured at the center of the specimen. Maximum stress measured at the pile locations was approximately 30 psi, for tension and compression. This level of stress is six percent of the tensile strength of the concrete and less than one-half of one percent of the compressive strength of the concrete. Stress levels at the piles were small compared to the stresses at the center of the specimen and well below the tensile and compressive strengths of the concrete. This explains why no cracks or other signs of concrete distress were recorded at the pile locations, and also allowed for the additional shear tests to be performed.

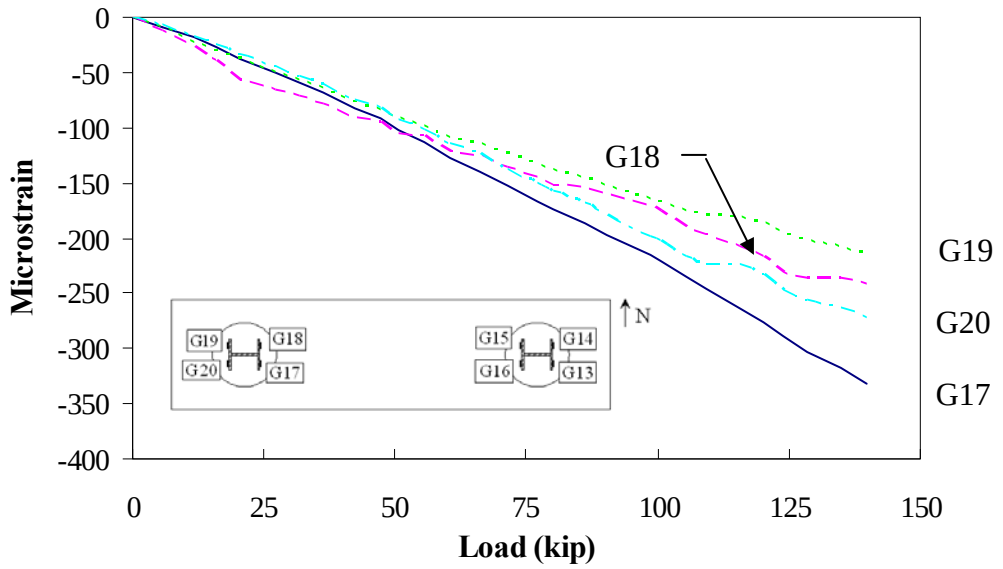

Figure 65. West pile steel strain in ADC1

Table 15. Strength properties for double pile abutment tests

Specimen	Concrete Compressive Strength (psi)	Concrete Tensile Strength (psi)	Modulus of Elasticity (ksi)
ADC1	6490	520-650	4885
ADC2	6515	520-650	4895

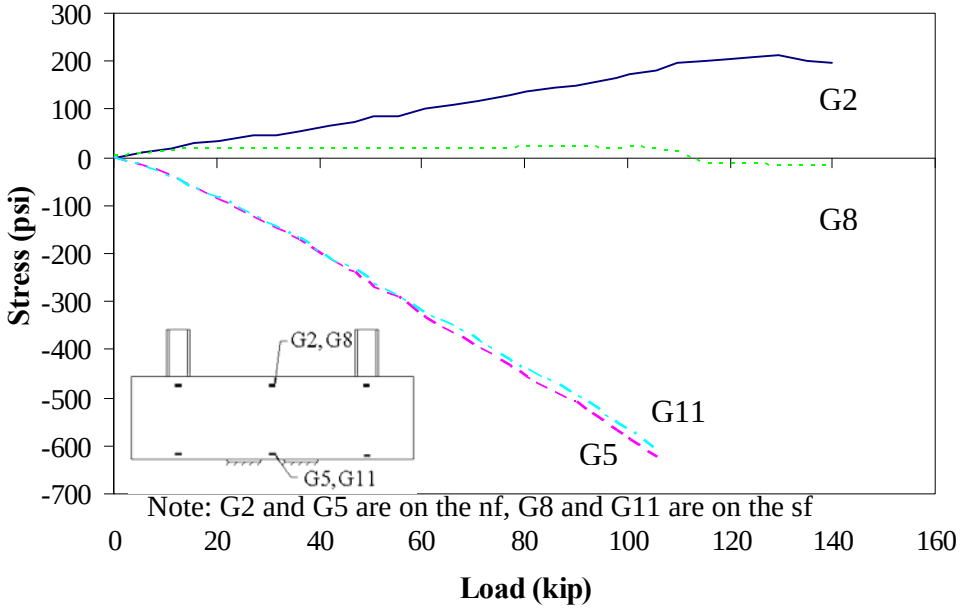

Figure 66. Concrete stresses at the center of ADC1

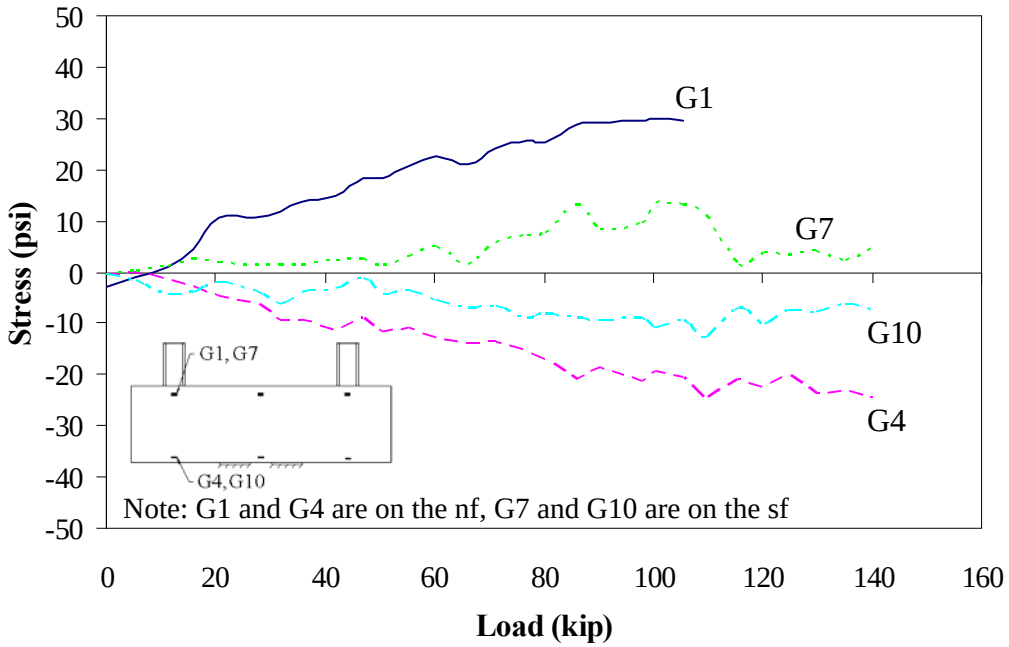

Figure 67. Concrete stresses at the east connection in ADC1

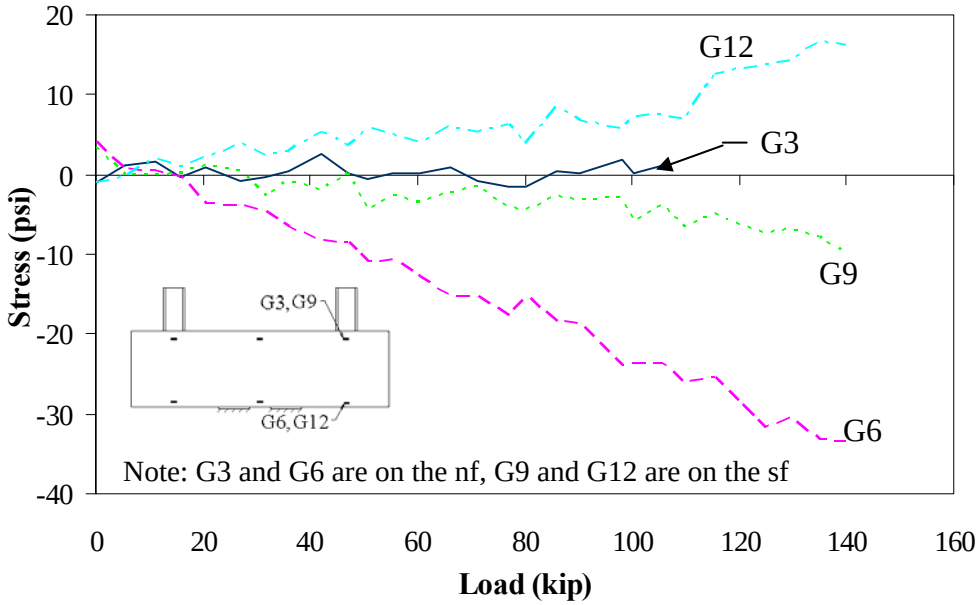

Figure 68. Concrete stresses at the west connection in ADC1

Unlike the single pile abutments, the concrete stress behavior did not show a clear indication when the cracking moment was reached. The cracking moment for the specimens was determined using the loads that were applied and when the first cracks in the specimen were noticed during testing. For both of the double pile tests, this was when each pile was loaded to approximately 70 kip, producing a moment of 290 kip-feet.

Deflection transducers were placed near each pile to measure differential movement between the precast concrete and the concrete in the CMP (see Figure 62). Differential movements for the east and west piles are shown in Figure 69 and Figure 70, respectively. The largest movements were measured from LVDT 3 and LVDT 5, the two gages located closest to the supports. Most likely, these two gages were measuring the flexural bending of the specimen along with differential movement. Even if these transducers were measuring differential movement, the maximum deflection measured was approximately 0.001 inches. The other six gages measured less than 0.005 inches, which is the tolerance of the LVDTs and therefore most likely picking up noise.

Total deflections of the specimen were also measured and are presented in Figure 71. Total deflection measurements are as expected: at the center of the specimen the specimen deflected upward (positive deflections) and the ends of the specimen deflected downward (negative deflections). In comparison with the total deflections, the magnitudes of the differential movements are very small, less than the LVDT precision in six of the transducers. As the figures have shown, the total deflection is two-hundred times greater than the differential movement.

Each pile in the double pile abutment specimens were loaded to at least 140 kip. Specimens were loaded to approximately 1.75 times the required design load of 80 kip for each pile, under more severe support conditions than the abutment would be subjected to in the field. The maximum applied load, the load producing the cracking moment, and the cracking moment determined through testing are presented in Table 16.

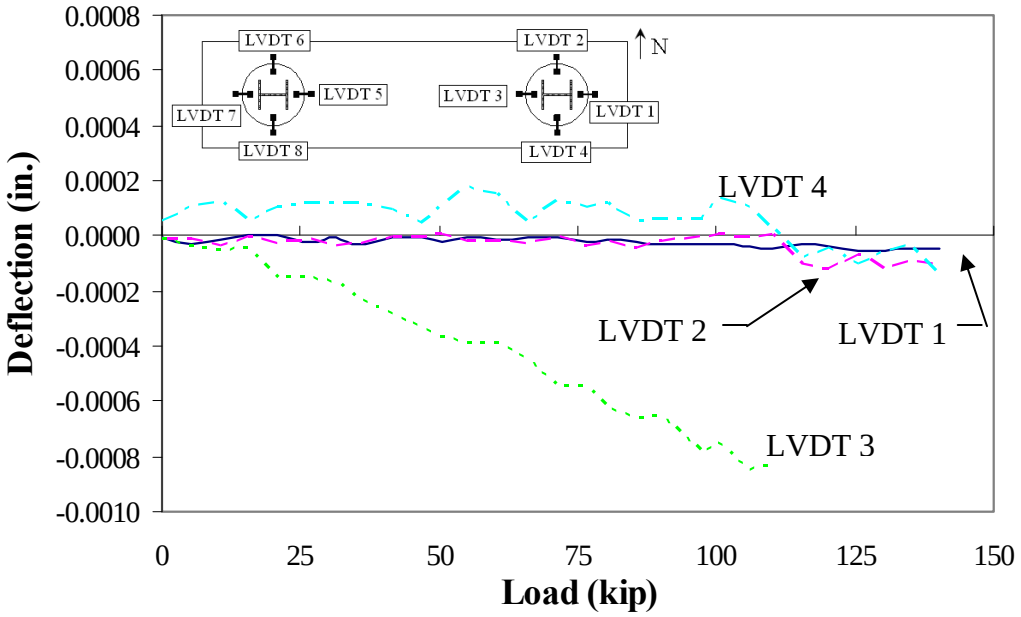

Figure 69. East pile differential deflections for ADC1

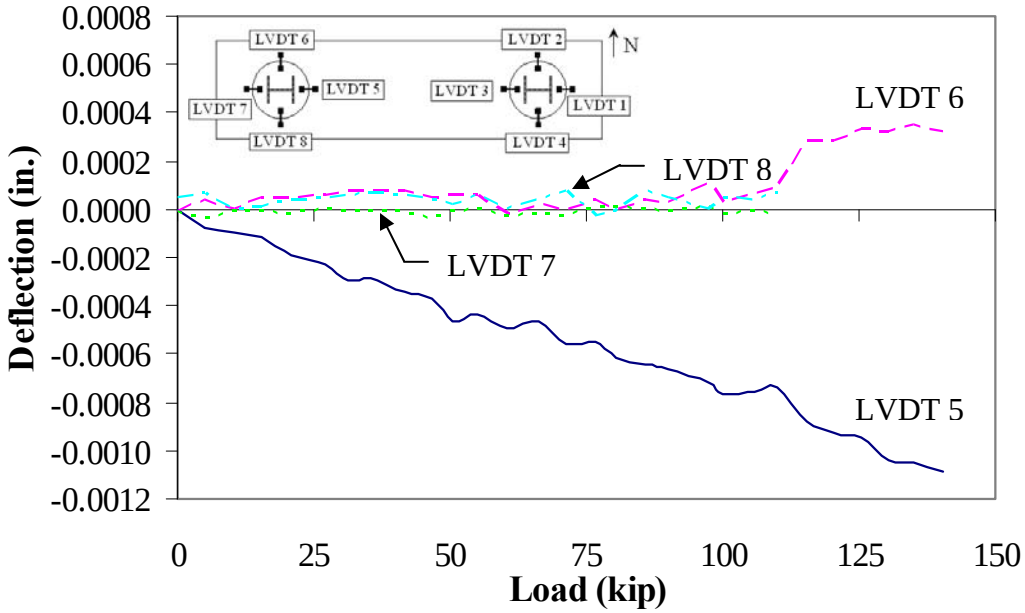

Figure 70. West pile differential deflections for ADC1

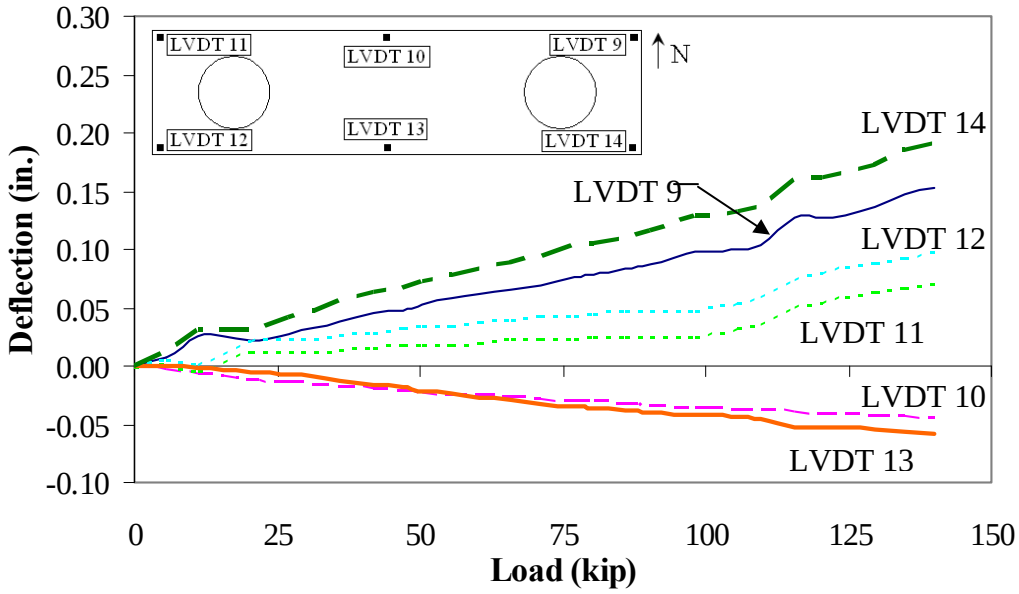

Figure 71. Total deflection of ADC1

Table 16. Double pile abutment tests results

Specimen	Maximum Applied Load (kip)	Applied Load at Cracking Moment (kip)	Cracking Moment (kip-feet)
ADC1	140	70	290
ADC2	150	70	290

In the double pile abutment tests, it was determined that the negative moment capacity for this loading was almost twice the design load of the abutment, under more severe conditions. The cracking moment was reached when each pile in the test was subjected to 70 kip. Note that the testing system and support conditions were not completely representative of the abutment field conditions. Also, for the double pile testing, the CMP in the specimens were only 70% full of concrete. Based on the beam spacing in the field, the abutment will never be subjected to this type of load and all of the CMPs are completely filled with concrete, so cracking under service loads should not occur.

4.3.2 Shear Test Results

After the negative moment tests were completed, no cracks were noticed near the H-piles, so each pile was tested individually. The support conditions were adjusted to provide minimal flexural bending and maximum shear in the piles and adjacent concrete. All four of the piles from the two double pile specimens were tested in this manner. In the shear tests, the same gage labeling and locations were used as were used in the single pile tests; the only difference being no bottom deflection transducers were used. Refer to Figure 44 and Figure 45 for instrumentation labels and locations.

Each pile was loaded to 400 kip - the maximum capacity of the hydraulic jack and load frame. Even at the maximum applied load, no differential movement was noticed and no cracks formed in the specimen. As previously noted, the CMP in these specimen were filled 70% with concrete, therefore, the connections in the field will have an even greater capacity since they are filled 100% with concrete. Because all the piles behaved in a similar manner, only the results from the shear Test 1 are presented and discussed in the following paragraphs; the complete results for Test 2 through Test 4 are presented in Appendix A.

Steel pile strains were first analyzed; strains for Test 1 are relatively linear as can be seen in Figure 72. There was a slight anomaly that occurred around 300 kip in two gages, which was likely due to unloading and reloading required since the load cell only had a capacity of 300 kip. Shortly after the load was reapplied, the strains stabilized and continued with the previous trend. There was a slight difference in the strains measured; the greatest difference was less than 150 μ-strains between gages G5 and G6. This was due to an eccentricity in the pile load, which has been previously discussed.

The strain gages on the concrete used in the double pile testing were reused for the shear testing. Strain data were converted into stresses using Hooke's law; ADC1 strength parameters and modulus of elasticity were used for shear Tests 1 and 2 and ADC2 strength parameters and modulus of elasticity were used for shear Tests 3 and 4. Concrete stresses occurring in shear Test 1 are shown in Figure 73.

Concrete located at the top of the specimen experienced low levels of compressive stresses - less than one-tenth of the compressive strength of the concrete. At the bottom of the specimen, the concrete was subjected to tensile stresses less than the tensile strength of the concrete (650 psi), thus the concrete did not crack. This is consistent with the fact no cracks were observed during

the shear test in any of the connections. Even though no visible sign of differential movement were noticed during testing, the differential movements measured by the top deflection transducers, presented in Figure 74, were analyzed.

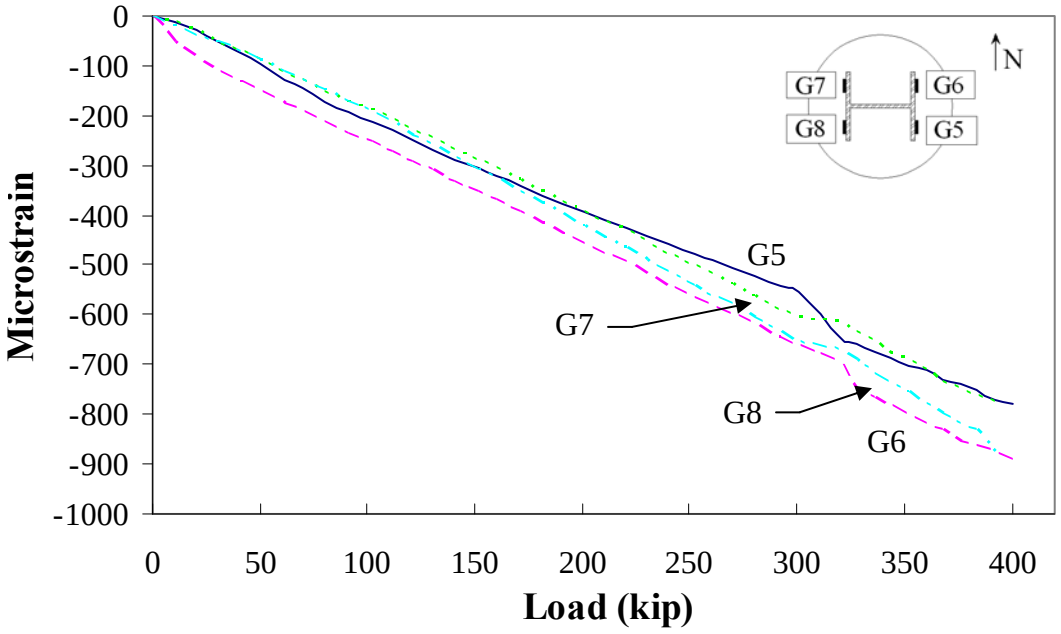

Figure 72. H-pile steel strains for Test 1, specimen ADC1

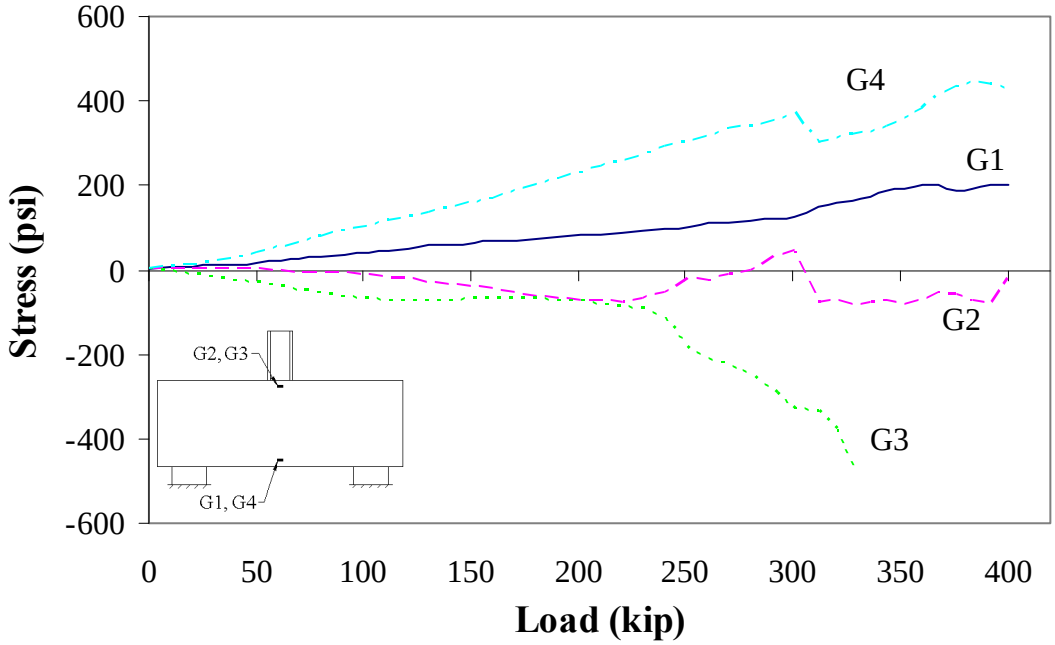

Figure 73. Concrete stresses for Test 1, specimen ADC1

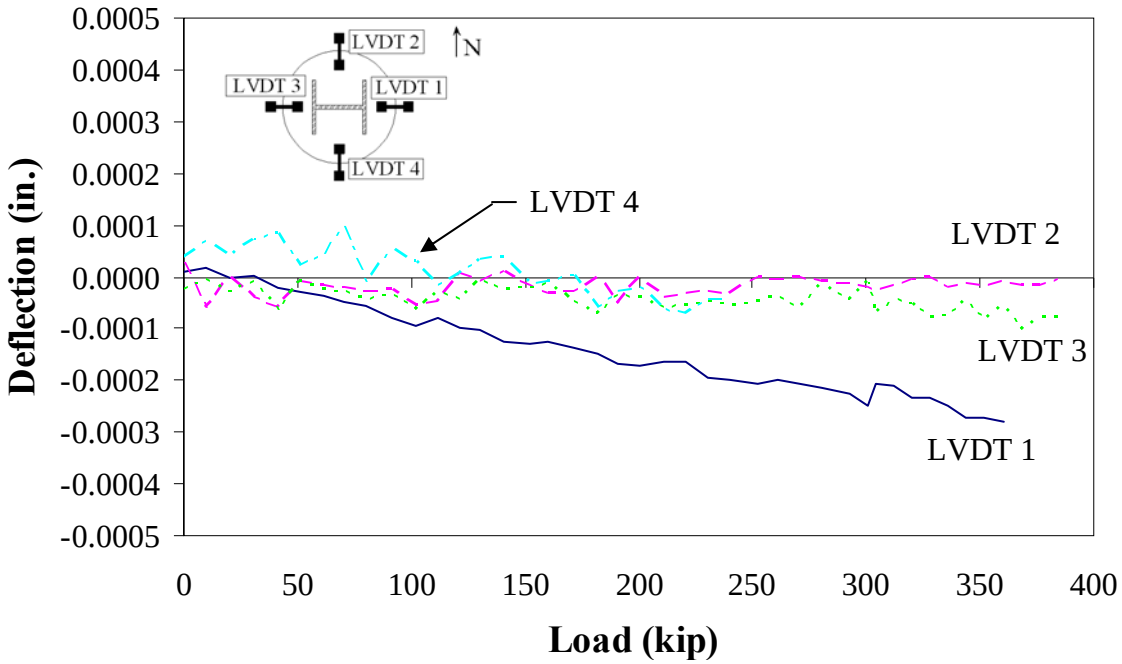

Figure 74. Top deflection for Shear Test 1, specimen ADC1

Differential deflections measured during Test 1 were less than 0.0003 inches for all transducers, which were less than the precision of the LVDT (0.0005 inches). Since the differential deflections measured were less than the transducer precision, the measurements were likely noise. Based on the low concrete stresses, the absence of cracks in the specimen, and the insignificant amount of differential movement, the shear capacity of the pile connection (filled only 70% with concrete) can safely be assumed greater than the maximum load of 400 kip. Under loads in the field, shear failure between the pile and the concrete, or shear failure between the precast concrete and the concrete in the CMP should not occur.

4.4 Abutment and Pier Cap Section Behavior Analysis

Substructure testing was successful in determining that shear failures would not be an issue for the actual abutments or pier caps. The piles in the abutments were designed to support a load of 80 kip each and the piles in the pier caps were designed to support a load of 72 kip each. All of the test specimen were load to at least 4.5 times the unfactored design load. The maximum load applied in the single pile tests are presented in Table 17.

While the pier cap specimen and the abutment specimens were loaded to approximately the same load, the stresses in the concrete and the crack patterns in the tested specimens indicate different behaviors. The crack pattern for ASC3 is shown in Figure 75 while the crack pattern for the PSC1 is presented in Figure 76. Note the cracks were scaled off the actual specimens using a three inch by three inch grid; thus the crack patterns shown are to scale.

Table 17. Maximum load for single pile tests

Specimen	Maximum Load (kip)
ASC1	360
ASC2	396
ASC3	384
ASO1	384
ASO2	384
PSC1	384

When comparing the two crack patterns, one sees two main differences in the way each specimen cracked under load. Cracks in the abutment (shown in Figure 75) started as flexural cracks, but as the cracks progresses to the top twelve inches of the concrete, the cracks changes direction. Instead of pure flexural cracks, the cracks become almost horizontal, and appear to follow the same slope as the CMP cast in the concrete. The angle of incline of the CMP was measured to be approximately twenty-five degrees; the abutment crack pattern is compared to the angle of incline of the CMP in Figure 77.

The presence of the angled cracks indicates that the specimen was reacting to more than pure flexural bending. Strains measured in all of the abutment specimens reinforce this observation. After the cracking moment was reached, the external concrete at the top of the specimen was subject to tensile stresses, as shown in Figure 47. Based on the crack patterns and the stress data from all of the abutments, the presence of the CMP caused localized tensile stresses in the concrete at the top of the specimen.

In the pier cap, there are no cracks that followed this angled behavior. The pier cap crack pattern reflects flexural bending, which agrees with the stresses measured in the concrete. As shown in Figure 57, the concrete at the top of the specimen was subjected to compressive stresses while the concrete at the bottom of the specimen was subjected to compressive stresses, which correlate with flexural bending.

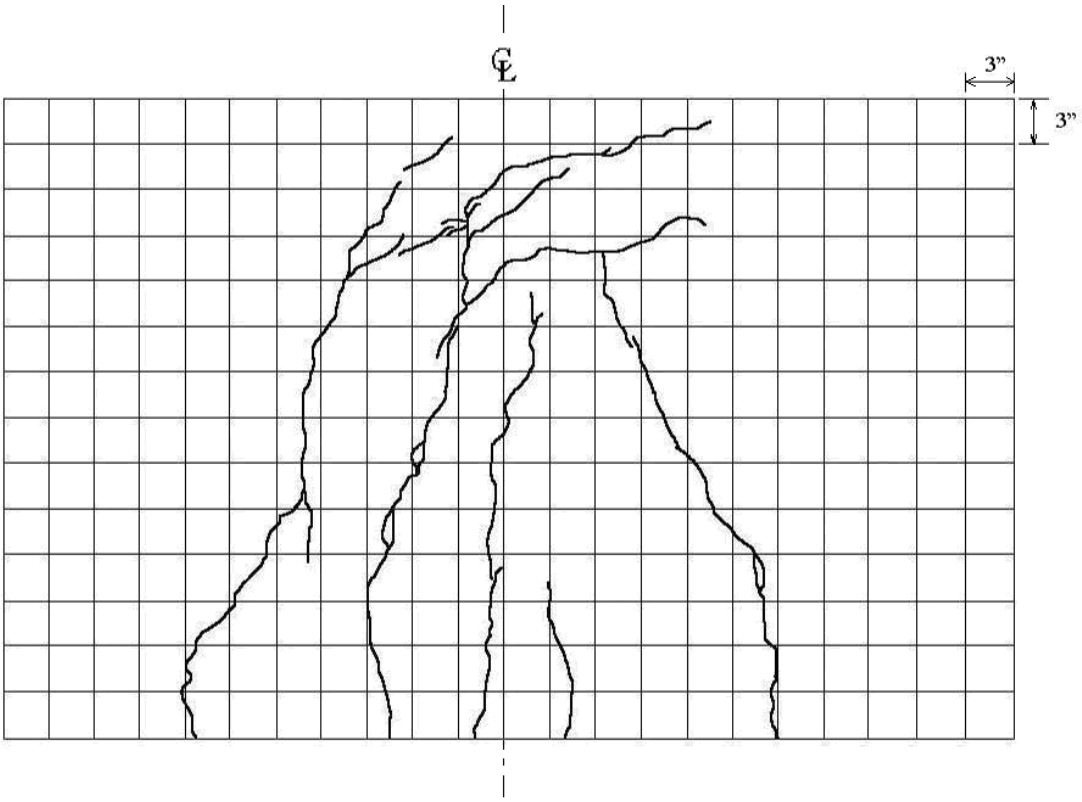

Figure 75. ASC3 crack pattern, north face

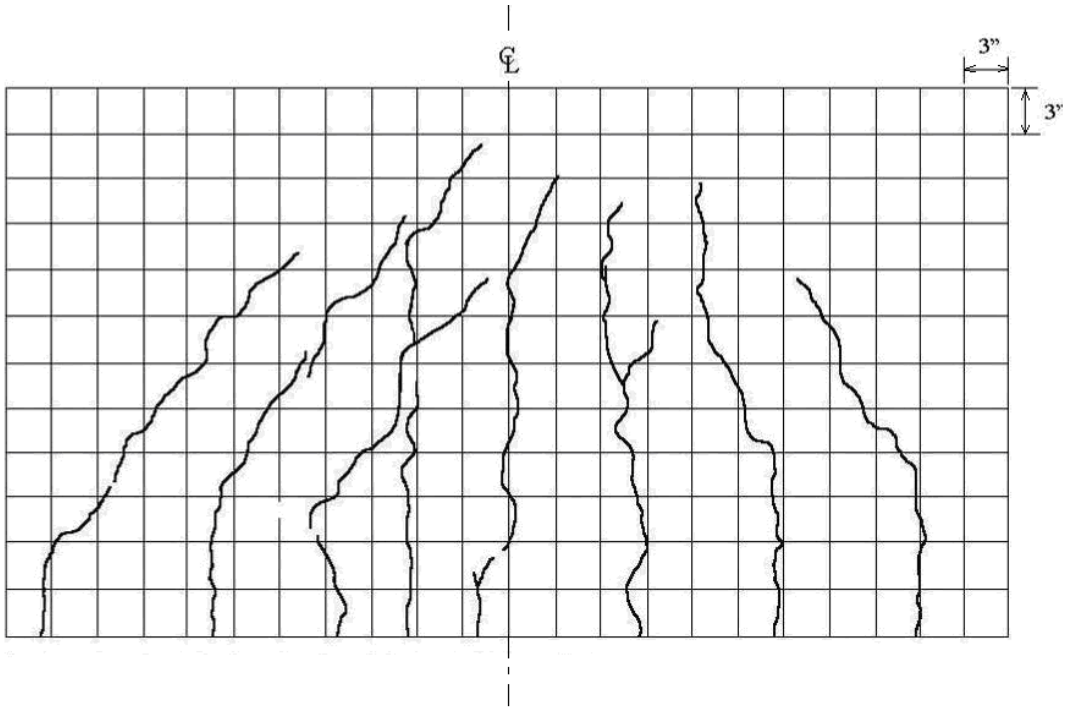

Figure 76. PSC1 crack pattern, north face

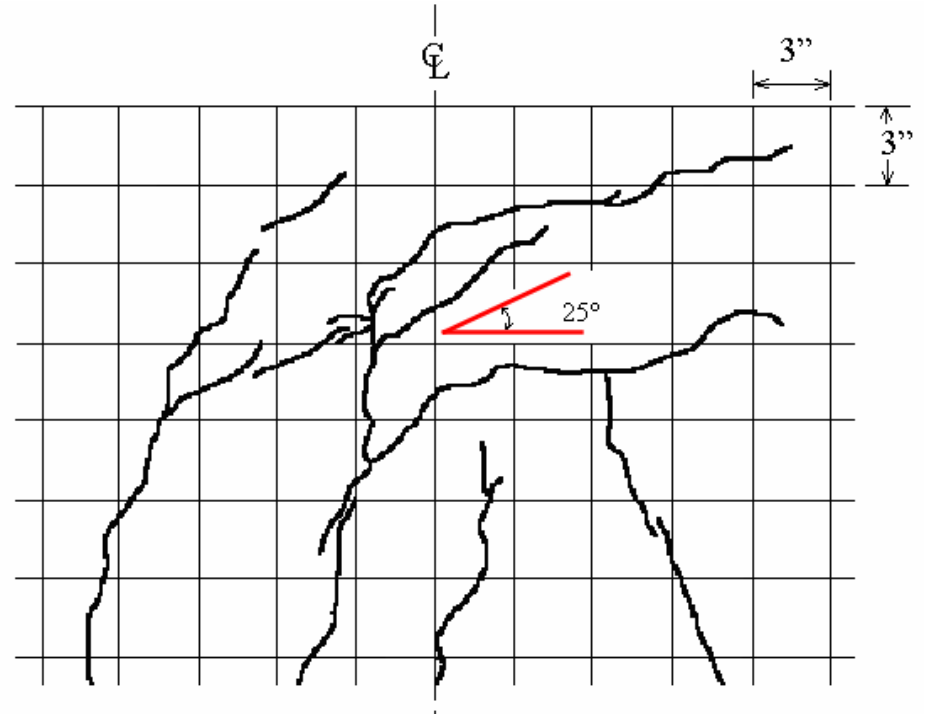

Figure 77. Abutment crack pattern compared with the CMP angle of incline.

The abutment specimens and pier caps were close in size and were loaded to approximately the same maximum load. To determine the reason for the differences in the behaviors of the abutment and pier cap, the reinforcement used in each specimen (shown in Figure 78) was compared.

As shown in Figure 78, the pier cap has a slightly smaller gross area of concrete (1,368 in^2 versus 1,512 in^2) than the abutment, but it has six additional No. 8 longitudinal bars. Spacing for the transverse reinforcement in the pier cap was almost half that in the abutment transverse reinforcement. To better compare the reinforcement in each section, the ratio of the area of longitudinal tensile reinforcing steel to the area of concrete, effective depth times the width (ρ), and the ratio of transverse steel to the area of concrete (ρ_t) were calculated using the definitions in the ACI Building Code (2005). The gross moment of inertia for each section was calculated, using a transformed section to account for the presence of the steel. All of these properties are presented in Table 18.

Based on percentages, the pier cap has almost twice the amount of longitudinal reinforcement as the abutment and 2.5 times the transverse reinforcement. The gross moment of inertia for the pier cap is lower than the abutment, but the contribution from the reinforcing steel is higher. As the concrete cracks, the specimen's moment of inertia decreases due to the cracking of the concrete, but the contribution from the reinforcement remains constant.

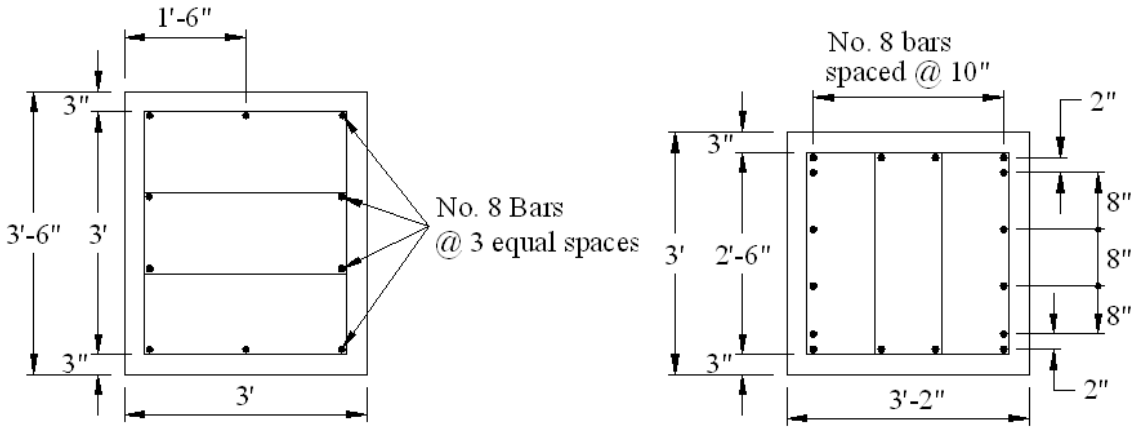

a) Abutment reinforcement **b) Pier cap reinforcement**

Figure 78. Comparison of the reinforcement used in the abutments and the pier caps

Table 18. Abutment and pier cap reinforcement ratios and moment of inertias

Section	□	□t	Igross (in4)
Abutment	0.0016	0.002	234,140
Pier Cap	0.0036	0.005	161,979

In the abutment testing, the CMP affected the behavior of the specimen as shown by the stresses measured and the crack patterns recorded. The reason the pier cap was not affected in the same manner is due to the larger area of longitudinal and transverse steel and a smaller cross-section, compared to the abutment. This also explains why the total deflection measured in the pier cap specimen was less than the total deflections measured in the abutment specimens. The behavior of the abutment was affected by the CMP connection, but in comparison to the pier caps, the combination of flexural and shear capacity of the specimen was not reduced.

4.5 Laboratory Testing Summary

4.5.1 Abutment Testing Summary

The single and double pile abutment tests have shown that there is no concern for a shear failure between the H-pile and the concrete, or between the precast concrete and the concrete in the CMP. For the single pile tests, the piles were loaded to at least 4.5 times the unfactored design load. For the double pile tests, which produced a more severe loading condition than actual field conditions, the specimens were loaded to approximately twice the unfactored design load. Shear failure was not detected in any of the tests; shear testing has shown the shear capacity of the pile and CMP connection to be greater than 400 kip.

Abutment testing has shown that even though the strength of the abutments was not compromised, the pile connection in the CMP did affect the stress behavior of the section. The presence of the CMP caused localized tensile stresses on the side of the abutment. The

experimental cracking moment determined by the single pile tests was in agreement with the experimental cracking moment determined by the double pile tests. Since the cross-section is symmetrical, the cracking moment for positive bending and negative bending were approximately the same. Experimental cracking moments for each of the abutment tests are presented in Table 19.

The cracking moment in a concrete section is dependent on the concrete strength at the time of testing. Based on an average concrete strength of 5450 psi, the average cracking moment in the abutment specimens was 295 kip-feet (an average single pile load of 142 kip with a clear distance of eight feet, four inches), which is much greater than the expected loads for the actual bridge abutments. The possibility of the abutments experiencing loads of this magnitude in the field is very small.

Table 19. Cracking moments for abutment specimens

Specimen	Cracking Moment (kip-feet)
ASC1	250
ASC2	260
ASO1	330
ASC3	330
ASO2	315
ADC1	290
ASC2	290

4.5.2 Pier Cap Testing Summary

Results from the pier cap tests have shown that the pier cap has approximately the same capacity as the abutment, even though the piles in the abutment are designed for an unfactored service load of 80 kip each and the piles in the pier cap are designed for an unfactored service load of 72 kip each. The pier cap specimen was subjected to a maximum load of 384 kip, more than five times the design load. During testing, no significant differential movement was detected between the precast concrete and the concrete in the CMP. The cracking moment was determined to be 312 kip-feet for the pier cap tested. Based on the tests performed, shear failure between the precast concrete and the concrete in the CMP is not a concern.

5. POST-TENSIONING TESTING AND VERIFICATION

5.1 Post-Tensioning Field Testing

The Boone County replacement bridge was the first post-tensioned bridge deck in the state of Iowa. One of the tasks in the proposed research included monitoring the post-tensioning process and verifying the forces in the strands reported by the contractor. Instrumentation was embedded in four deck panels and attached to four post-tensioning strands to monitor and verify the post-tensioning process, and to allow long-term monitoring of the deck. The instrumentation will also be used in the field service test associated with the project (not included in this report). This chapter presents the instrumentation layout, the post-tensioning monitoring process and the results obtained from the instrumentation.

Post-tensioning took place after all the interior and exterior deck panels were installed, leveled, and the transverse joints between panels were cast and had reached strength. The bridge was post-tensioned using a hydraulic, mono-strand jack system. Friction losses in the strands were essentially non-existent due to the strand layout and an average strand length of 144 feet and 9 inches. This allowed the entire post-tensioning operation to be performed from the west end of the bridge. Greg Gear P.E., a technical expert from Des Moines, was hired by the prime contractor to supervise the post-tensioning operation. Mr. Gear certified the jack calibrations prior to post-tensioning, and certified that the final forces in the strands met the limits set by the Iowa DOT after post-tensioning was complete; the certification from Mr. Gear is included in Appendix B.

The strand used was 0.6 inch diameter, 270 ksi post-tensioning strand with an area of 0.217 square inches. The bridge plans required each strand be tensioned to 41 kip; since there were 12 strands in each of the post-tensioning channels, this resulted in 984 kips of post-tensioning in each half of the bridge deck. The purpose of the post-tensioning testing was to verify the force in the strands as reported by the contractor, to measure losses between initial stressing and after the strands had been stressed, and to determine how the force in the strands was distributed through the deck panels.

Before the deck panels were cast, a total of twelve vibrating wire gages (VWG) were embedded in four of the deck panels so that strains in each of the panels could be measured during the post-tensioning operation. The strain data were then converted to deck panel stresses using Hooke's law. Location of the instrumented panels (Panels A, B, C, and D) and the number of gages in each panel are shown in Figure 79.

The instrumentation was concentrated around the southern-most post-tensioning channel. Gage identification and location is presented in Figure 80; the number of gages in each deck panel varied with the location of the panel. To simplify the comparison of the deck results, the numbering system for the deck panel gages was kept consistent between the panels. For example, gages A1, B1, C1and D1 were all located at Position 1. Number and location of the gages embedded in each of the four panels are presented in Table 20; the gage number corresponds to the positions shown in Figure 80.

The lead wires for the gages were threaded through the panel formwork and secured in the post-tensioning channel during casting and transportation of the panels. This allowed access to the wires from the deck for testing. Two of the VWGs attached to the panel reinforcement are shown in Figure 81 before the panel was cast. The gage lead wires can also be seen threaded through the formwork and secured in a channel in this figure as well.

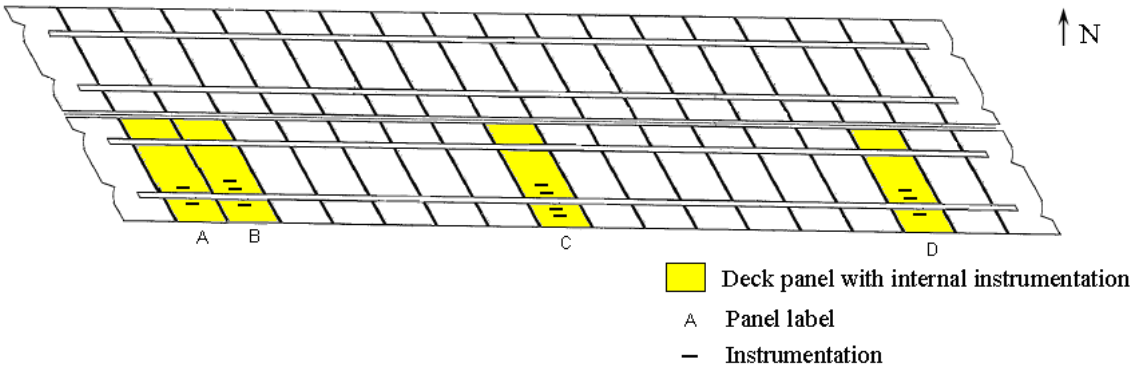

Figure 79. Location of instrumented panels

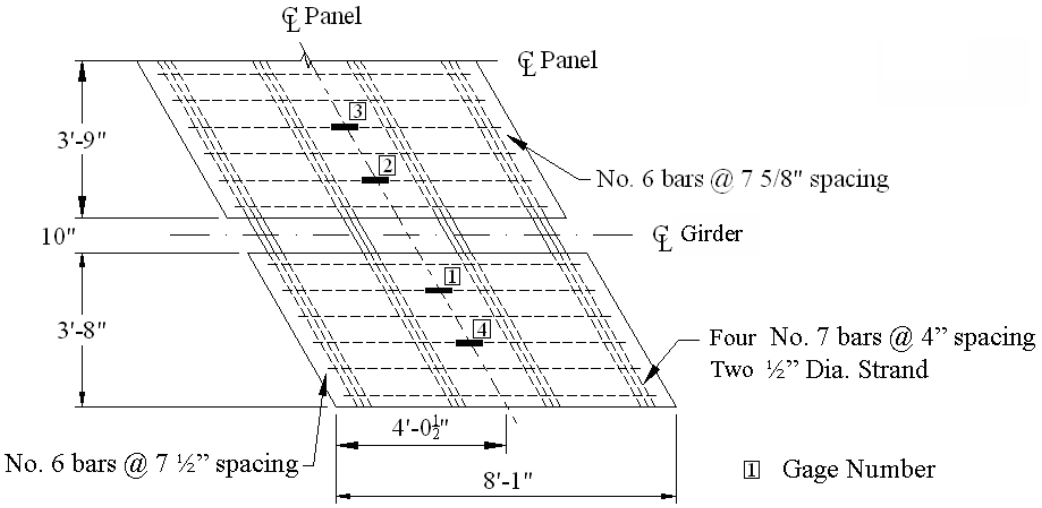

Figure 80. Deck panel internal instrumentation

Table 20. Number of gages and locations in each deck panel

Deck Panel	Number of Gages	Gage Location
A	2	A1, A2
B	3	B1, B2, B3
C	4	C1, C2, C3, C4
D	3	D1, D2, D3

Figure 81. Deck panel vibrating wire gages

As shown in Figure 82, seven VWGs were used on the post-tensioning strand. Gages (No. 3, 5, 6, and 7) were placed on the top center strand in each of the post-tensioning channels at the center of the bridge, approximately three and one half inches below the surface of the deck panel. Three additional gages (No. 1, 2, and 4) were placed along the strand previously instrumented in Channel 1. A VWG was placed one foot from the exterior edge of the first interior panel at both ends of the bridge. Another VWG was placed directly over the west pier, closest to the 'live' end of the jacking operation.

As previously noted, the gages were placed on the top interior strand in the channels; this was done to allow sufficient room for protection of the four gages to be embedded in the channels after post-tensioning and to allow for easy access for installation and removal of the gages. The strands instrumented were the first strand in each channel to be post-tensioned, according to the stressing sequence submitted by the contractor; the post-tensioning sequence for the south half of the bridge deck is presented in Figure 83. Instrumenting the initial strand stressed provides post-tensioning loss data throughout the entire stressing sequence.

The south half of the bridge (Channel 1 and Channel 2), which contained the majority of the panel and strand instrumentation, was stressed first. Since a single jack was used for all of the stressing, the contractor had to alternate between channels while post-tensioning (i.e. T1 and T2 in Channel 1, T3 through T6 in Channel 2, etc.). One of the VWGs attached to the post-tensioning strand is shown in Figure 84.

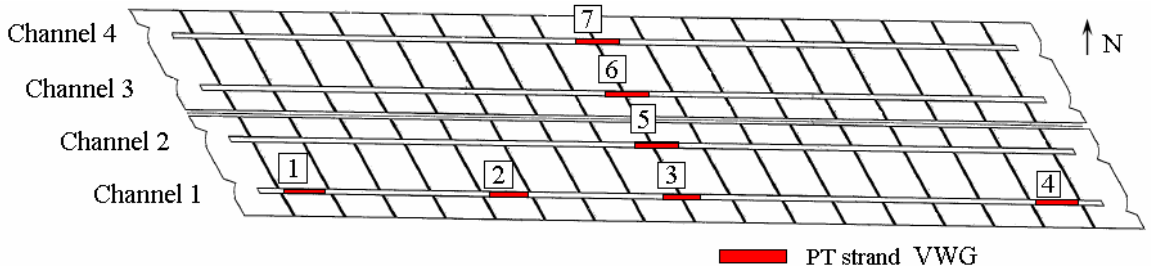

Figure 82. Post-tensioning VBG locations

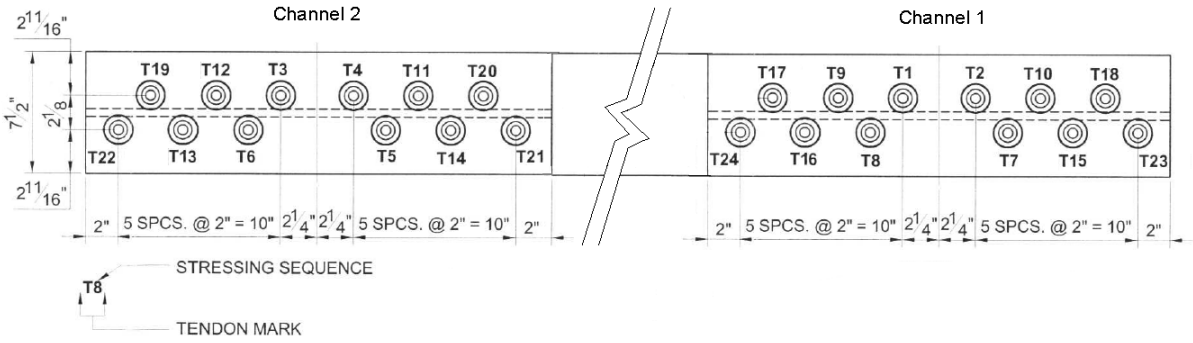

Figure 83. Post-tensioning stressing sequence (looking east)

Figure 84. PT strand vibrating wire gage

The entire post-tensioning process took approximately four hours. The mono-strand jack used for post-tensioning can be seen in Figure 85. The two halves of the bridge, which were post-tensioned separately, acted independently since the longitudinal joint connecting the two halves was not cast until the post-tensioning was completed. The initial gage readings for the deck and tendon gages were recorded before the post-tensioning operation started.

The stressing sequence was not followed exactly on the south half of the bridge due to an obstruction in one of the channels. After sixteen of the twenty-four strands were stressed, it was noticed that the concrete at one of the transverse joints (see Figure 86) was projecting into the post-tensioning channel and was creating a friction point for two strands. The stressing sequence on that half of the bridge was stopped and the obstruction was removed without disturbing the strands that had been previously stressed. While the excess concrete was being removed, the north half of the bridge deck, Channels 3 and 4, was stressed in its entirety, after which the remaining strands in the south half of the bridge were stressed without incident.

The VWGs used were not capable of providing continuous data readings and had to be read using a hand-held data collector. Data were recorded while the jacking hardware was moved from one channel to the next; stressing continued after the readings were taken. Since a data acquisition system was unavailable, all of the deck panel and strand gages were connected to two switch-and-balance units to make the data reading process faster. This allowed for sufficient data collection without slowing down the jacking operation.

On the day the bridge was post-tensioned, there was concern about inclement weather, thus in order to complete the jacking operation before the weather conditions worsened, data readings were only taken eight times. Table 21 presents the eight stages of post-tensioning after which readings were taken.

The first reading was taken after the first two strands in Channel 1 were stressed. Next, a second set of readings was taken after the six of the tendons in the south half of the bridge were stressed; two strands in the first channel and four strands in Channel 2. A third set of readings were taken after fourteen of the strands in the south half of the bridge had been stressed. Two additional strands were stressed in Channel 1 before the previously described obstruction in the channel was noticed. As previously noted, post-tensioning was then moved to the north half of the bridge while the obstruction was removed.

a) Mono-strand jack and hydraulic pump

b) Mono-strand jack in use

Figure 85. Mono-strand jack used for post-tensioning

Figure 86. Concrete obstruction in Channel 1

While stressing the north half of the bridge, a construction error was noticed. The anchor plates shown in Figure 83 were inverted during fabrication at the precast plant in Channel 3 and Channel 4. Thus, instead of post-tensioning the top interior strands first, the bottom interior strands were initially stressed; the stressing sequence used for the north half of the bridge is shown in Figure 87.

The fourth set of readings were taken after the first two strands, which were not instrumented, in the north half of the bridge were stressed. Since the instrumented strands were not initially stressed, the VWGs in the north half of the bridge did not provide force data during this reading. However, since two non-instrumented strands were stressed, the effects of elastic shortening in the deck were noticeable in VWGs on the unstressed strands in the north half of the deck; these results are presented later in this chapter.

Table 21. Description of post-tensioning stages

Stage	South Half of Deck				North Half of Deck			
	Channel 1		Channel 2		Channel 3		Channel 4	
	Tendons Stressed	Force (kip)	Tendons Stressed	Force (kip)	Tendons Stressed	Force (kip)	Tendons Stressed	Force (kip)
1	2	82	0	0	0	0	0	0
2	2	82	4	164	0	0	0	0
3	6	246	8	328	0	0	0	0
4	8	328	8	328	2	82	0	0
5	8	328	8	328	2	82	4	164
6	8	328	8	328	6	246	4	164
7	8	328	8	328	12	492	12	492
8	12	492	12	492	12	492	12	492

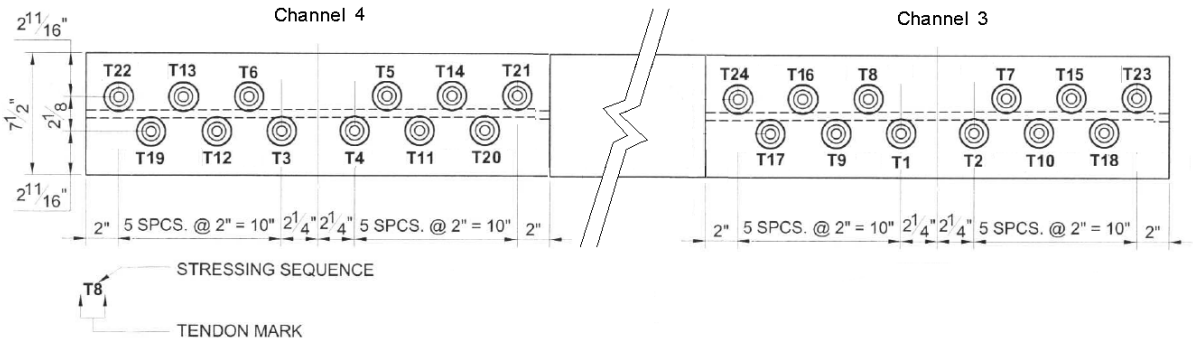

Figure 87. Post-tensioning sequence for the north half of the bridge (looking east)

Additional readings were taken after the first six tendons, and after fourteen tendons in the north half of the bridge were stressed. Last, two sets of readings were taken: after the north half of the bridge was stressed and after the south half of the bridge was stressed, respectively. After the post-tensioning operation was complete, final readings were taken from the embedded gages to use as initial values for long-term monitoring.

The four strand gages located along the centerline (No. 3, 5, 6, and 7) of the bridge were embedded in the post-tensioning channels when the longitudinal joints were cast and the other three gages were removed. Before the channels was grouted, each of the gages that were to be

embedded were protected with pre-cut PVC pipe, shown in Figure 88, that were sealed with a waterproof material and secured in place with two hose clamps.

The four embedded strand gages and the twelve internal deck panel gages will be used during the service load testing of the bridge and will make it possible for long-term monitoring of the deck system. All of the lead wires for the four gages were labeled, threaded through the formwork under the bridge deck and secured for future use.

Figure 88. Vibrating wire gage with PVC pipe cover

5.2 Post-Tensioning Test Results

5.2.1 Post-Tensioning Strand Results

The first task of the post-tensioning testing was to verify the force measured by the contractor in each of the post-tensioning strands. According to the plans, each strand was to be stressed to 41 kip, with a tolerance of ±5 percent (± 2.05kip). For the tendon gages all of the data was output in Digits, a unit used by the manufacturer, which can be converted into a change in length. The Digits reading is corrected for temperature effects and for the calibration of the individual gage. Data were converted from Digits to a corrected change in length using the following equation provided by the manufacturer, Geokon.

$$D_{corrected} = [(R_1 - R_0) \times C] + [(T_1 - T_0) \times K]$$

Where:

$D_{corrected}$ = the corrected change in length
R_1 = the current reading in Digits
R_0 = the initial reading in Digits
C = the calibration factor for each gage (provided by Geokon)
T_1 = the current temperature
T_0 = the initial temperature

K = the thermal coefficient for each gage

The thermal coefficient for each gage was determined based on the calibration factor and the current reading, using the following equation provided by the manufacturer:

$$K = [(R_1 \times 0.000295) + 1.724] \times C$$

All of the original test data, including the calibration factor for each gage, initial and subsequent gage readings (Digits), temperature readings, and thermal coefficient of each gage are presented in Appendix A. The final reading to be used for long-term monitoring, taken to get the correct temperature and final readings in Digits, is also presented in Appendix A.

The corrected change in length was calculated and then converted into strain based on a gage length of 7 ½ inches; strains were converted in stresses using an elastic modulus of 28,500 ksi, based on the PCI Design Handbook (2004) elastic modulus for 0.6-inch diameter strand with a yield stress of 270 ksi. Finally, the stress was converted into force using the area of the 0.6-inch diameter strand (0.217 in^2). The corrected change in length, strain, stress and force in each strand for each of the gages (Gage 1 – Gage 7) are presented in Table 22 through Table 29. Recall the location of the strand gages were identified in Figure 82.

There were difficulties in obtaining readings from Gage 4, as can be seen in Table 26, which were most likely the result of the rainy weather the day of the post-tensioning; this was the only strand gage that did not work properly during the post-tensioning operation. The percent of force lost during the post-tensioning operation was determined by using the force measured after each strand was initially stressed and comparing it to the force measured after post-tensioning was complete. The initial force, final force, force lost and percent of force lost are presented in Table 29.

According to the bridge plans, each strand was to be stressed to 41 kip, however, tolerances specified that strand force should be between 38.95 kip and 43.05 kip. The initial and final forces in all the strands monitored are well within the limits previously noted, as can be seen in Figure 89. The force in the strands initially stressed was expected to decrease as the final strands were post-tensioned. As may be seen in Figure 89, the tendons lost an average force of 0.80 kip or less than 0.02 percent of the initial force. Figure 89 compares the force loss between the tendons, from when each tendon was initially stressed until after all of the tendons were stressed.

Table 22. Post-tensioning results for Gage 1

Stage	Dcorrected (in.)	Strain (□)	Stress (ksi)	Force (kip)
1	0.000503	0.00675	192.2	41.7
2	0.050269	0.00674	192.0	41.7
3	0.050023	0.00667	190.1	41.3
4	0.049979	0.00666	189.7	41.2
5	0.049827	0.00665	189.6	41.1
6	0.049820	0.00665	189.6	41.1
7	0.049820	0.00665	189.5	41.1
8	0.049505	0.00661	188.3	40.9

Table 23. Post-tensioning results for Gage 2

Stage	Dcorrected (in.)	Strain (□)	Stress (ksi)	Force (kip)
1	0.050110	0.00668	190.4	41.3
2	0.049931	0.00666	189.7	41.2
3	0.049407	0.00659	187.7	40.7
4	0.049267	0.00657	187.2	40.6
5	0.049251	0.00657	187.2	40.6
6	0.049251	0.00657	187.2	40.6
7	0.049207	0.00656	187.0	40.6
8	0.048877	0.00652	185.7	40.3

Table 24. Post-tensioning results for Gage 3

Stage	Dcorrected (in.)	Strain (□)	Stress (ksi)	Force (kip)
1	0.050535	0.00674	192.0	41.7
2	0.050340	0.00671	191.3	41.5
3	0.049380	0.00658	187.6	40.7
4	0.049194	0.00656	186.9	40.6
5	0.049177	0.00656	186.9	40.6
6	0.049177	0.00656	186.9	40.6
7	0.049118	0.00655	186.6	40.5
8	0.048544	0.00647	184.5	40.0

Table 25. Post-tensioning results for Gage 4

Stage	Dcorrected (in.)	Strain (□)	Stress (ksi)	Force (kip)
1	0.050208	0.00669	190.8	41.4
2	NR*	-	-	-
3	0.049564	0.00661	188.3	40.9
4	NR	-	-	-
5	NR	-	-	-
6	0.049278	0.00657	187.3	40.6
7	0.049242	0.00657	187.1	40.6
8	NR	-	-	-

* NR = data collector could not get a reading

Table 26. Post-tensioning results for Gage 5

Stage	Dcorrected (in.)	Strain (□)	Stress (ksi)	Force (kip)
1	0.000503	0.00007	1.9	0.4
2	0.050269	0.00670	191.0	41.5
3	0.050023	0.00667	190.1	41.2
4	0.049979	0.00666	189.9	41.2
5	0.049827	0.00664	189.3	41.1
6	0.049820	0.00664	189.3	41.1
7	0.049820	0.00664	189.3	41.1
8	0.049505	0.00660	188.1	40.8

Table 27. Post-tensioning results for Gage 6

Stage	Dcorrected (in.)	Strain (□)	Stress (ksi)	Force (kip)
1	0.000629	0.00008	2.4	0.5
2	0.001250	0.00017	4.8	1.0
3	0.001288	0.00017	4.9	1.1
4	-0.000745**	-0.00010	-2.8	-0.6
5	-0.000651**	-0.00009	-2.5	-0.5
6	0.050243	0.00670	190.9	41.4
7	0.050214	0.00670	190.8	41.4
8	0.050170	0.00669	190.6	41.4

** indicates compressive values were measured due to post-tensioning in adjacent channel.

Table 28. Post-tensioning results for Gage 7

Stage	Dcorrected (in.)	Strain (□)	Stress (ksi)	Force (kip)
1	0.001373	0.00018	5.2	1.1
2	0.001402	0.00019	5.3	1.2
3	0.001500	0.00020	5.7	1.2
4	0.001183	0.00016	4.5	1.0
5	0.050358	0.00671	191.4	41.5
6	0.050220	0.00670	190.8	41.4
7	0.049901	0.00665	189.6	41.1
8	0.049616	0.00662	188.5	40.9

Table 29. Post-tensioning force and percent loss for each strand

VWG	Initial Force (kip)	Final Force (kip)	Force Lost (kip)	Percent Loss (%)
1	41.7	40.9	0.9	0.02
2	41.3	40.3	1.0	0.02
3	41.7	40.0	1.6	0.04
4	41.4	40.6	0.8	0.02
5	41.5	40.8	0.6	0.02
6	41.4	41.4	0.1	0.00
7	41.5	40.9	0.6	0.01

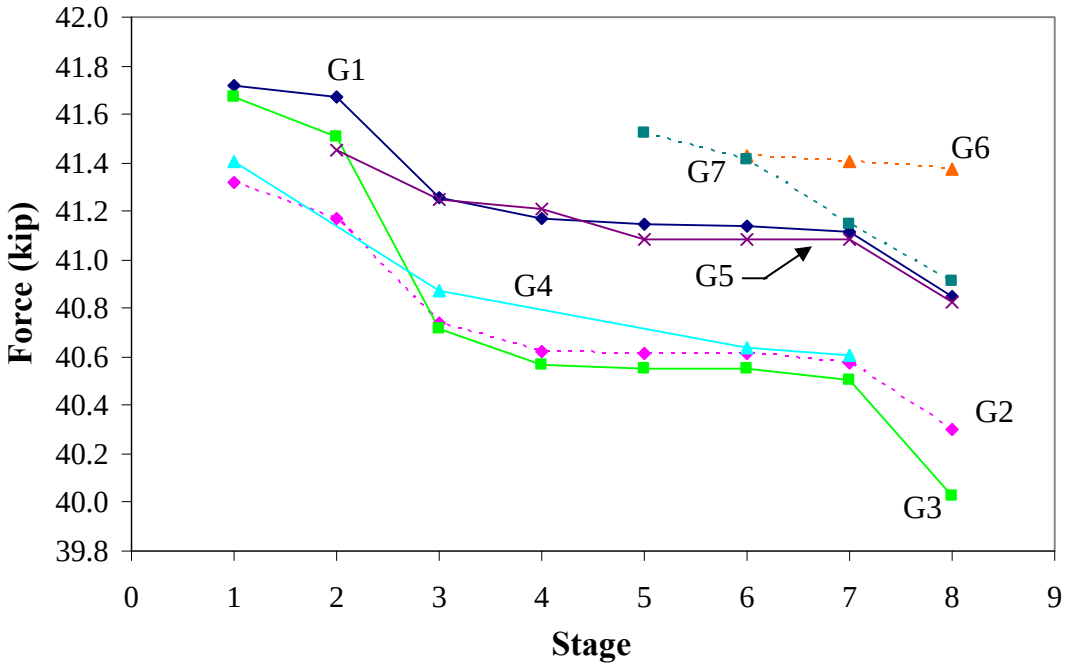

Figure 89. Force loss during the post-tensioning operation

For Gages 1 through 5, located in the south half of the bridge, noticeable losses occurred during the first three stages. Minimal losses occurred for stages four through seven which were when the north half of the bridge was post-tensioned. Since the two halves of the bridge were not connected, as previously discussed, Gages 1 through 5 were not expected to have any significant elastic shortening losses during these stages. Additional losses occurred after the south half of the bridge was completely post-tensioned.

Due to the construction error mentioned earlier, neither of the strands to which Gages 6 and 7 were attached were stressed during the fourth stage (while two other strands in the north half of the bridge were stressed) which provided an opportunity to examine the effects of elastic shortening in the tendons. Before the jacking operation was moved to the north half of the bridge, the readings from both Gage 6 and 7 indicated slight tensile force in each strand. After the first two strands in the north half of the bridge were stressed, the reading from Gages 6 and 7 showed a reduction in stress (strain); Gage 6 even showed negative tensile stress, as can be seen in Figure, which is a direct result of elastic shortening. Difference in stress reduction due to elastic shortening between Gages 6 and 7 could be due to friction points along each strand, which would cause the strands to behave differently.

Forces measured using the VWGs were compared to those provided by the contractor, who reported that every strand was stressed to 41 kip. After the post-tensioning was complete, the contractor verified the force in two of the strands by jacking from the 'dead' end of the strands. The force the contractor reported was the force in the strand outside the anchorage zone, which is higher than the force in the interior portion of the strand due to anchorage zone seating and some friction losses. According to the contractor, a force of 41 kip outside the anchorage zone corresponded to a force of 39.4 kip in the interior portion of the strand due to anchorage zone losses calculated by Dywidag, the supplier of the hydraulic jack and anchorage hardware. The contractor reported every strand was stressed to a force of 41 kip; worksheets with the gage values, final force in each strand, and elongation for each strand are presented in Appendix B.

Gage 1, as previously noted, was located one foot inside the first interior deck panel and thus the force measured by this gage should correspond to the 39.4 kip calculated by the contractor. As can be seen in Figure 90, the final force measured by Gage 1 was 40.1 kip, 0.7 kip greater than the force calculated by the contractor, however, well within tolerance. Forces measured along the strand in Channel 1 are presented in Figure 89. As shown in the figure, there is a slight difference in the force measured along the length of the strand. The greatest force occurred adjacent to the post-tensioning operation; loss of force along the tendon was most likely due to friction between the strands or friction between the strand and the leveling devices.

There are two reasons why the force calculated by the contractor does not correspond exactly to the force measured using the VWGs. The first reason is the accuracy of the pressure gage on the hydraulic jack (see Figure 90) the contractor was using. With this gage, getting a precise reading within 100 psi (which corresponds to a force of approximately 0.77 kip) would be difficult. Another reason for the difference is the complexity of calculating the anchor zone and friction losses. Post-tensioning losses are affected by several different factors including initial stress level, type of steel, curvature, and exposure conditions. Several different types of losses can

occur and it is common to determine losses as a lump sum value (ACI 318-05, 2005). Since it is difficult to separate losses due to elastic shortening, relaxation, seating, and friction immediately after stressing, it is very possible that the contractor's calculated losses for the anchor zone seating and friction have minor errors. It should be noted the difference between the force calculated by the contractor and the force measure by the VWGs is 1.7 percent and while the values don't correspond exactly, the difference is small enough to confirm the forces reported by the contractor.

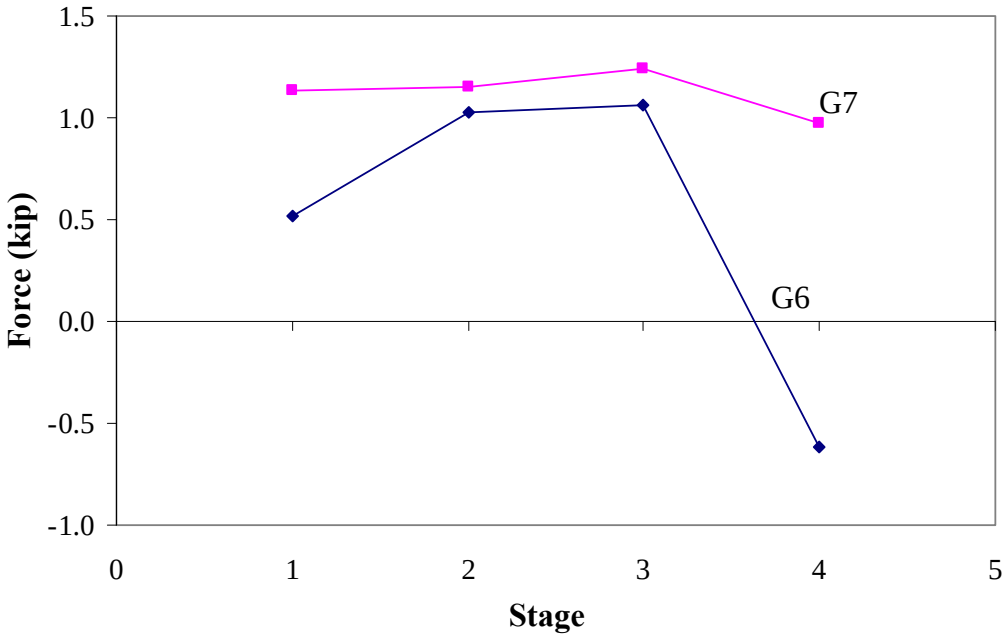

Figure 90. Elastic shortening losses in Gage 6 and Gage 7

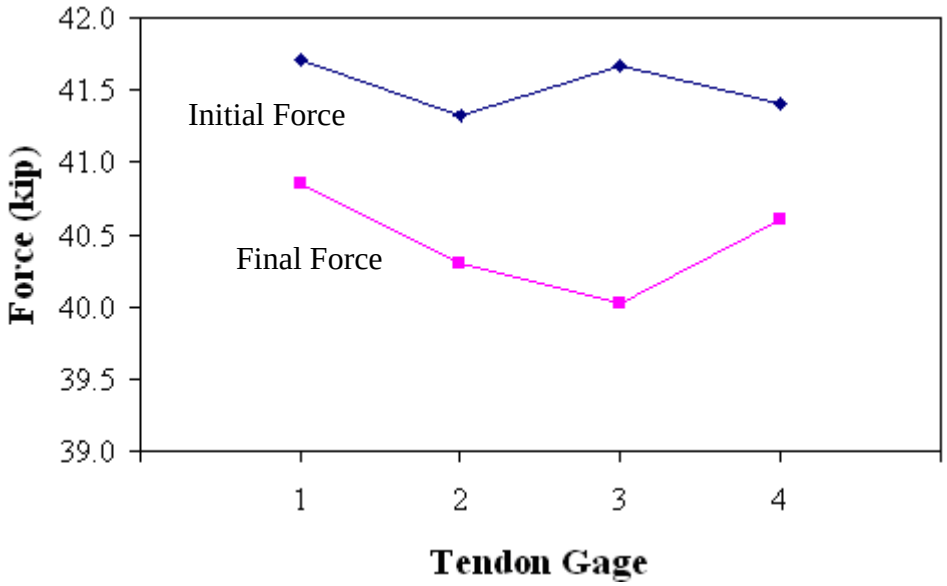

Figure 89. Initial and final force along the instrumented strand in Channel 1

Figure 90. Hydraulic mono-jack gage

5.2.2 Post-Tensioning Strand Summary

To summarize the post-tensioning strand test results, the forces reported by the contractor have been verified. All of the tendons were stressed within tolerance and the final stresses also meet tolerance requirements set by the Iowa DOT. On average, the tendons lost 0.8 kip of force, or about 0.02 percent of the initial stressing force, primarily due to elastic shortening. The largest force lost was 1.6 kip, measured at the midspan of the tendon in Channel 1, which is still less than 0.05 percent of the initial force.

5.2.3 Post-Tensioning Deck Panel Results

The reason for using instrumentation in the deck panels during the post-tensioning operation was to determine how the stresses from post-tensioning were distributed. In order to see how the stresses were distributed, twelve gages as shown in Figure 79, were placed in four deck panels located in the south half of the bridge. Strain data recorded directly with the hand-held data collector were obtained for each of the VWGs and were converted to stresses using the modulus of elasticity of the concrete deck panels. To determine the modulus of elasticity, the average compressive strength of the deck panels prior to delivery was used. The modulus of elasticity, calculated using a concrete strength of 6,800 psi and the relationship provided in Section 5.4.2.4 of the AASHTO LRFD Bridge Design Specification (1996), used for all of the stress calculations was 4,700 ksi.

On the morning of testing, problems were noticed in Gage B1. The connections were checked between the spliced wires, between the gage wires and the switch-and-balance unit, and between the switch-and-balance and the data collector; no connection problems were found. Most likely, Gage B1 was damaged prior to the field testing; thus, there are no results for Gage B1.

The gages used were very sensitive to loads and movements. When people were walking or moving equipment on the instrumented deck panels, there was a ‘spike’ in the strain reading.

Readings stabilized when people moved off the instrumented panels and/or stopped working. Since the reading were taken during the post-tensioning operation, it was impossible to clear the entire bridge while recording data. Besides the post-tensioning operation, the contractor was working on preparing the deck for the longitudinal joint closure pour. These two operations resulted in some inconsistent strain readings and is most likely the reason for higher stresses recorded in nine of the eleven working gages.

Strain readings taken during the post-tensioning of the deck are listed in Table 22. These results were then converted into stresses, which are presented in Table 23, using the modulus of elasticity; highlighted values represent inconsistent gage readings which occurred when the reading for a particular gage was not stable; often the unstable readings varied between 300 and 1200 micro-strains. As previously noted, the unstable readings were often the result of movement on the deck panels.

One gage in particular, Gage A2 produce variable readings on all but two of the data points. There are two possible reasons for the large number of variable readings for this gage. Although there were no problems with the connection to the switch-and-balance unit, there could have been wiring problems embedded in the deck panel. Secondly, Gage A2 may have been picking up the movement from the post-tensioning operation since Panel A was located adjacent to the end panel where the stressing took place and Gage A2 was located in between the two post-tensioning channels. Most of the movement from the post-tensioning was between Channel 1 and Channel 2 in the south half of the bridge. This could explain why the readings from Gage A2 were much more variable than Gage A1, which was located on the outside of Channel 1.

Stresses in the deck ranged from 1,670 psi to 1,775 psi for stable gage readings, below the allowable compressive stress of 4,080 psi (60% of the concrete strength) as specified by the AASHTO LRFD Bridge Design Specifications (1996). Even the highest variable gage reading produced a maximum deck panel stress of 3,545 psi, still below the allowable compressive stress due to post-tensioning. The original stress data for the deck panels, as can be seen in Figure 91, show a trend among ten of the eleven gages, disregarding Gage A2 and the higher stresses measured due to work on the bridge. Note the individual data points are ‘spikes’ in the data due to the contractor’s operations on the bridge deck.

The final stage of post-tensioning results in the largest respective stresses in all of the deck panels, due to the fact all of the strands in the deck were post-tensioned at this point. Actual stresses appear to be somewhat random, and not associated with the location of the panel in the bridge. Stresses in Panel D were the greatest, which was at the dead end of the bridge. Stresses at each gage location were compared to see if the deck panel stresses were highest in the panel closest to the post-tensioning operation. To compare the stress distribution between the instrumented panels, Gage locations 1, 2 and 3 (see Figure 80) were compared; since there was only one gage at Location 4, no comparison was made.

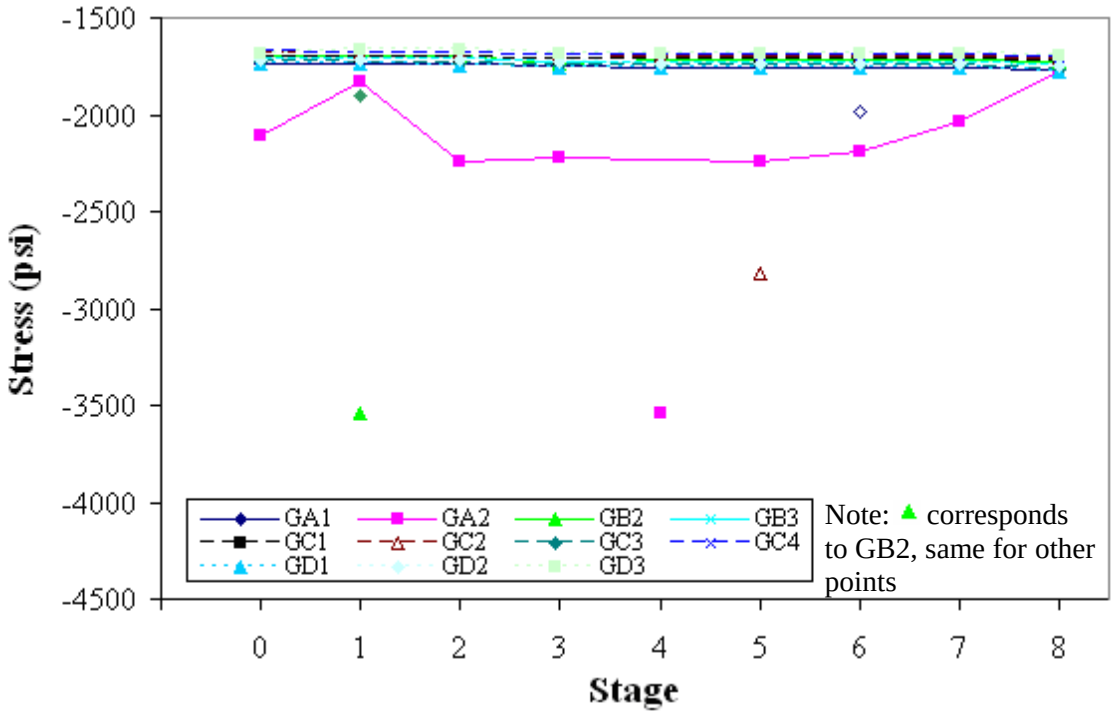

Figure 91. Complete stress results for the bridge deck post-tensioning

Table 22. Deck post-tensioning strains

Stage	Strain (m-strain)										
	A1	A2	B2	B3	C1	C2	C3	C4	D1	D2	D3
0	369	448	361	363	362	358	368	357	371	365	358
1	370	390	753	363	362	358	406	358	371	365	355
2	370	478	361	364	362	359	369	358	371	366	355
3	373	472	370	367	364	362	371	360	374	368	358
4	374	754	365	368	366	362	372	372	375	369	358
5	374	478	366	368	366	600	372	361	375	369	359
6	422	467	365	368	366	362	372	361	375	369	359
7	374	433	365	368	366	362	372	361	375	369	359
8	377	378	368	370	368	365	375	363	378	372	361

Highlighted cells had inconsistent readings

Table 23. Deck post-tensioning stresses

Stage	Stress (psi)										
	A1	A2	B2	B3	C1	C2	C3	C4	D1	D2	D3
0	1735	2105	1695	1705	1700	1685	1730	1675	1740	1715	1680
1	1735	1835	3540	1705	1700	1685	1905	1680	1740	1720	1670
2	1740	2245	1700	1710	1700	1690	1735	1680	1745	1720	1670
3	1750	2220	1740	1720	1715	1700	1745	1690	1755	1730	1680
4	1755	3545	1715	1730	1720	1705	1750	1750	1760	1735	1685
5	1755	2245	1720	1725	1720	2820	1750	1700	1760	1735	1685
6	1980	2195	1715	1725	1720	1705	1750	1700	1760	1735	1685
7	1755	2030	1715	1730	1720	1705	1750	1700	1760	1735	1685
8	1770	1775	1730	1740	1730	1715	1765	1710	1775	1750	1700

Highlighted cells had inconsistent readings

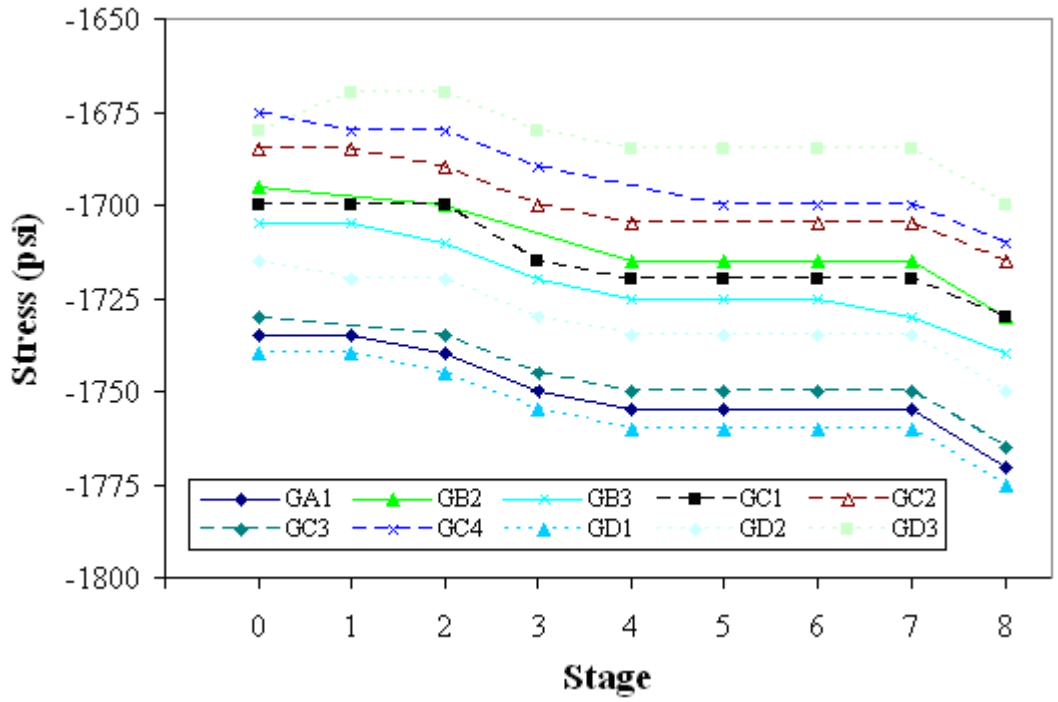

Figure 92. Deck panel stress results

Deck panel stresses at Location 1 (on the outside of Channel 1 in the cantilevered section of the panel) in Panel A, Panel C and Panel D are shown in Figure 93. Note deck Panel B is not shown because as previously noted, Gage B1 was not working.

The greatest stress levels at Location 1 was expected to be in deck Panel A, which was the closest to the post-tensioning operation and the lowest stress levels were expected to be in Panel D, at the dead end of the bridge. However, as shown in Figure 93, the highest stresses actually occurred in Panel D, at the dead end of the deck. Lowest stress levels were measured in Panel C, although the difference in final stress in Panels C and D was less than three percent. The difference in final stress between Panel A and Panel C was 0.3 percent. Stresses recorded at Location 1 do not seem to suggest there is a significant difference in stresses in the deck panels along the length of the bridge.

Stresses measured at Location 2 were compared next, without Gage A2. The gages at Location 2 were located between Channel 1 and Channel 2, on the reinforcing steel adjacent to Channel 1. Deck panel stresses at Location 2, shown in Figure 94, were expected to be the same as those at Location 1 - highest in the panel closest to the post-tensioning operation and decreasing along the length of the deck.

According to the data in Figure 94, the highest stress levels were again in Panel D and the lowest stress levels were in Panel C with Panel B approximately in between, however, there is not significant differences in stresses along the length of the bridge. The difference in final stress between Panel C and Panel D is less than two percent at Location 2.

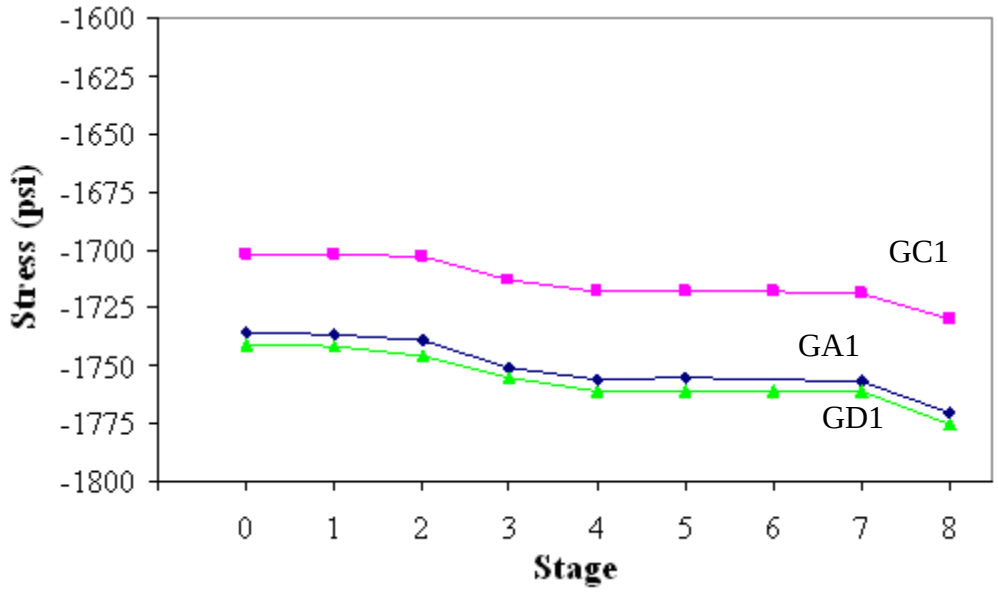

Figure 93. Comparison of deck stresses at Location 1

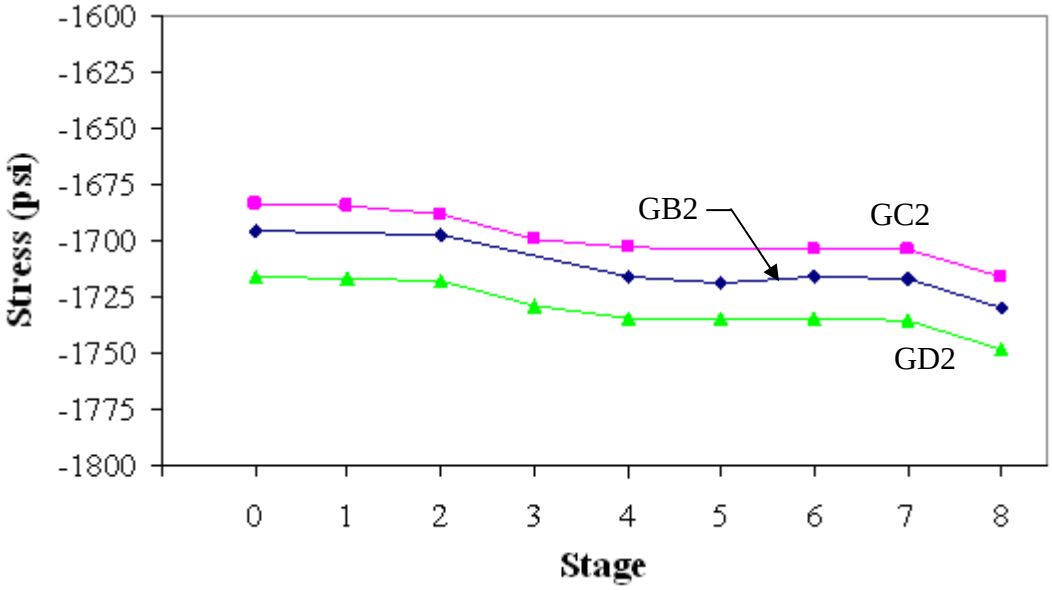

Figure 94. Comparison of deck stresses at Location 2

Stresses measured at Location 3 were also compared; gages at Location 3 were located between Channel 1 and Channel 2, approximately two feet farther away from the Channel 1 than Location 2. Deck panel stresses at Location 3 are shown in Figure 95; highest stresses occurred in Panel C and lowest stresses in Panel D. The difference in the final stress between Panel C and Panel D was 3.7 percent, which again suggests there is no significant difference in the stresses measured along the length of the bridge. When comparing the stress data from all three gage locations, the maximum and minimum stresses do not occur in the predicted panels and the maximum and minimum stresses at each location did not occur in the same panels. At each respective location,

the final stresses were all within four percent, showing no significant difference between the stresses measured in the panels. The locations of the highest and lowest stresses do not show a trend; the locations for the highest and lowest stresses are different at Location 3 than at Locations 1 and 2. Based on these results, stress distribution from the post-tensioning operation does not appear to decrease along the length of the bridge, as was expected.

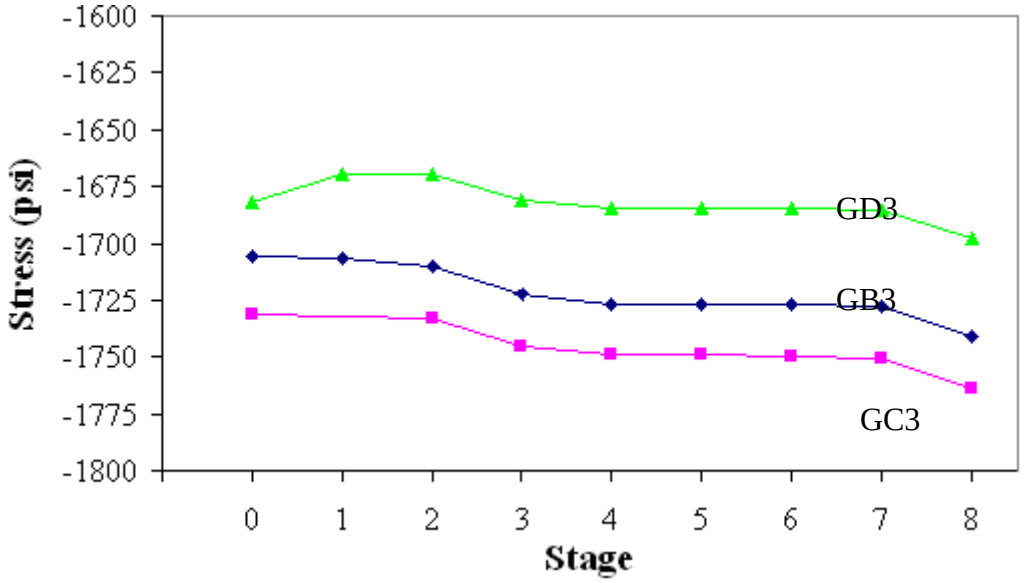

Figure 95. Comparison of deck stresses at Location 3.

Stresses within each panel were also compared. Highest stresses were expected at locations adjacent to Channel 1; as the distance from the and channel increased, stresses were expected to decrease. The stresses were also expected to be higher between Channel 1 and Channel 2 than in the cantilever section of the panels.

The stresses within Panel A were not compared due to the fact that Gage A1 was the only gage working properly during the post-tensioning. The stresses in Panel B were compared first and are presented in Figure 96; only two gages are shown because as previously mentioned, Gage B1 was not working.

The stresses in Panel B did not follow the expected behavior. As illustrated in Figure 96, the higher stresses were measured at Location B3, which was farther away from Channel 1 than Location B2. However, the difference in stress between the two locations was 11 psi, or less than one percent difference.

The stresses in Panel C, the panel with the most instrumentation, were compared next. Comparison of stresses in Panel C is shown in Figure 97; the highest stresses were expected at Location C2 and the lowest at Location C4. While lowest measured stresses did occur at Location C4, the stresses measured were only 9 psi less than the stresses at Location C2, which is adjacent to Channel 1. The highest stresses were at Location C3, which was the farthest from Channel 1. The largest difference in stresses measured in Panel C was between Locations C3

and C4; the difference in final stress between these two gages was 56 psi, or 3.2 percent. Measured stresses in Panel C did not follow the expected behavior; however, based on the final stress difference of 3.2 percent, the deck panel stresses do not change significantly within the deck panel.

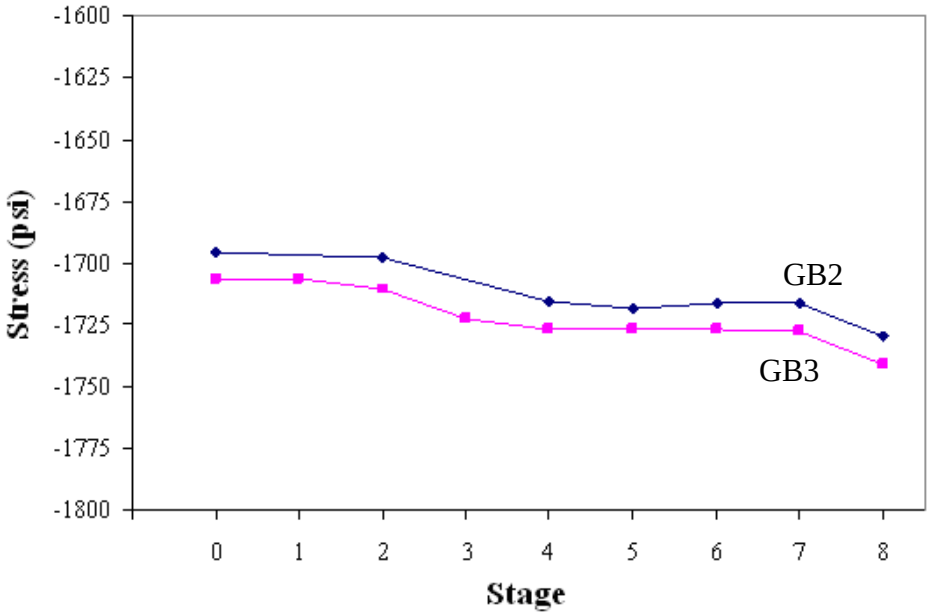

Figure 96. Comparison of deck stresses in Panel B

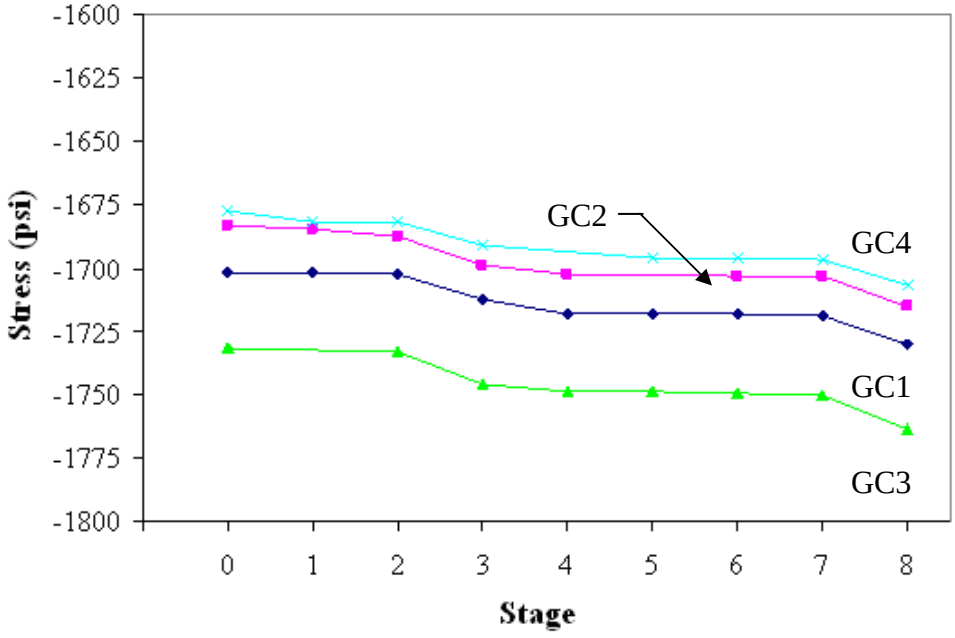

Figure 97. Comparison of deck stresses in Panel C

To better represent the stresses in the panel, the stresses were compared for each instrumented location. This stress comparison is presented in Figure 98. As shown in the figure, the stresses at each location increase as the post-tensioning operation progresses. The magnitudes of the stresses within the panel are relatively similar, as previously discussed. As shown in Figure 98, the stresses are the greatest at Location 3. This is because Location 3 was the closest to Channel 2 and was most likely measuring stresses from the force in Channels 1 and 2.

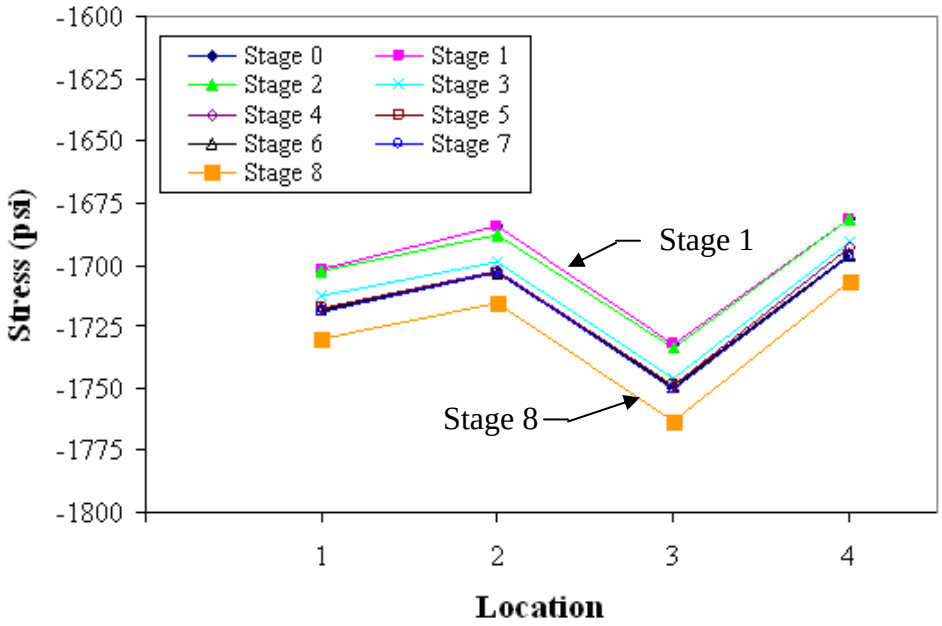

Figure 98. Comparison of deck stresses by location in Panel C

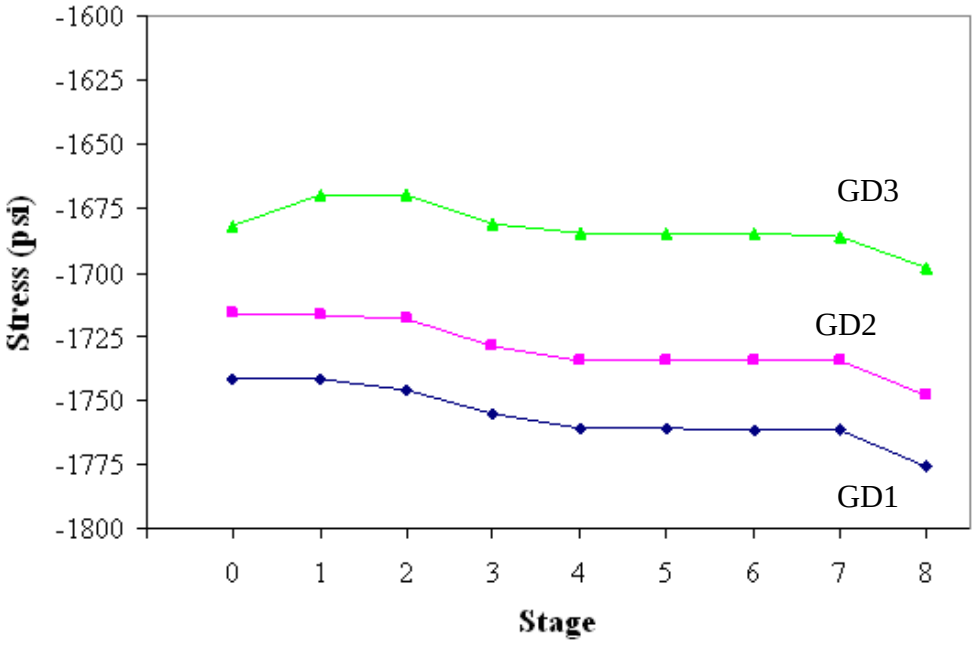

Figure 99. Comparison in deck stresses in Panel D

Stress levels in Panel D were compared last and are presented in Figure 99. Stresses in Panel D follow the expected behavior closer than the previous panels examined. The lowest stresses were measured at Location D3, the location farthest from Channel 1. However, the highest stress was measured at Location D1, which was located in the cantilevered section of the deck panel; the highest stress was expected to occur at Location D2. The final stress difference in Panel D between Locations D1 and D3 was 78 psi, or about 4.4 percent. This small percent difference indicates there is no significant difference in stresses within a given deck panel.

5.2.4 Post-Tensioning Deck Panel Summary

When considering all of the instrumented deck panels, there was minimal correlation between the deck stresses within a given panel. The stresses do not necessarily decrease with distance from the post-tensioning channel, and the stresses are not necessarily less in the cantilevered section of the deck panel than in the deck panel section between the two post-tensioning channels.

The location of the panel along the bridge deck also did not appear to correlate with a decrease in measured stresses; deck panel stresses did not necessarily decrease as the distance between the post-tensioning operation and the deck panel increased. After comparing all of the final stresses measured in the deck panels, the largest difference in stresses was 4.4 percent. Since the stresses measured at the locations in the panels were within five percent, it can be concluded that the stresses induced by the post-tensioning operation are essentially distributed uniformly throughout the deck, regardless of the proximity to the post-tensioning operation or to the post-tensioning channel. Finally, the measured stresses were below the allowable compressive deck panel stress of 4,080 psi, as previously described.

5.3 Post-Tensioning Testing and Verification Summary

Overall, the testing and verification of the post-tensioning operation was a success. Strand monitoring results have shown a loss of force in each strand between the initial stressing and after post-tensioning was completed. The strands exhibited a loss of force while that respective half of the bridge was being post-tensioned. When the opposite half of the bridge was being stresses, the strands showed no significant response.

The largest loss of force between the initial stress of each strand and the final stress was less than 0.05 percent of the initial force. Results from the strand monitoring also verified the strand forces provided by the contractor and verified that the strands with instrumentation were initially stressed within tolerance and remained in tolerance after the post-tensioning was complete. An unexpected result from the strand monitoring was the evidence of elastic shortening of the deck panels in the north half of the bridge.

Deck panel monitoring was performed to measure how the force from the post-tensioning operation was distributed through the deck panels. Results from the deck panels have shown the forces measured were evenly distributed through the deck, regardless of the location of the deck panel. Stress results also showed the stresses measured in the panels were below the allowable

compressive stress in the panels, as specified by AASHTO LRFD Bridge Design Specifications (1996).

6. CONSTRUCTION DOCUMENTATION

6.1 Construction Sequence

This chapter presents the documentation of the demolition of the previous Boone County Bridge over 120th Street, and the construction of the replacement bridge. A summary of feedback from the Boone County Engineer's Office, the prime contractor, the precast fabricator, and from the Iowa State University research team is presented at the end of the chapter.

The previous bridge was a single-span concrete Marsh Arch, shown in Figure 100, which was replaced due to width problems and weight restrictions on the bridge. Clear distance between the reinforced concrete arches was 19 feet and the bridge was 77 feet, 6 inches in length. The previous and existing road alignment can be seen in Figure 101; the bridge location remained the same while the intersecting road to the west of the bridge was moved further west to allow room for the larger replacement bridge.

Figure 100. Previous bridge on 120th Street, July 19

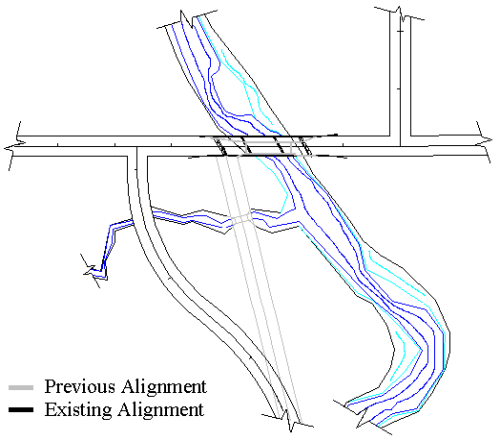

Figure 101. Previous and existing road alignment

Construction began on July 17, 2006 with the contractor focused on earthwork and grading. An access road south of the bridge was initially installed by the contractor before demolition began;

this causeway allowed access between the east and west banks after the original bridge was removed. Demolition of the bridge began the morning of July 24. The contractor used a back hoe with a hammer attachment, shown in Figure 102, to break apart the bridge deck and then used the back hoe to pull apart the bridge reinforcement.

Figure 102. Breaking apart the Marsh Arch bridge deck with a back hoe, July 24

In less than one day, the bridge was demolished and the abutment backwalls and wingwalls were removed. Footings from the abutments were left in place and buried under the creek bed since the location of the footings did not interfere with the substructure for the replacement bridge. Over the next several weeks, the contractor was clearing debris from the bridge and grading, due to the elevation change for the replacement bridge. Since the profile was raised over ten feet from the previous bridge, a large amount of earth fill was required. The graded bridge site and access road can be seen on August 7, 2006 in Figure 103.

During the week of August 7, the Boone and Ames area received approximately one-half inch of precipitation, which caused the access road constructed to wash out. Several working days were lost because the site conditions were too wet to use heavy equipment and the access road had to be reconstructed. Precipitation data for July, August, and September in the Boone/Ames area is presented in Appendix B. Rain damage to the site, along with the washed out access road can be seen in Figure 104.

When the access road was replaced, the contractor removed the original sixteen-inch culvert pipe that was placed under the access road and replaced it with large rock overlaid by sand and gravel. Grading and earth work continued until the bridge abutment locations were properly prepared for pile driving, the bridge site on September 5, 2006 with the west end of the bridge site graded and leveled for pile driving is shown in Figure 105.

Figure 103. Cleared bridge site, August 7

Figure 104. Access road and bridge site, August 11

Figure 105. West bridge abutment site prepped for pile driving, September 5

Pile driving began on the west end the bridge on September 14. For the abutments, five HP 10x57 steel piles were used. Between September 5 and September 15, over three inches of rain fell in the vicinity of the construction site. Rain and runoff caused the access road to wash for

the second time. Even though there was no access to the east side of the bridge, pile driving was finished on the west side; the bridge site after the effects of the additional rain is shown in Figure 106.

After driving piles was complete, 5/8-inch diameter studs were welded to the pile webs. The contractor used steel channels welded to the sides of the H-piles to provide a level surface for placement of the precast abutments. To ensure the channels were welded at the correct elevation, survey equipment was used. One of the piles on the west bank was driven incorrectly; the pile (which will be shown later) was rotated 90° from what the plans specified. Steel channels on the west end of the bridge before being blocked up to the correct elevation are shown in Figure 107.

Between September 15 and 20, the bridge site received an additional one and a half inches of rain. Although the access road hadn't been reconstructed, the additional rain washed away much of the material that had been used in the road. Because of the large amount of rain and wet condition of the bridge site, construction progress slowed. The state of the bridge site on September 20 can be seen in Figure 108.

The rain between the dates of September 15 and 20 caused more damage to the bridge site than the previous storms. The grading on both banks of the creek were damaged after the last storm and had to be repaired; damage to the west bank of the bridge site is shown in Figure 109.

Figure 106. Washed out access road, September 15

Figure 107. West abutment piles, driven and channels being blocked, September 15

The contractor continued work on the west bank when possible; however, most of the site was too wet to work on anything other than the west abutment piles. After the channels were welded in place, the wooden blocking was removed (see Figure 110). Note in Figure 110 the north-most pile, as previously noted, was driven incorrectly; this error required the channels to be positioned parallel to the longitudinal axis of the abutment, instead of perpendicular.

Figure 108. Bridge site on September 20

Figure 109. Damage to the west bank caused by the rain, September 20

The pipe piling for the west pier was driven on September 27 and 28. Each of the piers had nine, 16-inch diameter, closed-end steel pipe piles which were fitted with a pile point (shown in Figure 111) to make driving the piles easier and to prevent damage to the pile.

The two outside pier piles were batter driven at an angle of 4.8 degrees. After all of the piles in the west pier were driven, the piles were connected with steel beams and channels to provide a support for the precast pier cap, until it was installed and permanently grouted in place. The west pier as well as the west abutment piles can be seen in Figure 112.

After the pipe piling was in place and secured with steel falsework, the piles were filled with concrete and the reinforcement connections were embedded in the pier cap as the concrete was placed. Pipe piles with the embedded reinforcement can be seen in Figure 113, after concrete was placed inside the pipe piles. The H-piles for the east abutment were driven, cut to length, and had the studs and channels welded in place on October 10 and 11. H-piles for the east abutment can be seen in the background in Figure 113.

Figure 110. West abutment piles after wood blocking was removed, September 20

Figure 111. Steel pipe pile driving point, September 28

Figure 112. West pier and west abutment piling, September 28

Figure 113. Pipe pile reinforcement for pier cap connection, October 4

Figure 114. West abutment being lowered in place, October 4

a) abutment in final position

b) H-pile in the abutment

Figure 115. West precast abutment in place, October 4

On October 4, the precast abutment and pier cap for the west side of the bridge were transported to the site and placed; the abutment was delivered and set into place first. Unloading and setting the abutment in place, shown in Figure 114, took the contractor approximately fifteen minutes. There were no clearance issues with the H-piles, thus the operation went smoothly. To connect the precast portion of the abutment with the CIP portion, mechanical splicers were embedded in the precast portion to connect No. 5 reinforcing bars. In Figure 115a, the west abutment can be seen in place as well as the No. 5 reinforcing bars; in Figure 115b, one of the H-piles in the abutment is shown.

Next, the west pier cap was delivered, unloaded, and lowered into place on the falsework in approximately fifteen minutes as well. As shown in Figure 116, the pier cap was set on the falsework without any clearance issues with the pipe piles; the west pier cap is shown in place (Figure 117a) along with one of the pipe piles in the pier cap (Figure 117b).

The east abutment was delivered, unloaded, and set in place on October 4, in the same manner as the west abutment. Both abutments and the west pier cap were placed in approximately fifteen minutes each, and all were placed in the same day (October 4); the only delay in setting each element was waiting for the delivery truck. The east pier cap was the only precast substructure member that was not placed that day, due to the fact the site was still too wet to move the crane into place to drive the east pier piles. Shown in Figure 118 are the two abutments and the west pier cap on October 4. At this time, all three were in place. The external reinforcement attached to the west abutment can be seen in this figure as well.

The following day, the contractor grouted the nineteen piles into place (five in the east abutment, five in the west abutment, and nine in the west pier cap). There were difficulties with the special concrete mix meeting the slump and entrained air requirements and the first mix was rejected. The mix was corrected in the second truck and the contractor used a concrete bucket and crane to place the concrete in the CMP; the concrete was vibrated and finished by hand. Concrete being placed in the east abutment is shown in Figure 119; the finished concrete can be seen in Figure 120.

Figure 116. West pier cap being lowered into place, October 4

a) pier cap in place

b) pipe pile in the pier cap

Figure 117. West pier cap in place, in the field, October 4

Figure 118. Precast abutments and pier cap in place, October 4

Figure 119. Concrete being placed in the east abutment, October 5

Figure 120. Finished specialty concrete in the east abutment, October 5

By this time (October 5), the construction site had dried sufficiently for the contractor to rebuild the access road to the east side of the bridge. This time, the contractor used one sixteen-inch culvert pipe, one twelve-inch culvert pipe, and two twenty-four-inch culvert pipes, under the access road to increase the flow under the road to hopefully prevent another wash out. Once the road was finished, the crane was moved onto the access road (as shown in Figure 121) and pile driving for the east pier began on October 10.

After the east pier piles were driven and cutoff to the desired length, the piles were secured with steel falsework and filled with concrete. Reinforcement for the connection between the pipe piles and the pier cap was embedded in the concrete as it was being placed in the pipe piles. The exterior piles were driven at the same batter as previously noted for the west pier. The east pier cap pipe piles are shown in Figure 122, after being filled with concrete. Later that same day (October 12), as shown in Figure 123, the east pier cap was delivered, unloaded, and set in place without difficulty.

Figure 121. East pier pipe piles being driven, October 10

Figure 122. East pier pipe piles filled with concrete, October 12

Figure 123. East pier cap being set, October 12

On October 19, the contractor primed the exposed steel pipe piles and painted the piles on October 23 to prevent corrosion. After the concrete connecting the piles and substructure had reached strength, the contractor was able to set the prestressed concrete girders on the piers and abutment caps. The girders were delivered, three per truck, unloaded and set in place October 24. Center span girders were delivered and placed on the substructure first, followed by the west span girders, and finally the east span girders. Each girder was unloaded and set in place in approximately ten minutes; the first girder of the center span is shown being lifted into place in Figure 124.

All of the bridge girders were set in place on October 24. Small steel beams, shown in Figure 125, supported the girders on top of the pier caps and abutments to keep the girders at the correct elevation until the pier cap diaphragms and the CIP portion of the abutment caps were placed. A view of all of the erected bridge girders (looking east) is presented in Figure 126.

The first of the interior deck panels were delivered on October 25, four panels per truck, and erection thereof began that morning. The first two deck panels set were the panels at middle of the center span of the bridge. However, the panels were not set in the correct location; this error was not noticed until after eight panels had been set. Since the panels had to be set from midspan outwards, the contractor had to remove all eight panels and reset the first two panels. After the initial two panels were correctly positioned, the rest of the panels were then reset. One of the deck panels can be seen being lifted and placed on the girders in Figure 127.

Figure 124. The first bridge girder being lifted into place, October 24

Figure 125. Steel beams used to support the girders, October 24

Over half of the bridge deck panels, sixteen in total, were set on October 25. The remaining panels were delivered and set the next day, with the exception of the four end panels. Four sets steel plates and screws, one of which is shown in Figure 128, were used by the contractor to level the interior deck panels.

Once all of the deck panels were leveled to the correct elevation, the panels located over the piers were removed so the pier diaphragms could be cast. All of the panels had to be at final elevation

so the contractor could form the diaphragms under the panels to the correct height. The diaphragms for both east and west piers were placed on November 3, as shown in Figure 129. After the concrete was placed, the diaphragms were covered in wet burlap and plastic for curing; the west pier diaphragm can be seen in Figure 130, a day after the concrete was placed.

Figure 126. Erected bridge girders, October 24

Figure 127. Deck panel being reset on the bridge girders, October 25

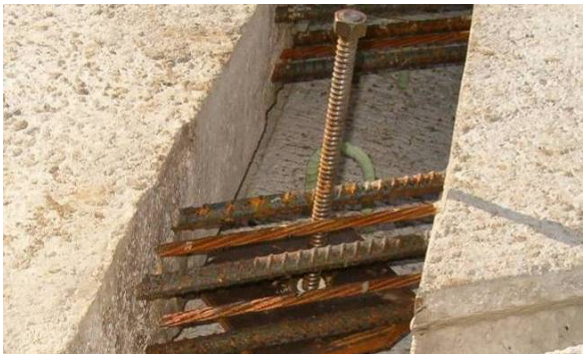

Figure 128. Deck panel leveling screw, October 26

Figure 129. Pier diaphragm before concrete placement was complete, November 3

Figure 130. West pier diaphragm covered with burlap and plastic, November 4

The panels over the piers were replaced after the pier diaphragm concrete had gained sufficient strength and the diaphragm formwork had been 'stripped'. While waiting for the diaphragm concrete to cure, the contractor formed the transverse joints between the deck panels, as shown in Figure 131. On November 8, all four of the end panels were delivered to the site and placed on the bridge; one of the east end panels being lowered into place is shown in Figure 132.

Figure 131. Transverse joint formwork, November 5

Figure 132. End panel being placed at the east end of the bridge, November 8

The transverse joints between the end panels and the adjacent panels were not formed and cast with the rest of the transverse joints, since the end panels had not reached the required 28-day strength. On November 8 the remaining transverse joints were placed. Several transverse joints can be seen in Figure 133, before being finished; a finished transverse joint is shown in Figure 134.

Post-tensioning strands were 'threaded' through the end panels and the four post-tensioning channels on November 13. End panels reached the required 28-day strength on November 16, after which concrete was placed in the transverse joints between the end panels and the adjacent interior panels.

Post-tensioning the bridge deck could not take place until the end panel transverse joints had reached a minimum strength of 3,500 psi. Since the temperature was dropping, the contractor used heating coils and thermal blankets to heat the joints and decrease the amount of time needed for the concrete in the joints to cure and reach strength. The Iowa DOT placed thermal couples in the transverse joint concrete, shown in Figure 135, so the internal temperature of the concrete could be monitored. Temperature data from the transverse joints are presented in Appendix B. One of the finished end transverse joints can be seen in Figure 136 covered with burlap and heating coils, before the thermal blankets were put in place.

Figure 133. Several transverse joints before finishing, November 8

Figure 134. Finished transverse joint, November 8

Figure 135. Thermal couple being inserted into end panel joint, November 16

The contractor was originally going to post-tension the bridge deck on November 21; the VWGs for monitoring some of the post-tensioning forces were attached to four of the tendons and calibrated that morning. One of the gages is shown being calibrated in Figure 137. However, there were problems keeping the joints sufficiently warm; around 2:00 a.m. on November 18, the generator for the heating coils lost power. Power was not restored until around 7:00 a.m. later that morning. Since the strength of the concrete in the end panel transverse joints was not at the required strength, post-tensioning had to be delayed one week for the concrete to cure sufficiently to meet the minimum strength requirements.

Figure 136. Burlap and heating coils on the west end panel joint, November 16

Figure 137. Calibration of one of the vibrating wire gages, November 21

The following week, the concrete in the joints had gained sufficient strength and the post-tensioning operation, shown in Figure 138, began approximately at 8:00 a.m. on November 28. The order of post-tensioning the various tendons was presented earlier in Section 5.1 of Chapter 5. The entire post-tensioning operation took less than four hours, including the time post-tensioning had to stop for data collection.

During the time spent waiting for the transverse joint concrete to reach the required strength, the contractor formed the longitudinal joint between the north and south half of the bridge and put up formwork for the four post-tensioning channels. Longitudinal joint formwork can be seen in Figure 139 from below the bridge deck. Formwork was attached to the deck using U-bolts.

After post-tensioning was completed, concrete was cast in the post-tensioning channels and longitudinal joint. The deck leveling plates and screws were left in place until the concrete in the joints had reached the desired strength; the screws were then removed from the deck and the holes were filled with grout in accordance with the Iowa DOT Materials Instructional Memoranda 491.13 Hydraulic Cement Grouts criteria. A finished post-tensioning channel, the

finished center longitudinal joint, and an unfinished post-tensioning channel can all be seen in Figure 140; note the leveling screws in the post-tensioning channels.

Figure 138. Post-tensioning in progress, November 28

Figure 139. Longitudinal joint formwork, November 28

Figure 140. Longitudinal joint and one channel finished, November 28

Concrete in the longitudinal center joint and the post-tensioning channels were covered with burlap, heating coils and thermal blankets to ensure the concrete cured with the cold temperatures. The next day, November 29, the contractor fabricated the formwork for the abutment cap and wing walls and placed the reinforcement in the formwork; both sets of abutment caps and wing walls were placed on November 29. Next, external reinforcement for the barrier rail was added to the deck panels using embedded mechanical splicers. The reinforcement for the CIP portion of the abutment can be seen in Figure 141 and the finished abutment cap is shown in Figure 142. Note the No. 5 reinforcing bars for the guard rail system attached to the deck panels can also be seen in Figure 142.

Next, the contractor fabricated the formwork for the CIP barrier rails, (shown in Figure 143), tied the reinforcement cages to be placed in the formwork, and connected the external reinforcement to the deck panels using the embedded mechanical splicers. The reinforcement cage for the barrier rail in the formwork is shown in Figure 144. Both barrier rails were placed and finished on December 8; the barrier rail can be seen after being placed, before final finishing in Figure 145. After finishing, the barrier rails were covered with wet burlap and plastic for curing.

Figure 141. Reinforcement in the west abutment cap, November 29

Figure 142. West abutment and wingwall, placed and finished, November 29

Figure 143. Barrier rail formwork, December 8

Figure 144. Barrier rail reinforcement, December 8

Figure 145. Barrier rail before final finishing, December 8

On December 11, the contractor began to 'strip' the formwork from the abutment caps and wing walls, and from the bottom of the post-tensioning channels and longitudinal joint. After the

formwork was removed, the contractor was able to compact granular fill material behind the abutments and grade the road to the bridge deck. Forms for the barrier rails were stripped on December 12.

The last construction task for the bridge was to grind the surface of the bridge deck. On December 27, the surface of the deck was ground, however, due to equipment breakdown, grinding wasn't completed until December 28. Due to clearance issues with the grinding equipment, shown in Figure 146, the three feet adjacent to the barrier rails were not ground. Figure 147 shows the surface of the bridge deck after the surface was ground.

There were some difficulties encountered with the deck grinding process. Several areas of the transverse joints were not finished high enough, causing low and uneven areas on the deck. Even after grinding, there were several areas where the transverse and longitudinal joints had noticeable low areas. One such area between the transverse joint and the precast panels can be seen in Figure 148. After the bridge deck was ground, the completed bridge shown in Figure 149 was officially opened.

Figure 146. Bridge deck grinding equipment on site, December 27

Figure 147. Bridge deck after the surface was ground, December 27

Figure 148. Low area in one transverse joint after deck grinding, December 27

Figure 149. Completed bridge, December 27

6.2 Construction Feedback

The Boone County engineering staff, along with the prime contractor and the precast manufacturer, was interviewed to obtain feedback on the bridge replacement project. Information obtained can be categorized into three main areas: project positives, project negatives, and suggestions to possibly improve the construction of such bridges.

6.2.1 Feedback from the Boone County Engineering Staff

Boone County was the owner of the bridge and responsible for the construction inspection throughout the project. Bob Kieffer, Boone County Engineer, and Scott Kruse, Assistant to the Engineer, were both interviewed after the bridge was completed for feedback from the owner. During construction of the bridge, Dave Anthony was the Boone County Engineer, however, Mr. Kieffer, as Assistant Engineer, was intimately involved with the project. Mr. Kruse was the field engineer responsible for the construction inspection and was at the bridge site on a daily basis. A summary of the feedback from the Boone County engineering staff follows.

Positive aspects of the project:

- The precast substructure caps were all set in a short amount of time and without difficulty.
- The deck panels were all set in a short amount of time and without difficulty. The delivery of the panels caused most of the delay while setting the panels, not the actual process of setting the panels.

Negative aspects of the project:

- The county did not save any time or money with this project. While the county was aware the project would be slightly more expensive than traditional construction, the engineers were under the impression there would be a time-savings involved.
- The Boone County engineers are not familiar with pipe piling. Concrete encased piles would have been preferred over the steel pipe piles. Repainting the piles will be more maintenance for the county.
- Boone County felt the design calculations for the piles were not conservative. Several piles had to be tapped the day after initial driving to meet bearing requirements.
- The quality of the panel finish was poor.
- Construction progress had to wait on the precast elements. The substructure could have been set earlier but the abutments had not been fabricated. Panel placement was also delayed because the panels were not on site.
- The precast abutment and pier caps cracked during transportation.
- The Iowa State Ready Mix representative was never present on the construction site when concrete was being placed. There were difficulties with the specialty concrete mix and having someone present from the concrete supplier would have been helpful.

Suggestions for improvement:

- The backer rod used in the transverse joints did not work well. Instead of the backer rod, expansive spray foam might work better in the transverse joints.
- Better workmanship on all of the joints could have prevented the need for grinding the bridge deck. If grinding is absolutely necessary, joints should be finished one-fourth of an inch high to ensure the joints are ground smooth and prevent low spots.
- The panels did not need a roughened finish since the deck was to be ground. The joints would be easier to finish if the panels were not roughened.

6.2.2 Feedback from Petersen Contractors, Inc.

Petersen Contractors, Inc. (PCI) was the prime contractor for the Boone County bridge replacement project. Justin Clausen, project manager, and John Benjamin, foreman for the project, were both given a chance to offer feedback. Mr. Clausen compiled his feedback in a document which can be found in Appendix B. Mr. Benjamin was interviewed over the phone. A summary of the feedback from PCI follows.

Positive aspects of the project:

- Deck panel sizes worked out well.
- Precast pier caps worked well.
- Precast abutments worked well.
- Post-tensioning worked very well.

Negative aspects of the project:

- There were difficulties with the specialty concrete. The designer should have a better handle on the mix design of that concrete and the admixtures being specified.
- The formwork for grouting the post-tensioning channels and under the deck panels was time consuming (putting up the formwork took at least 100 man-hours, not including the time to strip the formwork).
- The deck grinding was poor. The ends of the deck couldn't be properly ground because of the gravel approaches.

Suggestions for improvement:

- Use a beam with a wider top flange to allow more room for the post-tensioning channel.
- Modify the pier diaphragm pour so that none of the deck panels have to be removed.
- Coordinate letting, shop drawings, fabrication, and construction so that cold weather does not become an issue. If the project was let in the fall, the winter could have been used for shop drawing submissions and approval and fabrication of precast elements and construction could begin immediately in the spring.. This way, construction would not have to wait for the fabrication and delivery of precast elements and construction would be finished before cold weather.
- Review the end panel anchorages to make tendon placement easier.
- An overlay on the bridge would eliminate problems associated with grinding the bridge deck.
- A precast barrier rail would be much faster than the CIP barrier rail used.
- Use precast wing walls instead of CIP. The formwork for the wing walls was also time-consuming.

6.2.3 Feedback from Andrews Prestressed Concrete

Andrews Prestressed Concrete fabricated all of the precast elements associated with this project. Teresa Nelson, project manager, compiled feedback in a document, which can be found in Appendix B. A summary of the feedback from Andrews Prestressed Concrete follows.

Positive aspects of the project:

- ISU and PCI were easy to work with.
- It was easy to resolve fabrication issues or mistakes and oversights in the plans.

Negative aspects of the project:

- The anchor plate was not quite the full depth of the panel. This made it very difficult to assure that the plate was suspended off of the casting bed.

Suggestions for improvement:

- Look into a larger size mesh in end panels to allow for larger openings to aid in placement and consolidation of concrete.
- Change the design of the anchor plate in the end panels.
- Use larger diameter holes for the post-tensioning tendon to allow pipe sleeves to pass thru in lieu of butting against the anchor plate.

6.2.4 Feedback from Iowa State University

Researchers at Iowa State University provided feedback based on the fabrication and construction of the substructure elements tested in the laboratory. T.J. Wipf and F.W. Klaiber, as Co-Principal Investigators for the laboratory testing provided some feedback, a summary of which follows.

Positive aspects of the project:

- Reinforcement and the connection between the pile and CMP were easy to fabricate.

Negative aspects of the project:

- CMP was not a standard size; had to be special ordered.
- Pipe piling was hard to find and not a common size used in Iowa; pipe was obtained out of state.

Suggestions for improvement:

- Use standard CMP sizes to reduce cost and eliminate special orders.
- Use piles that are standard in Iowa. This will make the piles easier to obtain and ensure owners and contractors are familiar with the product (see comments from Boone County Engineers Office).

6.3 Construction Summary

Construction for the replacement bridge over 120th Street began on July 19, 2006 and took 108 working days to complete (see Table 32 at the end of this section for important events, delays and corresponding dates). Demolition of the previous bridge was completed in one day. Rain delayed the construction progress at the end of August and through most of September; in total, 21 working days were lost due to rain or wet site conditions. The piles were driven in late September and the precast substructure was set in early October; the girders and deck panels were set in late October after the substructure was complete. Transverse concrete joints were placed in late October and early November, during which time the post-tensioning tendons were placed and formwork for the post-tensioning channels and longitudinal center joint was installed.

Construction was delayed again due to cold weather effects on the concrete joints, therefore, the joints had to be heated to ensure the concrete reached the required strength. The deck was post-tensioned in late November and the post-tensioning channels and longitudinal joint were cast with concrete. In December, the CIP abutment caps, wing walls and barrier rails were placed. In late December, the excavated area behind the abutments and wingwalls were backfilled and compacted, the road was graded to the bridge deck elevation, and the bridge deck was ground smooth. After the bridge deck was ground, the completed bridge was opened to the public (December 28, 2006).

Feedback was received from the Boone County engineering staff, PCI contractors, and Andrews Prestressed Concrete on positive and negative aspects of the project and possible ways to improve the construction process. Some of the common comments include:

- The precast elements were all set without difficulty.
- There were difficulties with the specialty concrete mix.
- The deck grinding operation needs to be improved.

Table 32. Construction events, dates, and durations

Event	Date	Days
Construction begins	07/19/06	1
Previous bridge demolition and removal	07/24/06	5
Rain delay	08/02/06	9
Excavation and structure removal	08/03/06	15
Rain delay and repairing access road	09/11/06	6
Set up, pile driving, cutting and stud welding (abutments and west pier)	09/14/06	11
Setting precast abutments and west pier cap	10/04/06	1
Grouting piles in precast elements	10/05/06	1
Set up, pile driving, cutting, and stud welding (east pier)	10/09/06	3
Setting east pier cap	10/12/06	1
Grouting piles in east pier cap	10/13/06	1
Painted primer on pipe piles	10/16/06	2
Rain delay	10/17/06	3
Setting precast girders	10/24/06	1
Setting precast deck panels	10/25/06	2
Rain delay	10/26/06	1
Fabrication and placing pier diaphragms	10/30/06	5
Leveling deck panels	11/06/06	3
Rain/snow delay	11/10/06	1
Threading post-tensioning tendons	11/13/06	3
Forming CIP abutment diaphragms and longitudinal joints	11/13/06	8
Delay from cold weather/transverse joint strength	11/22/06	3
Post-tensioning the bridge deck and placing longitudinal joints	11/28/06	1
Placing CIP abutment diaphragms and wingwalls	11/29/06	2
Cold weather delay	11/30/06	1
Fabrication of barrier rails	12/04/06	3
Cold weather delay	12/07/06	1
Placing barrier rails and end sections	12/08/06	2
Stripping formwork and backfilling abutments	12/12/06	2
Cleaning site and shaping bridge approaches	12/14/06	2
Placing rip rap, stone, and guardrail	12/18/06	2
Delay waiting for the grinding operation	12/20/06	4
Grinding the bridge deck	12/27/06	2
Total Days	108	

7. SUMMARY AND CONCLUSIONS

7.1 Summary

This chapter presents a summary of the laboratory testing results, the post-tensioning results for the tendons and deck panels, and a summary of the construction documentation. Conclusions are also presented based on the results obtained from testing (laboratory and field) and feedback from the Boone County Engineer's Office, PCI, Andrews Prestressed Concrete, and the research team.

7.1.1 Laboratory Testing Summary

In total, eight laboratory tests were completed: five single pile abutment tests, two double pile abutment tests, and one pier cap test. Each single pile specimen resisted over four times the unfactored design load without any sign of failure. The double pile specimen supported approximately twice the unfactored design load without failure, even though the CMPs were only 70% full of concrete. Limiting the depth of the concrete was done in an attempt to actually fail the specimen. The experimental cracking moment from the double pile test agreed with the experimental cracking moment determined from the single pile tests. The pier cap resisted over five times the unfactored design load without any signs of failure. It was not possible to completely fail any of the eight laboratory specimens since their strength exceeded the capacity of the laboratory loading system.

7.1.2 Post-Tensioning Summary

Post-tensioning of the Boone County Bridge took place on the morning of November 28, 2007. The entire operation took approximately four hours, including the time needed for data collection. Vibrating wire gages were used to measure the force occurring in several of the post-tensioning strands, to measure the losses during the post-tensioning process, and to measure the distribution of the post-tensioning forces through the deck panels. The forces in the strands, calculated using data from the VWGs, were within two percent of the forces provided by the contractor. After the post-tensioning process was complete, all of the strands were within the tolerances specified by the Iowa DOT. The strains in the deck panels indicated that the post-tensioning force is distributed through the end panels to the interior deck panels almost immediately. Strains (stresses) measured in the panels were relatively constant throughout the deck, regardless of the location of the panel in the bridge, or the distance from the post-tensioning channels.

7.1.3 Construction Documentation Summary

Construction on the Boone County replacement bridge began on July 5, 2007, after demolition of the previous bridge at the site, which began on July 24. There were delays in construction due to heavy rain in August and September; a total 15 working days were lost to due rain and/or wet conditions at the site in August and September alone. In September, piles were driven and

erection of the precast substructure began October 4. The pile connections in the abutments and west pier cap were grouted in place October 5 and the east pier cap connections were grouted October 13. Once the grouted concrete reached strength, erection of the superstructure began on October 24.

The bridge girders were set on October 24; on the next day, the interior deck panels were set. The panels were leveled and the CIP diaphragms over the two piers were placed on October 30. End panels were delivered and set in place on November 8, which was followed by the casting of the interior transverse joints. Due to weather conditions, the transverse joints at the end panels (which had to be placed later when the end panels reached the desired strength) were slow to reach the required strength for post-tensioning. The post-tensioning operation was delayed until November 28, when the deck was post-tensioned and all of the longitudinal joints were placed.

Once the deck was finished, the contractor formed and cast the CIP portion of the abutments, the wingwalls, and the barrier rails. After the concrete reached the desired strength, the formwork was stripped, the approaches were backfilled and graded to the bridge deck elevation. On December 27, the bridge deck was ground and the bridge was opened to the public. The total construction time for the replacement bridge was 108 working days, with 21 days lost to rain and wet conditions throughout the project, and 9 days lost for miscellaneous reasons (78 actual working days).

7.2 Conclusions

7.2.1 Laboratory Testing Conclusions

The following conclusions are based on the eight laboratory tests of the substructure elements for the Boone County replacement bridge:

- The abutment section capacity is at least 4.5 times greater than the unfactored design load of 80 kip per pile.
- The pier cap section capacity is at least 5.3 times greater than the unfactored design load of 72 kip per pile.
- The CMP affected the behavior and crack pattern in the abutment sections, but had no influence in their capacity.
- The CMP had no apparent effect on the pier cap section.
- The measured cracking moments for the abutment and pier cap, based on observation and strain data, were approximately 264 kip-feet and 312 kip-feet, respectively.
- Essentially no differential movement was detected between the precast concrete and the concrete in the CMP in any of the abutment specimens or pier cap specimen. The movement measured was less than 0.0033 inches in every test.
- No movement was detected in the shear tests; measured movement was less than 0.0005, the LVDT precision.
- Shear failure was not detected between the H-pile in the abutment and the concrete in the CMP.

7.2.2 Post-Tensioning Tendon Forces and Deck Panel Stress Conclusions

The following conclusions are based on the verification of the post-tensioning forces and resulting strains in the precast deck panels:

- Small losses due to seating and elastic shortening of the bridge deck (less than 0.05 percent of the initial force) were measured during the post-tensioning operation.
- The forces in the strands provided by the contractor are in agreement with the forces measured in the four instrumented strands.
- The forces in all of the strands were within the required Iowa DOT tolerances and remained within these tolerances after post-tensioning was completed.
- The force from post-tensioning was distributed evenly through the deck panels, regardless of the panels' location in the bridge or distance from the post-tensioning channels.
- Stresses calculated from the measured strains in the deck were less than allowable compressive stress due to post-tensioning (AASHTO, 1996). The maximum measured stress (1,835 psi) was 45 percent lower than the maximum allowable compressive stress (4,080 psi).

7.2.3 Conclusions from Construction Documentation

The following conclusions were based on the construction documentation of the Boone County replacement bridge and the feed back provided by the Boone County Engineer's Office, PCI, and Andrews Prestressed Concrete:

- Construction began on July 5 and was completed on December 27, 78 days of actual construction.
- Delays in construction were caused by heavy rain and wet conditions (21 days).
- Setting all of the precast elements went quickly and smoothly with no problems.
- It was difficult to meet the slump and entrained air requirements for the specialty concrete mix used in the CMPs and in the transverse and longitudinal joints of the deck. The admixture to improve the workability of the mix only lasted about twenty minutes in the field.
- The post-tensioning process went smoothly and without any major difficulties. It is important to note that the post-tensioning was performed by the prime contractor (PCI), without any prior post-tensioning experience, with the supervision of a technical expert.
- Deck grinding was difficult; the entire deck could not be ground and low spots due to poor concrete finishing of the transverse joints were left on the deck.

8. RECOMMENDATIONS FOR FURTHER INVESTIGATION

This chapter summarizes the need for additional research on the precast bridge substructure, recommendations for monitoring the post-tensioned bridge deck, and recommendations to improve the construction sequence of this replacement bridge system in the future.

8.1 Substructure Recommendations

The following recommendations for the bridge substructure are based on the laboratory testing of the substructure elements:

- The cross-section and reinforcement in the abutment and pier cap should be evaluated to produce more economical sections.
- Additional research is required to quantify the effects of the CMP on the abutment.

8.2 Post-Tensioning Recommendations

The following recommendation is based on the verification of the post-tensioning of the Boone County bridge:

- Long-term monitoring of the bridge should be performed using the embedded instrumentation on the post-tensioning tendons and in the deck panels.

8.3 Construction Recommendations

The following recommendations were made based on the construction documentation of the Boone County Bridge and the feedback received from the Boone County Engineer's Office, PCI, and Andrews Prestressed Concrete:

- Construction scheduling for research projects should consider the time needed for shop drawings and approvals, and the schedule should be coordinated to avoid cold weather.
- Fabrication of precast elements should begin before on-site construction so progress in the field is not delayed by the fabrication of precast elements.
- The bridge deck grinding operation should be evaluated to produce a better riding surface for the bridge.
- Research is recommended on the specialty concrete mix to determine a mix design that meets the design requirements and is easier to place in the field.
- Additional research on this deck panel system is recommended to reduce the time required to install the formwork for the post-tensioning channels and center longitudinal closure joint.
- To reduce total construction time, the use of precast abutment caps, wingwalls, and barrier rails should be investigated (i.e. eliminate the need for the CIP concrete).

REFERENCES

American Association of State Highway and Transportation Officials. *AASHTO LRFD Bridge Design Specifications*, American Association of State Highway and Transportation Officials. Second Edition, 1998, pp 9-14.

American Association of State Highway and Transportation Officials. *AASHTO Standard Specifications for Highway Bridges*, American Association of State Highway and Transportation Officials. 16th Edition, 1996.

American Concrete Institute. *ACI 318-05 Building Code Requirements for Structural Concrete*, American Concrete Institute, 2005, pp 99.

Arditi, David, Uluc Ergin, and Suat Gunhan. *Factors Affecting the Use of Precast Concrete Systems*, Journal of Architectural Engineering. Vol. 6, No. 3, September 2000, pp. 79-86.

Badie, Sameh S., Baishya, Mantu C., Tadros, Maher K. *NUDECK – An Efficient and Economical Precast Prestressed Bridge Deck System*, PCI Journal. Vol.43, No.5, September/October 1998, pp 56-71.

Bonded Strand Post-Tensioning System, http://www.dywidag-systems.com/. 2007. http://www.dywidag-systems.com/products/Bonded_Strand_PT_System _Anchorages.html, Accessed January 31, 2007.

Billington, S.L., R.W. Barnes, J.E. Breen. *Alternate Substructure Systems for Standard Highway Bridges*, Journal of Bridge Engineering. Vol.6, No.2, March/April 2001, pp 87-94.

Billington, S.L., R.W. Barnes, J.E. Breen. *A Precast Segmental Substructure System for Standard Bridges*, PCI Journal. Vol. 44 No. 4, July/August 1999, pp56-72.

Cooper, Thomas and Pearson-Kirk, Donald. *Improving the Durability of Post-Tensioned Bridges,* Transportation Research Board 2006 Annual Meeting CD-ROM. pp 1-8.

Fallaha, Sam, Chuanbing Sun, Mark D. Lafferty, Maher K. Tadros. *High Performance Precast Concrete NUDECK Panel System for Nebraska's Skyline Bridge***,** PCI Journal. Vol. 49, No. 5, September/October 2004, pp 40-50.

Hale, W. Micah and Russell, Bruce W. *Effects of Allowable Compressive Stress at Release on Prestress Losses and on the Performance of Precast, Prestressed Concrete Bridge Girders,* PCI Journal. Vol. 51, No. 2, March/April 2006, pp 14-25.

Hamilton III, H.R., Wheat, H.G., Breen, J.E., and Frank, K.H. *Corrosion Testing of Grout for Posttensioning Ducts and Stay Cables,* Journal of Structural Engineering. Vol. 126, No. 2, February 2000, pp 163-170.

Haroon, Saif, Yazdani, Nur and Tawfiq, Kamal. *Posttensioned Anchorage Zone Enhancement with Fiber-Reinforced Concrete*, Journal of Bridge Engineering. Vol.11, No. 5, September/October 2006, pp 566-572.

Harrison, Alex and LeBlanc, N, David. *Design and Construction of a Full-Width, Full-Depth Precast Concrete Deck Slab on Steel Girder Bridge*, Transportation Research Record: Journal of the Transportation Research Board. No.1907, 2005, pp. 55-66.

Hieber, DG., JM. Wacker, MO Eberhard, and JF Stanton. *State-of-the-Art Report on Precast Concrete Systems for Rapid Construction of Bridges***,** Final Technical Report, Washington State Transportation and the Federal Highway Administration. March 2005, pp 1-85.

Issa, Moshen, Cyro L. Ribeiro do Valle, Hiba A. Abdalla, Shahid Islam, Mahmoud A. Issa. *Performance of Transverse Joint Grout Materials in Full-Depth Precast Concrete Bridge Deck Systems*, PCI Journal. Vol. 48, No. 4, July/August 2003, pp 92-103.

Issa, Moshen, Yousif, Alfred, Issa, Mahmoud, Kaspar, Iraj, and Khayyat, Salah. *Analysis of Full Depth Precast Concrete Bridge Deck Panels*, PCI Journal. Vol. 43, No.1, January/February 1998, pp 74-85.

Khayat, K.H., Yahina, A., and Duffy, P. *High-Performance Cement Grout for Post-Tensioning Application*, ACI Materials Journal. Vol. 96, No. 4, July-August 1999, pp 471-477.

Lounis, Z, Mirza M.S, and M. Z. Cohn, *Segmental and Conventional Precast Prestressed Concrete I-Bridge Girders*, Journal of Bridge Engineering. Vol. 2 No. 3, August 1997, pp 73-82.

Naaman, Antione. *Prestressed Concrete Analysis and Design Fundamentals*, Techno Press 3000. 2nd Edition, 2004.

NCHRP Project 20-58(1) *Detailed Planning for Research on Accelerating the Renewal of America's Highways (Renewal), Preliminary Draft Final Report*. February 28, 2003.

PCI Industry Handbook Committee. *PCI Design Handbook Precast and Prestressed Concrete*, Precast/Prestressed Concrete Institute, Sixth Edition, 2004, pp 2-1 – 2-10.

Russell, Henry G., Ralls, Mary Lou, Tang, Benjamin. *Prefabricated Bridge Elements and Systems in Japan and Europe*, Transportation Research Record: Journal of the Transportation Research Board. No.1928, 2005, pp 103-109.

Salas, R.M., Schokker, A.J., West, J.S., Breen, J.E. and Kreger, M.E. *Conclusions, Recommendations and Design Guidelines for Corrosion Protection of Post-Tensioned Bridges*, Texas Department of Transportation. Research Report 0-1405-9, February 2004, pp 1-73.

Schokker, A. J., Koester, B.D., Breen, J.E., and Kreger, M.E. *Development of High Performance Grouts for Bonded Post-Tensioned Structures,* Texas Department of Transportation. Research Report 1405-2, October 1999, 1-56.

Stamnas, Peter E. P.E. and Whittemore, Mark D. P.E. *All-Precast Substructure Accelerates Construction of Prestressed Concrete Bridge in New Hampshire ,* PCI Journal. Vol. 50 No. 3, May/June 2005, pp 26-39.

Tokerud, Roy. *Precast Prestressed Concrete Bridges for Low-Volume Roads,* PCI Journal. Vol. 24 No. 4, July/August 1979, pp 42-55.

VanGeem, Martha. *Achieving Sustainability with Precast Concrete,* PCI Journal. Vol. 51 No 1, January/February 2006, pp 42-55.

VSL Post-Tensioning Systems, http://www.vsl.net/. 2006. http://www.vsl.net/construction_systems/post_tensioning.html, Accessed January 31, 2007.

Yamane, Takashi, Tadros, Maher, Badie, Sameh, and Baishya, Mantu. *Full Depth Precast, Prestressed Concrete Bridge Deck System,* PCI Journal. Vol. 42, No. 3, May/June 1998, pp 50-66.

APPENDIX A. TEST DATA

Table 24. Slump test results

Test Name	Slump (in.)	
	Precast Concrete	Grouted Concrete
ASC1	3	4.5
ASC2	3	4.5
ASO1	3	4.5
ASC3	3.75	3.5
ASO2	3.75	3.5
ADC1	3.5	4.0
ADC2	3.5	4.0
PSC1	3.75	3.5

ASC1 Results: Figure 150 through Figure 152

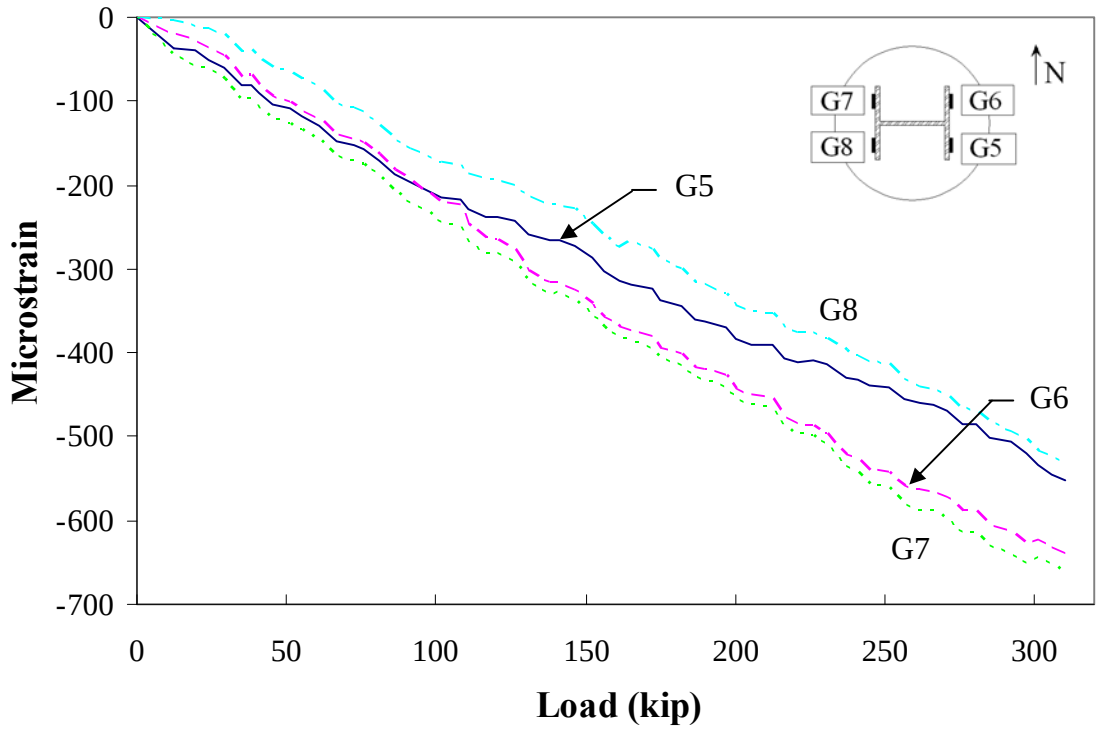

Figure 150. Steel strain for ASC1

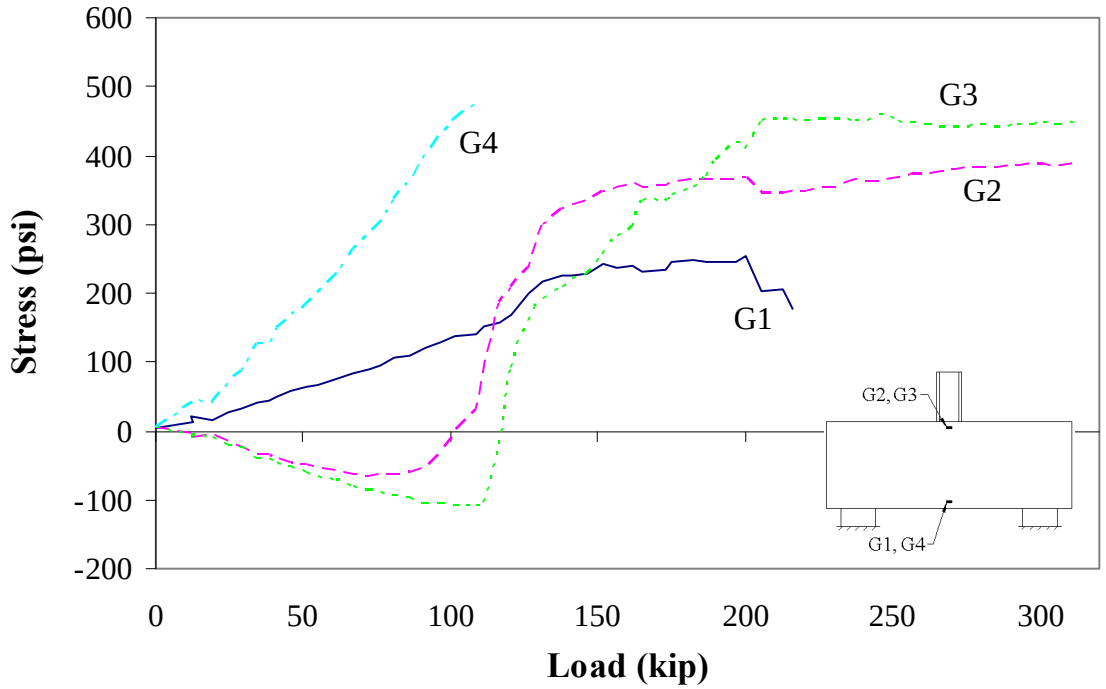

Figure 151. Concrete stress in ASC1

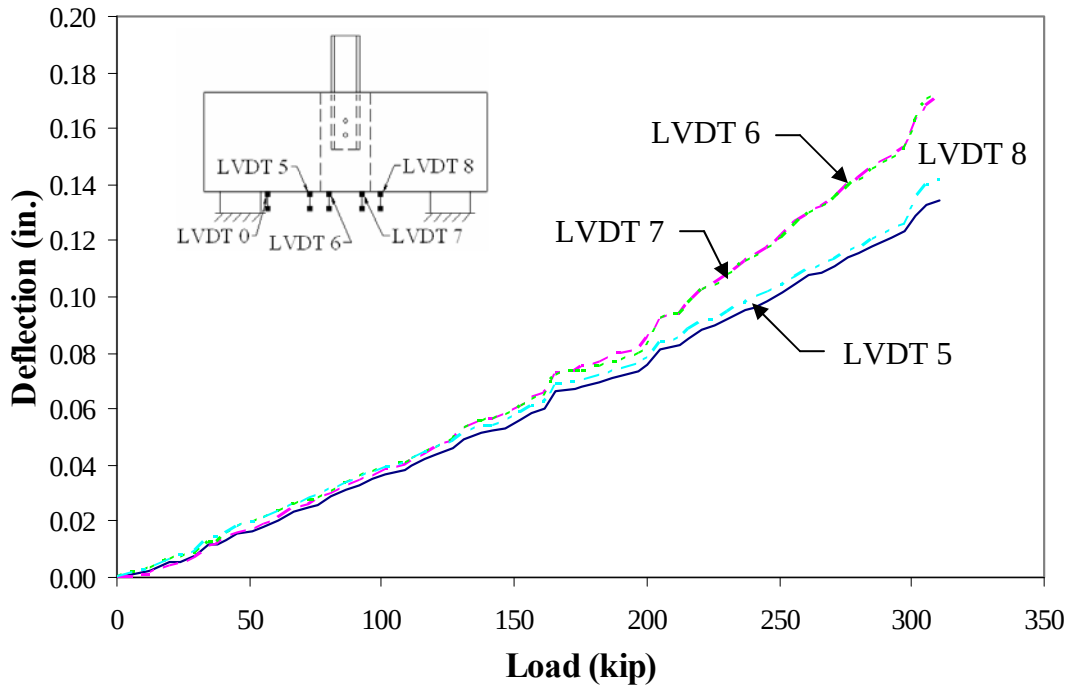

Figure 152. Total deflection for ASC1

ASC2 Results: Figure 153 through Figure 155

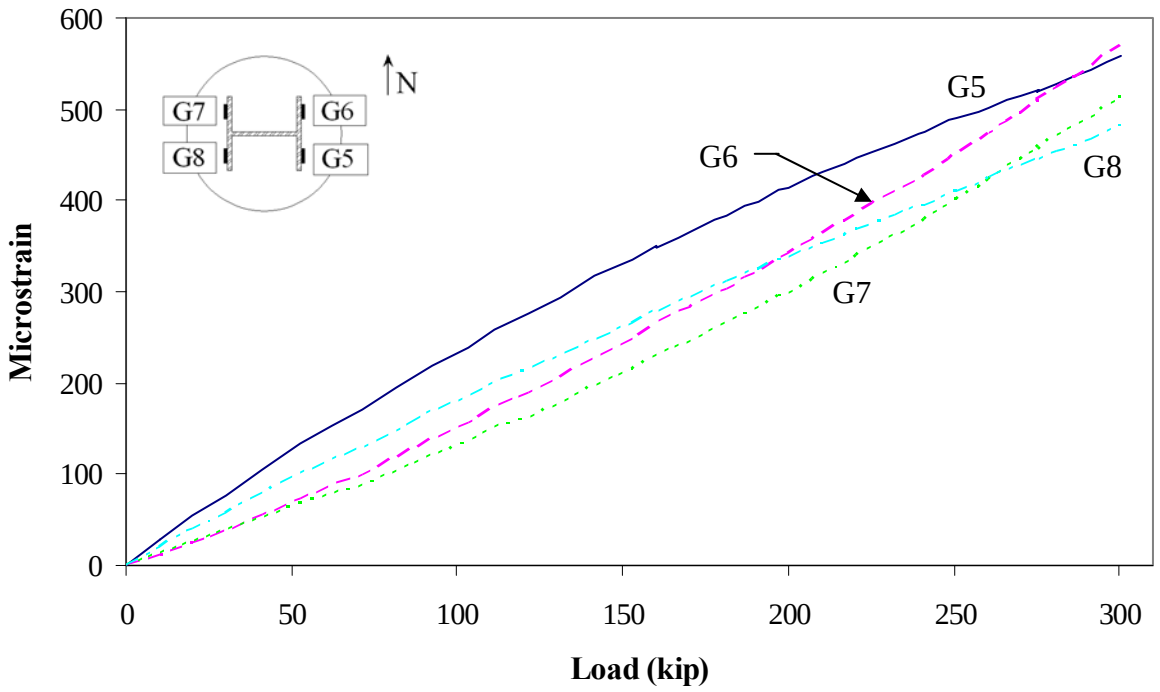

Figure 153. Steel strain for ASC2

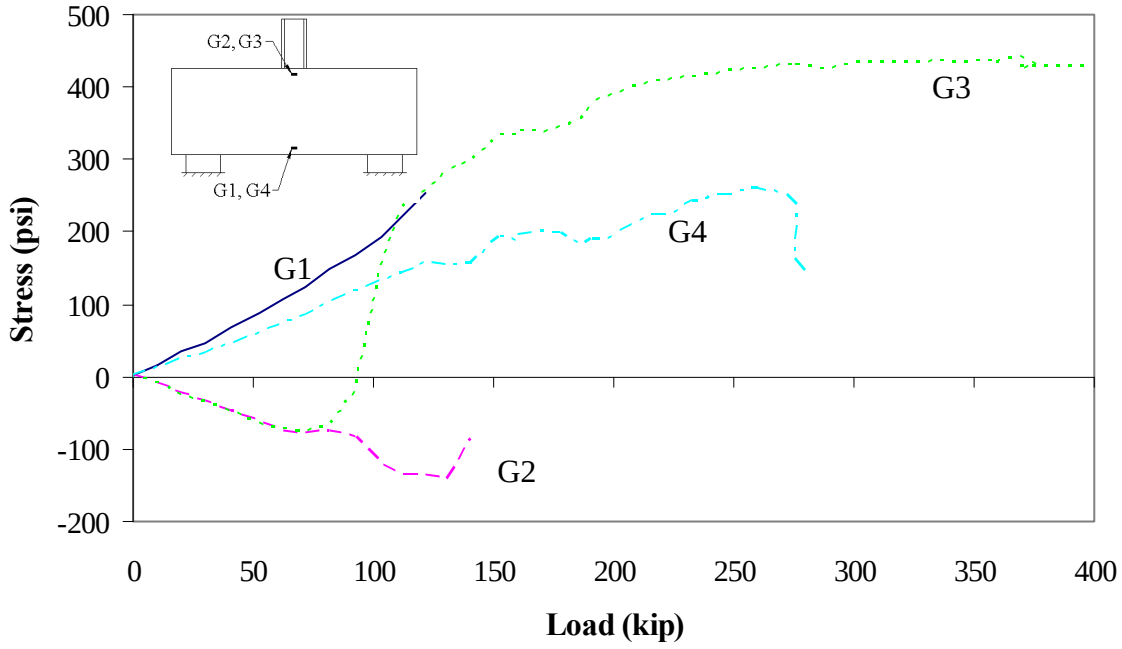

Figure 154. Concrete stress in ASC2

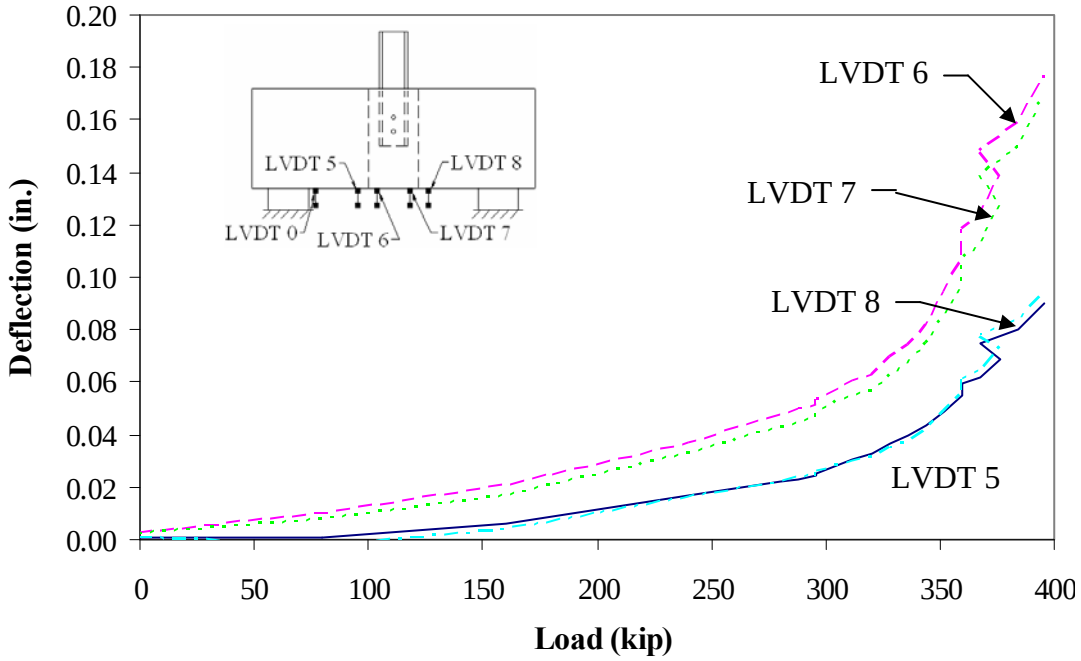

Figure 155. Total deflection for ASC2

ASO1 Results: Figure 156 through Figure 158

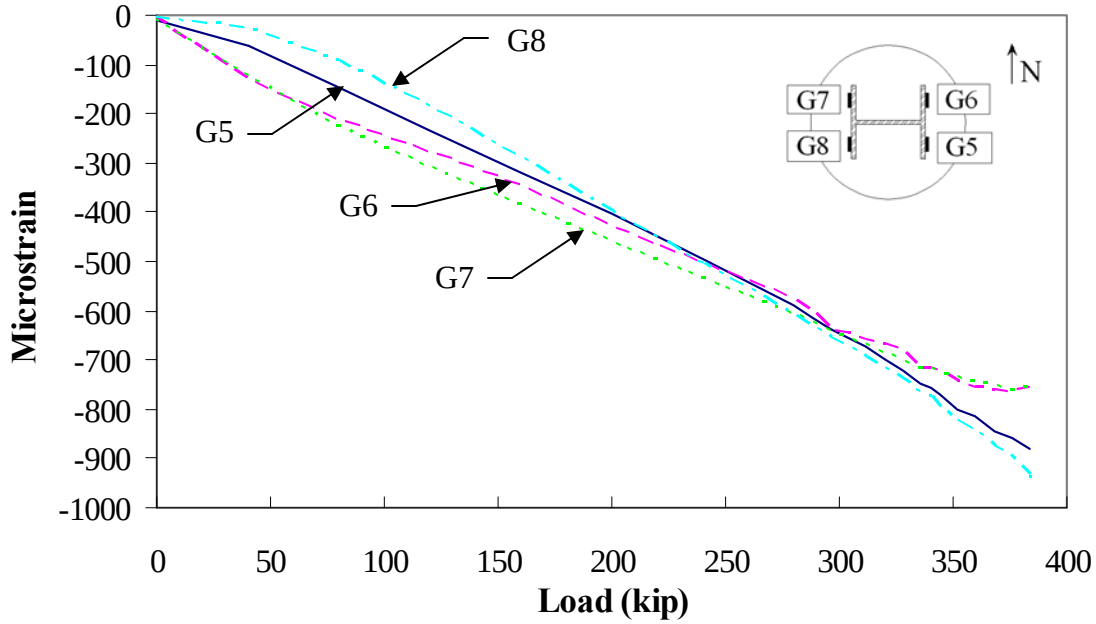

Figure 156. Steel strain for ASO1

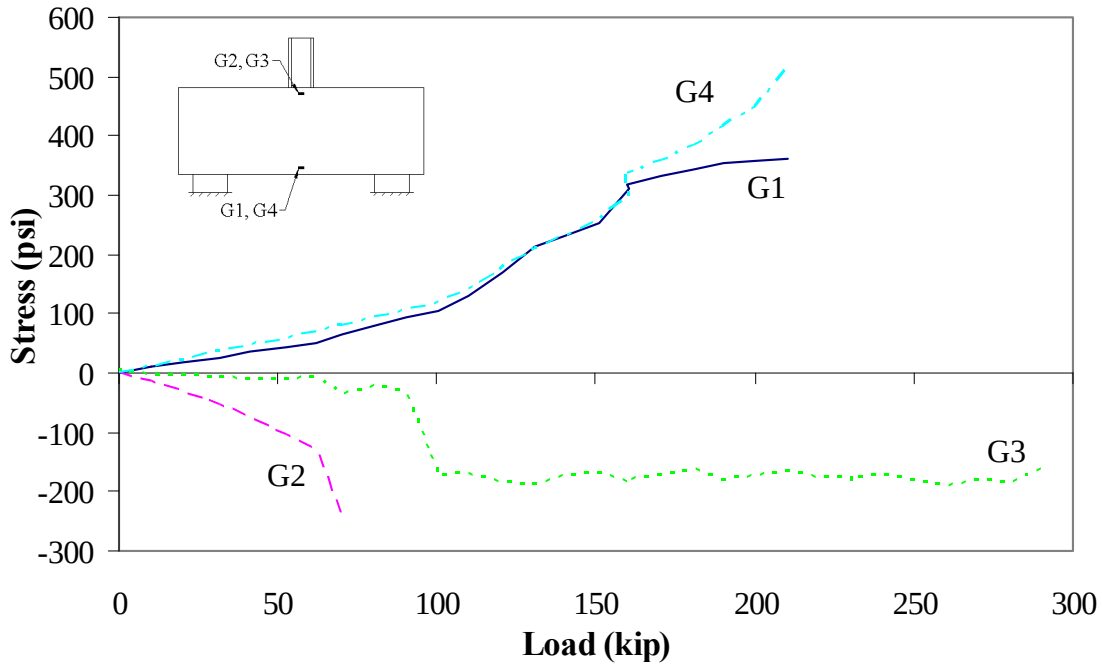

Figure 157. Concrete stress for ASO1

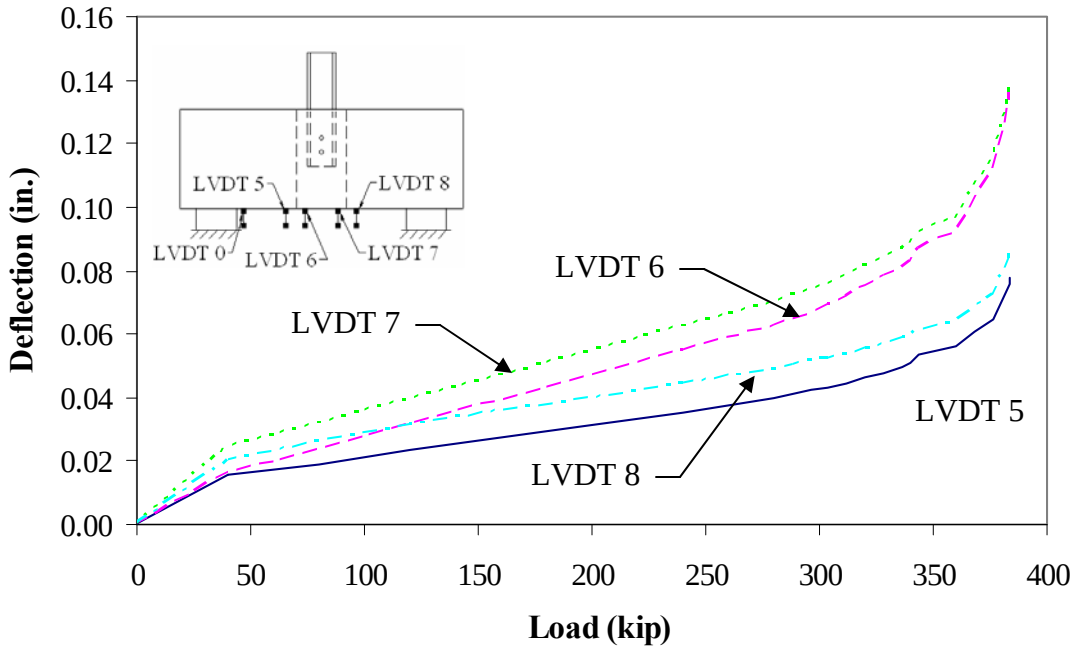

Figure 158. Total deflection for ASO1

ADC2 Results: Figure 159 through Figure 164

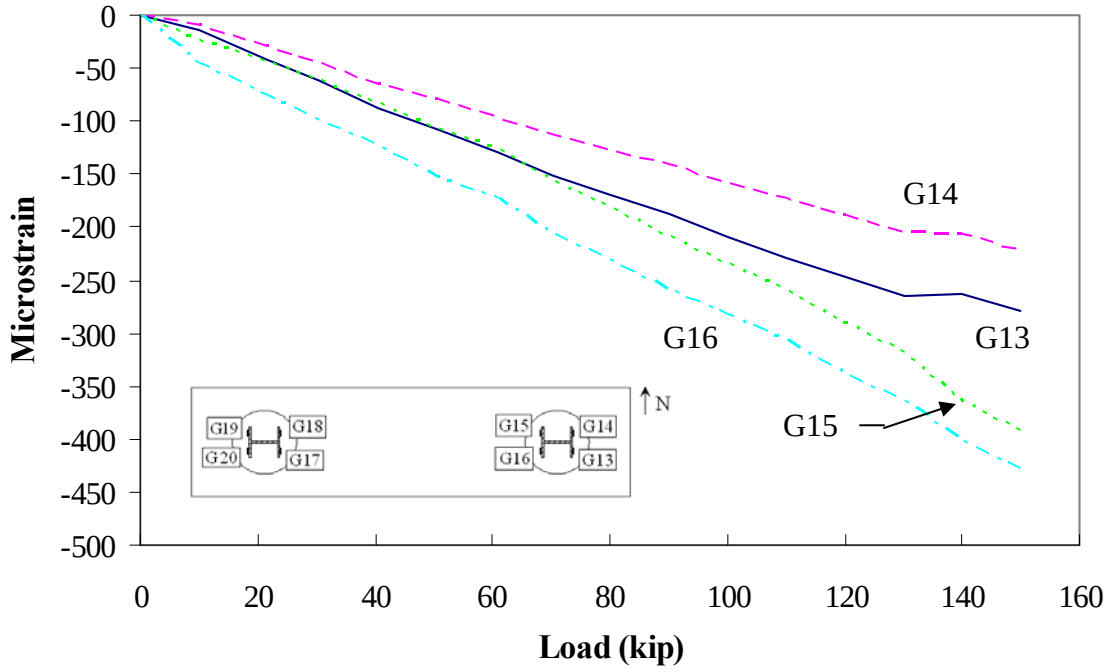

Figure 159. East pile steel strain for ADC2

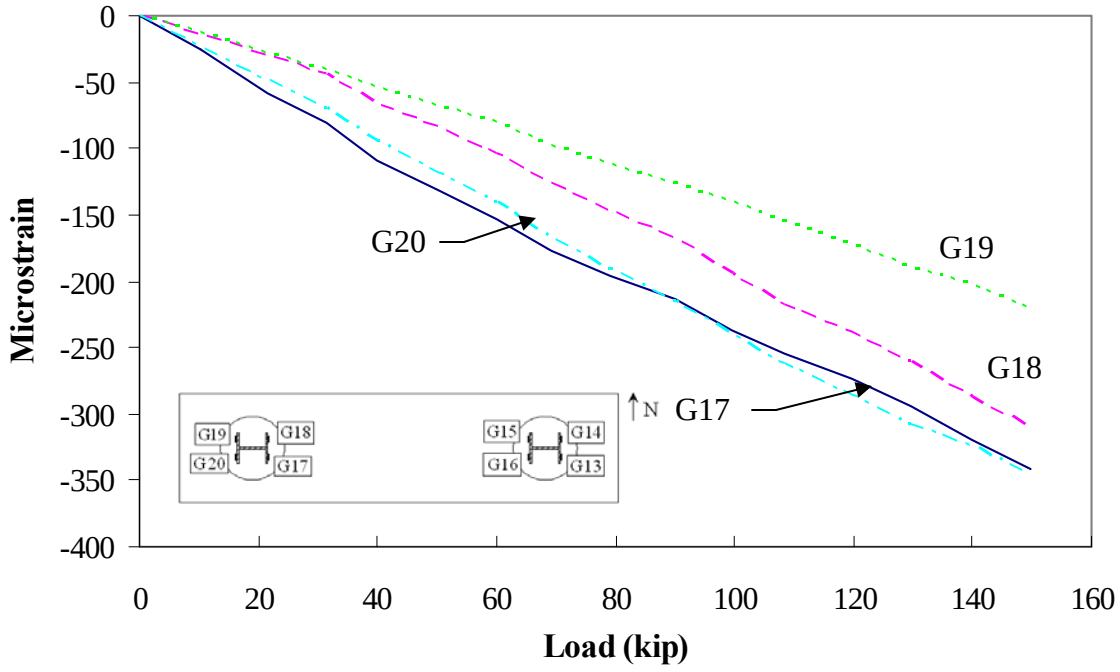

Figure 160. West pile steel strains for ADC2

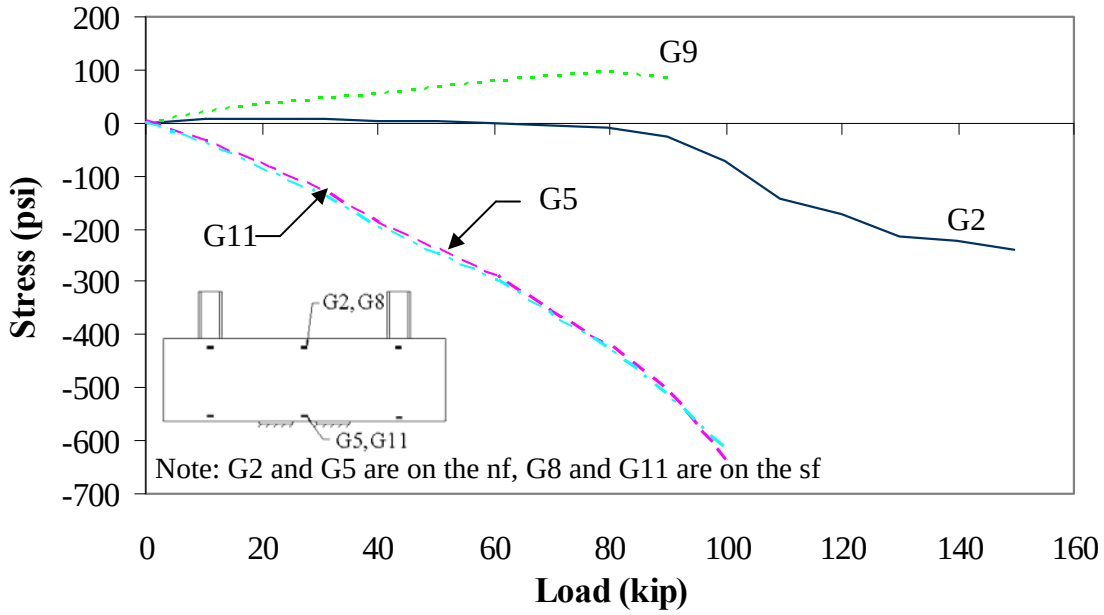

Figure 161. Concrete stresses at the center of ADC2

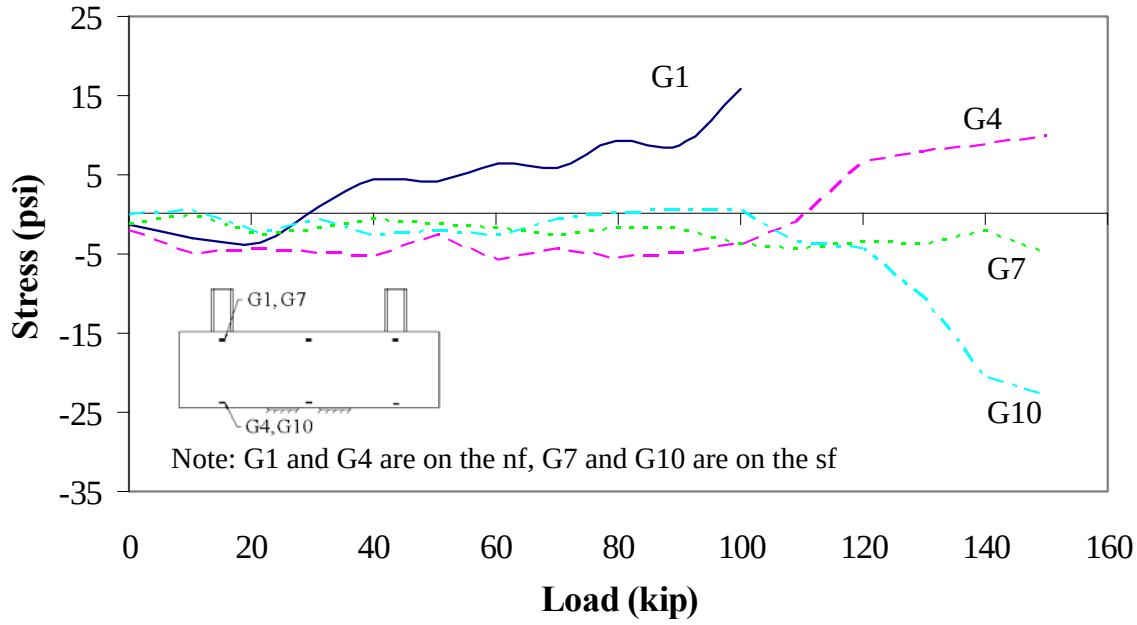

Figure 162. Concrete stresses at the east pile of ADC2

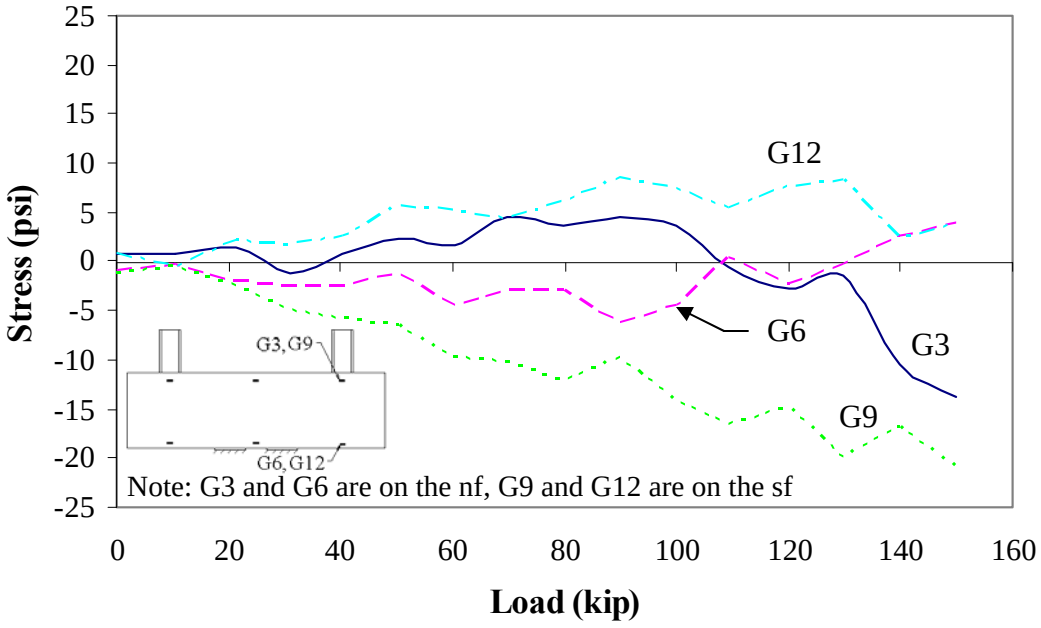

Figure 163. Concrete stresses at the west pile of ADC2

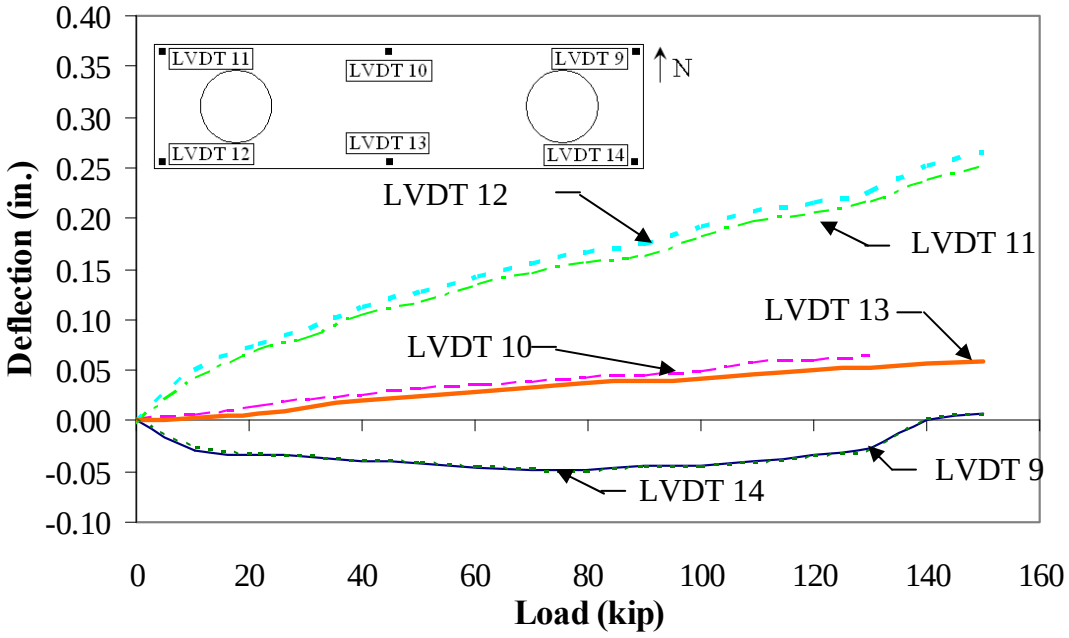

Figure 164. Total deflections for ADC2

Shear Test 2 Results: Figure 165 through Figure 167

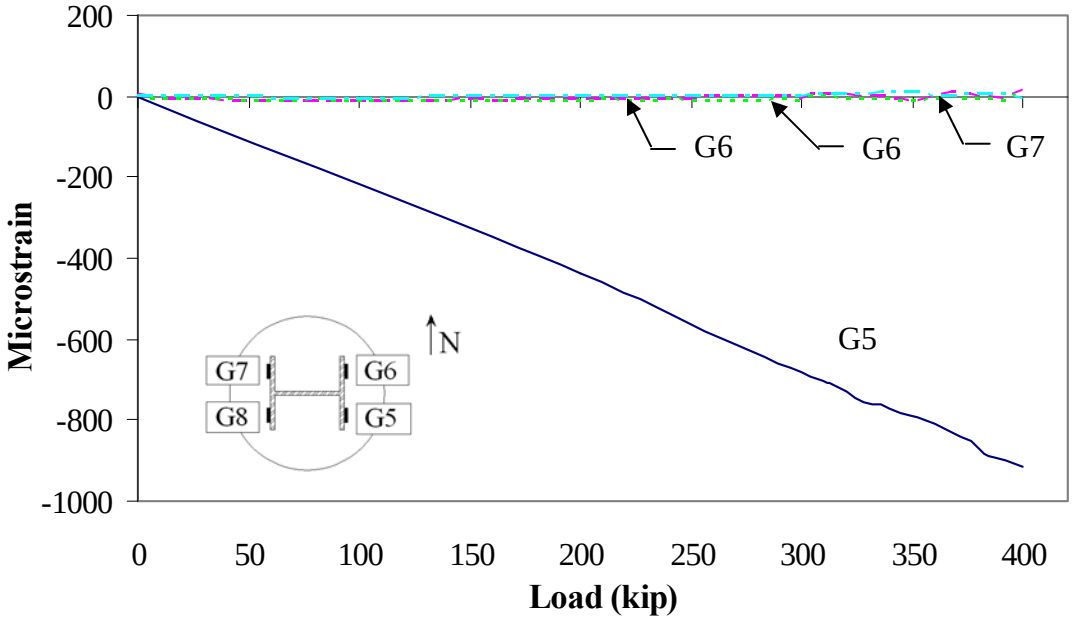

Figure 165. Steel strain for Shear Test 2

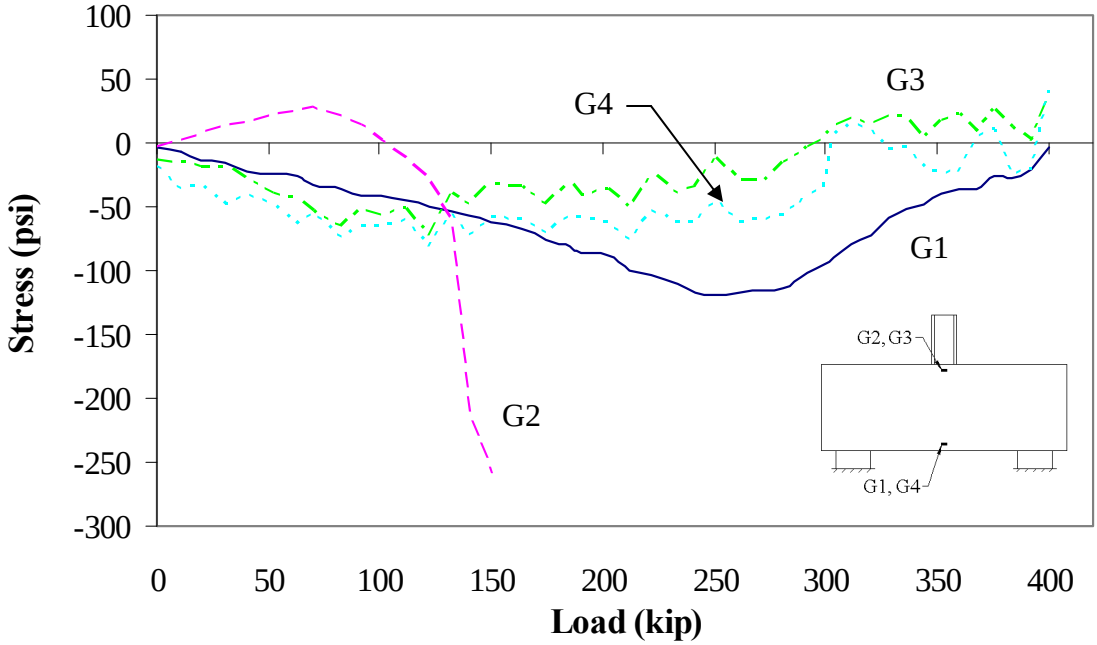

Figure 166. Concrete stress for Shear Test 2

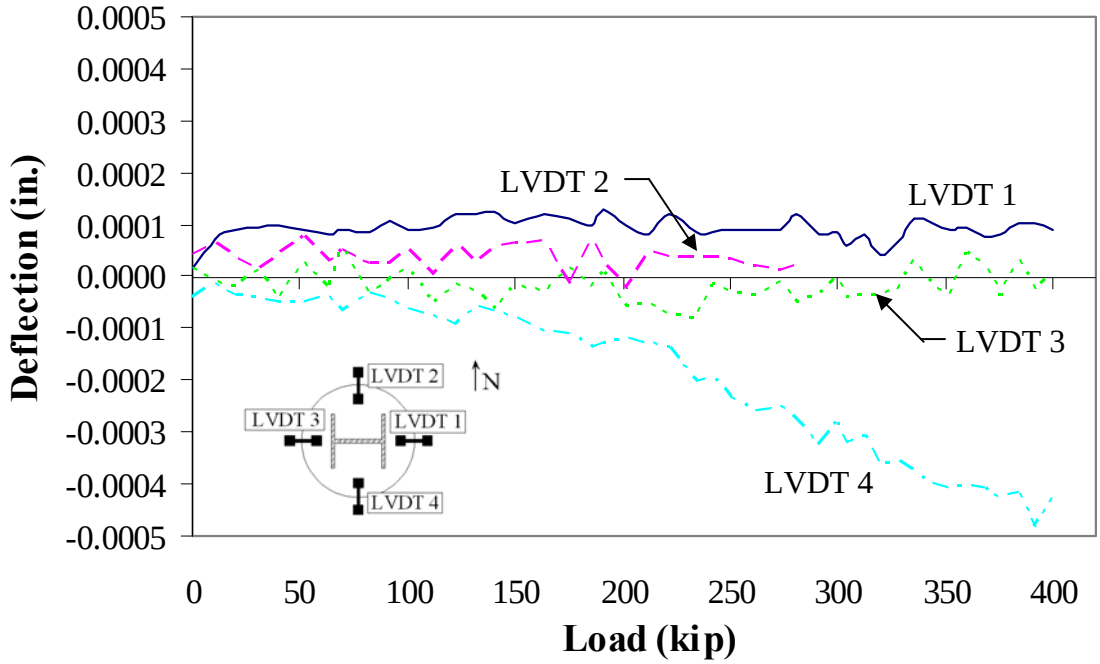

Figure 167. Top deflection for Shear Test 2

Shear Test 3 Results: Figure 168 through Figure 170

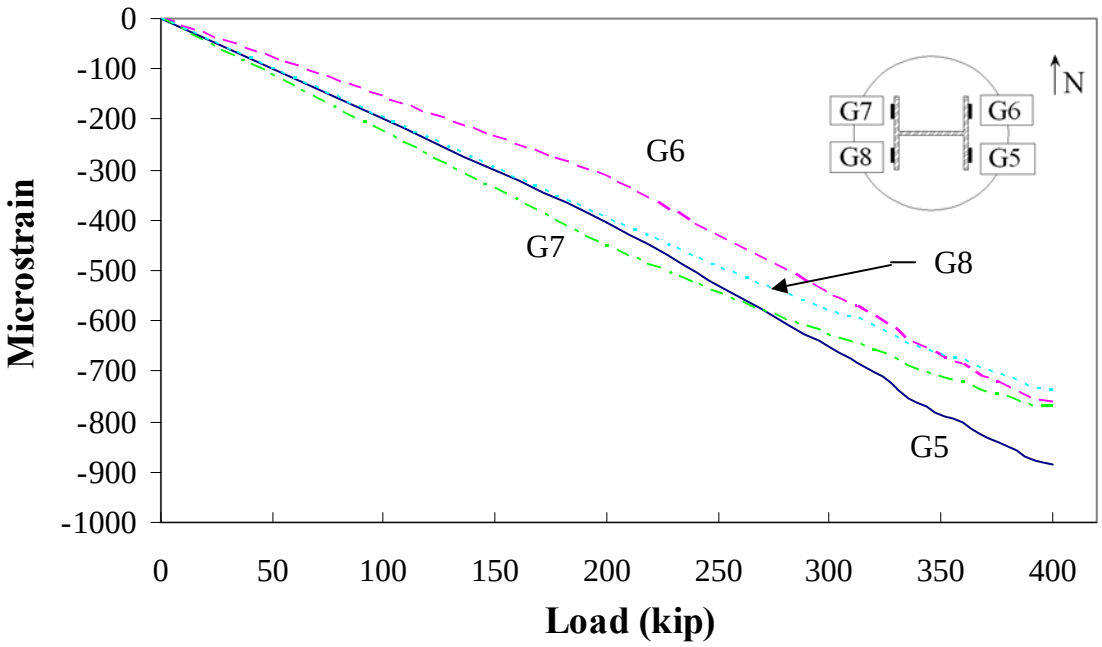

Figure 168. Steel strain for Shear Test 3

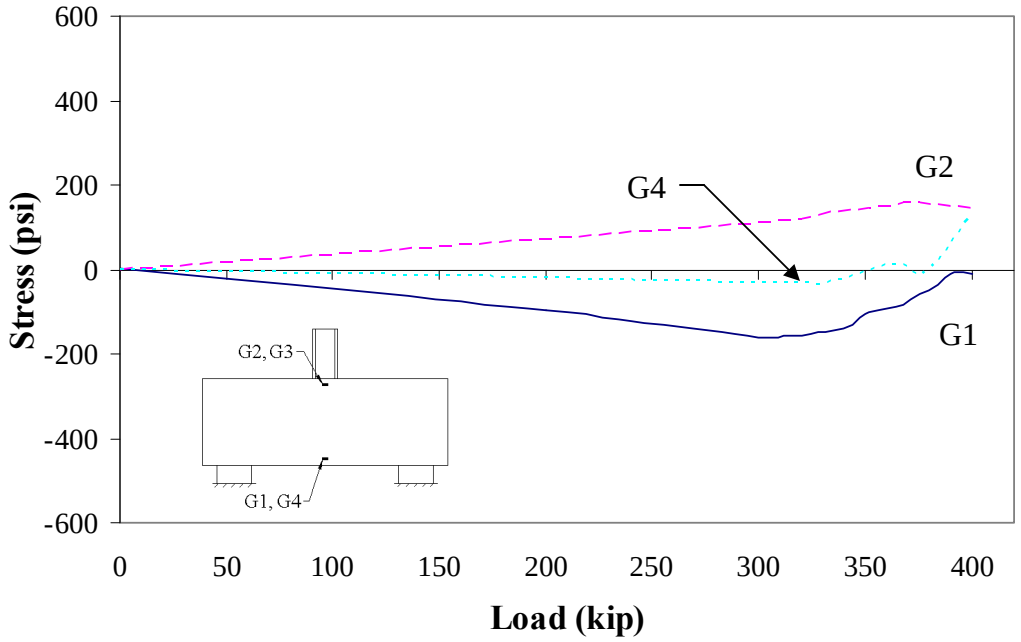

Figure 169. Concrete stress for Shear Test 3

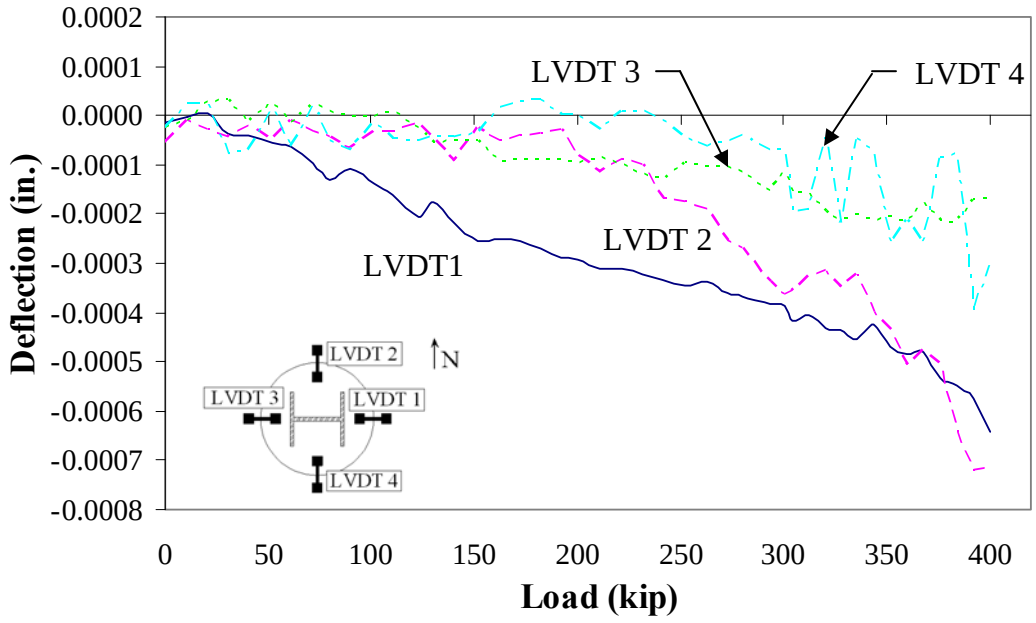

Figure 170. Top deflection for Shear Test 3

Shear Test 4 Results: Figure 171 through Figure 173

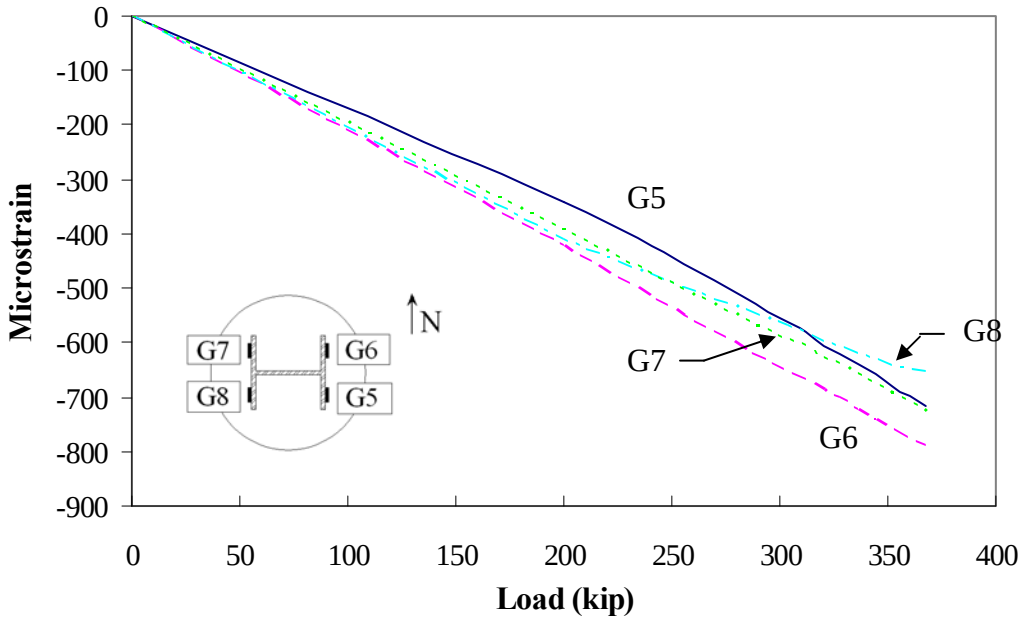

Figure 171. Steel strain for Shear Test 4

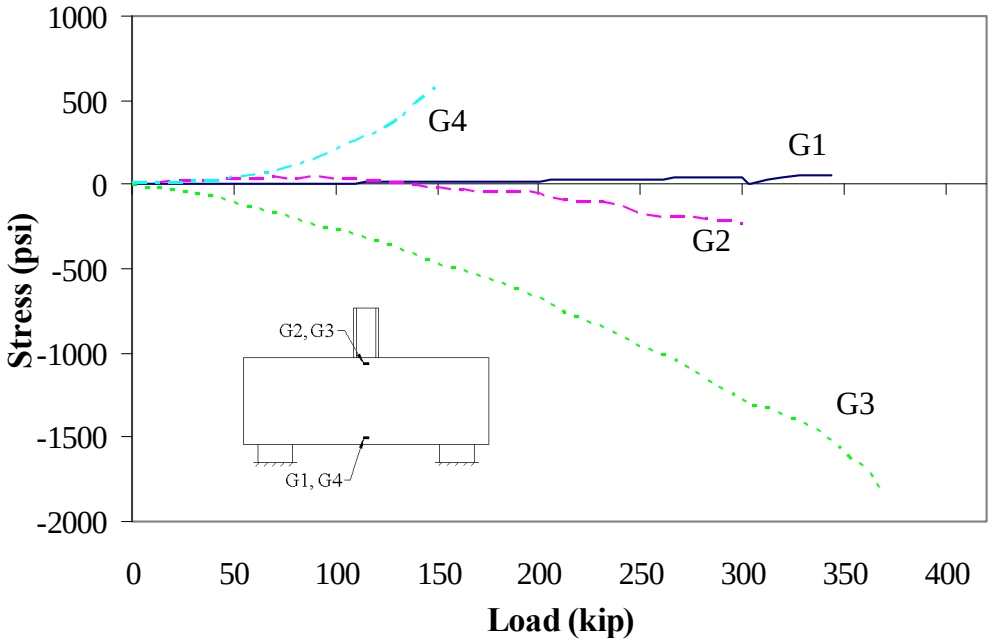

Figure 172. Concrete stress for Shear Test 4

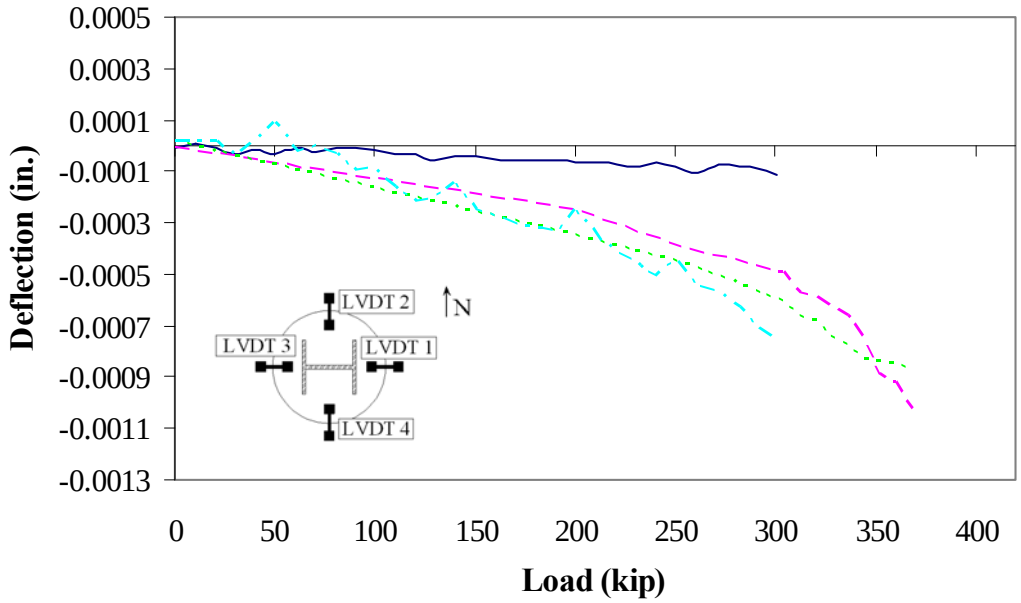

Figure 173. Top deflection for Shear Test 4

Post-Tensioning Test Data: Table 25 through Table 34

Table 25. Post-tensioned strand vibrating wire gage information

Gage Number	Correction (in/digit)	Serial Number
1	0.00002397	06-22965
2	0.00002456	06-22962
3	0.00002453	06-22964
4	0.00002468	06-22961
5	0.00002444	06-22960
6	0.00002457	06-22966
7	0.00002461	06-22959

Table 26. Gage 1 original post-tensioning data

Reading Number	R (Digits)	K	T (ºC)
0	2573.7	-	15.6
1	4681.8	7.443E-05	16.4
2	4677.9	7.440E-05	16.9
3	4654.2	7.423E-05	17.8
4	4650.0	7.421E-05	17.8
5	4646.6	7.418E-05	18.5
6	4646.5	7.418E-05	18.3
7	4643.5	7.416E-05	19.0
8	4627.6	7.405E-05	19.8

Table 27. Gage 2 original post-tensioning data

Reading Number	R (Digits)	K	T (ºC)
0	2581.3	-	15.4
1	4618.2	7.580E-05	16.5
2	4609.4	7.574E-05	17.0
3	4585.6	7.557E-05	17.8
4	4580.2	7.553E-05	17.7
5	4577.4	7.551E-05	18.4
6	4577.7	7.551E-05	18.3
7	4574.1	7.548E-05	18.9
8	4558.5	7.537E-05	19.6

Table 28. Gage 3 original post-tensioning data

Reading Number	R (Digits)	K	T (ºC)
0	2408.1	-	15.5
1	4464.6	7.460E-05	16.7
2	4455.4	7.453E-05	17.1
3	4414.8	7.424E-05	17.6
4	4406.9	7.418E-05	17.7
5	4404.4	7.416E-05	18.3
6	4404.4	7.416E-05	18.3
7	4400.8	7.414E-05	18.7
8	4375.6	7.395E-05	19.3

Table 29. Gage 4 original post-tensioning data

Reading Number	R (Digits)	K	T (ºC)
0	2533.3	-	15.6
1	4564.3	7.578E-05	16.7
2		4.255E-05	17.1
3	4533.9	7.556E-05	18.1
4		4.255E-05	18.1
5		4.255E-05	18.8
6	4520.5	7.546E-05	18.7
7	4517.2	7.544E-05	19.3
8	1500.0	5.347E-05	19.8

Table 30. Gage 5 original post-tensioning data

Reading Number	R (Digits)	K	T (ºC)
0	2372.3	-	15.4
1	2390.7	5.937E-05	16.3
2	4425.2	7.404E-05	16.7
3	4413.3	7.395E-05	17.3
4	4410.6	7.393E-05	17.6
5	4402.3	7.387E-05	18.3
6	4402.6	7.388E-05	18.1
7	4401.1	7.387E-05	18.6
8	4385.5	7.375E-05	19.5

Table 31. Gage 6 original post-tensioning data

Reading Number	R (Digits)	K	T (ºC)
0	2302.1	-	15.5
1	2325.3	5.921E-05	16.5
2	2349.6	5.939E-05	16.9
3	2349.7	5.939E-05	17.5
4	2266.5	5.879E-05	17.7
5	2269.4	5.881E-05	18.1
6	4339.5	7.381E-05	18.0
7	4337.1	7.379E-05	18.4
8	4333.5	7.377E-05	19.0

Table 32. Gage 7 original post-tensioning data

Reading Number	R (Digits)	K	T (ºC)
0	2598.8	-	15.4
1	2652.1	6.168E-05	16.4
2	2652.5	6.168E-05	16.7
3	2654.5	6.170E-05	17.5
4	2641.6	6.161E-05	17.5
5	4637.0	7.609E-05	18.0
6	4631.4	7.605E-05	18.0
7	4617.2	7.595E-05	18.4
8	4604.4	7.586E-05	18.8

Table 33. Final post-tensioning strand vibrating wire gage data

Gage	Final Reading (Digits)	Final Temperature (°C)
1	4627.6	17.3
2	4558.5	17.2
3	4375.6	16.9
4	4517.1	17.3
5	4385.5	17.0
6	4333.5	16.7
7	4604.4	16.6

Table 34. Final post-tensioning deck panel vibrating wire gage data

Gage	Final Reading (μ-strain)
A1	377
A2	378
B2	368
B3	370
C1	368
C2	365
C3	375
C4	363
D1	378
D2	372
D3	361

APPENDIX B. SUPPLEMENTAL POST-TENSIONING DATA AND CONSTRUCTION FEEDBACK

Summary of post-tensioning: Table 35 through Table 38
Document 1 through Document 3

Table 35. Channel 1 summary

PETERSON CONTRACTORS INC

PCI Job Number: J1692

IDOT Project Number: IBRC-C008(39)--8E-08

Date: November 28, 2006

Span: Far South

Tendon Number	Initial Tension		Final Tension		Final Elongation
	Kips	Gage Reading	Kips	Gage Reading	Measurement
T1	8.2 K	1040 psi	41 K	5300 psi	9-1/4"
T2	8.2 K	1040 psi	41 K	5300 psi	9-1/4"
T3	8.2 K	1040 psi	41 K	5300 psi	9"
T4	8.2 K	1040 psi	41 K	5300 psi	9"
T5	8.2 K	1040 psi	41 K	5300 psi	8-7/8"
T6	8.2 K	1040 psi	41 K	5300 psi	9"
T7	8.2 K	1040 psi	41 K	5300 psi	8-7/8"
T8	8.2 K	1040 psi	41 K	5300 psi	8-7/8"
T9	8.2 K	1040 psi	41 K	5300 psi	9"
T10	8.2 K	1040 psi	41 K	5300 psi	9"
T11	8.2 K	1040 psi	41 K	5300 psi	8-7/8"
T12	8.2 K	1040 psi	41 K	5300 psi	8-7/8"

PCI Representative: Justin A. Clausen

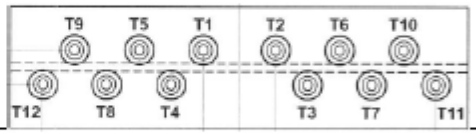

NOTES:

All Tension pulled from West End of Bridge

Tendon T1 was first tendon tensioned. Moved to East End of bridge to check tension. Jacked until 5300 psi on gage.

Measured 1/8" movement at 5300 psi.

Table 36. Channel 2 summary

PETERSON CONTRACTORS INC

PCI Job Number: J1692

IDOT Project Number: IBRC-C008(39)--8E-08

Date: November 28, 2006

Span: Mid South

Tendon Number	Initial Tension		Final Tension		Final Elongation
	Kips	Gage Reading	Kips	Gage Reading	Measurement
T1	8.2 K	1040 psi	41 K	5300 psi	9"
T2	8.2 K	1040 psi	41 K	5300 psi	8-7/8"
T3	8.2 K	1040 psi	41 K	5300 psi	9"
T4	8.2 K	1040 psi	41 K	5300 psi	8-3/4"
T5	8.2 K	1040 psi	41 K	5300 psi	9-1/8"
T6	8.2 K	1040 psi	41 K	5300 psi	8-7/8"
T7	8.2 K	1040 psi	41 K	5300 psi	8-7/8"
T8	8.2 K	1040 psi	41 K	5300 psi	9"
T9	8.2 K	1040 psi	41 K	5300 psi	8-7/8"
T10	8.2 K	1040 psi	41 K	5300 psi	9"
T11	8.2 K	1040 psi	41 K	5300 psi	9"
T12	8.2 K	1040 psi	41 K	5300 psi	8-7/8"

PCI Representative: Justin A. Clausen

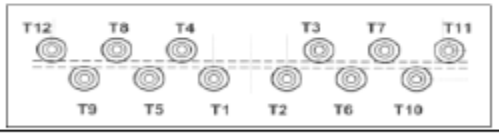

NOTES:

All Tension pulled from West End of Bridge

Table 37. Channel 3 summary

PETERSON CONTRACTORS INC

PCI Job Number: J1692

IDOT Project Number: IBRC-C008(39)--8E-08

Date: November 28, 2006

Span: Mid North

Tendon Number	Initial Tension		Final Tension		Final Elongation
	Kips	Gage Reading	Kips	Gage Reading	Measurement
T1	8.2 K	1040 psi	41 K	5300 psi	8-7/8"
T2	8.2 K	1040 psi	41 K	5300 psi	9-1/4"
T3	8.2 K	1040 psi	41 K	5300 psi	9-1/8"
T4	8.2 K	1040 psi	41 K	5300 psi	8-7/8"
T5	8.2 K	1040 psi	41 K	5300 psi	8-7/8"
T6	8.2 K	1040 psi	41 K	5300 psi	9"
T7	8.2 K	1040 psi	41 K	5300 psi	8-7/8"
T8	8.2 K	1040 psi	41 K	5300 psi	9"
T9	8.2 K	1040 psi	41 K	5300 psi	8-7/8"
T10	8.2 K	1040 psi	41 K	5300 psi	8-3/4"
T11	8.2 K	1040 psi	41 K	5300 psi	8-3/4"
T12	8.2 K	1040 psi	41 K	5300 psi	9"

PCI Representative: Justin A. Clausen

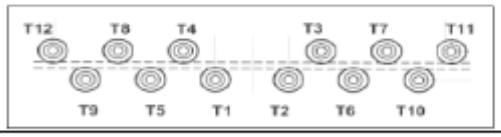

NOTES:

All Tension pulled from West End of Bridge

Table 38. Channel 4 summary

PETERSON CONTRACTORS INC

PCI Job Number: J1692

IDOT Project Number: IBRC-C008(39)--8E-08

Date: November 28, 2006

Span: Far North

Tendon Number	Initial Tension		Final Tension		Final Elongation
	Kips	Gage Reading	Kips	Gage Reading	Measurement
T1	8.2 K	1040 psi	41 K	5300 psi	9-1/8"
T2	8.2 K	1040 psi	41 K	5300 psi	9-1/8"
T3	8.2 K	1040 psi	41 K	5300 psi	9-1/8"
T4	8.2 K	1040 psi	41 K	5300 psi	9"
T5	8.2 K	1040 psi	41 K	5300 psi	8-7/8"
T6	8.2 K	1040 psi	41 K	5300 psi	9"
T7	8.2 K	1040 psi	41 K	5300 psi	8-3/4"
T8	8.2 K	1040 psi	41 K	5300 psi	8-3/4"
T9	8.2 K	1040 psi	41 K	5300 psi	8-7/8"
T10	8.2 K	1040 psi	41 K	5300 psi	9"
T11	8.2 K	1040 psi	41 K	5300 psi	8-3/4"
T12	8.2 K	1040 psi	41 K	5300 psi	8-1/8" + 5/8" = 8-3/4"

PCI Representative: Justin A. Clausen

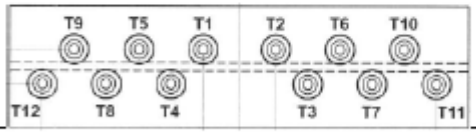

NOTES:

All Tension pulled from West End of Bridge

Tendon T12 same pulled from West end to required capacity 5300 psi = 41 kips, but only read 8-1/8" elongation.

Moved to East end of bridge and checked tension. Gage read 5300 psi. Increased tension to 5500 psi and tension cable "popped". Gage pressures fell but reading was not recorded. Gage pressure was brought back up to required tension (5300 psi) and elongation increased by 5/8", bringing overall elongation to 8-3/4".

Document 1. Mono-jack and post-tensioning force certification

The Pro-Firm, L.C.
Repairing the earth and the structures on it.

11-30-06

Peterson Contractors Inc.
104 Blackhawk Street
Reinbeck, Iowa 50669

Re: Bridge Deck Handling and Erection
Boone County Bridge and Approaches –PPCB
On 120th Street over Squaw Creek
IBRC-C008(39)—8E-08
Boone County, Iowa

Attn: Justin Clausen

Dear Justin:

This letter is to certify that I personally supervised the stressing of 48 - .6" diameter 270 ksi cable for the above referenced project. The cable run longitudinal with the bridge with 12 cable in each of 4 pour strips. All cables with stressed to 41000 lbs based on a gage pressure of 5300 psi. The elongations were recorded to verify strain in each cable. All recorded elongation were within the +/- 5% allowable by code. Jack calibrations dated 11-17-06 were presented to me certifying the load to pressure corralation.

In conclusion, all 48 cable were stressed to 41000 lbs +/- 1000 lbs

Sincerely;

Greg J. Gear P.E.
Structural Engineer
Iowa Registration No. 9377

Post-it® Fax Note 7671	Date 11-30-06	# of pages ▶ 1
To JUSTIN CLAUSEN	From GREG GEAR	
Co./Dept.	Co.	
Phone #	Phone #	
Fax #	Fax #	

☐ Henry D. Feeken, Manager
1449 NW 122nd St., Clive, IA 50325
Ph. (515) 223-9326
Fax (515) 225-4483

☑ Greg J. Gear, P.E., Manager
5020 Grand Ave., W Des Moines, IA 50265
Ph. (515) 221-9291
Fax (515) 221-9683

☐ Tammy Gear, Sales Consultant
529 4th St.,W Des Moines, IA 50265
Ph. (515) 255-2514
Fax (515) 277-8552

Document 2. Construction feedback from PCI

PETERSON CONTRACTORS, INC.

ADDRESS REPLY TO:
104 BLACKHAWK STREET
P.O. BOX A
REINBECK, IOWA 50669

HEAVY & HIGHWAY CONTRACTORS

PHONE: (319) 345-2713
FAX: (319) 345-2658

January 15, 2007

Boone County Bridge and Approaches on 120th St. over Squaw Creek.
IBRC-C008(39)—8E(08)

THINGS TO CHANGE:

- Better handle on mix design including any admixtures for small grout joints.
- Use a beam with a wider top flange so that the post-tensioning channel can be wider.
- Modify pier diaphragm pour so that all panels can be set and not have to be removed.
- Let the project earlier to allow all shop drawings to be approved and thus panels to be manufactured in time to take advantage of fast tracked construction. Do not rely strictly on quoted time frames to make panels and typically shop drawing turn around time frame. PCI made this point to DOT contracts office prior to the letting of the project. Because this is such a new system, the shop drawing/review/fabrication will take longer than anyone anticipates. It does not hurt to let the project early and allow the fabrication to happen so that the time needed to erect the few bridge will be more appealing to utilize this type of structure in the future.
- Plan the letting, fabrication, and erection schedule so that the colder weather is not a problem. The cold weather was a huge problem for this project. Let the project in the fall, use the winter to perform shop drawings/review, make panels in late winter/early spring, and construct late spring/early winter. This sort of time frame will miss the cold weather concreting of the small joints, allow the existing roadway to remain open longer prior to bridge replacement, and utilize the fast tracked progress of construction to its full potential.
- Review the end panel anchorage zones. I believe that shop drawings modified the zones to all the strands to bend easier.
- Possibly think about an overlay layer on bridge.

THINGS TO KEEP THE SAME:

- Panel sizes worked out well.
- Precast pier caps worked well.
- Precast abutments worked well.
- Post tensioning worked very well.
- Let the contractor choose how to level the panels. We went through a lot of different scenarios, but ultimately, everyone will choose a different way.

Please feel free to contact me should you have any questions or wish for more information regarding details of the project.

Respectfully,

Justin A. Clausen
Project Manager
Peterson Contractors Inc.

Document 3. Construction feedback from Andrews Prestressed Concrete

WebMAIL

From the desk of...
Samantha Hockerman

From: "Teresa Nelson" <tnelson@andrewsprestressedconcrete.com>
Wed, 7 Feb 2007 09:16:28 -0600
Boone Feedback

Positive
ISU and Contractor were easy to work with.
Resolving such matters as clearance issues due to mistakes or oversights in plans, i.e. placement of D14 wires fabric, placement of holes in end panels for tensioned strand and quantity and placement of inspection holes in end panels.

Negative

Would possibly look into a larger size mesh in end panels to allow for larger openings to aid in placement and consolidation of concrete.
Would suggest a different design on Jacking/tensioning plate on end panels.
Possibly larger diameter holes to allow pipe sleeves to pass thru in lieu of butting against the plate.
The plate was not quite full depth of the panel. This made it very difficult to assure that it was suspended off of the bed.

Teresa Nelson
Estimator/Project Manager
Andrews Prestressed Concrete, Inc
Ph. 641-357-5217
Cell-641-529-0026
Fax-641-357-8044

Boone/Ames Weather Data: Table 49 through 51

Note: Weather data is for the Ames weather station, approximately 20 miles south east of the construction site.
Site Name: AMES
Site ID: A130209

Table 39. July rain totals

Date	Daily Precip (in.)
7/1/2006 0:00	0.08
7/2/2006 0:00	0.43
7/3/2006 0:00	0.13
7/4/2006 0:00	0
7/5/2006 0:00	0
7/6/2006 0:00	0
7/7/2006 0:00	0
7/8/2006 0:00	0
7/9/2006 0:00	0
7/10/2006 0:00	0.13
7/11/2006 0:00	0.75
7/12/2006 0:00	0.28
7/13/2006 0:00	0.13
7/14/2006 0:00	0.1
7/15/2006 0:00	0.07
7/16/2006 0:00	0.03
7/17/2006 0:00	0.02
7/18/2006 0:00	0
7/19/2006 0:00	0
7/20/2006 0:00	0
7/21/2006 0:00	0.07
7/22/2006 0:00	0
7/23/2006 0:00	0
7/24/2006 0:00	0.14
7/25/2006 0:00	0.08
7/26/2006 0:00	0.47
7/27/2006 0:00	0.12
7/28/2006 0:00	0.06
7/29/2006 0:00	0.04
7/30/2006 0:00	0.01
7/31/2006 0:00	0
Sum:	3.14

Table 40. August rain totals

Date	Daily Precip (in.)
8/1/2006 0:00	0.18
8/2/2006 0:00	0.04
8/3/2006 0:00	0
8/4/2006 0:00	0
8/5/2006 0:00	0.14
8/6/2006 0:00	0.16
8/7/2006 0:00	0
8/8/2006 0:00	0
8/9/2006 0:00	0.19
8/10/2006 0:00	0.05
8/11/2006 0:00	0.05
8/12/2006 0:00	0.04
8/13/2006 0:00	0.05
8/14/2006 0:00	0.04
8/15/2006 0:00	0.04
8/16/2006 0:00	0.04
8/17/2006 0:00	0.05
8/18/2006 0:00	0.05
8/19/2006 0:00	0.05
8/20/2006 0:00	0.04
8/21/2006 0:00	0.06
8/22/2006 0:00	0.02
8/23/2006 0:00	0
8/24/2006 0:00	0
8/25/2006 0:00	0
8/26/2006 0:00	0
8/27/2006 0:00	0.23
8/28/2006 0:00	0.61
8/29/2006 0:00	0.1
8/30/2006 0:00	0.04
8/31/2006 0:00	0.04
Sum:	2.31

Table 41. September rain totals.

Date	Daily Precip (in.)
9/1/2006 0:00	0.04
9/2/2006 0:00	0.06
9/3/2006 0:00	0.05
9/4/2006 0:00	0.05
9/5/2006 0:00	0.06*
9/6/2006 0:00	0.07*
9/7/2006 0:00	0.08*
9/8/2006 0:00	0.04*
9/9/2006 0:00	0*
9/10/2006 0:00	1*
9/11/2006 0:00	0.22*
9/12/2006 0:00	0*
9/13/2006 0:00	0*
9/14/2006 0:00	0*
9/15/2006 0:00	0*
9/16/2006 0:00	0.72
9/17/2006 0:00	0.65
9/18/2006 0:00	0
9/19/2006 0:00	0
9/20/2006 0:00	0
9/21/2006 0:00	0.45
9/22/2006 0:00	0.02
9/23/2006 thru	0
9/28/2006 0:00	0
9/29/2006 0:00	0.01
9/30/2006 0:00	0.01
Sum:	3.53

*Note: The construction inspector noted the bridge site received over three inches of rain during the time period indicated.

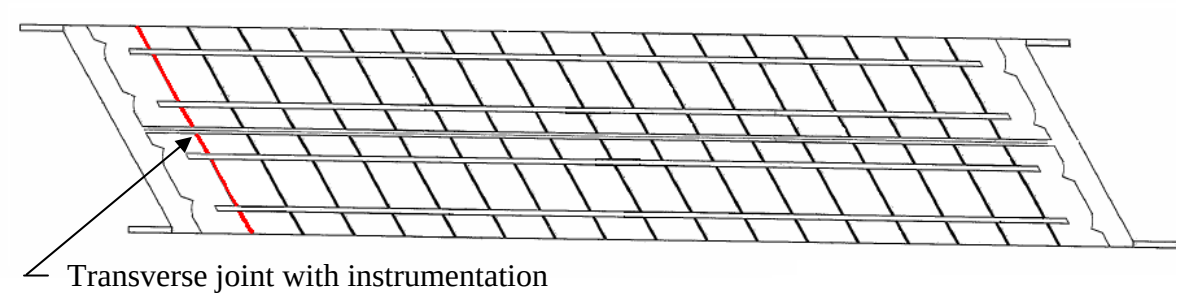

Figure 174. Location of west transverse joint with temperature instrumentation.

Table 42. West end panel transverse joint temperature data.

Reading Number	Time	Ambient Temp. (°C)	Cylinder Temp. (°C)	Joint Temp. (°C)	Ambient Temp. (°F)	Cylinder Temp. (°F)	Joint Temp. (°F)	Temp. Diff. Between Cylinder & Joint (°F)
1	11/16/06 2:30 PM	13.6	5.87	5.06	56.5	42.6	41.1	1.5
2	11/16/06 3:00 PM	12.6	6.65	6.34	54.7	44.0	43.4	0.6
3	11/16/06 3:30 PM	6.8	13.77	13.53	44.2	56.8	56.4	0.4
4	11/16/06 4:00 PM	7.6	15.83	12.31	45.7	60.5	54.2	6.3
5	11/16/06 4:30 PM	8	18.03	12.4	46.4	64.5	54.3	10.1
6	11/16/06 5:00 PM	7.8	19.34	12.51	46.0	66.8	54.5	12.3
7	11/16/06 5:30 PM	7.2	20.15	12.55	45.0	68.3	54.6	13.7
8	11/16/06 6:00 PM	6.7	20.39	12.56	44.1	68.7	54.6	14.1
9	11/16/06 6:30 PM	6.2	20.21	12.56	43.2	68.4	54.6	13.8
10	11/16/06 7:00 PM	5.7	20.48	12.69	42.3	68.9	54.8	14.0
11	11/16/06 7:30 PM	5.4	20.67	12.47	41.7	69.2	54.4	14.8
12	11/16/06 8:00 PM	5.2	20.5	12.39	41.4	68.9	54.3	14.6
13	11/16/06 8:30 PM	5	20.54	12.38	41.0	69.0	54.3	14.7
14	11/16/06 9:00 PM	5	20.79	12.26	41.0	69.4	54.1	15.4
15	11/16/06 9:30 PM	4.8	20.78	12.37	40.6	69.4	54.3	15.1
16	11/16/06 10:00 PM	4.8	20.9	12.12	40.6	69.6	53.8	15.8
17	11/16/06 10:30 PM	4.9	21.06	12.22	40.8	69.9	54.0	15.9
18	11/16/06 11:00 PM	5	21.16	11.93	41.0	70.1	53.5	16.6
19	11/16/06 11:30 PM	5.1	21.61	12.23	41.2	70.9	54.0	16.9
20	11/17/06 12:00 AM	5.1	21.92	12.03	41.2	71.5	53.7	17.8
21	11/17/06 12:30 AM	4.9	23.11	11.97	40.8	73.6	53.5	20.1
22	11/17/06 1:00 AM	4.2	24.13	11.71	39.6	75.4	53.1	22.4

Reading Number	Time	Ambient Temp. (°C)	Cylinder Temp. (°C)	Joint Temp. (°C)	Ambient Temp. (°F)	Cylinder Temp. (°F)	Joint Temp. (°F)	Temp. Diff. Between Cylinder & Joint (°F)
23	11/17/06 1:30 AM	3.9	23.82	11.79	39.0	74.9	53.2	21.7
24	11/17/06 2:00 AM	4.4	23.53	11.66	39.9	74.4	53.0	21.4
25	11/17/06 2:30 AM	4.4	22.83	12.1	39.9	73.1	53.8	19.3
26	11/17/06 3:00 AM	4.2	22.42	11.9	39.6	72.4	53.4	18.9
27	11/17/06 3:30 AM	4.1	21.87	11.93	39.4	71.4	53.5	17.9
28	11/17/06 4:00 AM	3.7	21.35	12.09	38.7	70.4	53.8	16.7
29	11/17/06 4:30 AM	3.3	20.78	12.27	37.9	69.4	54.1	15.3
30	11/17/06 5:00 AM	3.6	20.35	12.49	38.5	68.6	54.5	14.1
31	11/17/06 5:30 AM	3.8	19.92	12.63	38.8	67.9	54.7	13.1
32	11/17/06 6:00 AM	3.8	19.38	12.44	38.8	66.9	54.4	12.5
33	11/17/06 6:30 AM	3.2	18.94	12.1	37.8	66.1	53.8	12.3
34	11/17/06 7:00 AM	3.2	19.14	11.85	37.8	66.5	53.3	13.1
35	11/17/06 7:30 AM	3.8	18.75	11.44	38.8	65.8	52.6	13.2
36	11/17/06 8:00 AM	3.7	18.65	11.34	38.7	65.6	52.4	13.2
37	11/17/06 8:30 AM	3.3	18.44	11.01	37.9	65.2	51.8	13.4
38	11/17/06 9:00 AM	3.7	17.99	10.91	38.7	64.4	51.6	12.7
39	11/17/06 9:30 AM	3	16.97	10.71	37.4	62.5	51.3	11.3
40	11/17/06 10:00 AM	4.4	16.05	10.34	39.9	60.9	50.6	10.3
41	11/17/06 10:30 AM	6.4	16.15	10.25	43.5	61.1	50.5	10.6
42	11/17/06 11:00 AM	8.6	16.62	10.36	47.5	61.9	50.6	11.3
43	11/17/06 11:30 AM	9.1	16.81	10.48	48.4	62.3	50.9	11.4
44	11/17/06 12:00 PM	9.1	17.38	10.22	48.4	63.3	50.4	12.9
46	11/17/06 1:00 PM	9.2	17.45	10.7	48.6	63.4	51.3	12.2
47	11/17/06 1:30 PM	9.6	17.56	10.91	49.3	63.6	51.6	12.0

Reading Number	Time	Ambient Temp. (°C)	Cylinder Temp. (°C)	Joint Temp. (°C)	Ambient Temp. (°F)	Cylinder Temp. (°F)	Joint Temp. (°F)	Temp. Diff. Between Cylinder & Joint (°F)
48	11/17/06 2:00 PM	10	17.56	10.99	50.0	63.6	51.8	11.8
49	11/17/06 2:30 PM	10.4	17.92	11.26	50.7	64.3	52.3	12.0
50	11/17/06 3:00 PM	10.5	18.23	11.42	50.9	64.8	52.6	12.3
51	11/17/06 3:30 PM	9.9	18.31	11.65	49.8	65.0	53.0	12.0
52	11/17/06 4:00 PM	9.7	18.35	11.82	49.5	65.0	53.3	11.8
53	11/17/06 4:30 PM	9.5	18.37	12.12	49.1	65.1	53.8	11.3
54	11/17/06 5:00 PM	9.1	18.47	12.23	48.4	65.2	54.0	11.2
55	11/17/06 5:30 PM	9.3	18.2	12.17	48.7	64.8	53.9	10.9
56	11/17/06 6:00 PM	9.6	18.31	12.35	49.3	65.0	54.2	10.7
57	11/17/06 6:30 PM	9.7	17.98	12.26	49.5	64.4	54.1	10.3
58	11/17/06 7:00 PM	9.9	18.08	12.64	49.8	64.5	54.8	9.8
59	11/17/06 7:30 PM	9.4	18.31	12.72	48.9	65.0	54.9	10.1
60	11/17/06 8:00 PM	9.1	18.11	12.8	48.4	64.6	55.0	9.6
61	11/17/06 8:30 PM	8.8	18	12.75	47.8	64.4	55.0	9.5
62	11/17/06 9:00 PM	8.7	17.96	12.78	47.7	64.3	55.0	9.3
63	11/17/06 9:30 PM	8.6	17.8	12.49	47.5	64.0	54.5	9.6
64	11/17/06 10:00 PM	8.4	18.03	12.61	47.1	64.5	54.7	9.8
65	11/17/06 10:30 PM	8.2	17.83	12.47	46.8	64.1	54.4	9.6
66	11/17/06 11:00 PM	8.2	17.66	12.53	46.8	63.8	54.6	9.2
67	11/17/06 11:30 PM	8.2	17.66	12.35	46.8	63.8	54.2	9.6
68	11/18/06 12:00 AM	8.2	17.89	12.35	46.8	64.2	54.2	10.0
69	11/18/06 12:30 AM	8.2	17.56	12.22	46.8	63.6	54.0	9.6
70	11/18/06 1:00 AM	8.2	17.53	12.1	46.8	63.6	53.8	9.8
71	11/18/06 1:30 AM	8.2	17.68	11.97	46.8	63.8	53.5	10.3

Reading Number	Time	Ambient Temp. (°C)	Cylinder Temp. (°C)	Joint Temp. (°C)	Ambient Temp. (°F)	Cylinder Temp. (°F)	Joint Temp. (°F)	Temp. Diff. Between Cylinder & Joint (°F)
72	11/18/06 2:00 AM	8.1	17.58	11.87	46.6	63.6	53.4	10.3
73	11/18/06 2:30 AM	8	17.52	11.9	46.4	63.5	53.4	10.1
74	11/18/06 3:00 AM	7.9	17.48	11.67	46.2	63.5	53.0	10.5
75	11/18/06 3:30 AM	7.9	17.5	11.74	46.2	63.5	53.1	10.4
76	11/18/06 4:00 AM	7.8	17.22	11.76	46.0	63.0	53.2	9.8
77	11/18/06 4:30 AM	7.8	17.52	11.58	46.0	63.5	52.8	10.7
78	11/18/06 5:00 AM	7.7	17.49	11.6	45.9	63.5	52.9	10.6
79	11/18/06 5:30 AM	7.6	17.42	11.63	45.7	63.4	52.9	10.4
80	11/18/06 6:00 AM	7.6	17.2	11.38	45.7	63.0	52.5	10.5
81	11/18/06 6:30 AM	7.5	17.23	11.47	45.5	63.0	52.6	10.4
82	11/18/06 7:00 AM	7.4	17.25	11.05	45.3	63.1	51.9	11.2
83	11/18/06 7:30 AM	7.3	17.28	11.02	45.1	63.1	51.8	11.3
84	11/18/06 8:00 AM	7.2	17.18	11.04	45.0	62.9	51.9	11.1
85	11/18/06 8:30 AM	7.1	17.42	10.76	44.8	63.4	51.4	12.0
86	11/18/06 9:00 AM	7.1	17.37	10.7	44.8	63.3	51.3	12.0
87	11/18/06 9:30 AM	7.2	17.24	10.67	45.0	63.0	51.2	11.8
88	11/18/06 10:00 AM	7.1	17.37	10.57	44.8	63.3	51.0	12.2
89	11/18/06 10:30 AM	7.1	17.24	10.51	44.8	63.0	50.9	12.1
90	11/18/06 11:00 AM	7.1	17.3	10.38	44.8	63.1	50.7	12.5
91	11/18/06 11:30 AM	7.3	17.28	10.26	45.1	63.1	50.5	12.6
92	11/18/06 12:00 PM	7.5	17.41	10.27	45.5	63.3	50.5	12.9
93	11/18/06 12:30 PM	7.6	17.33	10.18	45.7	63.2	50.3	12.9
94	11/18/06 1:00 PM	7.6	17.26	10.18	45.7	63.1	50.3	12.7
95	11/18/06 1:30 PM	7.8	17.46	10.19	46.0	63.4	50.3	13.1

Reading Number	Time	Ambient Temp. (°C)	Cylinder Temp. (°C)	Joint Temp. (°C)	Ambient Temp. (°F)	Cylinder Temp. (°F)	Joint Temp. (°F)	Temp. Diff. Between Cylinder & Joint (°F)
96	11/18/06 2:00 PM	7.9	17.52	10.29	46.2	63.5	50.5	13.0
97	11/18/06 2:30 PM	8	17.66	10.33	46.4	63.8	50.6	13.2
98	11/18/06 3:00 PM	8	17.6	10.39	46.4	63.7	50.7	13.0
99	11/18/06 3:30 PM	8.1	17.66	10.3	46.6	63.8	50.5	13.2
100	11/18/06 4:00 PM	8.2	17.82	10.46	46.8	64.1	50.8	13.2
101	11/18/06 4:30 PM	8.1	17.97	10.49	46.6	64.3	50.9	13.5
102	11/18/06 5:00 PM	7.9	17.75	10.41	46.2	64.0	50.7	13.2
103	11/18/06 5:30 PM	7.8	17.86	10.75	46.0	64.1	51.4	12.8
104	11/18/06 6:00 PM	7.6	17.76	10.62	45.7	64.0	51.1	12.9
105	11/18/06 6:30 PM	7.6	17.94	10.43	45.7	64.3	50.8	13.5
106	11/18/06 7:00 PM	7.7	17.81	10.65	45.9	64.1	51.2	12.9
107	11/18/06 7:30 PM	7.5	17.84	10.58	45.5	64.1	51.0	13.1
108	11/18/06 8:00 PM	7.3	17.58	10.52	45.1	63.6	50.9	12.7
109	11/18/06 8:30 PM	7.5	17.83	10.64	45.5	64.1	51.2	12.9
110	11/18/06 9:00 PM	7.7	17.45	10.4	45.9	63.4	50.7	12.7
111	11/18/06 9:30 PM	7.8	17.33	10.57	46.0	63.2	51.0	12.2
112	11/18/06 10:00 PM	7.9	17.3	10.6	46.2	63.1	51.1	12.1
113	11/18/06 10:30 PM	7.8	17.36	10.44	46.0	63.2	50.8	12.5
114	11/18/06 11:00 PM	7.7	17.23	10.53	45.9	63.0	51.0	12.1
115	11/18/06 11:30 PM	7.6	17.41	10.49	45.7	63.3	50.9	12.5
116	11/19/06 12:00 AM	7.5	17.22	10.46	45.5	63.0	50.8	12.2
117	11/19/06 12:30 AM	7.3	17.18	10.32	45.1	62.9	50.6	12.3
118	11/19/06 1:00 AM	7.3	17.02	10.38	45.1	62.6	50.7	12.0
119	11/19/06 1:30 AM	7.1	16.86	10.12	44.8	62.3	50.2	12.1

Reading Number	Time	Ambient Temp. (°C)	Cylinder Temp. (°C)	Joint Temp. (°C)	Ambient Temp. (°F)	Cylinder Temp. (°F)	Joint Temp. (°F)	Temp. Diff. Between Cylinder & Joint (°F)
120	11/19/06 2:00 AM	7	16.94	10.22	44.6	62.5	50.4	12.1
121	11/19/06 2:30 AM	6.9	17.14	10.19	44.4	62.9	50.3	12.5
122	11/19/06 3:00 AM	6.8	17.01	10.09	44.2	62.6	50.2	12.5
123	11/19/06 3:30 AM	6.7	16.77	10.17	44.1	62.2	50.3	11.9
124	11/19/06 4:00 AM	6.6	16.55	10.01	43.9	61.8	50.0	11.8
125	11/19/06 4:30 AM	6.4	16.41	9.94	43.5	61.5	49.9	11.6
126	11/19/06 5:00 AM	6.3	16.61	9.78	43.3	61.9	49.6	12.3
127	11/19/06 5:30 AM	6.2	16.33	9.93	43.2	61.4	49.9	11.5
128	11/19/06 6:00 AM	6.1	16.48	9.51	43.0	61.7	49.1	12.5
129	11/19/06 6:30 AM	6	16.38	9.48	42.8	61.5	49.1	12.4
130	11/19/06 7:00 AM	5.9	15.86	9.38	42.6	60.5	48.9	11.7
131	11/19/06 7:30 AM	5.9	15.98	9.38	42.6	60.8	48.9	11.9
132	11/19/06 8:00 AM	5.9	15.98	9.19	42.6	60.8	48.5	12.2
133	11/19/06 8:30 AM	6.1	15.64	9	43.0	60.2	48.2	12.0
134	11/19/06 9:00 AM	6.4	15.58	8.98	43.5	60.0	48.2	11.9
135	11/19/06 9:30 AM	6.9	15.69	8.92	44.4	60.2	48.1	12.2
136	11/19/06 10:00 AM	7.4	16	8.85	45.3	60.8	47.9	12.9
137	11/19/06 10:30 AM	8	16.07	8.74	46.4	60.9	47.7	13.2
138	11/19/06 11:00 AM	8.3	16.33	8.79	46.9	61.4	47.8	13.6
139	11/19/06 11:30 AM	8.4	16.49	9.02	47.1	61.7	48.2	13.4
140	11/19/06 12:00 PM	8.2	16.79	8.88	46.8	62.2	48.0	14.2
141	11/19/06 12:30 PM	8.4	17.05	8.83	47.1	62.7	47.9	14.8
142	11/19/06 1:00 PM	8.7	17.01	9	47.7	62.6	48.2	14.4
143	11/19/06 1:30 PM	9.1	17.22	9.21	48.4	63.0	48.6	14.4

Reading Number	Time	Ambient Temp. (°C)	Cylinder Temp. (°C)	Joint Temp. (°C)	Ambient Temp. (°F)	Cylinder Temp. (°F)	Joint Temp. (°F)	Temp. Diff. Between Cylinder & Joint (°F)
144	11/19/06 2:00 PM	9.5	17.61	9.24	49.1	63.7	48.6	15.1
145	11/19/06 2:30 PM	9.9	17.85	9.51	49.8	64.1	49.1	15.0
146	11/19/06 3:00 PM	9.9	18.25	9.57	49.8	64.9	49.2	15.6
147	11/19/06 3:30 PM	9.7	18.49	9.75	49.5	65.3	49.6	15.7
148	11/19/06 4:00 PM	9.9	18.5	9.89	49.8	65.3	49.8	15.5
149	11/19/06 4:30 PM	9.9	18.66	10.26	49.8	65.6	50.5	15.1
150	11/19/06 5:00 PM	9.7	18.71	10.38	49.5	65.7	50.7	15.0
151	11/19/06 5:30 PM	9.3	18.84	10.48	48.7	65.9	50.9	15.0
152	11/19/06 6:00 PM	9	18.73	10.63	48.2	65.7	51.1	14.6
153	11/19/06 6:30 PM	8.8	18.53	10.56	47.8	65.4	51.0	14.3
154	11/19/06 7:00 PM	8.6	18.73	10.86	47.5	65.7	51.5	14.2
155	11/19/06 7:30 PM	8.5	18.36	10.95	47.3	65.0	51.7	13.3
156	11/19/06 8:00 PM	8.2	18.21	10.71	46.8	64.8	51.3	13.5
157	11/19/06 8:30 PM	8.1	18.36	10.68	46.6	65.0	51.2	13.8
158	11/19/06 9:00 PM	8	18.07	10.83	46.4	64.5	51.5	13.0
159	11/19/06 9:30 PM	7.9	18.16	10.73	46.2	64.7	51.3	13.4
160	11/19/06 10:00 PM	7.8	18	10.63	46.0	64.4	51.1	13.3
161	11/19/06 10:30 PM	7.7	17.9	10.84	45.9	64.2	51.5	12.7
162	11/19/06 11:00 PM	7.5	17.8	10.58	45.5	64.0	51.0	13.0
163	11/19/06 11:30 PM	7.4	17.89	10.62	45.3	64.2	51.1	13.1
164	11/20/06 12:00 AM	7.3	17.85	10.58	45.1	64.1	51.0	13.1
165	11/20/06 12:30 AM	7.1	17.34	10.57	44.8	63.2	51.0	12.2
166	11/20/06 1:00 AM	7.1	17.24	10.38	44.8	63.0	50.7	12.3
167	11/20/06 1:30 AM	7	17.33	10.28	44.6	63.2	50.5	12.7

Reading Number	Time	Ambient Temp. (°C)	Cylinder Temp. (°C)	Joint Temp. (°C)	Ambient Temp. (°F)	Cylinder Temp. (°F)	Joint Temp. (°F)	Temp. Diff. Between Cylinder & Joint (°F)
168	11/20/06 2:00 AM	6.8	17.23	10.4	44.2	63.0	50.7	12.3
169	11/20/06 2:30 AM	6.8	17.07	10.27	44.2	62.7	50.5	12.2
170	11/20/06 3:00 AM	6.7	17.16	9.99	44.1	62.9	50.0	12.9
171	11/20/06 3:30 AM	6.6	17.03	9.82	43.9	62.7	49.7	13.0
172	11/20/06 4:00 AM	6.5	16.9	9.79	43.7	62.4	49.6	12.8
173	11/20/06 4:30 AM	6.4	16.9	9.42	43.5	62.4	49.0	13.5
174	11/20/06 5:00 AM	6.3	16.76	9.71	43.3	62.2	49.5	12.7
175	11/20/06 5:30 AM	6.2	16.51	9.42	43.2	61.7	49.0	12.8
176	11/20/06 6:00 AM	6.1	16.29	9.39	43.0	61.3	48.9	12.4
177	11/20/06 6:30 AM	6.1	16.29	9.19	43.0	61.3	48.5	12.8
178	11/20/06 7:00 AM	6	16.34	9.15	42.8	61.4	48.5	12.9
179	11/20/06 7:30 AM	5.9	16.34	9.12	42.6	61.4	48.4	13.0
180	11/20/06 8:00 AM	6	16.15	9.15	42.8	61.1	48.5	12.6
181	11/20/06 8:30 AM	6.3	16.21	8.82	43.3	61.2	47.9	13.3
182	11/20/06 9:00 AM	6.8	16.36	8.63	44.2	61.4	47.5	13.9
183	11/20/06 9:30 AM	7.3	16.08	8.62	45.1	60.9	47.5	13.4
184	11/20/06 10:00 AM	7.8	16.42	8.73	46.0	61.6	47.7	13.8
185	11/20/06 10:30 AM	8	16.43	8.81	46.4	61.6	47.9	13.7
186	11/20/06 11:00 AM	8.4	16.66	8.95	47.1	62.0	48.1	13.9
187	11/20/06 11:30 AM	8.5	16.62	9.05	47.3	61.9	48.3	13.6
188	11/20/06 12:00 PM	8.6	17.06	9.03	47.5	62.7	48.3	14.5
189	11/20/06 12:30 PM	8.8	16.99	9.29	47.8	62.6	48.7	13.9
190	11/20/06 1:00 PM	8.9	17.13	9.8	48.0	62.8	49.6	13.2
191	11/20/06 1:30 PM	8.9	16.82	9.94	48.0	62.3	49.9	12.4

Reading Number	Time	Ambient Temp. (°C)	Cylinder Temp. (°C)	Joint Temp. (°C)	Ambient Temp. (°F)	Cylinder Temp. (°F)	Joint Temp. (°F)	Temp. Diff. Between Cylinder & Joint (°F)
192	11/20/06 2:00 PM	9.3	16.73	10.05	48.7	62.1	50.1	12.0
193	11/20/06 2:30 PM	9.6	16.84	10.47	49.3	62.3	50.8	11.5
194	11/20/06 3:00 PM	9.7	16.93	10.79	49.5	62.5	51.4	11.1
195	11/20/06 3:30 PM	9.6	17.02	10.85	49.3	62.6	51.5	11.1
196	11/20/06 4:00 PM	9.4	17	10.97	48.9	62.6	51.7	10.9
197	11/20/06 4:30 PM	9.4	16.95	11.28	48.9	62.5	52.3	10.2
198	11/20/06 5:00 PM	9.6	17.57	11.64	49.3	63.6	53.0	10.7
199	11/20/06 5:30 PM	10.7	18.79	12.21	51.3	65.8	54.0	11.8
200	11/20/06 6:00 PM	11.1	19.74	12.73	52.0	67.5	54.9	12.6
201	11/20/06 6:30 PM	11.3	20.73	13.24	52.3	69.3	55.8	13.5
202	11/20/06 7:00 PM	11.5	21.16	13.75	52.7	70.1	56.8	13.3
203	11/20/06 7:30 PM	11.4	21.79	14	52.5	71.2	57.2	14.0
204	11/20/06 8:00 PM	11.4	21.62	14.36	52.5	70.9	57.8	13.1
205	11/20/06 8:30 PM	11	21.4	14.84	51.8	70.5	58.7	11.8
206	11/20/06 9:00 PM	10.5	21.21	15.08	50.9	70.2	59.1	11.0
207	11/20/06 9:30 PM	9.9	20.91	15.31	49.8	69.6	59.6	10.1
208	11/20/06 10:00 PM	8.6	19.57	15.26	47.5	67.2	59.5	7.8
209	11/20/06 10:30 PM	7.6	18.16	15.03	45.7	64.7	59.1	5.6
210	11/20/06 11:00 PM	7	16.89	14.48	44.6	62.4	58.1	4.3
211	11/20/06 11:30 PM	6.4	15.33	13.76	43.5	59.6	56.8	2.8
212	11/21/06 12:00 AM	5.9	14.1	13.24	42.6	57.4	55.8	1.5
213	11/21/06 12:30 AM	5.4	12.55	12.62	41.7	54.6	54.7	-0.1
214	11/21/06 1:00 AM	4.8	11.35	12	40.6	52.4	53.6	-1.2
215	11/21/06 1:30 AM	4.7	10.58	11.6	40.5	51.0	52.9	-1.8

Reading Number	Time	Ambient Temp. (°C)	Cylinder Temp. (°C)	Joint Temp. (°C)	Ambient Temp. (°F)	Cylinder Temp. (°F)	Joint Temp. (°F)	Temp. Diff. Between Cylinder & Joint (°F)
216	11/21/06 2:00 AM	4.5	9.76	11.15	40.1	49.6	52.1	-2.5
217	11/21/06 2:30 AM	4.3	9.2	10.8	39.7	48.6	51.4	-2.9
218	11/21/06 3:00 AM	4.2	8.91	10.29	39.6	48.0	50.5	-2.5
219	11/21/06 3:30 AM	4	8.58	9.97	39.2	47.4	49.9	-2.5
220	11/21/06 4:00 AM	3.8	8.2	9.52	38.8	46.8	49.1	-2.4
221	11/21/06 4:30 AM	3.8	7.64	9.08	38.8	45.8	48.3	-2.6
222	11/21/06 5:00 AM	3.9	7.49	8.76	39.0	45.5	47.8	-2.3
223	11/21/06 5:30 AM	3.9	7.62	8.57	39.0	45.7	47.4	-1.7
224	11/21/06 6:00 AM	3.9	7.44	8.45	39.0	45.4	47.2	-1.8
225	11/21/06 6:30 AM	3.7	7.18	8.25	38.7	44.9	46.9	-1.9
226	11/21/06 7:00 AM	3.5	7.22	7.73	38.3	45.0	45.9	-0.9
227	11/21/06 7:30 AM	3.3	6.71	7.62	37.9	44.1	45.7	-1.6
228	11/21/06 8:00 AM	3.1	6.64	7.36	37.6	44.0	45.2	-1.3
229	11/21/06 8:30 AM	3.2	6.55	7.14	37.8	43.8	44.9	-1.1
230	11/21/06 9:00 AM	3.7	6.56	6.89	38.7	43.8	44.4	-0.6
231	11/21/06 9:30 AM	5.5	7.11	6.73	41.9	44.8	44.1	0.7
232	11/21/06 10:00 AM	7.4	7.9	6.63	45.3	46.2	43.9	2.3
233	11/21/06 10:30 AM	8.8	9.37	6.69	47.8	48.9	44.0	4.8
234	11/21/06 11:00 AM	9.8	10.72	7.21	49.6	51.3	45.0	6.3
235	11/21/06 11:30 AM	10.8	11.97	8	51.4	53.5	46.4	7.1
236	11/21/06 12:00 PM	9.8	14.04	8.63	49.6	57.3	47.5	9.7
237	11/21/06 12:30 PM	10.8	16.1	9.35	51.4	61.0	48.8	12.2
238	11/21/06 1:00 PM	11.4	17.44	10.17	52.5	63.4	50.3	13.1
239	11/21/06 1:30 PM	12.3	18.11	11.48	54.1	64.6	52.7	11.9

Reading Number	Time	Ambient Temp. (°C)	Cylinder Temp. (°C)	Joint Temp. (°C)	Ambient Temp. (°F)	Cylinder Temp. (°F)	Joint Temp. (°F)	Temp. Diff. Between Cylinder & Joint (°F)
240	11/21/06 2:00 PM	13.7	18.85	12.27	56.7	65.9	54.1	11.8
241	11/21/06 2:30 PM	13.7	19.4	13.19	56.7	66.9	55.7	11.2
242	11/21/06 3:00 PM	14	19.44	13.71	57.2	67.0	56.7	10.3
243	11/21/06 3:30 PM	14	19.4	13.99	57.2	66.9	57.2	9.7
244	11/21/06 4:00 PM	13.8	18.84	14.21	56.8	65.9	57.6	8.3
245	11/21/06 4:30 PM	13.7	18.55	14.38	56.7	65.4	57.9	7.5
246	11/21/06 5:00 PM	13.2	18.59	14.53	55.8	65.5	58.2	7.3
247	11/21/06 5:30 PM	12.3	20.99	15.1	54.1	69.8	59.2	10.6
248	11/21/06 6:00 PM	10.5	24.99	16.05	50.9	77.0	60.9	16.1
249	11/21/06 6:30 PM	8.3	28.52	17.45	46.9	83.3	63.4	19.9
250	11/21/06 7:00 PM	7	31.2	18.62	44.6	88.2	65.5	22.6
251	11/21/06 7:30 PM	6.1	33.94	19.73	43.0	93.1	67.5	25.6
252	11/21/06 8:00 PM	5	36.13	20.62	41.0	97.0	69.1	27.9
253	11/21/06 8:30 PM	4.3	37.3	21.41	39.7	99.1	70.5	28.6
254	11/21/06 9:00 PM	3.9	39.05	22.12	39.0	102.3	71.8	30.5
255	11/21/06 9:30 PM	3.5	39.97	22.9	38.3	103.9	73.2	30.7
256	11/21/06 10:00 PM	3.5	41.18	23.43	38.3	106.1	74.2	32.0
257	11/21/06 10:30 PM	2.6	42.05	24.05	36.7	107.7	75.3	32.4
258	11/21/06 11:00 PM	2.3	43.01	24.59	36.1	109.4	76.3	33.2
259	11/21/06 11:30 PM	2.1	43.53	24.87	35.8	110.4	76.8	33.6
260	11/22/06 12:00 AM	1.6	44.04	25.24	34.9	111.3	77.4	33.8
261	11/22/06 12:30 AM	1.4	44.38	25.53	34.5	111.9	78.0	33.9
262	11/22/06 1:00 AM	1.8	44.64	25.67	35.2	112.4	78.2	34.1
263	11/22/06 1:30 AM	2.6	44.95	25.97	36.7	112.9	78.7	34.2

Reading Number	Time	Ambient Temp. (°C)	Cylinder Temp. (°C)	Joint Temp. (°C)	Ambient Temp. (°F)	Cylinder Temp. (°F)	Joint Temp. (°F)	Temp. Diff. Between Cylinder & Joint (°F)
264	11/22/06 2:00 AM	3.1	45.36	26.38	37.6	113.6	79.5	34.2
265	11/22/06 2:30 AM	3	45.35	26.4	37.4	113.6	79.5	34.1
266	11/22/06 3:00 AM	2	45.48	26.44	35.6	113.9	79.6	34.3
267	11/22/06 3:30 AM	2.6	45.62	26.57	36.7	114.1	79.8	34.3
268	11/22/06 4:00 AM	2.8	45.71	26.7	37.0	114.3	80.1	34.2
269	11/22/06 4:30 AM	1.4	45.67	26.92	34.5	114.2	80.5	33.8
270	11/22/06 5:00 AM	1	45.75	27.15	33.8	114.4	80.9	33.5
271	11/22/06 5:30 AM	0.4	45.98	27.18	32.7	114.8	80.9	33.8
272	11/22/06 6:00 AM	0.3	46.07	27.23	32.5	114.9	81.0	33.9
273	11/22/06 6:30 AM	0.3	45.91	27.16	32.5	114.6	80.9	33.8
274	11/22/06 7:00 AM	0.5	46.05	27.19	32.9	114.9	80.9	33.9
275	11/22/06 7:30 AM	0.9	45.79	27.24	33.6	114.4	81.0	33.4
276	11/22/06 8:00 AM	1.1	46.06	27.11	34.0	114.9	80.8	34.1
277	11/22/06 8:30 AM	1.4	46.49	26.85	34.5	115.7	80.3	35.4
278	11/22/06 9:00 AM	2.1	46.37	27.13	35.8	115.5	80.8	34.6
279	11/22/06 9:30 AM	3.1	45.53	26.74	37.6	114.0	80.1	33.8
280	11/22/06 10:00 AM	4.1	42.31	26.82	39.4	108.2	80.3	27.9
281	11/22/06 10:30 AM	6	42.12	26.57	42.8	107.8	79.8	28.0
282	11/22/06 11:00 AM	6.7	38.78	26.2	44.1	101.8	79.2	22.6
283	11/22/06 11:30 AM	8.1	35.76	25.23	46.6	96.4	77.4	19.0
284	11/22/06 12:00 PM	10.4	36.4	24.55	50.7	97.5	76.2	21.3
285	11/22/06 12:30 PM	12.4	37.32	23.99	54.3	99.2	75.2	24.0
286	11/22/06 1:00 PM	13.6	38.09	23.83	56.5	100.6	74.9	25.7
287	11/22/06 1:30 PM	14.6	38.69	23.99	58.3	101.6	75.2	26.5

Reading Number	Time	Ambient Temp. (°C)	Cylinder Temp. (°C)	Joint Temp. (°C)	Ambient Temp. (°F)	Cylinder Temp. (°F)	Joint Temp. (°F)	Temp. Diff. Between Cylinder & Joint (°F)
288	11/22/06 2:00 PM	15.7	39.42	23.81	60.3	103.0	74.9	28.1
289	11/22/06 2:30 PM	16	40.35	24.07	60.8	104.6	75.3	29.3
290	11/22/06 3:00 PM	16.8	39.45	24.04	62.2	103.0	75.3	27.7
291	11/22/06 3:30 PM	16.9	38.27	23.54	62.4	100.9	74.4	26.5
292	11/22/06 4:00 PM	16.1	36.82	23.2	61.0	98.3	73.8	24.5
293	11/22/06 4:30 PM	15.5	35.34	22.47	59.9	95.6	72.4	23.2
294	11/22/06 5:00 PM	14.4	33.93	22.02	57.9	93.1	71.6	21.4
295	11/22/06 5:30 PM	13.5	32.23	21.67	56.3	90.0	71.0	19.0
296	11/22/06 6:00 PM	12	30.74	21	53.6	87.3	69.8	17.5
297	11/22/06 6:30 PM	10.2	29.11	20.32	50.4	84.4	68.6	15.8
298	11/22/06 7:00 PM	8.8	27.63	19.87	47.8	81.7	67.8	14.0
299	11/22/06 7:30 PM	8.3	26.41	19.32	46.9	79.5	66.8	12.8
300	11/22/06 8:00 PM	8.4	25.43	18.79	47.1	77.8	65.8	12.0
301	11/22/06 8:30 PM	7.9	24.25	18.46	46.2	75.7	65.2	10.4
302	11/22/06 9:00 PM	7.2	23.31	18.04	45.0	74.0	64.5	9.5
303	11/22/06 9:30 PM	6.8	22.37	17.68	44.2	72.3	63.8	8.4
304	11/22/06 10:00 PM	6.1	21.57	17.25	43.0	70.8	63.1	7.8
305	11/22/06 10:30 PM	5.2	20.36	16.54	41.4	68.6	61.8	6.9
306	11/22/06 11:00 PM	3.7	19.52	16.24	38.7	67.1	61.2	5.9
307	11/22/06 11:30 PM	3.7	18.96	15.66	38.7	66.1	60.2	5.9
308	11/23/06 12:00 AM	3.1	18.27	15.11	37.6	64.9	59.2	5.7
309	11/23/06 12:30 AM	2.9	17.18	14.77	37.2	62.9	58.6	4.3
310	11/23/06 1:00 AM	2.4	16.77	14.31	36.3	62.2	57.8	4.4
311	11/23/06 1:30 AM	2.1	16.16	13.98	35.8	61.1	57.2	3.9

Reading Number	Time	Ambient Temp. (°C)	Cylinder Temp. (°C)	Joint Temp. (°C)	Ambient Temp. (°F)	Cylinder Temp. (°F)	Joint Temp. (°F)	Temp. Diff. Between Cylinder & Joint (°F)
312	11/23/06 2:00 AM	1.8	15.28	13.33	35.2	59.5	56.0	3.5
313	11/23/06 2:30 AM	1.5	14.96	12.85	34.7	58.9	55.1	3.8
314	11/23/06 3:00 AM	1.1	14.27	12.79	34.0	57.7	55.0	2.7
315	11/23/06 3:30 AM	0.9	13.86	11.99	33.6	56.9	53.6	3.4
316	11/23/06 4:00 AM	0.7	12.99	11.93	33.3	55.4	53.5	1.9
317	11/23/06 4:30 AM	0.6	12.92	11.42	33.1	55.3	52.6	2.7
318	11/23/06 5:00 AM	0.4	12.27	11.13	32.7	54.1	52.0	2.1
319	11/23/06 5:30 AM	0.2	11.76	10.61	32.4	53.2	51.1	2.1
320	11/23/06 6:00 AM	0.1	11.71	10.3	32.2	53.1	50.5	2.5
321	11/23/06 6:30 AM	-0.1	11.31	10.2	31.8	52.4	50.4	2.0
322	11/23/06 7:00 AM	-0.6	10.72	9.84	30.9	51.3	49.7	1.6
323	11/23/06 7:30 AM	-0.5	10.47	9.39	31.1	50.8	48.9	1.9
324	11/23/06 8:00 AM	-0.6	9.93	9.2	30.9	49.9	48.6	1.3
325	11/23/06 8:30 AM	-0.6	9.94	8.73	30.9	49.9	47.7	2.2
326	11/23/06 9:00 AM	-0.1	9.77	8.55	31.8	49.6	47.4	2.2
327	11/23/06 9:30 AM	1.4	9.72	8.55	34.5	49.5	47.4	2.1
328	11/23/06 10:00 AM	3.7	9.91	8.59	38.7	49.8	47.5	2.4
329	11/23/06 10:30 AM	5.2	10.38	8.91	41.4	50.7	48.0	2.6
330	11/23/06 11:00 AM	6.5	10.94	8.88	43.7	51.7	48.0	3.7
331	11/23/06 11:30 AM	7.9	11.77	9.15	46.2	53.2	48.5	4.7
332	11/23/06 12:00 PM	9.4	12.1	9.55	48.9	53.8	49.2	4.6
333	11/23/06 12:30 PM	10.6	12.77	9.69	51.1	55.0	49.4	5.5
334	11/23/06 1:00 PM	11.3	13.56	10.2	52.3	56.4	50.4	6.0
335	11/23/06 1:30 PM	12.7	14.03	10.71	54.9	57.3	51.3	6.0

Reading Number	Time	Ambient Temp. (°C)	Cylinder Temp. (°C)	Joint Temp. (°C)	Ambient Temp. (°F)	Cylinder Temp. (°F)	Joint Temp. (°F)	Temp. Diff. Between Cylinder & Joint (°F)
336	11/23/06 2:00 PM	13.8	14.86	11.45	56.8	58.7	52.6	6.1
337	11/23/06 2:30 PM	15.3	14.85	12.03	59.5	58.7	53.7	5.1
338	11/23/06 3:00 PM	15.1	15.07	12.43	59.2	59.1	54.4	4.8
339	11/23/06 3:30 PM	14.9	15.27	13.03	58.8	59.5	55.5	4.0
340	11/23/06 4:00 PM	14.7	15.34	13.34	58.5	59.6	56.0	3.6
341	11/23/06 4:30 PM	13.8	15.18	13.55	56.8	59.3	56.4	2.9
342	11/23/06 5:00 PM	13.2	14.79	13.55	55.8	58.6	56.4	2.2
343	11/23/06 5:30 PM	11.8	14.59	13.52	53.2	58.3	56.3	1.9
344	11/23/06 6:00 PM	10.5	14.16	13.68	50.9	57.5	56.6	0.9
345	11/23/06 6:30 PM	9.8	13.81	13.42	49.6	56.9	56.2	0.7
346	11/23/06 7:00 PM	9.3	13.64	13.28	48.7	56.6	55.9	0.6
347	11/23/06 7:30 PM	8.4	13.24	13.29	47.1	55.8	55.9	-0.1
348	11/23/06 8:00 PM	8.1	13.03	12.96	46.6	55.5	55.3	0.1
349	11/23/06 8:30 PM	8.2	12.51	12.53	46.8	54.5	54.6	0.0
350	11/23/06 9:00 PM	7.8	12.53	12.48	46.0	54.6	54.5	0.1
351	11/23/06 9:30 PM	7.4	12.49	12.32	45.3	54.5	54.2	0.3
352	11/23/06 10:00 PM	7.1	12.21	12.16	44.8	54.0	53.9	0.1
353	11/23/06 10:30 PM	7	11.79	11.81	44.6	53.2	53.3	0.0
354	11/23/06 11:00 PM	6.9	11.94	11.45	44.4	53.5	52.6	0.9
355	11/23/06 11:30 PM	6.8	11.71	11.47	44.2	53.1	52.6	0.4
356	11/24/06 12:00 AM	6.7	11.45	11.46	44.1	52.6	52.6	0.0
357	11/24/06 12:30 AM	6.4	11.23	11.14	43.5	52.2	52.1	0.2
358	11/24/06 1:00 AM	6.2	11.19	10.85	43.2	52.1	51.5	0.6
359	11/24/06 1:30 AM	6.1	11.13	10.57	43.0	52.0	51.0	1.0

Reading Number	Time	Ambient Temp. (°C)	Cylinder Temp. (°C)	Joint Temp. (°C)	Ambient Temp. (°F)	Cylinder Temp. (°F)	Joint Temp. (°F)	Temp. Diff. Between Cylinder & Joint (°F)
360	11/24/06 2:00 AM	6	10.94	10.38	42.8	51.7	50.7	1.0
361	11/24/06 2:30 AM	6	10.95	10.3	42.8	51.7	50.5	1.2
362	11/24/06 3:00 AM	6	10.58	10.23	42.8	51.0	50.4	0.6
363	11/24/06 3:30 AM	5.7	10.65	9.87	42.3	51.2	49.8	1.4
364	11/24/06 4:00 AM	4.7	10.31	9.69	40.5	50.6	49.4	1.1
365	11/24/06 4:30 AM	4.4	10.04	9.51	39.9	50.1	49.1	1.0
366	11/24/06 5:00 AM	4	10.32	9.14	39.2	50.6	48.5	2.1
367	11/24/06 5:30 AM	3.1	9.77	9.05	37.6	49.6	48.3	1.3
368	11/24/06 6:00 AM	2.4	9.78	8.89	36.3	49.6	48.0	1.6
369	11/24/06 6:30 AM	2.1	9.65	8.74	35.8	49.4	47.7	1.6
370	11/24/06 7:00 AM	1.8	9.4	8.48	35.2	48.9	47.3	1.7
371	11/24/06 7:30 AM	1.3	9.07	8.18	34.3	48.3	46.7	1.6
372	11/24/06 8:00 AM	1.1	8.96	8.03	34.0	48.1	46.5	1.7
373	11/24/06 8:30 AM	0.9	8.67	7.67	33.6	47.6	45.8	1.8
374	11/24/06 9:00 AM	1.4	8.48	7.5	34.5	47.3	45.5	1.8
375	11/24/06 9:30 AM	2.3	8.78	7.79	36.1	47.8	46.0	1.8
376	11/24/06 10:00 AM	6	9.14	7.99	42.8	48.5	46.4	2.1
377	11/24/06 10:30 AM	8.4	9.84	8.25	47.1	49.7	46.9	2.9
378	11/24/06 11:00 AM	10	10.47	8.57	50.0	50.8	47.4	3.4
379	11/24/06 11:30 AM	11.3	11.33	9.44	52.3	52.4	49.0	3.4
380	11/24/06 12:00 PM	12.6	12.13	9.64	54.7	53.8	49.4	4.5
381	11/24/06 12:30 PM	13.4	12.79	10.46	56.1	55.0	50.8	4.2
382	11/24/06 1:00 PM	13.9	13.7	11.03	57.0	56.7	51.9	4.8
383	11/24/06 1:30 PM	14.5	13.98	11.42	58.1	57.2	52.6	4.6

Reading Number	Time	Ambient Temp. (°C)	Cylinder Temp. (°C)	Joint Temp. (°C)	Ambient Temp. (°F)	Cylinder Temp. (°F)	Joint Temp. (°F)	Temp. Diff. Between Cylinder & Joint (°F)
384	11/24/06 2:00 PM	15.1	14.41	11.91	59.2	57.9	53.4	4.5
385	11/24/06 2:30 PM	15.2	14.7	12.43	59.4	58.5	54.4	4.1
386	11/24/06 3:00 PM	14.9	14.79	12.75	58.8	58.6	55.0	3.7
387	11/24/06 3:30 PM	15	15.11	13.34	59.0	59.2	56.0	3.2
388	11/24/06 4:00 PM	14.6	15.02	13.36	58.3	59.0	56.0	3.0
389	11/24/06 4:30 PM	13.2	14.55	13.27	55.8	58.2	55.9	2.3
390	11/24/06 5:00 PM	12.5	14.28	13.63	54.5	57.7	56.5	1.2
391	11/24/06 5:30 PM	11.3	13.98	13.49	52.3	57.2	56.3	0.9
392	11/24/06 6:00 PM	9.8	13.52	13.38	49.6	56.3	56.1	0.3
393	11/24/06 6:30 PM	8.2	13.22	13.36	46.8	55.8	56.0	-0.3
394	11/24/06 7:00 PM	7.3	12.91	13.21	45.1	55.2	55.8	-0.5
395	11/24/06 7:30 PM	6.2	12.35	13.02	43.2	54.2	55.4	-1.2
396	11/24/06 8:00 PM	5.7	11.92	12.73	42.3	53.5	54.9	-1.5
397	11/24/06 8:30 PM	4.7	11.56	12.62	40.5	52.8	54.7	-1.9
398	11/24/06 9:00 PM	3.7	11.5	12.34	38.7	52.7	54.2	-1.5
399	11/24/06 9:30 PM	3.4	10.76	11.9	38.1	51.4	53.4	-2.1
400	11/24/06 10:00 PM	2.6	10.46	11.62	36.7	50.8	52.9	-2.1
401	11/24/06 10:30 PM	2.1	10.25	11.51	35.8	50.5	52.7	-2.3
402	11/24/06 11:00 PM	1.8	9.92	11.36	35.2	49.9	52.4	-2.6
403	11/24/06 11:30 PM	1.1	9.92	11.11	34.0	49.9	52.0	-2.1
404	11/25/06 12:00 AM	0.7	9.46	10.84	33.3	49.0	51.5	-2.5
405	11/25/06 12:30 AM	0.7	9.18	10.55	33.3	48.5	51.0	-2.5
406	11/25/06 1:00 AM	0.8	9.29	10.37	33.4	48.7	50.7	-1.9
407	11/25/06 1:30 AM	1.2	9.37	10.11	34.2	48.9	50.2	-1.3

Reading Number	Time	Ambient Temp. (°C)	Cylinder Temp. (°C)	Joint Temp. (°C)	Ambient Temp. (°F)	Cylinder Temp. (°F)	Joint Temp. (°F)	Temp. Diff. Between Cylinder & Joint (°F)
408	11/25/06 2:00 AM	1.8	8.99	9.88	35.2	48.2	49.8	-1.6
409	11/25/06 2:30 AM	2	8.84	9.71	35.6	47.9	49.5	-1.6
410	11/25/06 3:00 AM	2	9.09	9.42	35.6	48.4	49.0	-0.6
411	11/25/06 3:30 AM	1.6	8.78	9.17	34.9	47.8	48.5	-0.7
412	11/25/06 4:00 AM	1.6	8.35	9.28	34.9	47.0	48.7	-1.7
413	11/25/06 4:30 AM	1.6	8.59	8.86	34.9	47.5	47.9	-0.5
414	11/25/06 5:00 AM	1.3	8.02	8.85	34.3	46.4	47.9	-1.5
415	11/25/06 5:30 AM	1.1	8.19	8.58	34.0	46.7	47.4	-0.7
416	11/25/06 6:00 AM	0.9	8.06	8.28	33.6	46.5	46.9	-0.4
417	11/25/06 6:30 AM	0.7	7.6	8.02	33.3	45.7	46.4	-0.8
418	11/25/06 7:00 AM	0.5	7.57	7.96	32.9	45.6	46.3	-0.7
419	11/25/06 7:30 AM	0.3	7.4	7.88	32.5	45.3	46.2	-0.9
420	11/25/06 8:00 AM	0.2	7.34	7.55	32.4	45.2	45.6	-0.4
421	11/25/06 8:30 AM	0.1	7.24	7.44	32.2	45.0	45.4	-0.4
422	11/25/06 9:00 AM	0.4	7.27	7.01	32.7	45.1	44.6	0.5
423	11/25/06 9:30 AM	0.8	7.42	6.88	33.4	45.4	44.4	1.0
424	11/25/06 10:00 AM	2.5	7.56	6.89	36.5	45.6	44.4	1.2
425	11/25/06 10:30 AM	3.7	8.14	6.95	38.7	46.7	44.5	2.1
426	11/25/06 11:00 AM	5.2	8.36	6.82	41.4	47.0	44.3	2.8
427	11/25/06 11:30 AM	6.7	8.92	7.04	44.1	48.1	44.7	3.4
428	11/25/06 12:00 PM	8.6	9.43	6.88	47.5	49.0	44.4	4.6
429	11/25/06 12:30 PM	9.1	9.75	7.24	48.4	49.6	45.0	4.5
430	11/25/06 1:00 PM	10.1	10.42	7.47	50.2	50.8	45.4	5.3
431	11/25/06 1:30 PM	11.4	10.89	7.74	52.5	51.6	45.9	5.7

Reading Number	Time	Ambient Temp. (°C)	Cylinder Temp. (°C)	Joint Temp. (°C)	Ambient Temp. (°F)	Cylinder Temp. (°F)	Joint Temp. (°F)	Temp. Diff. Between Cylinder & Joint (°F)
432	11/25/06 2:00 PM	12	11.34	8.1	53.6	52.4	46.6	5.8
433	11/25/06 2:30 PM	12.9	11.75	8.71	55.2	53.2	47.7	5.5
434	11/25/06 3:00 PM	12.8	11.95	8.82	55.0	53.5	47.9	5.6
435	11/25/06 3:30 PM	12.3	11.97	9.02	54.1	53.5	48.2	5.3
436	11/25/06 4:00 PM	12	11.75	9.7	53.6	53.2	49.5	3.7
437	11/25/06 4:30 PM	10.8	11.74	9.92	51.4	53.1	49.9	3.3
438	11/25/06 5:00 PM	9.9	11.37	9.76	49.8	52.5	49.6	2.9
439	11/25/06 5:30 PM	8.9	11.36	9.49	48.0	52.4	49.1	3.4
440	11/25/06 6:00 PM	8.1	11.25	9.97	46.6	52.3	49.9	2.3
441	11/25/06 6:30 PM	7.6	10.95	9.96	45.7	51.7	49.9	1.8
442	11/25/06 7:00 PM	8.4	10.8	10.02	47.1	51.4	50.0	1.4
443	11/25/06 7:30 PM	8.1	10.8	9.86	46.6	51.4	49.7	1.7
444	11/25/06 8:00 PM	7.4	10.54	9.69	45.3	51.0	49.4	1.5
445	11/25/06 8:30 PM	7.4	10.45	9.97	45.3	50.8	49.9	0.9
446	11/25/06 9:00 PM	7.2	10.32	9.81	45.0	50.6	49.7	0.9
447	11/25/06 9:30 PM	7.1	10.41	9.71	44.8	50.7	49.5	1.3
448	11/25/06 10:00 PM	7.1	10.37	9.96	44.8	50.7	49.9	0.7
449	11/25/06 10:30 PM	7	10.45	9.82	44.6	50.8	49.7	1.1
450	11/25/06 11:00 PM	6.9	10.19	9.85	44.4	50.3	49.7	0.6
451	11/25/06 11:30 PM	6.8	10.17	9.7	44.2	50.3	49.5	0.8
452	11/26/06 12:00 AM	6.6	10.09	9.62	43.9	50.2	49.3	0.8
453	11/26/06 12:30 AM	6.7	9.97	9.65	44.1	49.9	49.4	0.6
454	11/26/06 1:00 AM	6.5	9.93	9.59	43.7	49.9	49.3	0.6
455	11/26/06 1:30 AM	5.7	9.76	9.6	42.3	49.6	49.3	0.3

Reading Number	Time	Ambient Temp. (°C)	Cylinder Temp. (°C)	Joint Temp. (°C)	Ambient Temp. (°F)	Cylinder Temp. (°F)	Joint Temp. (°F)	Temp. Diff. Between Cylinder & Joint (°F)
456	11/26/06 2:00 AM	4.6	9.28	9.46	40.3	48.7	49.0	-0.3
457	11/26/06 2:30 AM	4	9.23	9.32	39.2	48.6	48.8	-0.2
458	11/26/06 3:00 AM	3.7	9.13	9.01	38.7	48.4	48.2	0.2
459	11/26/06 3:30 AM	3.1	8.67	8.92	37.6	47.6	48.1	-0.4
460	11/26/06 4:00 AM	3	8.66	8.76	37.4	47.6	47.8	-0.2
461	11/26/06 4:30 AM	2.6	8.36	8.8	36.7	47.0	47.8	-0.8
462	11/26/06 5:00 AM	2.9	8.57	8.51	37.2	47.4	47.3	0.1
463	11/26/06 5:30 AM	3.1	8.9	8.48	37.6	48.0	47.3	0.8
464	11/26/06 6:00 AM	4.3	8.62	8.33	39.7	47.5	47.0	0.5
465	11/26/06 6:30 AM	5	8.61	8.13	41.0	47.5	46.6	0.9
466	11/26/06 7:00 AM	5.4	8.87	8.23	41.7	48.0	46.8	1.2
467	11/26/06 7:30 AM	5.7	8.86	8.22	42.3	47.9	46.8	1.2
468	11/26/06 8:00 AM	5.9	9.16	8.16	42.6	48.5	46.7	1.8
469	11/26/06 8:30 AM	6	8.99	8.34	42.8	48.2	47.0	1.2
470	11/26/06 9:00 AM	6.3	9.38	8.29	43.3	48.9	46.9	2.0
471	11/26/06 9:30 AM	6.7	9.33	8.35	44.1	48.8	47.0	1.8
472	11/26/06 10:00 AM	6.9	9.62	8.29	44.4	49.3	46.9	2.4
473	11/26/06 10:30 AM	7.1	9.77	8.34	44.8	49.6	47.0	2.6
474	11/26/06 11:00 AM	7.2	9.7	8.27	45.0	49.5	46.9	2.6
475	11/26/06 11:30 AM	7.6	10.05	8.61	45.7	50.1	47.5	2.6
476	11/26/06 12:00 PM	7.9	10.28	8.61	46.2	50.5	47.5	3.0
477	11/26/06 12:30 PM	8.5	10.52	8.93	47.3	50.9	48.1	2.9
478	11/26/06 1:00 PM	9.1	10.9	8.73	48.4	51.6	47.7	3.9
479	11/26/06 1:30 PM	9.9	11.43	9.01	49.8	52.6	48.2	4.4

Reading Number	Time	Ambient Temp. (°C)	Cylinder Temp. (°C)	Joint Temp. (°C)	Ambient Temp. (°F)	Cylinder Temp. (°F)	Joint Temp. (°F)	Temp. Diff. Between Cylinder & Joint (°F)
480	11/26/06 2:00 PM	11.5	12.04	9.25	52.7	53.7	48.7	5.0
481	11/26/06 2:30 PM	12.7	12.39	9.63	54.9	54.3	49.3	5.0
482	11/26/06 3:00 PM	12.4	12.7	9.9	54.3	54.9	49.8	5.0
483	11/26/06 3:30 PM	12.2	12.62	10.18	54.0	54.7	50.3	4.4
484	11/26/06 4:00 PM	11.9	12.76	10.38	53.4	55.0	50.7	4.3
485	11/26/06 4:30 PM	11.7	12.73	10.45	53.1	54.9	50.8	4.1
486	11/26/06 5:00 PM	11.4	12.58	10.91	52.5	54.6	51.6	3.0
487	11/26/06 5:30 PM	11.2	12.45	10.84	52.2	54.4	51.5	2.9
488	11/26/06 6:00 PM	10.8	12.53	10.92	51.4	54.6	51.7	2.9
489	11/26/06 6:30 PM	10.6	12.59	11.2	51.1	54.7	52.2	2.5
490	11/26/06 7:00 PM	10.5	12.37	11.14	50.9	54.3	52.1	2.2
491	11/26/06 7:30 PM	10.5	12.33	11.2	50.9	54.2	52.2	2.0
492	11/26/06 8:00 PM	10.4	12.34	11.31	50.7	54.2	52.4	1.9
493	11/26/06 8:30 PM	10.3	12.31	11.43	50.5	54.2	52.6	1.6
494	11/26/06 9:00 PM	10.2	12.26	11.43	50.4	54.1	52.6	1.5
495	11/26/06 9:30 PM	10.1	12.3	11.55	50.2	54.1	52.8	1.3
496	11/26/06 10:00 PM	9.8	12.27	11.46	49.6	54.1	52.6	1.5
497	11/26/06 10:30 PM	9.1	12.13	11.33	48.4	53.8	52.4	1.4
498	11/26/06 11:00 PM	7.9	11.77	11.2	46.2	53.2	52.2	1.0
499	11/26/06 11:30 PM	7.2	11.2	11.04	45.0	52.2	51.9	0.3
500	11/27/06 12:00 AM	6.4	11.2	10.63	43.5	52.2	51.1	1.0
501	11/27/06 12:30 AM	5.7	10.83	10.67	42.3	51.5	51.2	0.3
502	11/27/06 1:00 AM	5.2	10.25	10.23	41.4	50.5	50.4	0.0
503	11/27/06 1:30 AM	4.7	10.61	9.85	40.5	51.1	49.7	1.4

Reading Number	Time	Ambient Temp. (°C)	Cylinder Temp. (°C)	Joint Temp. (°C)	Ambient Temp. (°F)	Cylinder Temp. (°F)	Joint Temp. (°F)	Temp. Diff. Between Cylinder & Joint (°F)
504	11/27/06 2:00 AM	4.5	10.11	9.81	40.1	50.2	49.7	0.5
505	11/27/06 2:30 AM	4.8	9.92	9.29	40.6	49.9	48.7	1.1
506	11/27/06 3:00 AM	5.1	10.03	9.24	41.2	50.1	48.6	1.4
507	11/27/06 3:30 AM	5.4	9.77	9.14	41.7	49.6	48.5	1.1
508	11/27/06 4:00 AM	5.7	9.83	9.05	42.3	49.7	48.3	1.4
509	11/27/06 4:30 AM	5.5	9.85	8.99	41.9	49.7	48.2	1.5
510	11/27/06 5:00 AM	5.5	9.47	8.97	41.9	49.0	48.1	0.9
511	11/27/06 5:30 AM	5.2	9.4	8.78	41.4	48.9	47.8	1.1
512	11/27/06 6:00 AM	4.7	9.05	8.62	40.5	48.3	47.5	0.8
513	11/27/06 6:30 AM	4.2	9.21	8.47	39.6	48.6	47.2	1.3
514	11/27/06 7:00 AM	4.1	9.24	8.35	39.4	48.6	47.0	1.6
515	11/27/06 7:30 AM	4.2	9.34	8.26	39.6	48.8	46.9	1.9
516	11/27/06 8:00 AM	4.4	8.96	8.26	39.9	48.1	46.9	1.3
517	11/27/06 8:30 AM	4.5	8.97	8.15	40.1	48.1	46.7	1.5
518	11/27/06 9:00 AM	4.5	9.09	8.15	40.1	48.4	46.7	1.7
519	11/27/06 9:30 AM	4.7	9.18	8.07	40.5	48.5	46.5	2.0
520	11/27/06 10:00 AM	5	8.84	7.82	41.0	47.9	46.1	1.8
521	11/27/06 10:30 AM	5.4	9.05	8.17	41.7	48.3	46.7	1.6
522	11/27/06 11:00 AM	5.3	9.05	7.9	41.5	48.3	46.2	2.1
523	11/27/06 11:30 AM	5.4	9.11	8.03	41.7	48.4	46.5	1.9
524	11/27/06 12:00 PM	5.7	9.43	7.99	42.3	49.0	46.4	2.6
525	11/27/06 12:30 PM	6.2	9.37	7.84	43.2	48.9	46.1	2.8
526	11/27/06 1:00 PM	6.7	9.62	7.84	44.1	49.3	46.1	3.2
527	11/27/06 1:30 PM	7.2	9.43	7.94	45.0	49.0	46.3	2.7

Reading Number	Time	Ambient Temp. (°C)	Cylinder Temp. (°C)	Joint Temp. (°C)	Ambient Temp. (°F)	Cylinder Temp. (°F)	Joint Temp. (°F)	Temp. Diff. Between Cylinder & Joint (°F)
528	11/27/06 2:00 PM	7.2	9.66	7.92	45.0	49.4	46.3	3.1
529	11/27/06 2:30 PM	7.2	9.53	8.14	45.0	49.2	46.7	2.5
530	11/27/06 3:00 PM	7.3	9.52	8.24	45.1	49.1	46.8	2.3
531	11/27/06 3:30 PM	7.3	9.83	8.32	45.1	49.7	47.0	2.7
532	11/27/06 4:00 PM	7.4	9.73	8.28	45.3	49.5	46.9	2.6

Volume 1-2. Laboratory Testing of Full-Depth Precast, Prestressed Concrete Deck Panels: Boone County Bridge

Technical Report Documentation Page

1. Report No. IHRB Project TR-561	2. Government Accession No.	3. Recipient's Catalog No.	
4. Title and Subtitle Precast Concrete Elements for Accelerated Bridge Construction: Laboratory Testing of Full-Depth Precast, Prestressed Concrete Deck Panels, Boone County Bridge		5. Report Date January 2009 6. Performing Organization Code	
7. Author(s) Terry J. Wipf, F. Wayne Klaiber, Brent Phares, and Ryan P. Bowers		8. Performing Organization Report No. CTRE Project 06-262	
9. Performing Organization Name and Address Bridge Engineering Center Iowa State University 2711 South Loop Drive, Suite 4700 Ames, IA 50010-8664		10. Work Unit No. (TRAIS) 11. Contract or Grant No.	
12. Sponsoring Organization Name and Address Iowa Highway Research Board Iowa Department of Transportation 800 Lincoln Way Ames, IA 50010		13. Type of Report and Period Covered Final Report 14. Sponsoring Agency Code	
15. Supplementary Notes Visit www.ctre.iastate.edu for color PDF files of this and other research reports.			
16. Abstract This second section of Volume 1 focuses on the laboratory testing of full-depth precast, prestressed concrete deck panels used in the construction of a continuous four-girder, three span bridge over Squaw Creek on 120th Street in Boone County, Iowa. Various laboratory tests were conducted on a single panel and on two panels connected by a closure pour. These tests ranged from determining physical properties of the panel (compressive strength and prestressing force), to determining the panel's response in various circumstances (moving with a crane, during field leveling, and under loading). This report details the results of these laboratory tests.			
17. Key Words accelerated bridge construction—Boone County, Iowa—field testing—laboratory strength testing—precast concrete abutments, pier caps, deck panels—prestressed concrete girders		18. Distribution Statement No restrictions.	
19. Security Classification (of this report) Unclassified.	20. Security Classification (of this page) Unclassified.	21. No. of Pages 105	22. Price NA

Form DOT F 1700.7 (8-72) **Reproduction of completed page authorized**

PRECAST CONCRETE ELEMENTS FOR ACCELERATED BRIDGE CONSTRUCTION:
LABORATORY TESTING OF FULL-DEPTH PRECAST, PRESTRESSED CONCRETE DECK PANELS: BOONE COUNTY BRIDGE

Final Report
January 2009

Principal Investigator
Terry J. Wipf, Director, Bridge Engineering Center
Center for Transportation Research and Education, Iowa State University

Co-Principal Investigators
F. Wayne Klaiber, Professor of Civil, Construction, and Environmental Engineering
Iowa State University

Brent M. Phares, Associate Director, Bridge Engineering Center
Center for Transportation Research and Education, Iowa State University

Mike D. LaViolette, Former Bridge Engineer
Iowa State University

Research Assistant
Ryan P. Bowers

Authors
Terry J. Wipf, F. Wayne Klaiber, Brent Phares, and Ryan P. Bowers

Sponsored by
the Iowa Highway Research Board (IHRB Project TR-561)
and Boone County, Iowa, through the Federal Highway Administration's
Innovative Bridge Research and Construction Program

Preparation of this report was financed in part through funds provided by
the Iowa Department of Transportation through its research management agreement with
the Center for Transportation Research and Education (CTRE Project 06-262).

A report from
Center for Transportation Research and Education
Iowa State University
2711 South Loop Drive, Suite 4700
Ames, IA 50010-8664
Phone: 515-294-8103
Fax: 515-294-0467
www.ctre.iastate.edu

TABLE OF CONTENTS

LIST OF FIGURES

LIST OF TABLES

ACKNOWLEDGMENTS

The authors would like to thank the Iowa Highway Research Board, the Iowa Department of Transportation, Boone County and the Federal Highway Administration for providing funding, design expertise, and research collaboration for this project. Special recognition is give to the following individuals for their significant contributions to the research: Ahmad Abu-Hawash, Jim Nelson, Stuart Nielsen, and many other staff from the Office of Bridges and Structures at the Iowa Department of Transportation; Curtis Monk, Iowa Division, Federal Highway Administration; Dave Anthoney (recently retired), Bob Kieffer and Scott Kruse, Boone County; and Doug Wood, Iowa State University along with numerous undergraduate students, including Matt Goliber, Matt Becker, Nathan Hardisty, Tom Lewin, Carl Zeigler, Casey Faber, Ryan Evans, Jacob Wilson, Jill Barada, Greg Cabalka, and Laura Scott. Finally, thanks are given to the following graduate students for their help with the laboratory testing: Vernon Wineland, Mark Currie, Adam Faris, Samantha Kevern, and Jeremy Koskie.

EXECUTIVE SUMMARY

As the United States highway infrastructure is in need of rehabilitation due to increasing traffic needs and structural inadequacies, use of precast concrete elements is increasing. Use of precast concrete systems provide various advantages, including minimizing traffic disruption, increasing the quality of the final product, and lowering life-cycle costs. Both the Federal Highway Administration and the Iowa Department of Transportation have recognized the benefits of using precast concrete elements in bridge construction to help reduce the duration of construction projects.

This second section of Volume 1 of the report focuses on the laboratory testing of full-depth precast, prestressed concrete deck panels used in the construction of a continuous four-girder, three span bridge over Squaw Creek on 120th Street in Boone County, Iowa. Various laboratory tests were conducted on a single panel and on two panels connected by a closure pour. These tests ranged from determining physical properties of the panel (compressive strength and prestressing force), to determining the panel's response in various circumstances (moving with a crane, during field leveling, and under loading).

Tests were conducted to determine physical characteristics of a deck panel such as compressive strength and stress in the mild reinforcing due to prestressing. The average compressive strength of the concrete core samples was 7,600 psi, which exceeded the specified compressive strength of 5,000 psi. Prestressing strands in one post-tensioning channel were cut to determine the amount of stress in each strand due to prestressing. Of the six bars instrumented, five were found to have a stress lower than that expected from the initial prestressing force.

Stresses in the mild reinforcing bars were monitored in the laboratory while a panel was lifted with a crane. Two different strap configurations were used to lift the panel; the first configuration used four lifting straps, and the second used two lifting straps. Results from these tests showed the strap configuration did not have a significant effect on the stresses induced in the mild reinforcing bars. The total flexural and axial strength of a bar used during these tests had a maximum value of 61%. Panels were also leveled in the laboratory to monitor the stresses in the mild reinforcement. Bars were found to utilize only 70% of their flexural and axial strength during this process.

Service load tests were performed on both a single panel and two panels connected by a closure pour. Through these tests it was determined that the deck panels had adequate strength under service loads. Panels also met American Association of State Highway and Transportation Officials (AASHTO) requirements for deflection under service loads.

Both a single panel and two connected panels were tested to failure. Ultimate load tests included testing a single panel and two connected panels to a flexural failure, and testing the connected panels to a punching shear failure. The connected panels also experienced a combination punching shear and flexure failure during one test. Failures during each test occurred at loads much greater than the service loads the panels are expected to experience in the field.

1. INTRODUCTION

1.1 Background

Due to factors including increasing traffic needs, inadequacies of the structure, and increasing truck weights, the highway infrastructure in the United States (U.S.) is in need of rehabilitation or replacement. In order to ensure the safety of the public, this rehabilitation/replacement must be conducted in a manner that both minimizes congestion and improves safety. A way to meet these goals is through the use of prefabricated concrete systems (Russell *et al*., 2005).

Prefabricated concrete systems provide various advantages over the use of cast-in-place (CIP) systems. Use of prefabricated concrete systems can:

- Minimize traffic disruption
- Improve constructability
- Improve work-zone safety
- Minimize construction impact on the environment
- Increase the quality of the final product
- Lower life-cycle costs

Use of precast bridge elements also allows construction to proceed during cold weather. Bridges can be constructed quicker because of the elimination of cure times from the critical path of the construction schedule (Russell *et al*., 2005).

Both the Federal Highway Administration (FHWA) and Iowa Department of Transportation (DOT) have recognized the need for use of precast concrete elements in bridge construction. This report focuses on the use of precast elements in the construction of the substructure and superstructure of a bridge constructed in Boone County, Iowa. The work presented in the report was sponsored by the FHWA and Iowa DOT.

The bridge in Boone County, Iowa is located over Squaw Creek on 120th Street. Shown in Figure 1.1 is a map of Boone County with the location of the bridge marked. A continuous, four-girder, three-span bridge design was chosen to replace an existing Marsh Arch bridge at the site. A photograph of the Marsh Arch bridge that was replaced is shown in Figure 1.2a, while the replacement bridge is shown in Figure 1.2b. Dimensions of the replacement bridge are 151 ft - 4 in. long and 33 ft - 2 in wide. Span lengths are 47 ft - 5 in., 56 ft - 6 in., and 47 ft - 5 in. The original Marsh Arch bridge was a single span arch 76 ft in length and 18 ft wide.

Precast elements used for this bridge include abutment caps and pier caps for the substructure and girders and full-depth deck panels for the superstructure. Deck panels were prestressed in the transverse direction of the bridge and had two full-depth channels over the girders for post-tensioning. After all the deck panels were placed, the bridge was post-tensioned in the longitudinal direction. Performance of the individual components was evaluated in the laboratory, and the overall performance of the bridge was tested in the field.

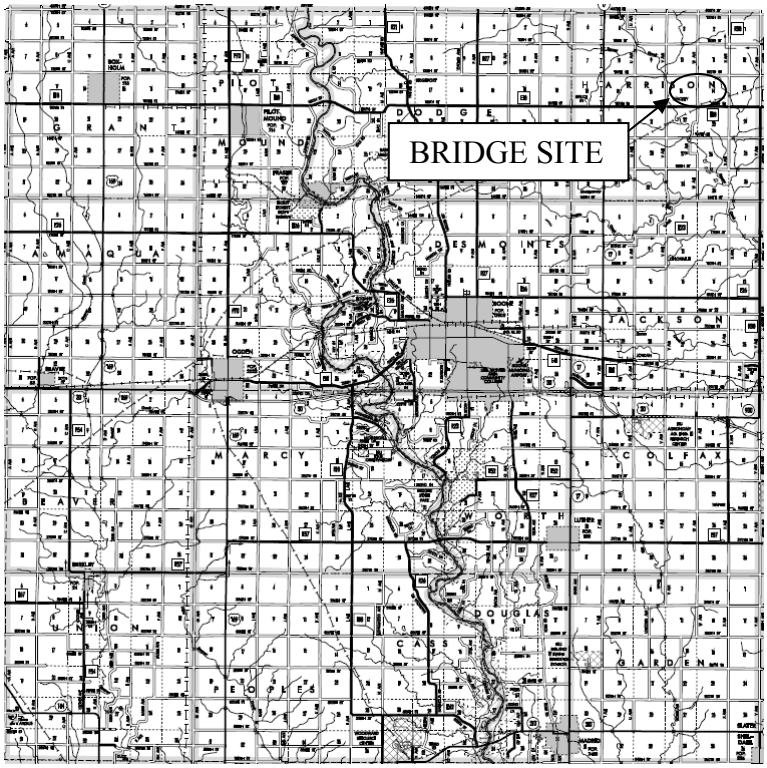

a) Map of Boone County

b) Location of bridge

Figure 1.1. Location of Boone County bridge

a) Replaced Marsh Arch bridge

b) Completed replacement bridge

Figure 1.2. Original and replacement Boone County bridges

1.2 Research Objectives

Objectives of this research were based on input from the Iowa DOT and Iowa State University (ISU) Bridge Engineering Center (BEC) researchers involved with the project. The following objectives were the focus of this research project:

- Determine the actual strength of the connection between the precast abutment cap and the piles
- Determine the strength and behavior of the longitudinal closure joint connecting deck panels
- Monitor the stresses present in the mild reinforcing bars during lifting and leveling of the deck panels

- Observe the flow of concrete in the post-tensioning channels to ensure no void spaces are created
- Document the construction process, particularly any problems or difficulties that occurred
- Install instrumentation to allow for long-term monitoring of the bridge deck
- Monitor and evaluate the deck panels and post-tensioning strand forces during the post-tensioning operation
- Determine the response of the field bridge to loading

These objectives were met through various laboratory and field tests performed on specimens; test details and test results will be presented in this report.

1.3 Scope of Research

The first task for this project was the completion of a review of literature related to the project. First, literature relating to accelerated precast concrete superstructure elements was reviewed which was followed by a more focused review of projects involving various deck panel systems. A summary of the literature reviewed for this project is presented in Section 0.

Once the literature review was completed, laboratory testing of the deck panels was conducted. A variety of tests were executed to meet the previously stated project objectives. An explanation of the various laboratory setups and tests conducted is presented in Chapter 2.

Test results from the various laboratory tests along with a discussion of the results are presented in Chapter 0. Also, a comparison of the results to design standards and material yield strengths is provided. A summary of the research, conclusions, and recommendations based on the laboratory tests are presented in Chapter 4.

1.4 Literature Review

An increase in costs coupled with a decrease in highway revenues have had a serious impact on the highway construction program, leading to the need for economical bridge systems. Because of this, the use of precast bridge elements has become more prevalent in the construction industry (Tokerud, 1979). Using precast bridge elements in place of CIP elements offers various advantages. Precast concrete construction contributes to the practice of sustainability by incorporating integrated design, using materials efficiently, and reducing construction site disturbance, waste, and noise (VanGeem, 2006). Economics also influence the decision to use CIP or precast elements.

By using precast elements, major time-consuming tasks such as the erection and removal of formwork, placement of reinforcing steel and concrete, and concrete curing are not completed at the job site. Instead, these tasks are completed off-site, and the finished element is delivered to the construction site and placed when needed for the construction to continue. This can significantly compress the project timeline and reduce traffic disruption. Reducing the

construction schedule is important in colder climates where a large number of construction projects must be completed in the short period of time when the weather conditions are favorable (Bell III *et al*., 2006).

A second advantage of using precast concrete elements is that fabrication occurs in a controlled environment with stringent quality control. By fabricating at a plant, the fabricator can take as much time as necessary to properly fabricate the elements. This leads to greater durability and uniformity of the elements (Hieber *et al*., 2005). Also, this allows for greater control of the concrete cover over the reinforcing steel, decreasing the likelihood of inadequate cover and surface spalling (VanGeem, 2006).

Work-zone safety is improved by using precast concrete elements. Workers are exposed to high-speed traffic and other on-site construction hazards for a shorter amount of time due to the elimination of constructing formwork and casting concrete on-site (Hieber *et al*., 2005). Safety is also increased because less work is done in close proximity to power lines and over water (Bell III *et al*., 2006).

Precast elements provide some economic advantages. A more durable product typically results from precasting, which in turn can decrease life cycle costs. Another economic benefit is the potential the same precast elements can be used at different projects, resulting in a repeatability of the use of the design (Bell III *et al*., 2006). CIP concrete has seen an increase in cost due to rising labor costs. Labor requirements for CIP concrete include the construction of falsework, forms, placing steel, and casting and finishing the concrete (Tokerud, 1979).

Construction of CIP concrete bridges has a greater impact on the environment than using precast elements. Erection and removal of the formwork required for CIP bridges requires workers and equipment to access the underside of the bridge. This causes a great disturbance to the surrounding environment and increases the probability of materials falling into the waterway (Bell III *et al*., 2006).

CIP concrete decks do provide some advantages over using precast elements. Adjustments can be made to CIP decks in the field, allowing for the production of a smooth roadway profile. Also, CIP concrete decks provide composite action. However, use of CIP decks result in a low construction speed, the need for strict field quality control, and cracking due to shortening of the deck as a result of cooling during cement hydration cycle and differential creep and shrinkage. Because of cracking, CIP concrete decks often will require major repair or replacement within 15 to 25 years of construction (Fallaha *et al*., 2004). CIP decks also have a high cost because of the need to install formwork, require an extensive amount of fieldwork, and are limited in use during cold or inclement weather (Badie *et al*., 1998).

Overall, use of prefabricated elements and systems is increasing. Some of the major problems inhibiting the implementation of broader use of prefabricated systems are the initial cost, lack of standardization, lack of specialized contractors, and problems with the connections between elements (Ehmke, 2006).

1.4.1 Superstructure Types

Four types of precast concrete superstructure systems are prevalent. These systems are partial-depth precast concrete deck panels, full-depth precast concrete deck panels, prestressed concrete multibeam superstructures, and pre-constructed composite units (PCUs) (Hieber *et al*., 2005).

1.4.1.1 Partial-Depth Precast Concrete Deck Panels

Partial-depth precast concrete deck panels typically are 3.5 in. deep, 8 ft long in the longitudinal direction, and wide enough to span between bridge girders. Because the panels are only 3.5 in. deep, a CIP deck is cast once the panels are placed. The panels serve as stay-in-place forms for the CIP deck (Hieber *et al*., 2005).

Reinforcing in the deck panels is provided by pretensioning strands. Panels are pretensioned in the transverse direction. Strands are located at the mid-depth of the panel and serve as the bottom layer of reinforcing steel in the bridge deck. After the panel is placed in the field, the top layer of reinforcing steel is placed, and the CIP concrete portion of the deck is cast. Once completed, the CIP concrete and precast panels act as a composite slab (Hieber *et al*., 2005).

One problem observed with this system is the presence of reflective cracking of the CIP deck at the panel edges (Fallaha *et al*., 2004). This occurs because the deck panels are not connected at the transverse joint. Individual panels therefore can deflect differentially at the transverse joint, resulting in cracking of the CIP deck.

Experimentation has shown another problem with this system is the reduced panel arching action due to a lack of beam support anchorage for the transverse pretensioning strand in the individual panels. This in turn reduces the load capacity of the system compared to full-bridge width CIP or panel systems. Another disadvantage is the cost associated with having to construct conventional formwork for the bridge overhangs (Fallaha *et al*., 2004).

One of the first projects using partial-depth panels was the Illinois Tollway project in the 1950's. Currently partial-depth panels are used by at least 28 states and Canadian provinces. In the state of Washington, previous applications using partial-depth panels had higher construction costs but overall savings. Savings were a result of the reduced amount of traffic control required (Hieber *et al*., 2005).

The NUDECK system is a variation of the partial-depth panel system. Six inch precast concrete panels pretensioned transversely are used. Prestressing is provided by pairs of ½ in. diameter, Grade 270 low-relaxation strands at a 24 in. spacing. The pretensioning strands have a 1 in. clear spacing vertically. An effective pretensioning stress of 350 psi after losses is achieved. High-strength wire spirals are placed around the final 24 in. of each strand pair to ensure a short transfer length of the prestress force (Fallaha *et al*., 2004).

NUDECK panels contain an opening over the girder lines for running post-tensioning strands. Using an open post-tensioning channel reduces interference between the strands and shear studs

and simplifies the process of post-tensioning in the longitudinal direction. Post-tensioning is executed after a strength of approximately 1500 psi is reached in the transverse joints and prior to composite action developing. If post-tensioning is done at this time, the post-tensioning force is applied to only the deck, with none of the force distributed to the stiffer beams. Once post-tensioned, the deck is highly resistant to transverse cracking (Fallaha *et al*., 2004)

To preserve the tension in the prestressing strands through the open longitudinal channel, four #7 reinforcing bars are grouped with each pair of strands. Number 7 bars were used because of the need to resist buckling in the reinforcement during the release of the prestress and bending during handling and erection. Longitudinal reinforcement for NUDECK panels is provided by #5 steel bars spaced on 12 in. centers (Fallaha *et al*., 2004).

Conclusions based on the use of the NUDECK system are: 1) use results in control of the transverse cracking of the deck frequently observed in CIP decks due to shrinkage; 2) the continuity in both the transverse and longitudinal directions eliminates reflective cracking over joints; 3) the NUDECK system exhibits improved fatigue resistance and crack control in the longitudinal direction over the girder lines; 4) construction speed is improved because of the elimination of field forming (Badie *et al*., 1998).

1.4.1.2 Full-Depth Precast Concrete Deck Panels

Full-depth precast concrete deck panels typically are 8 in. thick, 10 ft long, and span the full width of the bridge. A wearing course is not required for full-depth panels, but one may be applied to create a smooth driving surface. The transverse joint between panels is grouted to construct a shear key for transferring load between adjacent panels. Shear studs or reinforcing bars extend from the girders and connect the girders to the panels to develop composite action. This connection is made by grouting the open channel in the deck panel in which the steel lies (Hieber *et al*., 2005).

Panels are typically pretensioned in the transverse direction; however, mild reinforcement may also be present. If panels are not prestressed in the transverse direction, cracking may occur under service load conditions (Fallaha *et al*., 2004). Recent applications of full-depth panels include post-tensioning longitudinally. Longitudinal post-tensioning places the transverse joint in compression, thus improving durability and promoting monolithic behavior of the system (Hieber *et al*., 2005).

Full-depth deck panels have been used since the early 1960's. Currently, over 18 states, Japan, Great Britain, Canada, and Mexico use full-depth panels. The primary use for these panels is for replacing deteriorated CIP decks; however their use in new bridge construction is increasing (Hieber *et al*., 2005). The majority of applications using full-depth panels have involved steel girder bridges. One explanation for this is that most older bridges requiring a deck replacement have steel girders (Slavis, 1982).

Full-depth precast concrete panels have been used in Japan in recent years because of the following benefits: improved durability, lower creep deformation, and fast construction time.

The use of full-depth panels reduces construction time by eliminating the need for formwork and CIP concrete. In Japan, deck panels are not post-tensioned in the longitudinal direction (Russell *et al*., 2005).

Other countries, such as France, use a slightly modified design for full-depth deck panels. In France, deck panels are longitudinally post-tensioned together and contain screws used to adjust the elevation of the panel. Instead of match casting panels, a transverse CIP joint can be cast between the panels (Russell *et al*., 2005).

An advantage of using full-depth panels over CIP decks is the ability to use a wider girder spacing. Also, because the deck panels are connected to the girders by shear studs, a positive connection for lateral load is provided that was not included in the bridge design. Transverse continuity is accomplished through the use of overlapping hoop bars extending from the deck panels (Russell *et al*., 2005).

The full-depth, full width precast deck panel system could become a low cost solution for deck replacement projects if the panels are standardized. Use of the system needs to be widespread enough that contractors become familiar with the construction process. This system is very durable because all of the components are cast in a controlled environment, which alleviates the early age deck cracking and differential and restrained shrinkage cracking (Menkulasi and Carin, 2005).

1.4.1.3 Prestressed Concrete Multibeam Superstructures

Use of prestressed concrete multibeam superstructures has been extensive throughout the U.S. This system is common for bridges subjected to low traffic volumes and in remote areas where fresh concrete is difficult to obtain. Prestressed concrete multibeam superstructures consist of precast/prestressed concrete girders such as double tees, box beams, deck bulb-tees, and channels placed adjacently and spanning in the longitudinal direction of the bridge (Hieber *et al*, 2005).

Girders in multibeam superstructures serve as both the deck and support system for the superstructure. Adjacent girders are connected by one of or a combination of grout-filled shear keys, mechanical fasteners, or transverse post-tensioning. A non-composite wearing course is added to provide a smooth riding surface. In the state of Washington, poor performance of the longitudinal joint under heavy traffic has been observed (Hieber *et al.*, 2005).

Of the various multibeam superstructure shapes being used, the bulb tee is the most efficient. However, double tees and channels are more stable during handling and placing, and therefore are the preferred shape of contractors. Shapes such as the channel and box beam provide an additional advantage of having near-vertical flush sides; this allows adjacent members to be connected directly to each other and eliminates the need for intermediate diaphragms. Even though the box beam is less efficient than tees and channels, it is used extensively in many regions (Tokerud, 1979).

Precast prestressed concrete box girder bridges were widely used in Illinois state highways during the 1960s and 1970s. Use of these bridges was discontinued due to corrosion problems. Approximately 10 percent of prestressed box girder bridges inventoried on Illinois state highways had experienced significant corrosion, leading to a decreased bridge rating and required load restrictions. Because these bridges are economical to build, they are still widely used on county roads throughout Illinois (Hawkins *et al*., 2002).

Illinois DOT box girders are either 36 in. or 48 in. wide and vary in depth. Shallower beams contain circular voids and welded wire fabric for the shear reinforcement. Deeper beams contain rectangular voids and the shear reinforcement consists of deformed bars. The deeper beams are limited to the 36 in. width to restrict the weight and size of the girders. This allows for easy transportation to the project site and placement with a mobile crane (Hawkins *et al*., 2002).

Differential deflections between adjacent girders allowed the development of reflective cracks along the longitudinal joint between girders. Corrosion of the prestressing strands resulted from salt laded water seeping through the cracked joint and into the girder. County engineers believe a lack of transverse load distribution between adjacent girders is the cause for the longitudinal cracking (Hawkins *et al*., 2003).

Two solutions used by the Illinois DOT to resolve this problem include transversely post-tensioning the girders together and providing a composite cast-in-place concrete deck. Both solutions have worked satisfactorily, but add considerably to the cost of construction, do not ensure that corrosion will be prevented, and make replacing damaged girders more difficult. Currently these are no reasonable solutions for retrofitting bridges in service (Hawkins *et al*., 2003).

The Ohio DOT requires 1 in. diameter steel tie bars spaced at distances no greater than 25 ft to be used in box girder bridges in the state. Tie bars are placed at midheight of the girder and pass through precast ducts. However, shear key failures and large relative deflections of adjacent girders were still observed. Suggestions to improve shear key performance in Ohio include increasing the depth of the shear key and increasing the level of transverse post-tensioning (Huckelbridge *et al*., 1995).

1.4.1.4 Pre-Constructed Composite Units

Pre-constructed composite units (PCUs) are concrete or steel girders with a composite concrete bridge deck that are prefabricated. Fabrication takes place off-site and the PCUs are transported to the job by barge, truck, or rail. Once on-site, entire units are lifted into place, reducing construction time. After several units are set, the joints between units are grouted. Longitudinal and transverse post-tensioning is conducted to put the joints into compression (Hieber *et al*., 2005).

While on a scanning tour in April 2004, the Federal Highway Administration (FHWA) and the American Association of State Highway and Transportation Officials (AASHTO) observed the use of a partial depth panel system in Germany similar to the PCU system. The German system

involved casting a partial depth panel on a beam prior to erecting the beam. Beams are then set into place so the panels almost touch. Because of the closeness of the panels, there is no need for additional formwork prior to placing the CIP concrete (Russell *et al*., 2005). A project using this system can be seen in Figure 1.3.

One advantage of PCUs is the ability to fabricate units with nonstructural elements such as barrier walls, light posts, and wearing surfaces. This helps reduce the construction time of the project. Use of PCUs has been limited mostly to large projects. The first applications of PCUs were large-scale superstructure replacement projects in the 1990's (Hieber *et al*., 2005).

Figure 1.3. Placement of partial depth panels cast on beams (Russell *et al*., 2005)

1.4.2 Superstructure Element Connection Methods

The method used to connect the precast superstructure element varies with the type of element being used. Closure joints, shear keys, and cast-in-place concrete toppings are various methods used to connect precast elements and aid in load transfer.

1.4.2.1 Closure Joint

Closure joint details were observed by the FHWA and AASHTO while on the scanning tour in 2004. Prefabricated deck systems require longitudinal and transverse joints to provide continuity for live load distribution and seismic resistance. One method to accomplish this is by overlapping hoop bars that project from the edge of the slabs. The hoop bars are then overlapped by continuous loop bars, and straight bars pass through all the loops to provide continuity. This joint detail may provide better continuity between adjacent elements and better crack control along the joint than details used in the U.S (Russell *et al*., 2005).

Details similar to those observed in other countries have been used in the state of New York and are being developed for use in Texas. However, issues concerning the amount of concrete cover, loop bar bend radius, type of reinforcement to be used, properties of concrete used for the closure joint, sealing of the interface between the precast panels and CIP, and the need for an overlay need to be addressed. Several research projects sponsored by the National Cooperative Highway Research Program (NCHRP) are underway to evaluate the use of these joints (Russell *et al*., 2005).

A 1995 survey found the use of female to female joints was a common was to connect deck panels in the U.S. A variety of problems have been encountered with the use of these joints. Some of these problems are related to material quality, construction procedures, and maintenance. One problem frequently cited was leaking occurring at the joint (Issa *et al*., 1995).

1.4.2.2 Shear Key

The transverse joint must be able to resist vertical shear caused from wheel loads crossing the joint and bending induced by moving vehicular loads. The joint may be subjected to tension through drying shrinkage of the grouting material and transverse shortening of the precast concrete slabs. If the grouting material cannot resist the stresses induced during service, cracking will occur. Cracking will allow foreign materials to penetrate into the joint, gradually weakening the joint (Issa *et al*., 2003).

A visual inspection of various joint systems in bridges throughout the U.S. was conducted in 1995. From this inspection, the conclusion was drawn that the transverse joints between precast slabs should be female-to-female (shear key) with a minimum nominal width of 1 ¼ in. at the top and ½ in. at the bottom. Longitudinal post-tensioning should also be provided to compress all of the joints (Issa *et al*., 2003). If longitudinal post-tensioning is not done, a debonding of the transverse joint can occur (Issa *et al*., 1998).

A failure of the longitudinal shear key affects the strength and serviceability of the bridge. Failure compromises the lateral load distribution of the bridge, resulting in individual girders being exposed to greater live loads than designed for. Also, excessive relative displacements between adjacent girders can develop if the shear key fails. Excessive relative displacements occur because each girder acts individually with no load transfer between them (Bell III *et al*., 2006).

1.4.2.3 Cast-In-Place Topping

Use of a CIP concrete topping is another method to connect precast elements. A CIP topping will allow for production of a smooth riding surface. The topping will connect adjacent elements, allowing for continuity within the deck system and a means for transverse load transfer. CIP toppings can be made to act compositely with precast elements, improving the structural performance of the system. To achieve composite behavior, either shear reinforcement protruding from the precast sections or roughening of the contact surfaces of the elements or a combination of both are used (Bell III *et al*., 2006).

There are various drawbacks to using a CIP topping to achieve continuity between precast elements. Using CIP toppings leads to relatively slow construction speeds, the need for strict field quality control, and the possibility of cracking due to differential shrinkage between the CIP topping and the precast sections. Longitudinal reflective cracking often develops in the CIP topping about the joints formed between adjacent precast sections. Once cracking develop, water and deicing chemicals penetrate the cracks, leading to staining and spalling along with corrosion of the reinforcement (Bell III *et al*., 2006).

1.4.2.4 Post-tensioning

Providing post-tensioning is another method for connecting adjacent precast members to achieve continuity. Post-tensioning tendons are typically run perpendicular to the prestressing strands present in the member. Use of post-tensioning along with prestressing in full-depth panels eliminates concerns of cracking because the panel is compressed in both directions throughout its service life, resulting in a durable deck system (Fallaha *et al*., 2004).

The use of post-tensioning does have disadvantages. A large amount of post-tensioning is typically required for superstructures such as full-depth deck panels, which adds an additional cost and time in the field to the project (Badie *et al*., 1999). Use of post-tensioning requires the mobilization of a specialty contractor and increased construction monitoring, which increases the initial construction costs (Bell III *et al*., 2006).

One major problem associated with the use of post-tensioning is the possibility of corrosion. A walk-through inspection of 70 Florida bridges using post-tensioning revealed 44 with "indications of possible post-tensioning problems," 16 with "minor defects," and 10 with "no visible defects." However corrosion problems are not limited to Florida and not considered a problem specific to the environment of that state, as corrosion problems have been discovered in post-tensioned bridges in other states (Poston *et al*., 2003).

Corrosion problems found in the United States are the result of numerous factors, including deficient grouting specifications, possible deficiencies related to construction, and the effects of aggressive marine environments. Voids in the grout at the tendon anchorages have also been cited as a source of corrosion initiation. These problems have resulted in tendon failures within the bridges' first 10 years of service (Poston *et al*., 2003).

2. LABORATORY TESTING

Deck panels were fabricated at Andrews Prestressed Concrete, Inc. of Clear Lake, Iowa and delivered to ISU. ISU received three precast deck panels for testing. The project proposal called for the testing of two deck panels; however, ISU was able to purchase a third deck panel which had been rejected by the Iowa DOT due to the presence of a cold joint. Laboratory testing included concrete coring to determine the concrete compressive strength, determination of the compressive force in the #7 reinforcing bars due to prestressing, determination of strains in the panels while leveled and while lifted with a crane, service load testing, and ultimate load testing. A photograph of one of the precast deck panels used in this project is presented in Figure 2.1.

Figure 2.1. Full-depth precast concrete deck panel (courtesy of Iowa DOT)

2.1 Deck Panel Properties

Dimensions of the deck panels are given in Figure 2.2. As can be seen, the panels had a 60 degree skew; the dimension of the panels perpendicular to the centerline of the bridge was 16 ft - 1 in. This allowed each deck panel to span half the transverse width of the bridge. Each panel was 8 ft - 1 in. in the direction parallel to the centerline of the bridge; thus 36 panels were required to complete the bridge deck.

Each panel consisted of three segments connected by prestressing strands and mild reinforcement. The purpose of the mild reinforcement was to “hold open” a channel between the segments for the post-tensioning strands which were placed in the field. Both 10 in. channels ran in the longitudinal direction of the bridge and were aligned over the prestressed concrete girders of the bridge.

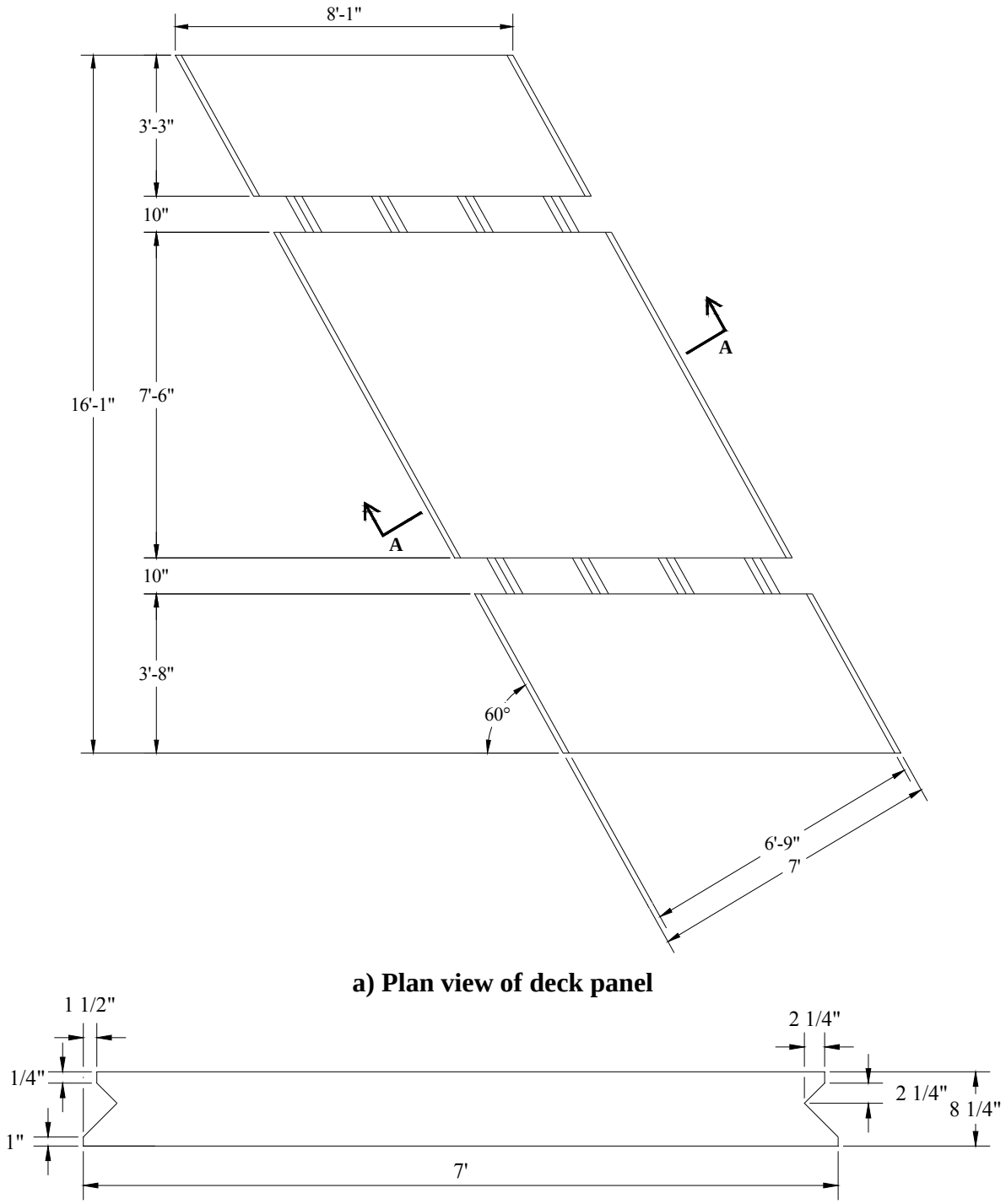

a) Plan view of deck panel

b) Section A-A

Figure 2.2. Deck panel dimensions

Also of note in Figure 2.2 is that the bottom of the panels is 3 in. wider than the panel top. This provides an opening for placing the concrete for the shear key between the individual panels. The shear key runs transversely and provides continuity between the deck panels. As shown in

Figure 2.3, the shear key surface had a diamond pattern to provide a better bond between the concrete in the panels and the concrete placed in the shear key.

Figure 2.3. Textured surface of transverse joint

Reinforcement in the deck panel is shown in Figure 2.4. All panels were reinforced the same, with the only difference among them being the presence of a cold joint in the third panel. The cold joint was a result of an equipment breakdown during casting. Grade 60 mild reinforcing bars were used for all the reinforcement; a modulus of elasticity equal to 29,000 ksi was assumed for the reinforcing steel as none of the reinforcing was tested. Number 7 and #6 reinforcing bars were used in the transverse and longitudinal directions, respectively. Four #7 bars surrounded every two prestressing strands to carry the compressive force in the strands across the open longitudinal post-tensioning channels.

Eight prestressing strands were used in each of the deck panels. Prestressing strands were uncoated, seven-wire, low relaxation steel strand with a nominal diameter of ½ in.; a modulus of elasticity equal to 27,000 ksi was assumed by the Iowa DOT for the prestressing strands. Strands were to be tensioned to 31 kips prior to release, resulting in an initial stress of approximately 158 ksi in each strand. Deck panels were specified to have a concrete strength of 4,000 psi at stress transfer and a 28 day strength of 6,000 psi.

A 1 in. pitch spiral 2 ft in length with a 4.5 in. outer diameter and 4 in. inner diameter, ASTM A227 steel, is present at each end of the prestressing strands to help with confinement of the prestressing force. Eight pairs of #5 hook bars are shown at the top of the panel in Figure 2.4a. These bars are the reinforcing steel for the longitudinal closure pour located at the longitudinal center of the bridge for transferring load between adjacent transverse panels.

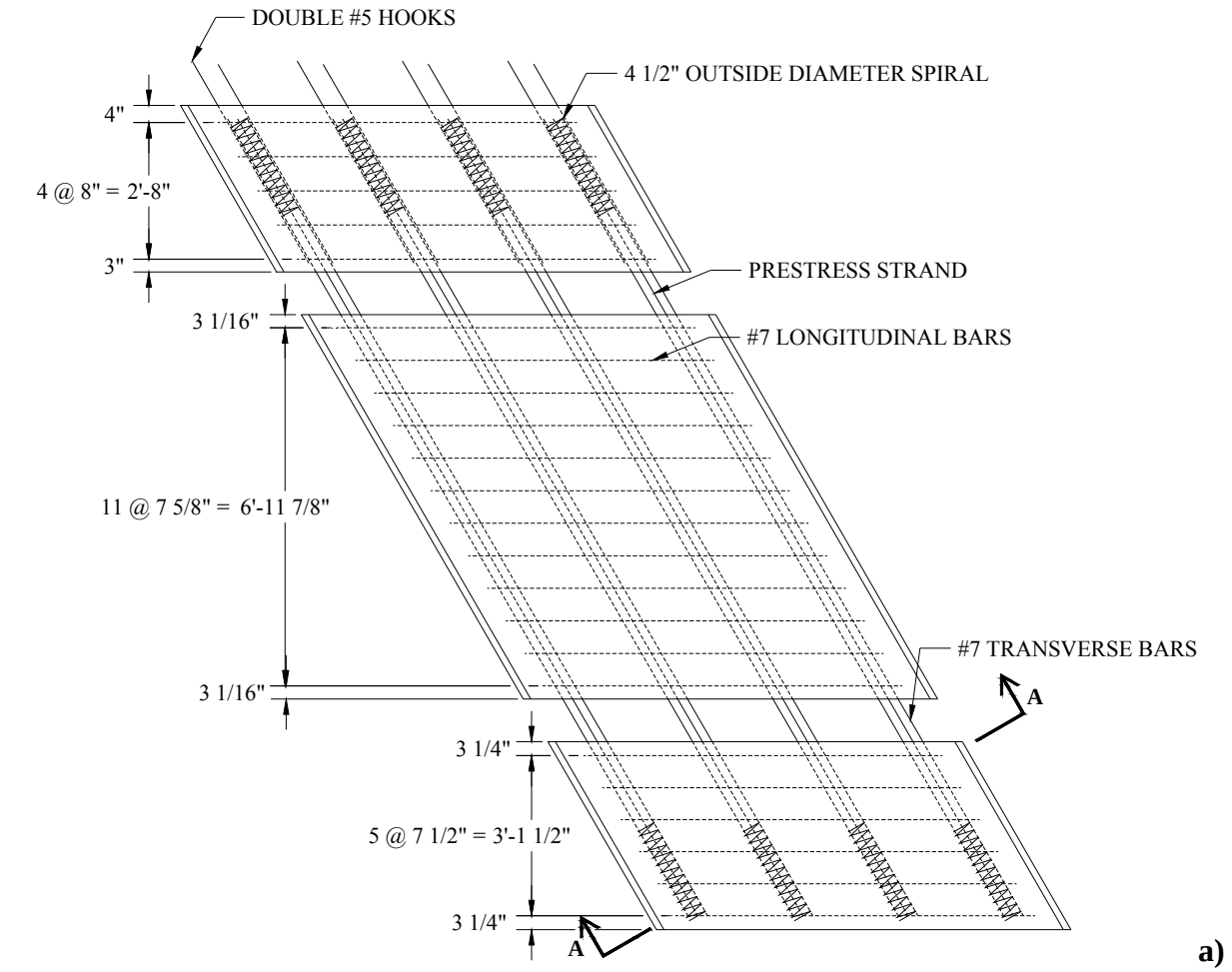

Figure 2.4. Reinforcing steel in deck panels

Shown in Figure 2.5 is the steel reinforcement in the deck panel casting beds. The four groups of prestressing steel and mild steel are visible in both figures, as well as the spirals encasing the ends of the prestressing strands. The additional steel seen in between the spirals in Figure 2.5a is the reinforcement for the barrier rail connections. Prestressing steel exiting the formwork and the double hooks are visible in Figure 2.5b.

a) Deck panel reinforcing steel

b)

b) Double hooks and prestressing strands

Figure 2.5. Deck panel reinforcing steel in formwork (courtesy of Iowa DOT)

2.2 Instrumentation

Instrumentation on the deck panels consisted of concrete strain gages, steel strain gages, and deflection transducers. In this section, the location of each type of gage installed as well as the numbering system for each type of strain measured will be presented. As will be detailed later, not every gage installed was used in every test. The specific gages used in a particular test will be presented during the discussion of the individual tests.

A general numbering system was created for identifying concrete and steel strain measurements taken during testing; it follows the pattern PW-XYZ. The first letter, P, indicates the strain is in a deck panel and the second letter, W, is 1, 2, or 3 indicating the strain of interest is in Panel 1, Panel 2, or Panel 3, respectively. The next letter, X, is either C or S and signifies the strain is in the concrete (C) or steel (S). The fourth variable, Y, is a number from 1 to 10 that identifies the location of the strain being discussed; figures displaying the locations of the strains are in the following sections. The final variable, Z, will be a T or B and denotes if the strain was measured in the top or bottom surface if it is a concrete strain, or in the bar closest to the top or bottom surface if it is a steel strain. All steel strains were measured in the top surfaces of the bars.

A similar numbering system is used for concrete and steel strains measured in the closure pour. For these strains, the general numbering system is CP-XYZ. In this system, CP designates the strain as in the closure pour. The variables X, Y, and Z have the same meaning as previously described for the deck panel strains.

Deflections are designated by PW-V. In this nomenclature, P signifies the deflection is that of a deck panel, W is either 1, 2, or 3 and designates the panel being discussed, and V varies from 1 to 10 and identifies the location of the deflection of interest. For closure pour deflections, the general naming system is CP-V. CP identifies the deflection as that of the closure pour, and V is a variable identifying the location of interest.

2.2.1 Concrete Strains

The location of the concrete strain gages used is shown in Figure 2.6a. Locations were the same for each deck panel and for both the bottom and top surfaces of the deck panel. In the longitudinal direction of the bridge, gages were placed along a line parallel to the skew. Strains were measured at the center of each panel segment and at the quarter points of the interior segment. In the transverse direction, strains were measured along two lines located in one-third of the panel width from the panel edge. A total of ten strain locations are shown in Figure 2.6a.

Strain locations are numbered in Figure 2.6b. An example of a strain designation is P2-C3T. This designation indicates the following: the strain is in deck panel (P) two (2); a concrete strain is being discussed (C); a strain at location number 3 in Figure 2.6b (3); and the strain is located on the top surface of the panel (T).

Shown in Figure 2.6c are the locations and numbering for the concrete strains in the closure pour connecting Panel 1 and Panel 2. Strains were measured 2 ft - 3 in. from the transverse edge of the panel and along the longitudinal center of the joint. Concrete strains were measured only on the top surface of the closure pour.

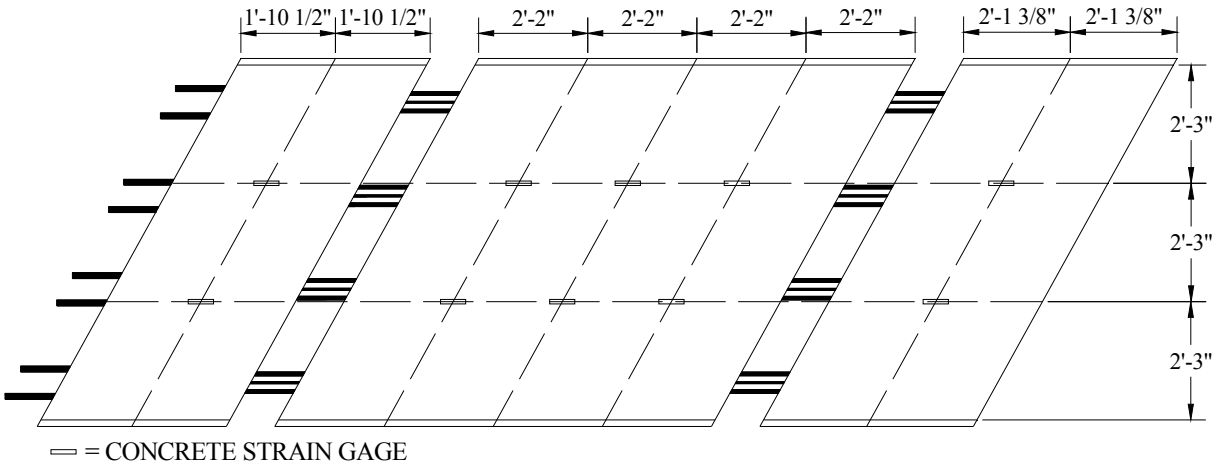

a) Location of deck panel concrete strain gages

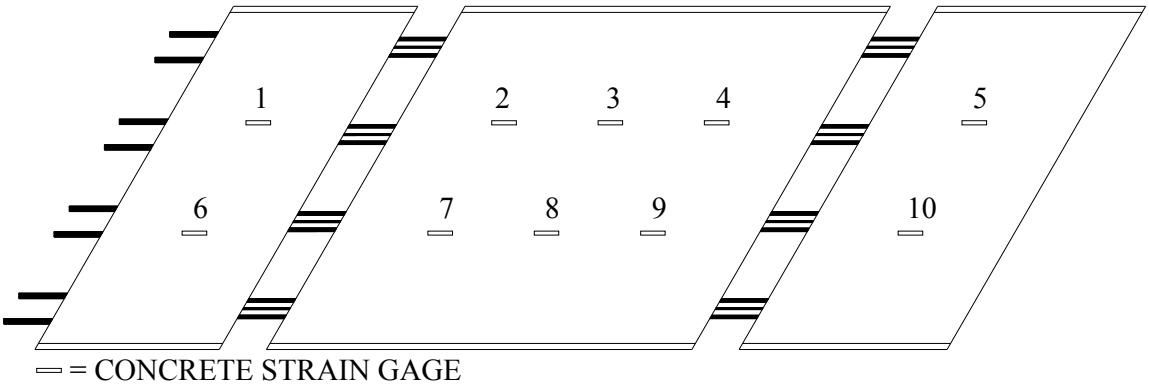

b) Numbering of deck panel concrete strain locations

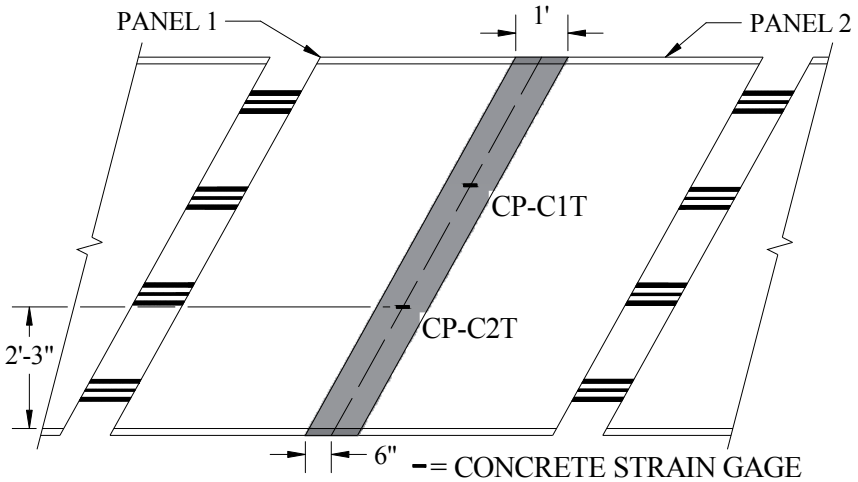

c) Closure pour concrete strain location numbering system

Figure 2.6. Location and identification of concrete strains

2.2.2 Steel Strains

Presented in Figure 2.7a and b are the numerical labels for the steel reinforcing bars for a deck panel. The number in Figure 2.7a refers to the vertical plane the measured strain is in. As illustrated in Figure 2.7b, T or B is used to indicate if a strain is in a top or bottom reinforcing bar in a particular vertical plane. An example of a number for a steel strain in a deck panel bar is P3-S3T; this strain would be in deck panel (P) three (3), is a steel strain (S) in Bar 3 (3), and in the top bar of the vertical plane (T).

Instrumentation of the closure pour hook bars is also shown in Figure 2.7; as illustrated, strains were measured for ten of the hook bars. The bar the strain was in can be seen in Figure 2.7c, and the locations of the strain measurements on the hook are shown in Figure 2.7d. As seen in Figure 2.7d, strains were only measured in the top surface of the bars, however strains in both the top and bottom bars of the hooks were measured. An example strain designation for the closure pour steel strains is CP-S7B, with CP meaning a closure pour strain, S for a steel strain, 7 being the bar number, and B meaning the bottom bar in the hook.

2.2.3 Deflections

Locations of deflections measured during testing are illustrated by black squares in Figure 2.8; deflection transducers were positioned at each location to measure the deflections. In a given test, a maximum of ten of the eleven deflection transducers were used. Deflection locations included: the four corners of the panel; the midpoints of the transverse edges; the center-point of the panel; and the midpoint between bar groups in the post-tensioning channel.

Presented in Figure 2.8b is the numbering system used for deck panel deflections. An example of the deflection numbering system is P2-3. This label is explained as follows: the deflection being analyzed is for deck panel (P) two (2); the deflection is for location 3 in Figure 2.8b.

A different configuration of deflection measurements was required once Panel 1 and Panel 2 were connected with the closure pour. Deflections measured at the deck panel corners near the closure pour were replaced with three measurements along the centerline of the closure pour. These deflections were labeled CP-1 through CP-3, as can be seen in Figure 2.8c.

2.3 Concrete Strength Testing

Concrete cores were taken to determine the actual concrete compressive strength of the deck panels at the time of testing. Cores were taken from Panel 1 after all testing on this panel was completed. Locations of the cores are shown in Figure 2.9. Panel 1 was selected for coring because this panel had sustained the least damage during loading. All cores were taken from the end span of the panel because this span was the only section that had not cracked during loading.

ASTM C 42 was followed to obtain three concrete cores from the deck panel. Cores had a diameter of 3 in. and a height of 8.25 in. Once removed from the deck panels, both ends of each core were cut resulting in a 6 in. specimen. The cores were cut to reduce the length to diameter

ratio to two and also to provide a flat and smooth surface for testing. Cores were then tested in accordance to ASTM C 39 to determine the compressive strength of the concrete.

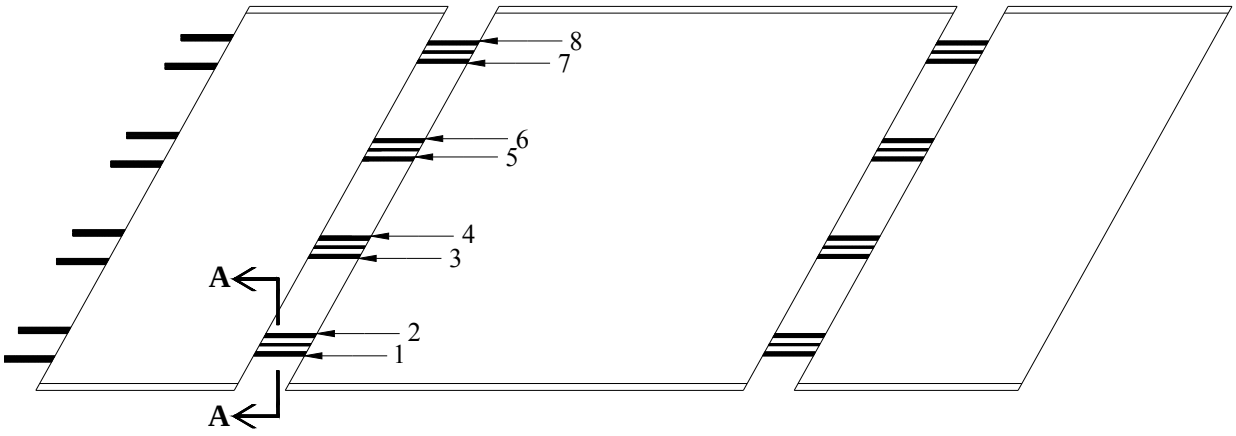

a) Deck panel bar numbering

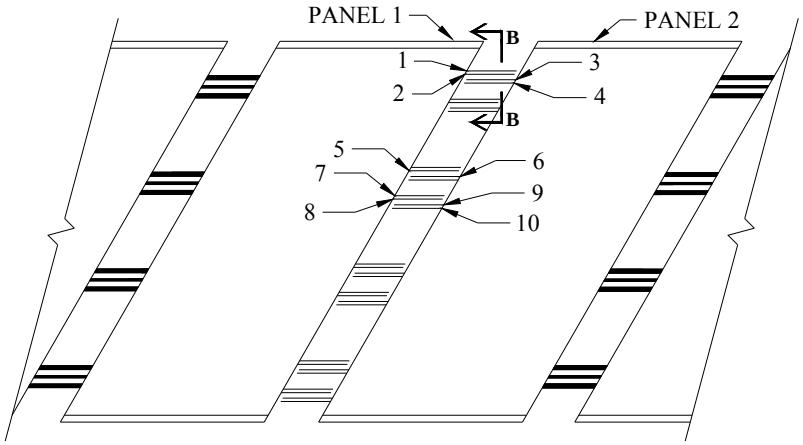

b) Closure pour bar numbering

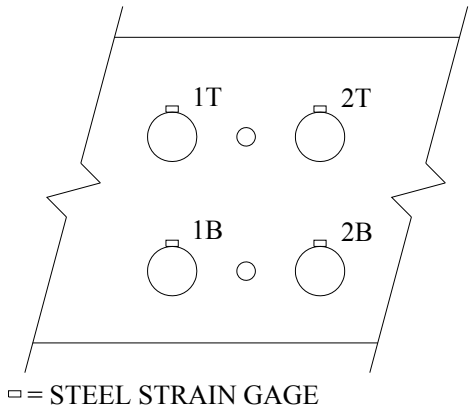

c) Section A-A

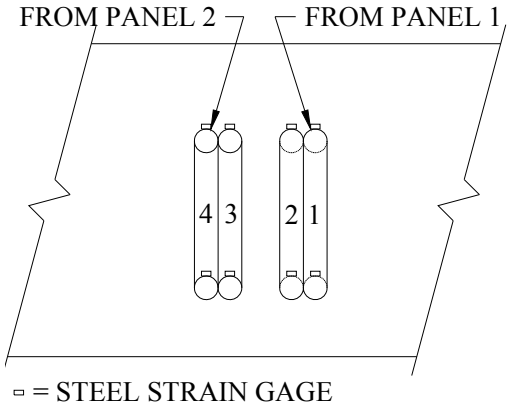

d) Section B-B

Figure 2.7. Location and identification of steel strains

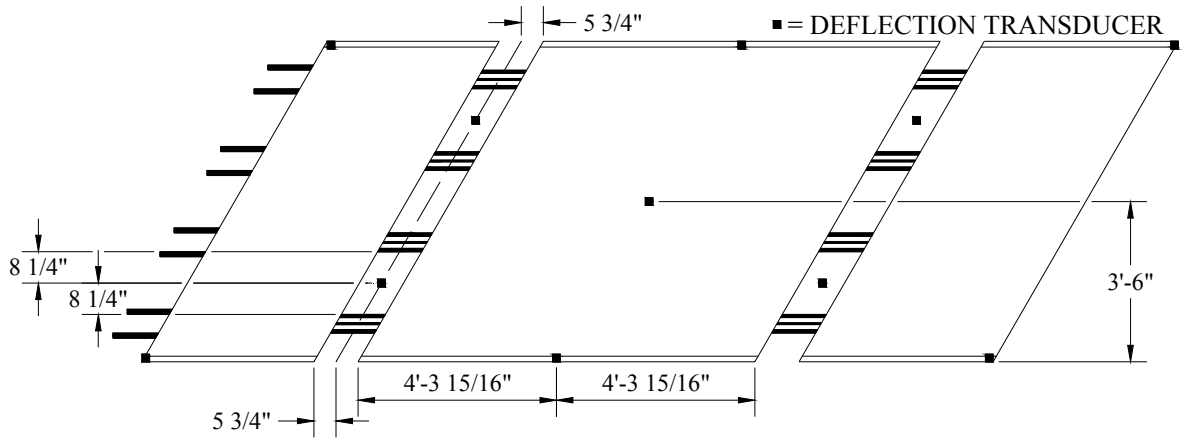

a) Location of deflection measurements

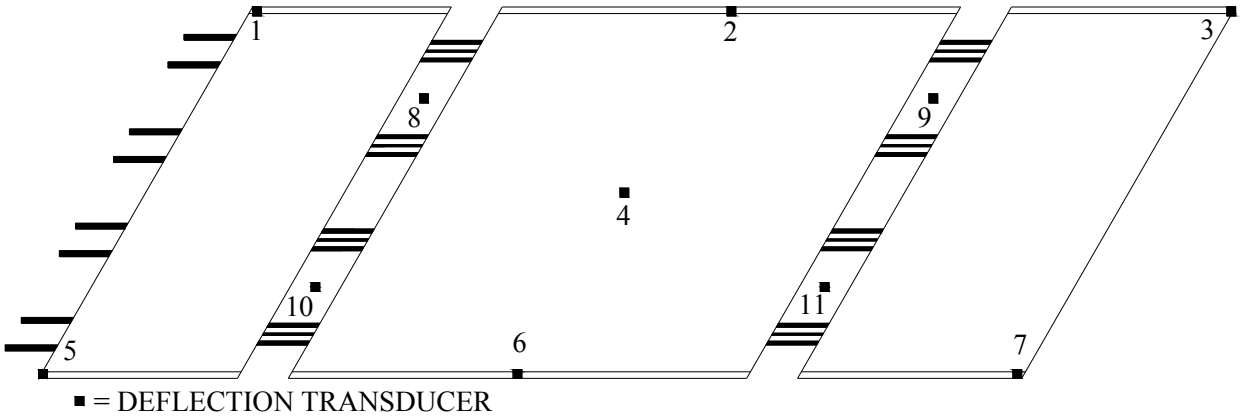

b) Deck panel deflection numbering system

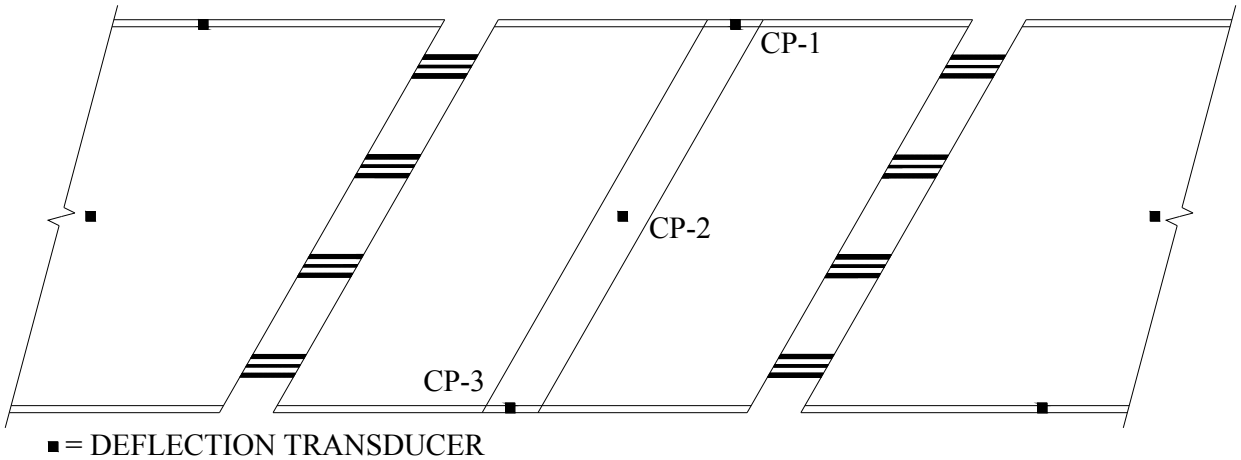

c) Closure pour deflection numbering system

Figure 2.8. Location and identification of deflection measurements

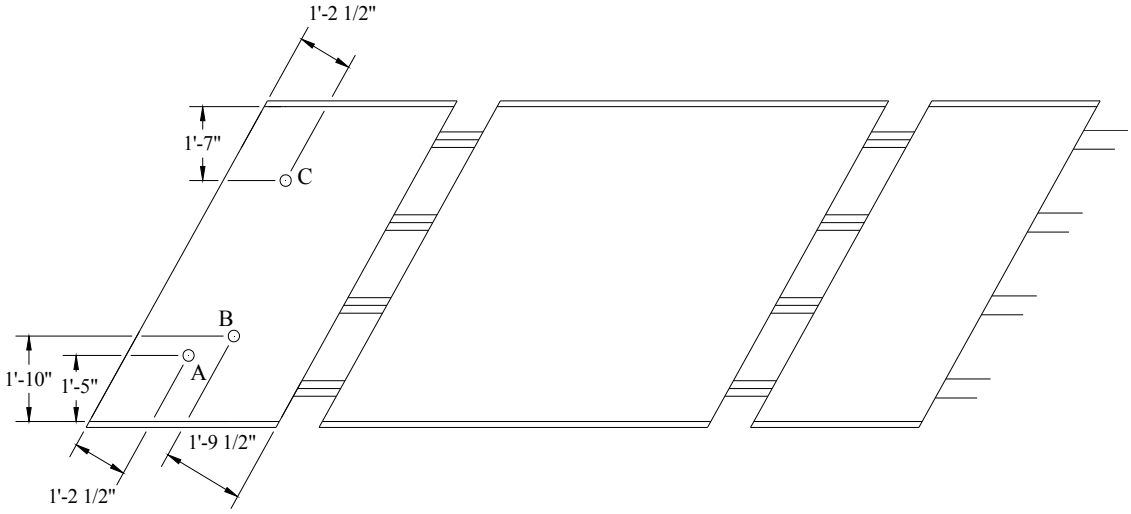

Figure 2.9. Core locations

2.4 Stresses in Panel Mild Reinforcement Due to Prestressing

The eight prestressing strands present in one longitudinal channel of Panel 3 were cut to determine the compressive force in the mild reinforcement due to prestressing. Strains were measured while cutting the strands by installing strain gages on six of the twelve mild reinforcing bars. Bars 1T, 1B, 2T, 2B, 8T, and 8B (shown in Figure 2.7a) were instrumented; a photograph of these strain gages is shown in Figure 2.10.

Figure 2.10. Reinforcing bars instrumented with steel strain gages

An initial strain reading was taken prior to beginning the test in order to record the "zero" strain in the bars. After this, the top strand between Bars 1 and 2 was cut using a torch, as shown in Figure 2.11a. Once the strand was cut data readings were taken. Next the entire top prestressing strand was removed to provide better access to the lower strand, and then the lower strand was cut. The cut strands (top and bottom) are shown in Figure 2.11b.

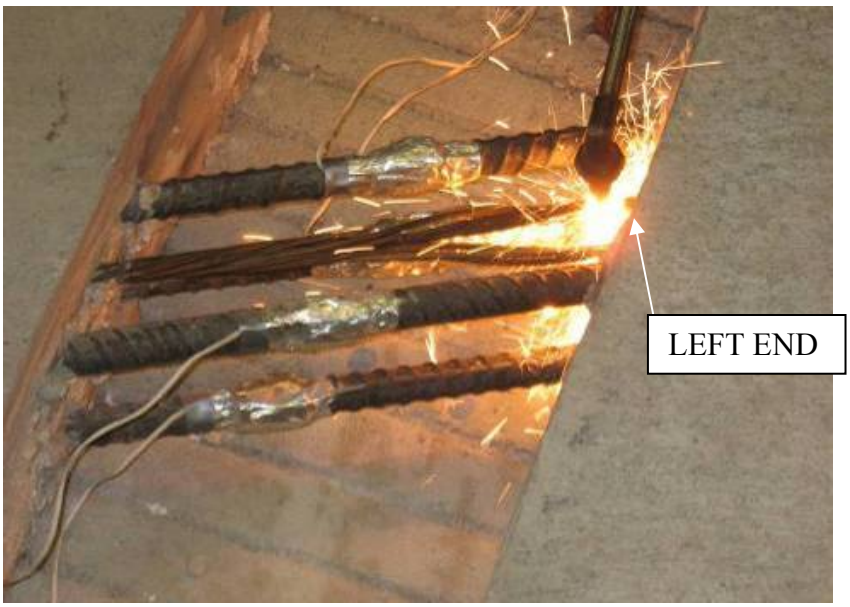

a) Cutting the first prestress strand

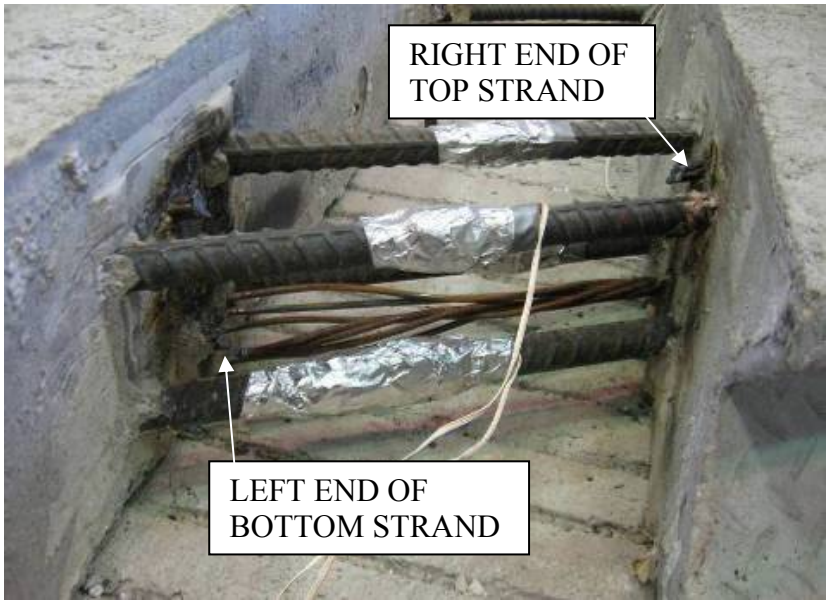

b) After removal of the prestress strands

Figure 2.11. Torch cutting of the prestress strands

Once the prestressing strands between Bars 1 and 2 were cut, the process was repeated to cut the strands between Bars 7 and 8, with data being recorded after each strand was cut. After these

strands were cut, the strands between Bars 5 and 6 were cut, followed by the strands between Bars 3 and 4. The strands were cut in this order to reduce the extra compressive force in Bars 7 and 8 after the first two strands were cut.

2.5 Lifting Panel Strains

One concern about the deck panels was the additional stress exerted on the exposed mild reinforcing bars during lifting and transporting. Panel 2 and Panel 3 were instrumented and lifted with a crane in the laboratory to determine the additional stresses induced in the exposed reinforcement. Straps were connected to the panels in two different configurations (four lifting straps and two lifting straps) and strain measurements were taken during lifting.

2.5.1 Four Lifting Straps

The first lifting configuration used four straps to lift the panel. Each strap was wrapped around two groups of reinforcing steel bars, after which the ends of two straps were paired together; the crane hook was then put through the ends of the straps to lift the panel. A photograph and sketch of the straps wrapped around the bar groups are shown in Figure 2.12. Directions of the forces exerted on the reinforcing bars are shown in Figure 2.12c. Straps had to be wrapped around the bar groups in different configurations in order to have a balanced pick of the panel. Panel 2 and Panel 3 were tested in this configuration. Eight gages on Bars 1, 2, 7 and 8 shown in Figure 2.7 were used to collect data in both panel tests. Each panel was lifted twice and the results compared.

a) Photograph of lifting the deck panel with four straps

Figure 2.12. Setup of lifting test using four straps

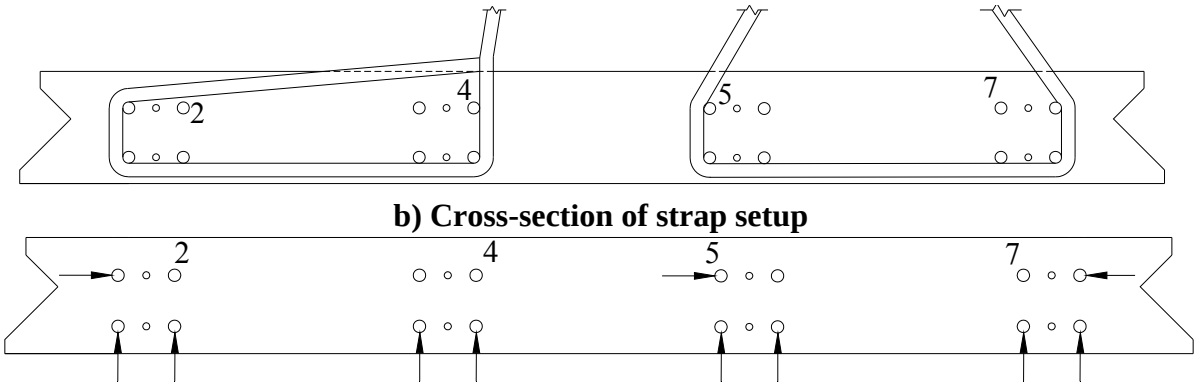

b) Cross-section of strap setup

c) Primary forces acting on reinforcing bars due to lifting straps

Figure 2.12. Setup of lifting test using four straps

2.5.2 Two Lifting Straps

The second lifting configuration used two straps to lift the panel. Each strap was wrapped around the four bar groups in the longitudinal channel, as shown in Figure 2.13. Once both straps were in place, the panel was lifted and strain readings taken. Only Panel 3 was tested with this setup, and data were collected from four lifts. Steel strains using six strain gages on Bars 1, 2, and 8 were recorded during the tests.

a) Photograph of two strap setup prior to lifting

Figure 2.13. Setup of lifting test using two straps

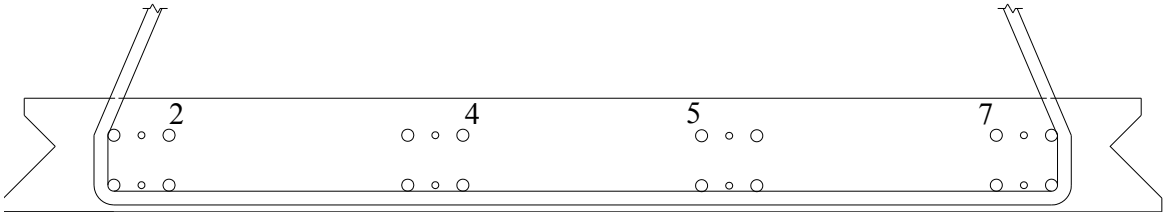

b) Cross-section of strap setup

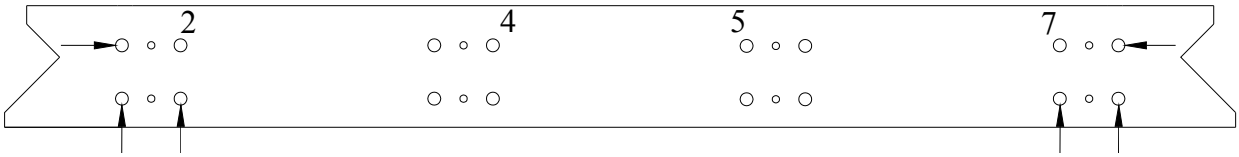

c) Primary forces acting on reinforcing bars due to lifting strap

Figure 2.13. Setup of lifting test using two straps

2.6 Leveling Test

In addition to during moving and transporting, there was concern about the stresses in the mild reinforcing steel during the leveling of the panels. Therefore, Panel 2 was tested in the laboratory to determine the magnitude of the stresses exerted on the mild reinforcing steel during panel leveling. For this test, two supports simulating the precast girders in the field were cast to support the panels; the simulated beams were 18 in. tall, 14 in. wide, and 10 ft long. Panel 2 supported by two simulated girders is shown in Figure 2.14.

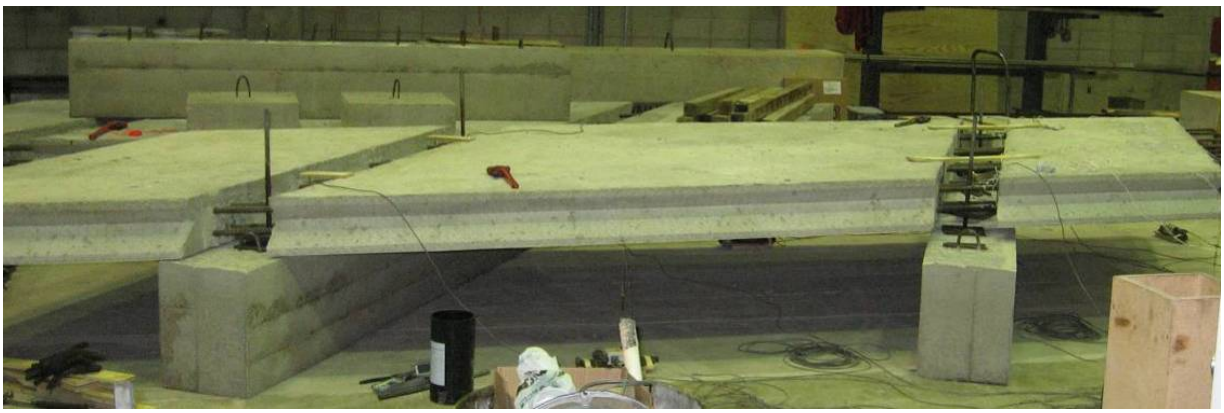

Figure 2.14. Deck panel setup for leveling test

For the field bridge, panels were leveled to a 2% transverse slope using a device designed by the contractor and approved by the Iowa DOT. Four devices were used to level each panel. Each device was placed under a group of exterior reinforcing bars, as shown in Figure 2.15. The leveling device consisted of a 3/4 in. coil nut welded to the bottom of a 3/4 in. plate that had a 13/16 in. hole. A 3/4 in. diameter coil bolt was then threaded through the nut, and the bolt was turned to adjust the height of the panel.

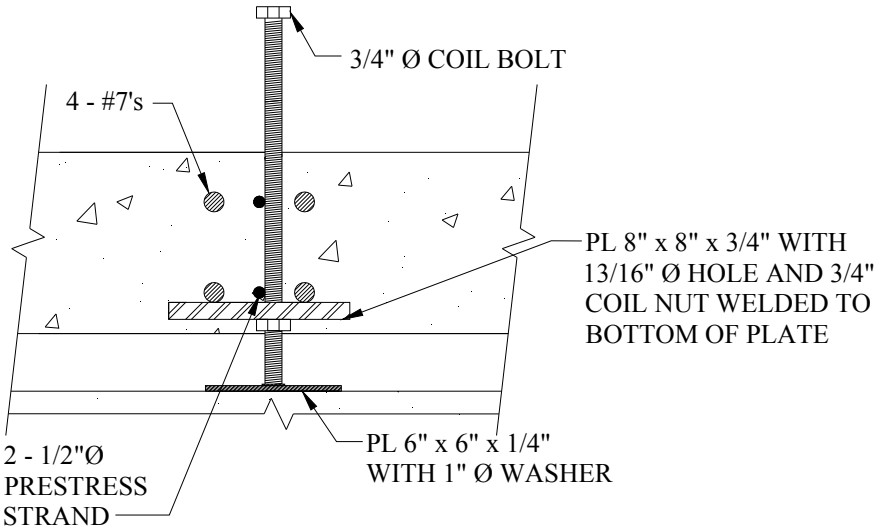

a) Cross-section of leveling device

b) Photograph of leveling device

Figure 2.15. Leveling device used to achieve correct elevation and 2% slope of the deck panels

One variation made in the laboratory test setup was the addition of a 1/4 in. plate for the rod to bear on. A washer was welded to the plate to keep the rod from moving on the plate. The plate and washer were added because the test panel was not confined by other panels as would be the situation in the field. In the field, these other panels would keep the panel and leveling devices from moving along the prestressed girder. The additional plate and washer used in the laboratory can be seen in Figure 2.15b.

To achieve the desired elevation of the panels, four leveling devices were used per panel. Using four devices allowed each corner of the deck panel to be adjusted separately until the required

elevation and slope were achieved. A photograph of one leveling device and two deflection transducers in a simulated post-tensioning channel is shown in Figure 2.16. Through the use of the deflections measured at Points 8, 9, 10, and 11 shown in Figure 2.8, the slope of the panel was calculated and adjusted until a 2% slope was reached, as required in the field. The slope was calculated by dividing the difference in the height of the panels at Points 8 and 9 (and 10 and 11) and dividing by 8 ft – 4 in., which was the distance between deflection transducers.

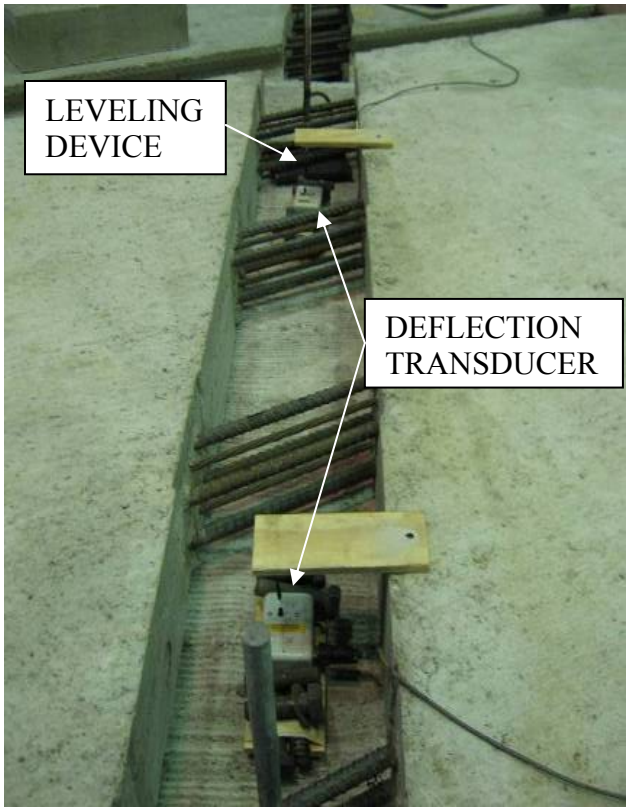

Figure 2.16. Leveling devices and transducers used in panel leveling tests

In addition to leveling the panel to the desired field slope, various combinations of the four leveling devices were raised to a height of 1 in. to determine the panel response for different scenarios. These tests included the following: raising one corner of the panel, raising one side, raising opposite corners, and raising three panel corners. During each test, readings (strains and deflections) were taken for every 1/8 in. increment the leveling device was raised. Presented in Table 2.1 are the different tests conducted (i.e. adjusting the various leveling devices). The number in the table corresponds to the deflection closest to the leveling device being adjusted.

The panel was not lowered to the original position prior to each test listed in Table 2.1. For example, once the deflection at Point 9 reached 1 in. in Test 1, the leveling device next to deflection Point 11 was adjusted until the deflection at Point 11 reached 1 in. (Test 2 in Table 2.1). The leveling device next to deflection Point 9 was not adjusted during Test 2. Following Test 2, the leveling devices near Points 9 and 11 were untouched while the deflection at Point 8

Table 2.1. Tests conducted with leveling devices

Test Number	Leveling Device Adjusted
1	Pt 9 to 1 in.
2	Pts 9 and 11 to 1 in.
3	Pts 8, 9, and 11 to 1 in.
4	Pt 8 to 1 in.
5	Pts 8 and 9 to 1 in.
6	Pts 8 and 11 to 1 in.
7	Pt 10 to 1 in.
8	Pts 8 and 10 to 1 in.
9	"Field Leveling"

was adjusted upward 1 in. (Test 3). Next, the panel was lowered to the zero position and Test 4 undertaken. This process was continued for all of the tests, with the panel only being lowered to the zero position after Tests 3 and 6.

The "Field Leveling" test was conducted to determine the stresses developed in the mild reinforcing steel during leveling of the panel to field requirements. For this test, the panel was to be leveled to a 2% slope in the transverse direction. To achieve this, a difference of 3.86 in. was required between Points 1 and 3 and Points 5 and 7, located at the corners of the panel. This resulted in a difference of 2 in. between Points 8 and 9 and Points 10 and 11.

2.7 Longitudinal Post-Tensioning Channel Concrete Placement Test

One concern about the deck panel system was the placement of concrete in the post-tensioning channel (i.e. could concrete could flow around all of the steel in the post-tensioning channel?). Shown in Figure 2.17 is a photograph of one of the post-tensioning channels in the bridge prior to placement of concrete. In order to check this concern, a model of the channel was constructed in the laboratory and concrete was placed multiple times to determine if any void spaces were left around the steel.

2.7.1 Channel Construction

The laboratory channel model was to have the same dimensions and all of the steel present in the field bridge channel. Therefore, the channel was 10 in. wide, 8 1/4 in. deep, and 6 ft long. A 6 ft channel length was chosen because this allowed construction of a channel where observations could be made on both the concrete flow around the leveling devices and through only the prestress strand. Figure 2.18 provides illustrations of the channel constructed.

Elements composing the completed model included a simulated deck panel with mild steel and prestress strands, a simulated girder, and concrete beams to support the simulated deck panel. Plywood was placed at the ends of the channel to close the channel and support the post-tensioning strands. The plywood could be removed between tests to allow for cleaning of the specimen before reuse. Presented in Figure 2.18a is a photograph of the constructed test specimen.

Figure 2.17. Photograph of longitudinal post-tensioning channel prior to casting concrete in the field

a) Constructed channel used in concrete placement tests (courtesy of Iowa DOT)

Figure 2.18. Channel constructed for longitudinal post-tensioning channel concreteplacement test

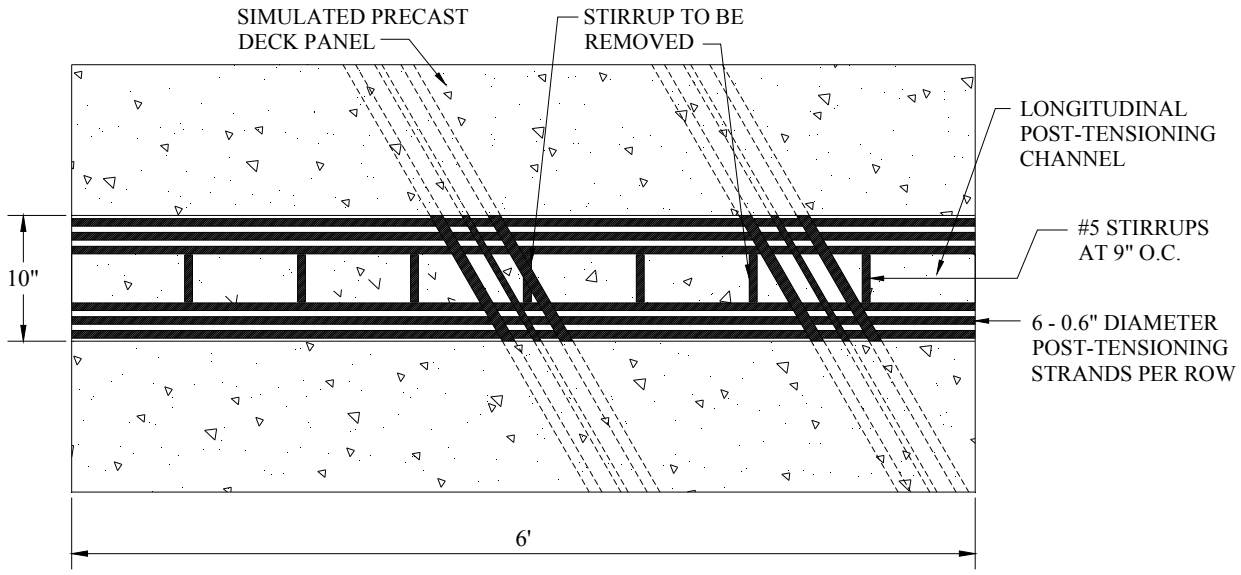

b) Plan view of channel constructed

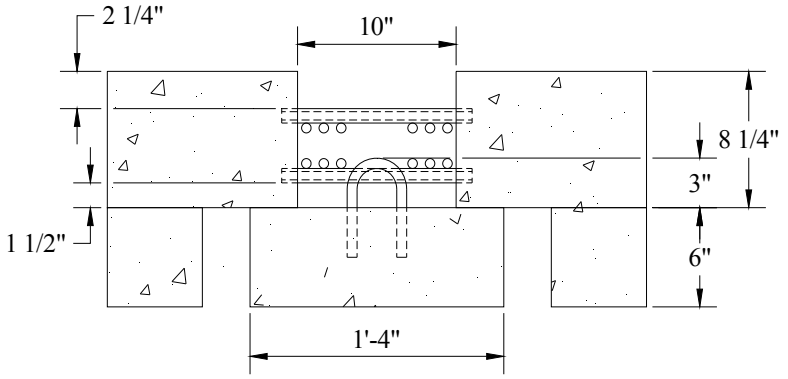

c) Cross-section of channel constructed

Figure 2.18. Channel constructed for longitudinal post-tensioning channel concreteplacement test

As can be seen in Figure 2.18c, a cross-section of the channel, the following are present in the channel: stirrups extending from the girder to provide composite action with the deck, two layers of prestressing strands, two layers of mild reinforcement, and 12 post-tensioning strands (6 in the top layer and 6 in the bottom layer) along the length of the channel. Excluded from the figure for simplicity is the leveling device.

Stirrups were spaced on 9 in. centers to simulate the worst-case spacing which occurred near the end of the girders. Two stirrups were removed from the beam prior to placing the simulated deck panel on the beam because the stirrups would interfere with either the mild steel reinforcement or the leveling device. The specifications for the project also called for removal of any stirrups in the field that may interfere with installation of the deck panels.

Three inches of each stirrup were left exposed from the beam instead of the 4 1/2 in. specified in the plans, because in the field the panels would be raised and not resting on the girders once leveled. Leveling decreases the overlap of the stirrups with the post-tensioning strands and other bars. For this reason, the exposed length of the stirrups was reduced so the top of the stirrups would be located at a lower height on the model channel and closer simulate the field conditions.

Twelve post-tensioning strands ran the length of the channel. For the tests, the strands were not post-tensioned. In order to eliminate any sag in the strands, the strands were tied to the mild steel reinforcement and supported at the ends by plywood. The holes in the plywood were not oversized, allowing for a tight fit of the strands.

2.7.2 Concrete Placement

Placement testing was conducted on two days, November 9, 2006 and May 17, 2007. A total of three tests were conducted, two on the first test day and one on the second day. The third test will be the focus of this section. Unlike the first two tests, which took place inside the laboratory due to weather conditions, the third test was conducted outdoors. Photographs of the setup of the channel outside of the laboratory are presented in Figure 2.19.

Another change from the first two tests was the addition of the leveling devices to the channel. In the first two tests, the focus was to ensure the concrete left no void spaces among the mild reinforcement and post-tensioning strands; therefore the leveling devices were left out so this was easier to observe. Leveling devices were in-place during the third test, resulting in a worst-case scenario for obstructions in the channel and replicating field conditions. This test setup provided a worse-case scenario for the opening between the leveling device plate and the girder because in the field, the plate would be raised higher due to leveling the deck panels. During this test, the space between the plate and the girder was 1 1/4 in. A photograph of a leveling device in the channel prior to testing is shown in Figure 2.19b.

An O-4-S35 concrete mix was ordered from Iowa State Ready Mix for all three tests. This mix met the following requirements: a class O-4WR; maximum top size of aggregate of 3/8 in.; 35% replacement with ground granulated blast furnace slag (GGBFS); maximum water cement ratio of 0.38; maximum slump at the plant of 3 in.; maximum slump after addition of high range water reducer of 8 in.; and a minimum concrete temperature at time of placement of 70° F.

Testing began at 11:00 A.M. on May 17, 2007. Air temperature at the time of the test was 61°F. The temperature of the channel concrete was 45°F. Slump of the concrete at time of arrival was measured at 3 3/4 in. After the addition of 40 ounces of super plasticizer per cubic yard of concrete, the slump was 8 in. For comparison, the air temperature was 55°F and the slump at arrival was 2 in. for the first two tests. A 5 in. slump after the addition of super plasticizer was measured for the first test and the slump was 6 1/2 in. for the second test, after the addition of extra super plasticizer.

Concrete placement for the third test began near the mild steel, which is the right end of Figure 2.18. For this test, concrete from the concrete truck was placed into a wheel barrow, and then

placed by the shovelful into the channel and vibrated. One location of the channel was filled at a time, and as the channel filled, placement continued until the channel was full.

a) Outdoor test setup

b) Steel in channel

Figure 2.19. Concrete placement test setup

2.8 Service Load Tests

A series of service load tests were conducted to determine the response of the deck panels to loads placed at various locations. Load magnitudes typically were 40 kips for interior spans and 20 kips on the cantilevered sections. Service load tests were first preformed on panels prior to the closure pour being cast, with concrete strains, steel strains, and deflection data recorded. Next, the closure pour was cast between two panels and service load testing repeated, with the results between the series of tests compared to determine the effect of the closure pour on the system. All service loads were completed applying loads to a 9 in. square footprint.

2.8.1 Individual Panel Service Load Tests

Setup for the service load tests began with placing four simulated precast girders at the proper spacing on the laboratory floor. Once the girders were set in place, two deck panels were lowered into position. Leveling devices designed by the contractor were used to adjust the slope of the panels to 2%, matching the slope of the panels in the field bridge. Next, plywood formwork was attached to the beam below the deck panel and at both ends of the longitudinal post-tensioning channel, as shown in the photograph in Figure 2.20a.

Once the formwork was constructed, concrete could be placed in the post-tensioning channels. A C-4 mix with 3/8 in. chips and a 4 in. slump was used for the post-tensioning channel concrete. Concrete in the channels was placed on February 15, 2007; a photograph of the concrete placement in one of the channels is shown in Figure 2.20b.

Load locations used for the two panels are presented in Figure 2.21. Load locations were laid out along three lines in the transverse direction (A, B, and C) and fourteen lines in the longitudinal direction (1-14). Lines A, B, and C were equally spaced at 1 ft - 9 in., measured from the bottom of the transverse shear key. Lines 1 through 14 were spaced on 3 ft increments, with Line 1 approximately 2 in. from the corner of Panel 1. This was done so point B8 would be positioned over the center of the closure pour for the connected panel service load tests.

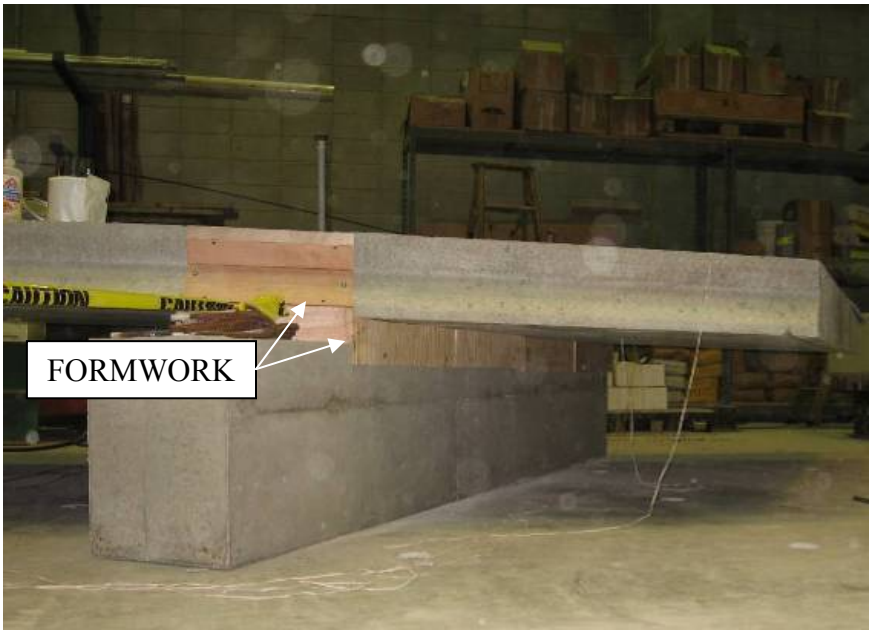

a) Formwork along bottom of channel

b) Placement of concrete in channel

Figure 2.20. Casting concrete in the post-tensioning channel

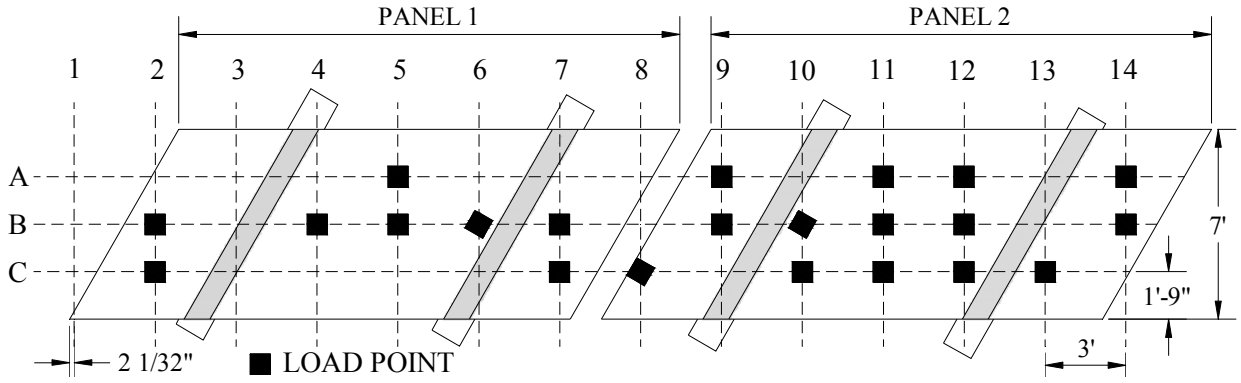

Figure 2.21. Load locations for service load tests on individual panels

More instrumentation was installed on Panel 2 than on Panel 1, and therefore Panel 2 was tested more extensively, as illustrated in Figure 2.21. Each test point on Panel 1 was chosen to correspond to a point on Panel 2, allowing for a comparison of the data from the two panel tests. This it was possible to see how both panels responded to the same loading.

Also of note in Figure 2.21 are load locations B6 and B10. The footprint at these points is parallel to the support beams. This was done so the load would not be applied directly to the support, which would occur if the footprint was not rotated. Point C8 was also rotated so the load footprint would not overhang the deck panel.

Service load testing began on Panel 2 on February 22, 2007, seven days after the post-tensioning channel concrete was placed. The 7 day strength of the concrete in the channel was 4,650 psi. Loading of the panel began at Point B14, and shown in Figure 2.22 is the test setup for various load points. Each point was loaded twice to ensure consistent results. For Panel 2, loading varied from 32 kips for points on cantilevered sections to 40 kips for interior spans, with the load increased in 4 kip increments. All points on Panel 1 were loaded to 20 kips in 2 kip increments. A load cell was used to measure the applied load.

a) Service load at Position B9

b) Service load at Position C10

Figure 2.22. Individual panel service load test setup

c) Service load at Position B14

Figure 2.22. Individual panel service load test setup

2.8.2 Connected Panels Service Load Tests

After the service load tests on the individual panels were completed, the closure pour was cast, connecting the two panels. Shown in Figure 2.23 is a photograph of the closure pour connection prior to concrete placement. Present in the joint are sixteen #5 double hooked bars and four #5 longitudinal bars.

Figure 2.23. Longitudinal closure between panels prior to concrete placement

Load points used for the connected panel service load tests are presented in Figure 2.24. There were multiple goals considered in determining these load points. These goals were to: determine

the panels' response as the load moved in the transverse direction; determine the response of the closure to loading; and determine the general effect the closure had on the system.

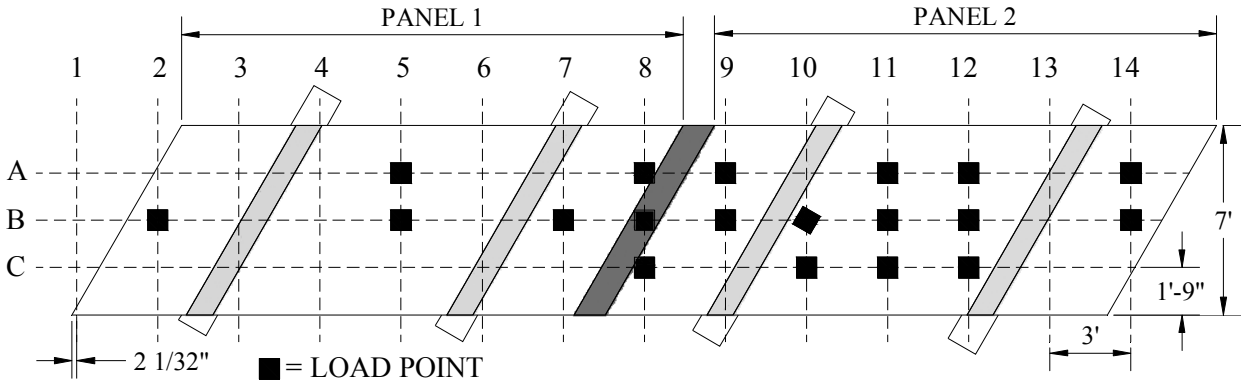

Figure 2.24. Load points used in connected panel service load tests

The first test goal was to determine the panel response as a load moved transversely across the system. This was accomplished by applying load at multiple locations along Line B in Figure 2.24 and measuring the resulting concrete strains, steel strains, and deflections.

Another objective of the connected panel service load tests was to measure the response of the closure to loading. To do this, multiple load points were positioned in the vicinity of the closure, with concrete strains, steel strains, and deflections measured and recorded.

Finally, the general effect the closure had on the response of the system was to be determined. This was accomplished by comparing the response data between the individual panel tests and closure tests with the load in the same locations.

Review of Figure 2.24 reveals Panel 2 has the majority of the load points. There are two reasons for this. First, as previously noted Panel 2 had the majority of the instrumentation; therefore by loading this panel, a better idea of the response would be obtained. Also, Panel 2 was subjected to more tests during the individual panel service load tests than Panel 1. Testing Panel 2 extensively again allowed for a better comparison of data between the two sets of service load tests.

The test setup in the laboratory for the connected panel tests is shown in Figure 2.25. Testing went from Column 14 to 1 and Row A to C in Figure 2.24. As previously noted, a 9 in. square footprint was used for each test, and each point was loaded twice to ensure consistent results. Loading varied from 20 kips for points on Columns 2 and 14 (the cantilevered sections), to 40 kips for all the points in the interior spans. Instrument readings were taken ten times for each test, resulting in readings in 2 kip increments for the cantilevered spans and 4 kip increments for the interior spans. A load cell was used to measure the applied load. Instrumentation locations for this test were presented earlier in Section 0.

a) Service load at Position B2

b) Service load at Position B12

Figure 2.25. Test setup for connected panel service load tests

c) Service load at Position A14

Figure 2.25. Test setup for connected panel service load tests

2.9 Ultimate Strength Tests

A series of ultimate load tests were conducted to determine flexural and punching shear capacities of the connected deck panels. Testing was done on both the single panel (Panel 3) and connected panels (Panels 1 and 2). Footprints used for the tests included a 9 in. square, tandem wheels, and line load.

2.9.1 Test of a Single Panel

Panel 3 was tested to determine the flexural capacity of a single panel. This was accomplished by applying a line load at the midspan of the panel. As previously noted, Panel 3 also contained a cold joint, so this test would help determine if the cold joint affected the strength of the panel. The position of the line load is shown in Figure 2.26a.

Presented in Figure 2.26b is a photograph of the laboratory setup prior to the start of the test. The line load was applied by loading a 6 ft long HP10x42 section. Neoprene pads were placed between the load beam and deck panel to account for the roughness in the deck panel surface and to evenly distribute the load. A 300 kip load cell was placed between the load beam and the actuator. Deflection transducers were installed at the ends and midpoint of the load beam so the load distribution through the beam could be monitored. Data were collected for every 10 kip increment of load applied to the panel.

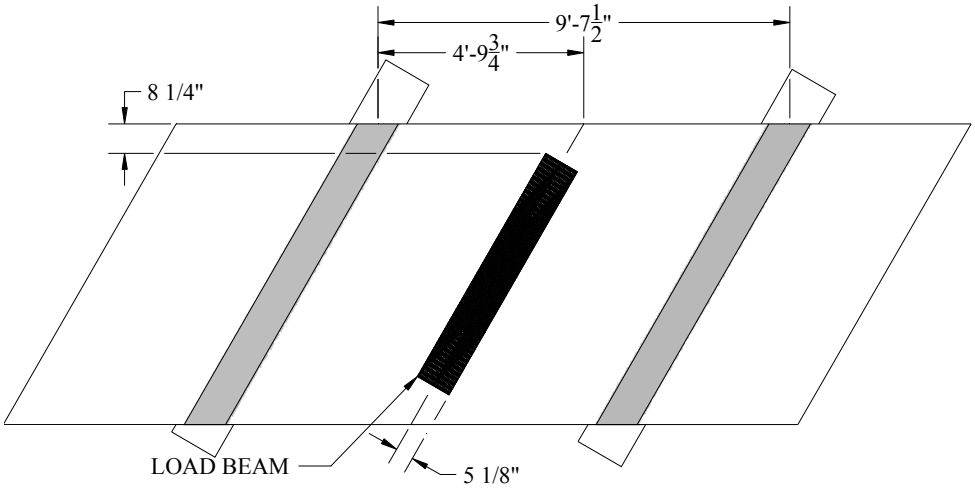

a) Location of line load for Panel 3 test

b) Panel 3 setup prior to testing

Figure 2.26. Laboratory setup for Panel 3 ultimate load test

2.9.2 Test Using 9 in. Square Footprint

The goal of this ultimate strength test was to determine the strength of the longitudinal closure pour. Because of the anticipated strength of the closure pour and the capacities of the laboratory equipment, the decision was made to place a point load to one side of the joint for the test. This was done instead of placing one point load on each side of the joint and subjecting the joint to pure flexure. The reasoning for this was to expose the joint to both flexure and shear – a more severe loading condition.

A 9 in. square footprint was used to keep consistency between this test and the service tests to allow for data comparison. Location of the footprint relative to the closure joint can be seen in Figure 2.27a. The footprint was parallel to and 4 1/2 in. from the joint and 2 ft – 8 in. from the panel edge. Shown in Figure 2.27b is a photograph of the applied load relative to the closure joint and concrete strain gages on the specimen.

Steel beams were used to tie the specimen to the floor. This was done because of an anticipated uplift force at the exterior beams during loading. The locations of the restraining beams relative to the support beams can be seen in Figure 2.27a. Locations of the restraining beams were controlled by the locations of the inserts in the tie down floor. The entire test setup with the two restraining beams is shown in the photograph in Figure 2.27c.

Loading was to continue during the test until either the specimen failed or the capacity of the actuator was reached, which was 400 kips. Instrumentation readings were collected at 10 kip increments until failure occurred. A load cell was used to measure the applied load.

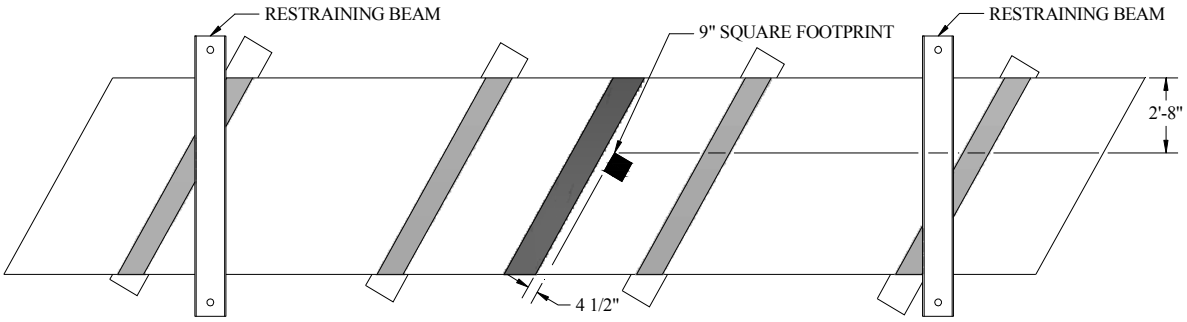

a) Location of 9 in. square footprint

b) Test setup for closure pour ultimate load test

Figure 2.27. Laboratory setup for closure joint ultimate load test

c) Restraining beams positioned for ultimate load test

Figure 2.27. Laboratory setup for closure joint ultimate load test

2.9.3 Testing Using Tandem Wheel Footprint

A tandem wheel footprint was used for the third ultimate load test. The load was positioned as close to midspan of Panel 2 as possible based on the layout of the tie down floor. Shown in Figure 2.28a is the exact position of the load. A steel beam was positioned over one of the support beams to keep the panel from lifting during loading due to uplift forces. Presented in Figure 2.28b and c are photographs of the test setup.

Shown in Figure 2.28c is a photograph of an overall view of the tandem wheel footprint. The following can be seen in this figure: two neoprene pads each with dimensions of 10 in. by 10 in., steel plates approximately 20 in. x 10 in., 9 in. square steel plates, a 300 kip load cell, and a 400 kip actuator. Load was applied until either a failure in the deck panel occurred or the capacity of the actuator was reached. Data were recorded for every 10 kip increments of load applied.

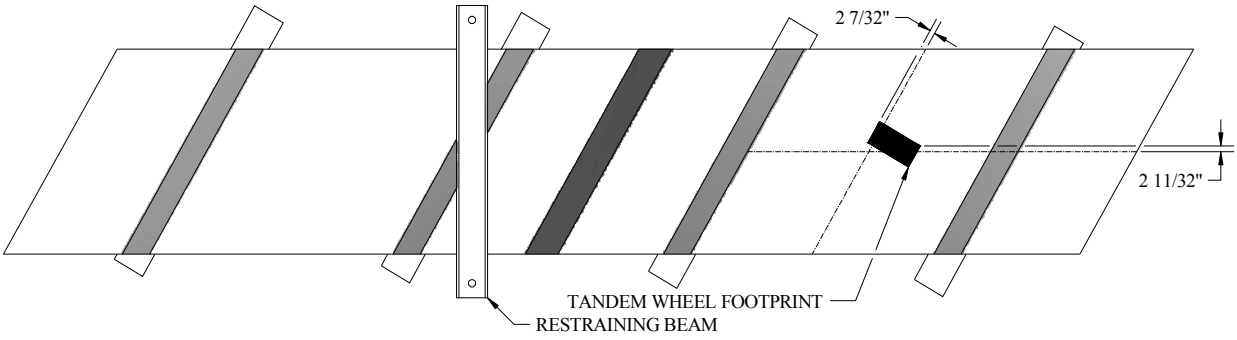

a) Load position for tandem wheel footprint ultimate load test

Figure 2.28. Load position and laboratory setup for tandem wheel ultimate load test

b) Laboratory setup

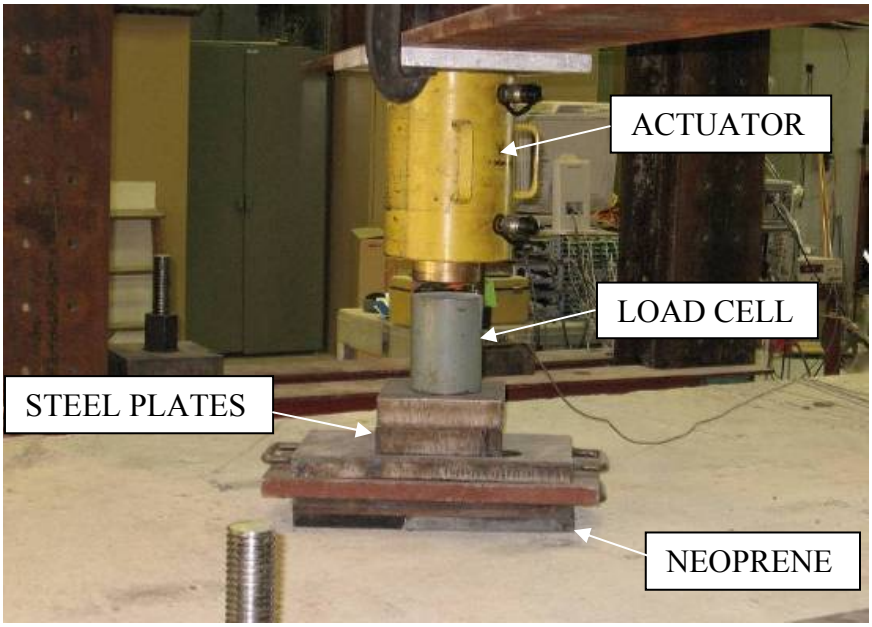

c) Tandem wheel footprint

Figure 2.28. Load position and laboratory setup for tandem wheel ultimate load test

2.9.4 Line Load

A line load was applied to test a span of Panel 1 in flexure. The load was applied until a deck panel failure occurred. Data were recorded for every 10 kip increment of load applied to the panel; applied loads were measured with a load cell.

The line load was applied by loading a 6 ft long HP10x42 section. Neoprene pads were placed between the load beam and deck panel to account for the roughness in the deck panel surface and to evenly distribute the load. A 300 kip load cell was placed between the load beam and the actuator. Deflection transducers were installed at the ends and midpoint of the load beam so the load distribution through the beam could be monitored. A photograph of the setup in the laboratory prior to testing is shown in Figure 2.29a.

a) Laboratory setup for line load ultimate load test

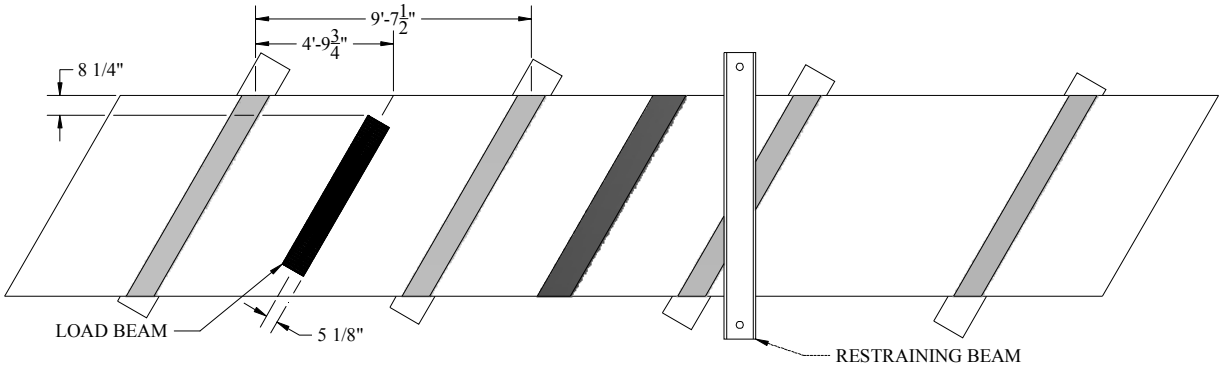

b) Location of line load on Panel 1

Figure 2.29. Laboratory setup for ultimate load test using a line load

Shown in Figure 2.29b is the position of the line load on Panel 1. The line load was placed at the midspan of the panel. Also shown is the location of the restraining beam used for this test. The restraining beam was needed to transfer the uplift forces developed in Panel 2 to the tie down floor.

3. LABORATORY TEST RESULTS

In this chapter, results for the various laboratory tests performed on the deck panels are presented. Test results presented include concrete compressive strengths, prestressing force measurements, strains measured in the deck panel during lifting, and strains measured during leveling. Observations made during placement of concrete in the longitudinal post-tensioning channel are discussed. Lastly, strain and deflection data from the service load tests and ultimate strength tests of the panels are presented.

3.1 Concrete Strength Test Results

Compressive strength results for the concrete cores taken from the Panel 1 are presented in Table 3.1. Results for this panel were assumed to be representative of the compressive strength of the concrete in all the deck panels tested. The compressive strengths ranged from 7,530 psi to 9,570 psi. Because the strength of Core A was significantly greater than Cores B and C, only the Core B and C strengths were used to calculate the average concrete compressive strength of 7,600 psi. By not using the high compressive strength of Core A, a conservative value was obtained. The average compressive strength exceeded the specified concrete strength of 5,000 psi by 27 percent.

Table 3.1. Deck panel concrete compressive strengths

Core	Strength (psi)
A	9,570*
B	7,670
C	7,530
Average	7,600

*excluded from average

3.2 Stresses in Panel Mild Reinforcement Due to Prestressing

Presented in this section are the stresses calculated from strains measured in six reinforcing bars when the prestressing strands in one longitudinal channel were cut. Locations of the instrumented bars can be seen in Figure 2.7. The experimental stress in each mild reinforcing bar was compared to the design stress for the mild bars. To determine the design stress in each bar, estimated losses were subtracted from one-half the initial stress in one prestressing strand. Estimated losses included losses due to creep, shrinkage, relaxation, and elastic shortening and were taken as a lump sum value of 40 ksi (Naaman, 2004). The design stress in each reinforcing bar without considering losses was 25.8 ksi and 20.7 ksi considering losses.

Calculated stresses for each instrumented bar are given in Table 3.2. Hooke's Law and an assumed steel modulus of elasticity equal to 29,000 ksi were used to determine stresses from the measured strains. Experimental stresses ranged from 13.0 ksi to 21.5 ksi. One of the six bars was stressed greater than the design stress less losses by 0.8 ksi. The average experimental

stress was 16.1 ksi, which is 4.6 ksi less than the design stress less losses. Therefore losses in the prestressing force were greater than expected.

Table 3.2. Stress in each instrumented bar

Bar	Stress (ksi)	Difference from Design Value Less Losses (%)
1T	13.8	-33
1B	17.2	-17
2T	13.0	-37
2B	21.5	+4
8T	15.8	-24
8B	15.1	-27

In Table 3.3 the average stress in the top and bottom bars is presented. The average stress in the bottom bars (17.9 ksi) was higher than that in the top bars (14.2 ksi); however both stresses were less than the design stress less losses. A reason for the difference in stresses could be that the bottom prestressing strands were stressed higher than the top strands; this is supported by comparing the values of 1T and 1B, or 2T and 2B. Both bottom strands were stressed higher than the corresponding top strands.

Table 3.3. Average stress in each bar layer

Bar	Stress (ksi)	Difference from Design Value Less Losses (%)
Top	14.2	-31
Bottom	17.9	-14

3.3 Lifting Panel Strain Results

Presented in this section are the results for the crane lifting tests. A deck panel was lifted multiple times with two different strap configurations (see Figure 2.12 and Figure 2.13). Strains induced in the mild reinforcing bars were measured during each test to determine the state of stress in the bars.

3.3.1 Four Lifting Strap Test Results

Shown in Figure 3.1 is a plot of the strains experienced in each instrumented bar while the panel was lifted from the support beams. Locations of the instrumented bars are presented in Figure 2.7, and the configuration of the straps around the bars is shown in Figure 2.12. Strains measured in the test presented (the first test) agree with results from the other tests conducted with the same strap configuration. All strains plotted were temporary because they only occur during lifting; once lifting is completed and the panel is in place, the only strains present in the mild reinforcing bars are due to the prestressing force and bending of the cantilevered sections over the supports due to the self-weight of the panel.

As can be seen in the graph, half the bars experienced tension and half were in compression. However, not all the top bars experienced tension and not all the bottom bars experienced compression, as one would expect. Three of the top bars (1T, 7T, and 8T) and one bottom bar

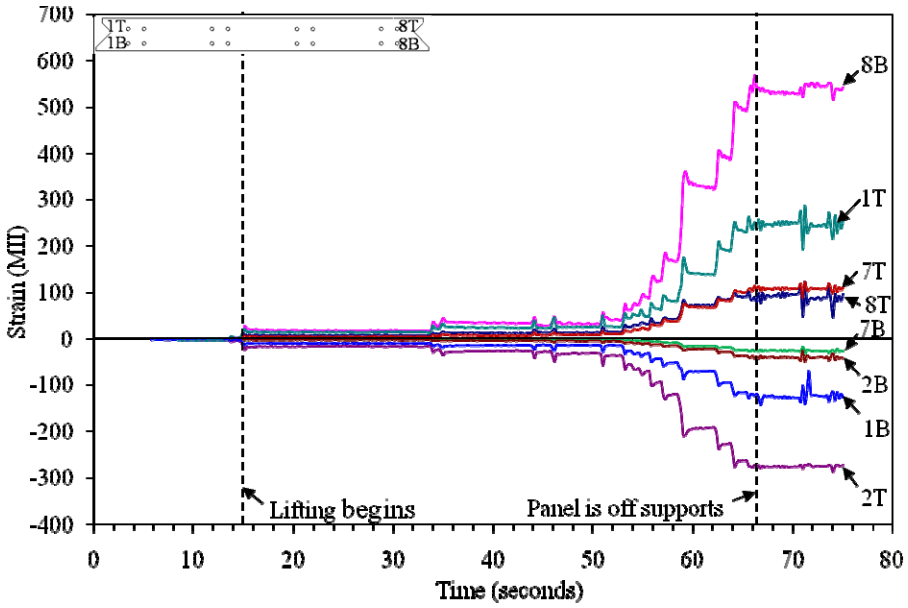

Figure 3.1. Strain results for first lift of Panel 2 with four straps

(8B) were in tension. The tension in the bottom bar, 8B, was due to a localized effect caused by bearing of the lifting strap directly on the bar near the strain gage. Bar 1T experienced the largest tensile strain (251 MII) if Bar 8B is neglected, and Bar 2T had the largest compressive strain (-278 MII).

Presented in Table 3.4 are the maximum strains measured for each instrumented bar during the four strap lifting tests. The strain magnitudes were converted to stresses using Hooke's Law and then to the moment values presented. To use Hooke's Law, linear behavior and a steel modulus of elasticity equal to 29,000 ksi were assumed. Moments were calculated using the stress with the following equation:

$$M = \frac{I\,\sigma_{max}}{c} \qquad (1)$$

Where M = resultant internal moment
I = moment of inertia of one bar about the neutral axis
σ_{max} = maximum stress in the member
c = perpendicular distance from the neutral axis to a point farthest away from the neutral axis

Next, Equation H1-1a in the American Institute of Steel Construction, Inc. (AISC) Steel Construction Manual, 13th Edition (2006) was used to determine if the bar was adequate under combined flexure and compressive forces. This equation is presented as Equation 2:

$$\frac{P_r}{\phi_c P_n} + \frac{8}{9}\left(\frac{M_{rx}}{\phi_b M_n} + \frac{M_{ry}}{\phi_b M_n}\right) \leq 1.0 \quad (2)$$

Where P_r = required axial compressive strength
P_n = nominal axial compressive strength
M_r = required flexural strength
M_n = nominal flexural strength
$\phi_b = \phi_c$ = strength reduction factor = 0.90

Table 3.4. Strains, moments, and percent utilization of the #7 bars' yield stress during four strap lifting

Bar	Maximum Strain Measured (MII)	Calculated Moment (in.-kips)	Utilization (%)
1T	251	0.48	60
1B	-204	0.39	59
2T	-278	0.53	61
2B	79	0.15	55
7T	143	0.27	57
7B	-40	0.08	54
8T	93	0.18	56

The solution of the left-hand side of Equation 2 results in the percent utilization value given in Table 3.4, which is the percentage of the total strength of the bar being used. Bars with utilization less than 100% have reserve strength. A compressive force of 15.5 kips was used in the AISC interaction equation, which is the design force value and does not include any of the previously discussed losses. Use of 15.5 kips results in a conservative value from the interaction equation because the actual compressive force present in each bar would be less due to prestress force losses. Bar 2T had the highest percent utilization at 61%. All instrumented bars were utilized between 55% and 61%.

3.3.2 Two Lifting Strap Results

Six bars were instrumented when a deck panel was lifted with two straps; locations of each strain can be seen in Figure 2.7 and the layout of the straps can be seen in Figure 2.13. Strains induced while lifting a deck panel with two straps are plotted in Figure 3.2. Of the six bars instrumented, four experienced tension (1T, 8T, 2B, and 8B) and two were in compression (1B and 2T). As previously noted, these strains were temporary because they only occurred during lifting; once the panel was set in place, the only strains present in the mild reinforcing bars were due to the

prestressing force and bending of the cantilevered sections over the supports due to the self-weight of the panel.

Bar 8B had the largest strain, stabilizing at a strain of 1780 MII. However, this strain was caused by a localized effect from the lifting strap bearing directly on the bar near the strain gage. Neglecting this strain, all the instrumented bars experienced strains less than 250 MII. The strains measured during the two lifting strap tests were of a similar magnitude to those measured during the four lifting strap tests, even though the strap configuration was different. This shows that for the instrumented bars, the configuration of the lifting straps did not affect the strains in the bars.

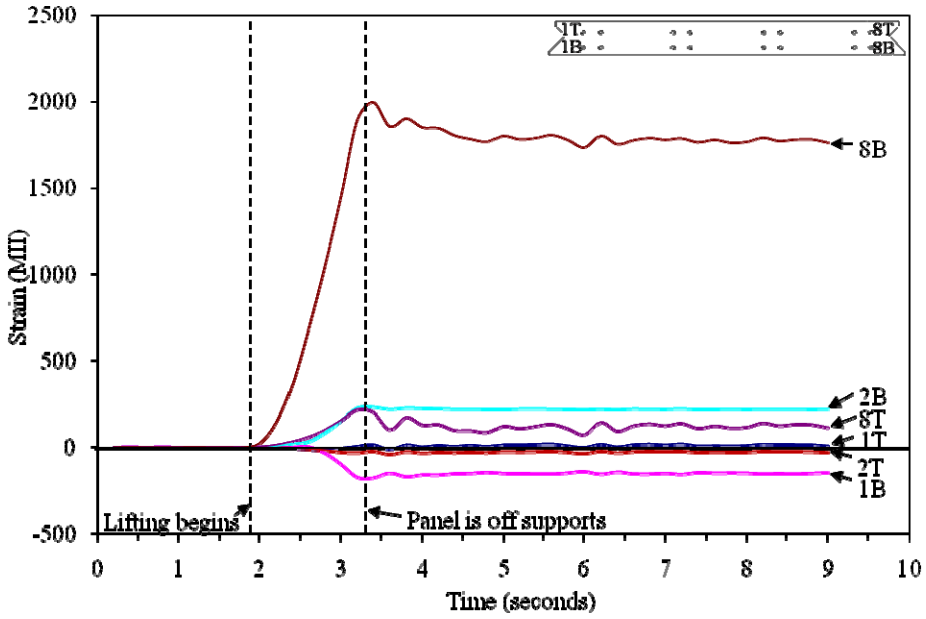

Figure 3.2. Strain results for fourth lift of Panel 3 with two straps

In Table 3.5 the maximum strains in each instrumented bar during the two strap lifting tests are presented. The strain magnitudes were converted to stresses using Hooke's Law and a value of 29,000 ksi for the steel modulus of elasticity. To use Hooke's Law, linear behavior was assumed. Moments were calculated from the stresses using Equation 1.

Table 3.5. Strains, moments, and percent utilization of #7 bars during two strap lifting

Bar	Maximum Strain Measured (MII)	Calculated Moment (in.-kips)	Utilization (%)
1T	22	0.04	54
1B	-177	0.34	58
2T	-38	0.07	54
2B	231	0.44	60
8T	217	0.41	59

Once moments were calculated, the percent utilization value given in Table 3.5 was calculated. Calculation of percent utilization values was presented in Section 0 and used Equation 2. Bar 2B had the highest percent utilization at 60%; all the bars were utilized between 54% and 60%. This range is similar to that for the four lifting strap results (55% to 61%). which is the same range as the results from the four strap lifting tests. Therefore the strap configuration did not have a significant effect on the bar utilization.

3.4 Leveling Test Results

Strains experienced during the various leveling tests conducted are presented in **Figure 3.4**. Tests conducted and the order leveling devices were raised were presented in Section 0; locations of the instrumented mild reinforcing bars were shown in Figure 2.7. Each event plotted on the horizontal axis in **Figure 3.4** represents an increase of 1/8 in. in height of the leveling rod being adjusted.

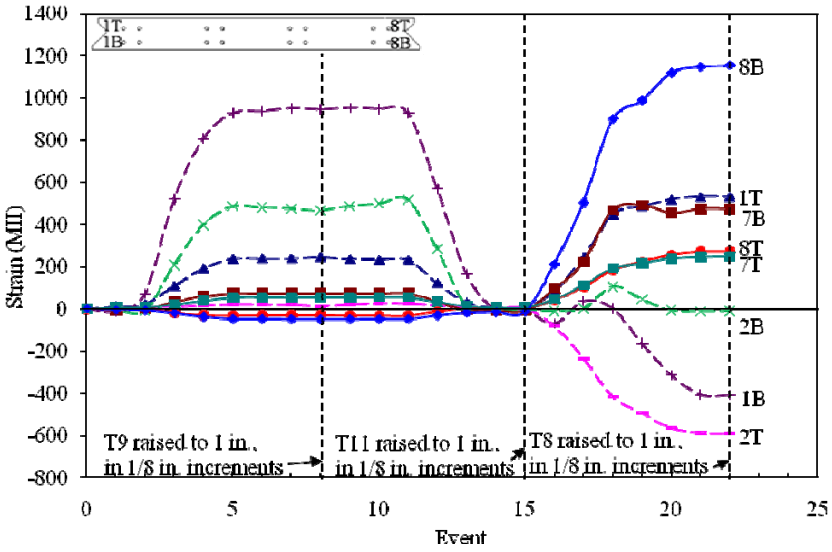

a) Strains for all instrumented bars during Test 1

Figure 3.3. Measured steel strains in Panel 2 mild reinforcing bars during leveling tests

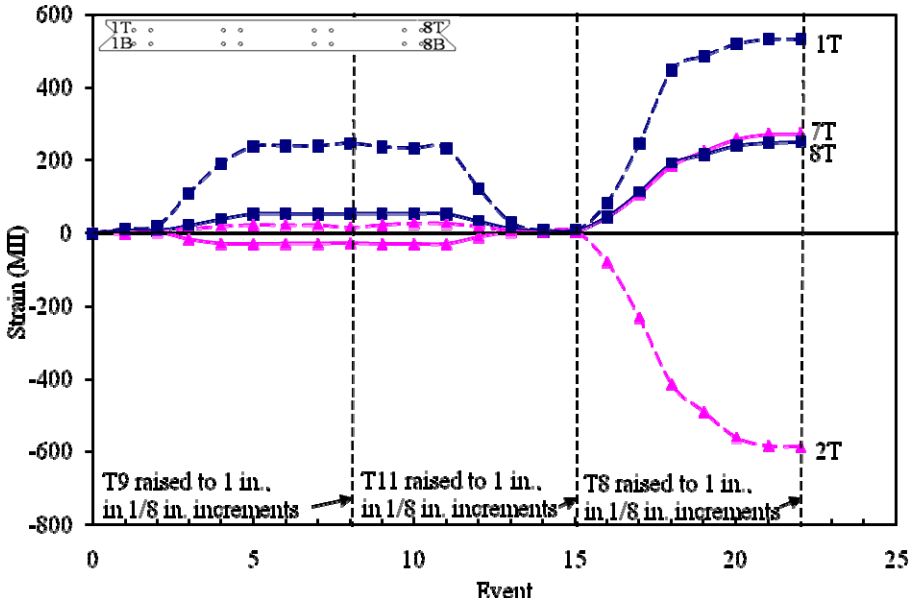

b) Top bar strains in Tests 1, 2, and 3

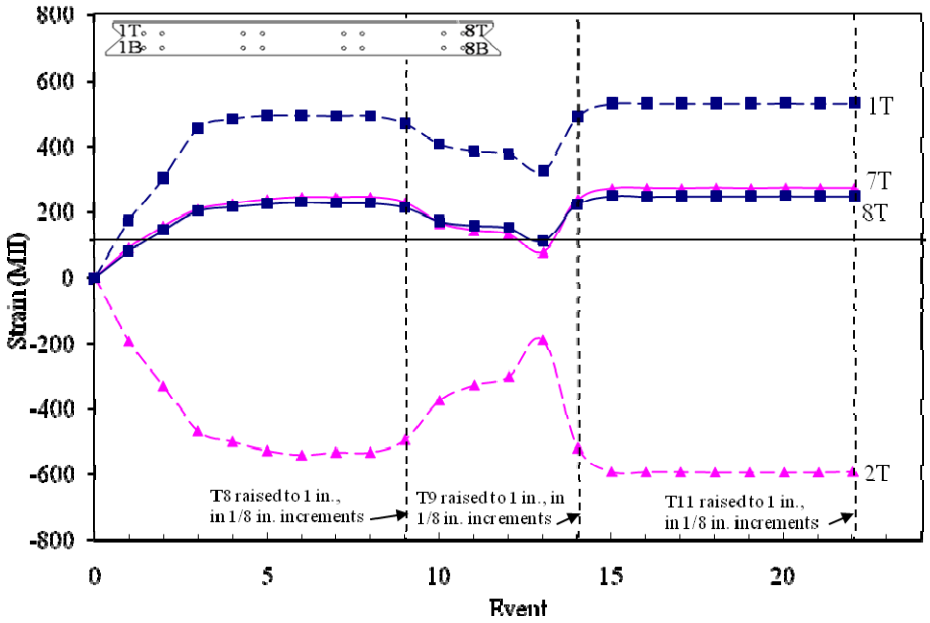

c) Top bar strains in Tests 4, 5, and 6

Figure 3.4. Measured steel strains in Panel 2 mild reinforcing bars during leveling tests

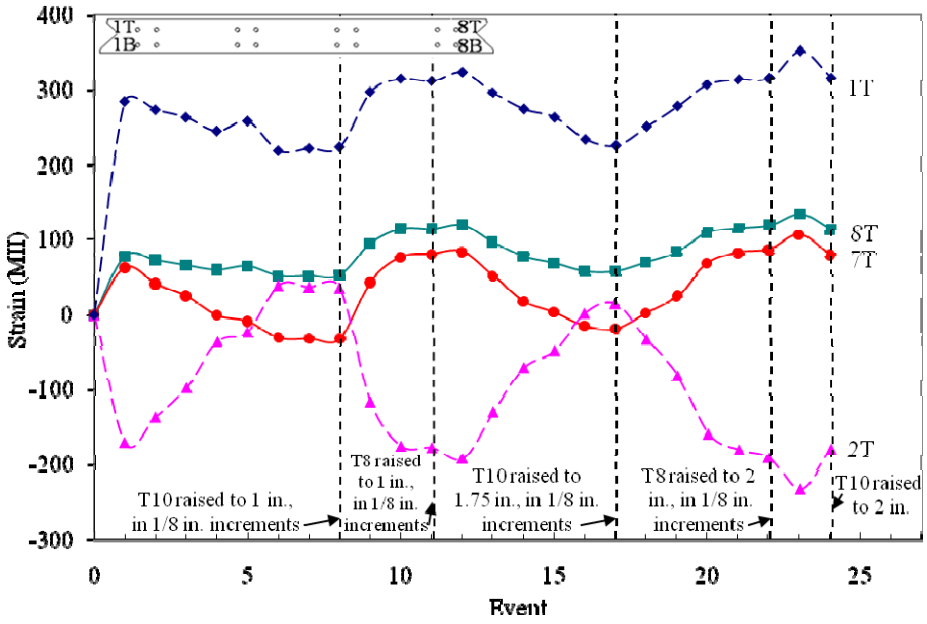

d) Top bar strains in Test 7, 8, and 9

Figure 3.5. Measured steel strains in Panel 2 mild reinforcing bars during leveling tests

Shown in Figure 3.4a are the strains measured for each instrumented bar during Tests 1, 2, and 3. Bar 8B experienced the largest strain (1194 MII) during the test, with a strain twice that of the next largest strain. Strain data for all the bottom bars are disregarded in Figure 3.4b through d because these strains were the result of a localized effect caused by the bar bearing on the leveling plate.

Bar 2T and Bar 7T were the only bars to experience compressive strains during testing, and Bar 7T was the only bar that was always in compression. The maximum strain measured in the top bars during testing was approximately -600 MII. Another observation from the plots is that strains tended to change over the first 1/2 in. of adjusting a leveling device and then remained constant as the leveling device is raised the final 1/2 in. to a height of 1 in.

An observation that can be made from the results of the test replicating field leveling (Tests 7, 8, and 9) shown in Figure 3.4d is the maximum strain experienced by any of the bars was independent of the height of the bar. Strains induced in bars were essentially the same when a leveling device was at 1 in. or when the same device reached 2 in.

Maximum strains measured for each instrumented bar during the leveling tests are presented in Table 3.6. The strain magnitudes were converted to stresses using Hooke's Law, assumed linear behavior, and a steel modulus of elasticity equal to 29,000 ksi. Moment values presented were calculated using Equation 1.

Table 3.6. Strains, moments, and percent utilization during leveling tests

Bar	Maximum Strain Measured (MII)	Calculated Moment (in.-kips)	Utilization (%)
1T	533	1.02	68
2T	-595	1.13	70
7T	273	0.52	61
8T	249	0.47	60

Percent utilization values were calculated and listed in Table 3.6. The equations used and assumptions made when calculating these values were presented in Section 0. Bar 2T had the highest percent utilization at 70%. Utilization of bars during the leveling tests ranged from 60% to 70%.

Values given in Table 3.6 were temporary because all strains went to zero once the deck panel was placed in a horizontal position on the support girders. However, because deck panels are left in a leveled position in the field, strains due to leveling may be permanent strains in the reinforcing bars.

3.5 Longitudinal Post-Tensioning Channel Concrete Placement Results

The photographs in Figure 3.6 address concerns the Iowa DOT had about the flow of concrete in the post-tensioning channel, specifically the flow around all of the steel present in the channel. In Figure 3.6a, one can see the concrete flowed through the channel in three layers, first under the prestress strand, then between and around the strands, and finally above the strands. This was typical of all three tests conducted. Shown in Figure 3.6b is concrete flowing between the prestressing strands, addressing concerns of the Iowa DOT if concrete would leave void space between the strands.

a) Concrete flowing in channel

b) Concrete flowing between post-tensioning strands

Figure 3.6. Concrete flow during longitudinal post-tensioning channel concrete placement tests

c) Concrete below the leveling device

Figure 3.6. Concrete flow during longitudinal post-tensioning channel concrete placement tests

Concrete can be seen below the leveling device in Figure 3.6c, eliminating another concern of the Iowa DOT. Because concrete is beneath the leveling device, load is transferred from the deck panels by bearing on concrete and not through the leveling device rod. The leveling device was only present in the third test.

3.6 Service Load Tests Results

Presented in the following sections are results for the individual panel and connected panel service load tests. Concrete strains, steel strains, and deflection data are presented along with comparisons to service values where appropriate.

3.6.1 Individual Panel Service Test Results

The following section presents the results from the service load tests conducted prior to the closure pour being cast. A total of 22 load points were used; 8 points on Panel 1 and 14 points on Panel 2 (see Figure 2.21). In this section, results for loads positioned at B5, B11, and B14 are presented. Load placed at B5 and B11 resulted in the largest strains and deflections for the cases of the load positioned between the support beams. A load at B14 resulted in the largest deflections in the deck panel. Results for these three load positions are representative of the results obtained from the other 19 load cases. Magnitude of loads applied varied however all were greater than the 16 kip wheel load of a HS 20-44 truck used in design.

Strains induced for a load varying from 0 to 48 kip positioned at B11 are plotted in Figure 3.7. Refer to Figure 2.7 for the location of each steel strain. All the steel strains for this load location resulted from bending of the cantilevered portion of the deck panel about the support beam.

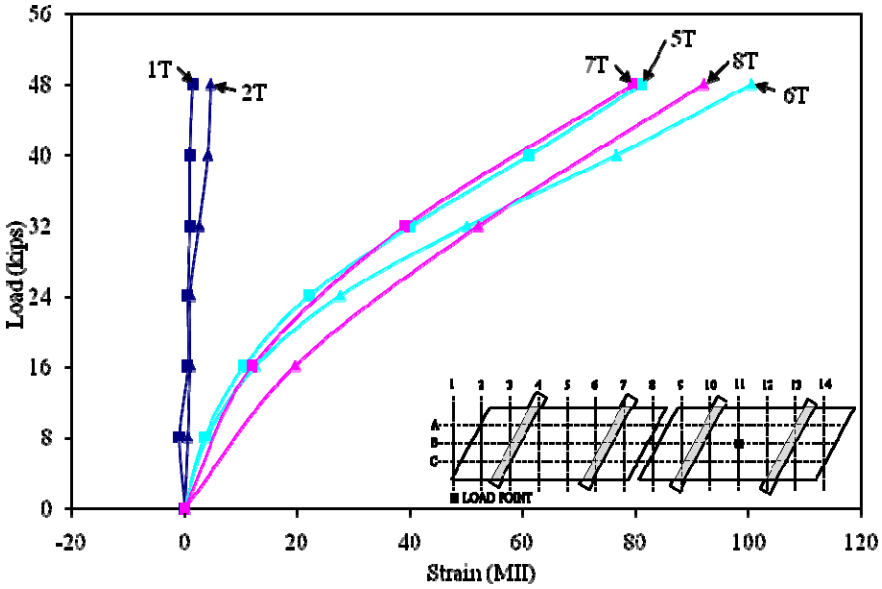

Figure 3.7. Steel strain versus load, load at B11, Panel 2

Bottom bar strains were compressive and less than 20 MII and were not plotted for clarity. From Figure 3.7 one can see the top bars were in tension and the majority of the bending due to self weight occurred in Bars 5, 6, 7, and 8. The maximum steel strain measured during this test was 101 MII in Bar 6T.

Plotted in Figure 3.8 are deflections for a load varying from 0 to 48 kip at B11; locations of the deflections are shown in Figure 2.8. These deflection results are typical for tests with a load located between the support beams. For this load case, the cantilevered sections deflected upward (positive direction), and the loaded span deflected downward (negative direction). Each panel corner deflected a similar amount, with the deflections at P2-3 and P2-7 being slightly greater because these points were farther from the support than Points P2-1 and P2-5. The largest measured deflection (0.067 in.) was directly under the applied load.

Deflections for each span were compared to the deflection limits in the AASHTO LRFD Bridge Design Specifications (2002). The AASHTO deflection guideline for vehicular loads is L/800 for spans supported at both ends and L/300 for cantilevered spans, where L is the span length. This results in a deflection limit of 0.125 in. for the 8 ft – 4 in. interior span, 0.147 in. for the 3 ft – 8 in. cantilever, and 0.163 in for the 4 ft – 1 in. cantilever. Because the applied load exceeds the HS 20-44 loading for which the deck panel was designed, and the deflection is less than the limits specified by AASHTO, the deck panel meets deflection requirements.

The largest concrete strain (-253 MII) for load varying from 0 to 48 kip at B11 occurred at P2-C8T. This strain was the closest to the applied load (1 ft - 9 ½ in. away). P2-C2T and P2-C3T are the second and third closest strains to the load, respectively, which agrees with the strains measured (-184 MII and -162 MII). P2-C4T was over 4 ft from the load, explaining why the strain was 2 MII. All concrete strains are presented in Figure 3.9 with locations of the strains shown in Figure 2.6. Concrete strains measured in the cantilever sections were less than 2 MII and therefore were not included in the figure for clarity.

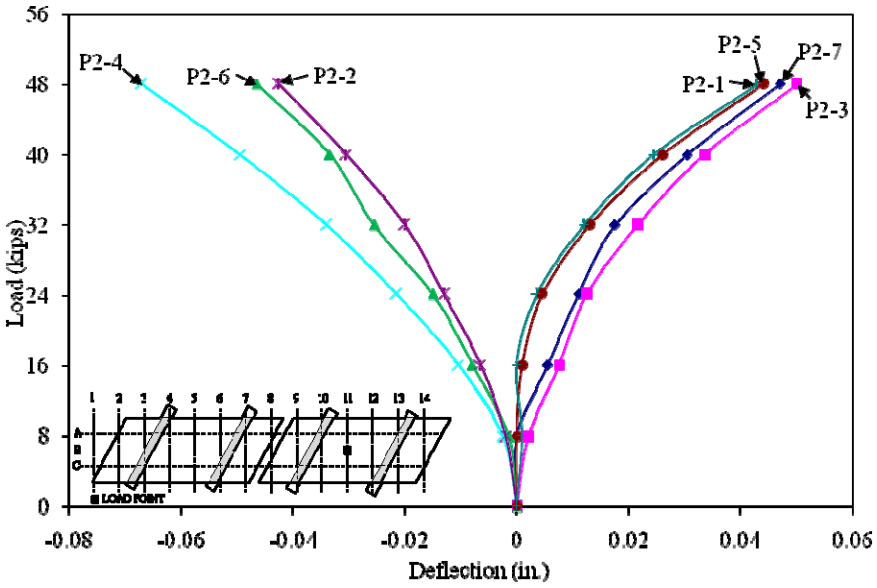

Figure 3.8. Deflection versus load, load at B11, no closure pour

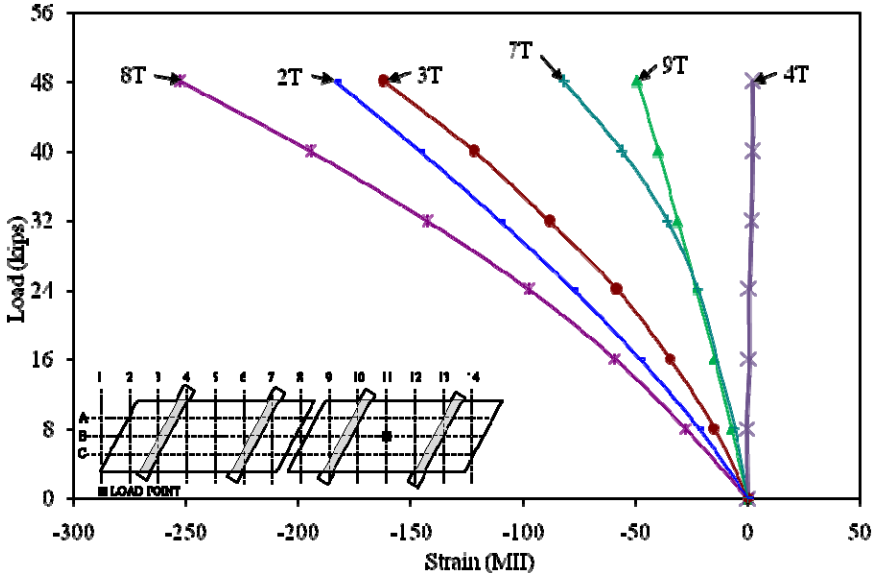

Figure 3.9. Concrete strains versus load, load at B11, Panel 2

The largest changes in deflection for a single panel occurred with a load at B14. Deflections for a 0 kip to 32 kip load at this point are plotted in Figure 3.10. A 32 kip load was used for load at B14 because the panel began to rotate about the near support at loads greater than 32 kips. Point P2-3 deflected 0.433 in. under the 32 kip load. However, P2-3 deflected 0.146 in. for a 16 kip load, the wheel load of a HS 20-44 truck. The AASHTO deflection limit for a 4 ft-1 in. cantilevered span is 0.163 in (L/300). Therefore cantilever deflections for the design wheel load are within the AASHTO limits.

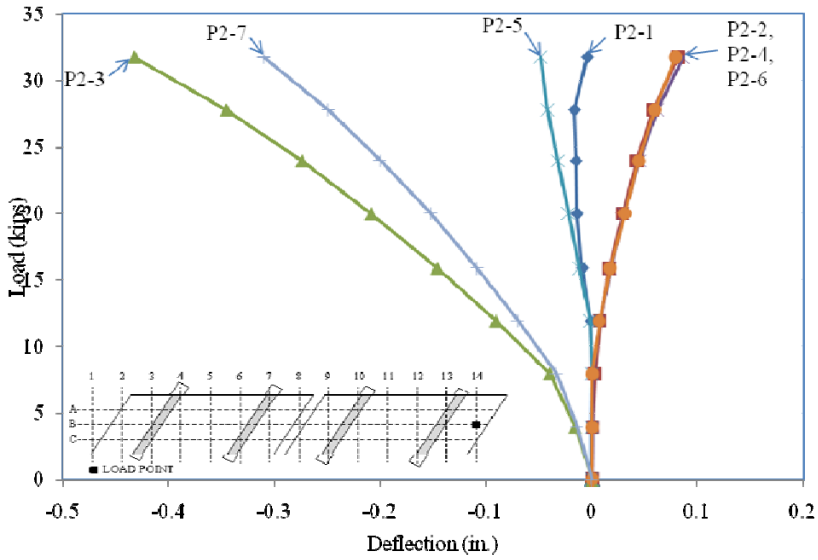

Figure 3.10. Deflection versus load, load at B14, no closure pour

A comparison of the deflection of the individual panels with a load at B5 on Panel 1 and B11 on Panel 2 are plotted in Figure 3.11. Panel 1 was loaded 0 to 20 kips, while Panel 2 was loaded 0 to 24 kips. These load ranges were plotted because 20 kips was the maximum load applied at B5, whereas B11 was loaded to 48 kips in 8 kip increments. In order to plot the data over a similar load range and because data were not recorded at 20 kips, 24 kips was chosen as the maximum load to plot for B11. Locations of each measured deflection are presented in Figure 2.8. These results are presented to show that the two deck panels when loaded similarly responded essentially the same way; the deflections for the two panels are within 0.005 in.

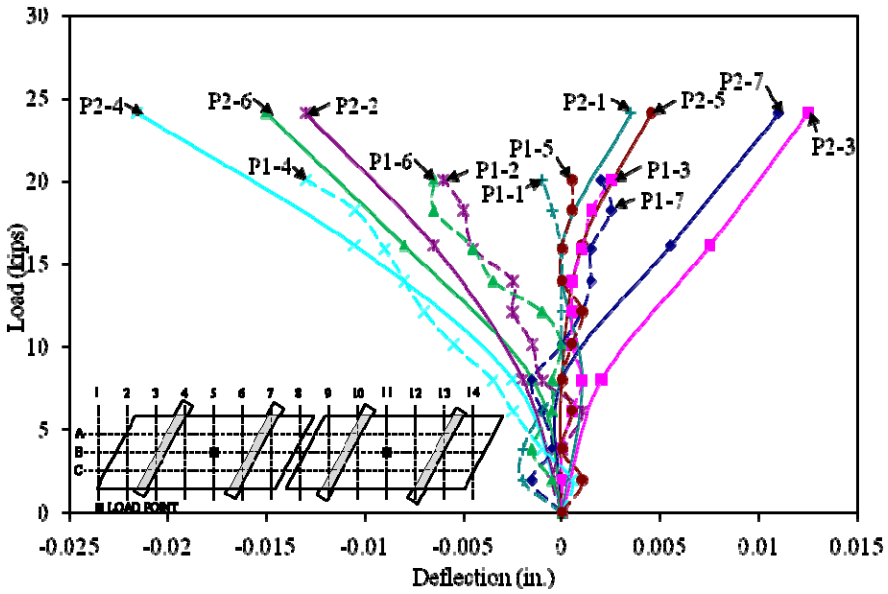

Figure 3.11. Comparison of deflection versus load results, for loads at B5 (on Panel 1) and B11 (on Panel 2)

3.6.2 Connected Panel Service Load Test Results

Nineteen points on the deck panels were loaded after the closure pour was cast (see Figure 2.24). These points were chosen to meet the test objectives stated in Section 0. The results for a load at B8 are presented to show the response of the closure pour to load. Plots illustrating the response of the system as a load moves longitudinally or transversely are also shown, along with a plot showing deflections of the deck panels with and without the closure pour in place.

Steel strains measured for the closure pour hooked bars for a load 0 to 40 kips at B8 are plotted in Figure 3.12, and the locations of the strains are shown in Figure 2.7. Strain gages on Bars CP-S3T and CP-S5B were damaged when the closure pour was cast and no strain in these bars are shown in the plot. Bottom bars in a hook were in tension and top bars in compression during loading at B8. Bars experienced greater tensile strains than compressive strains because the bars were at different depths in the cross-section; bottom bars had 1 1/2 in. of clear cover and top bars had 2 1/4 in. of clear cover. The largest strain measured was 307 MII in Bar CP-S8B, which was located at the location of the load and is less than the yielding strain of 2069 MII.

Adjacent bars comprising a double hook had tensile strains within 15 MII, and bars in compression were within 45 MII of each other. One reason as to why the compressive strains varied more than the tensile strains is because the gages were wrapped in foil to protect them prior to placing concrete (see Figure 2.23) , the concrete may not have bonded as well to some of the bars. Therefore some bars had to carry a larger compressive force than other bars.

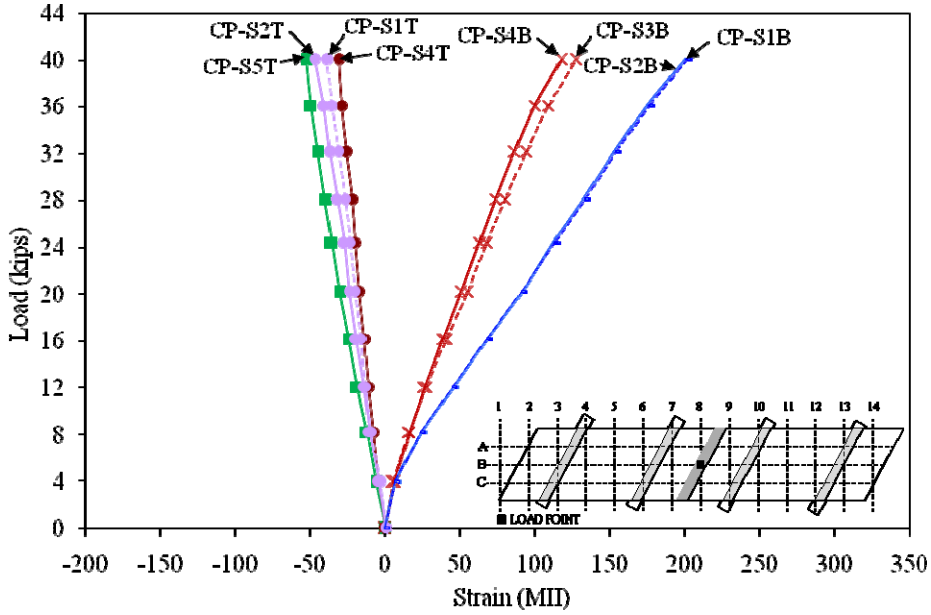

a) Strains CP-S1 through CP-S5, top and bottom bars

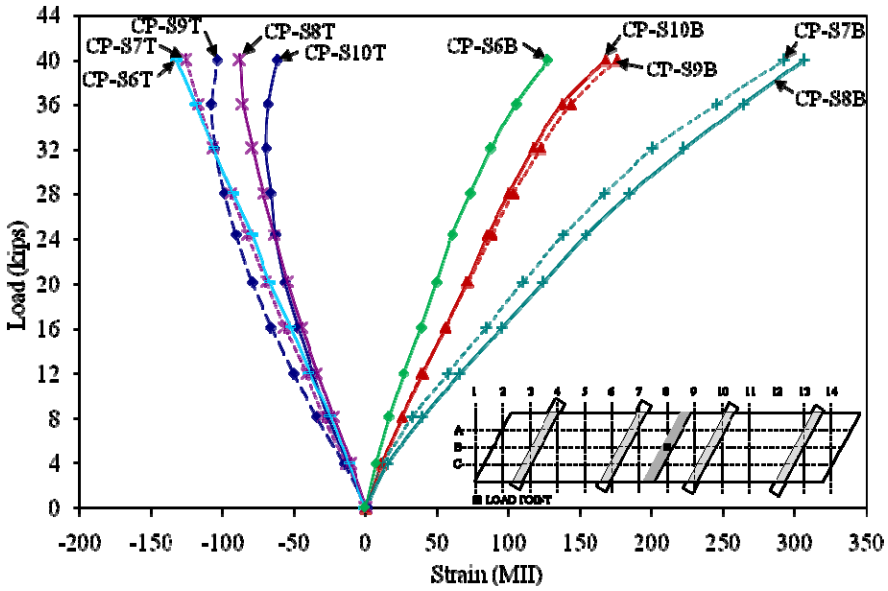

b) Strains CP-S6 through CP-S10, top and bottom bars

Figure 3.12. Closure pour steel strains versus load, load at B8, closure pour in place

Bar P1-S8T was the only bar to experience a compressive strain for a 40 kip load at B8, and the strain was -20 MII. Reinforcing bars with strains greater than 20 MII are plotted in Figure 3.13; bars with strains less than 20 MII are not shown for clarity. Refer to Figure 2.7 for the locations of the bars. The largest strain was 278 MII and occurred in Bar P2-S2T, a top bar. Top bars experienced larger strains than bottom bars because the panel had negative bending over the support beam, therefore subjecting the top bars to larger strains than the bottom bars; top bars

were at a different depth in the cross-section than bottom bars due to panel leveling. All of the reinforcing steel strains were less than the yielding strain of 2069 MII.

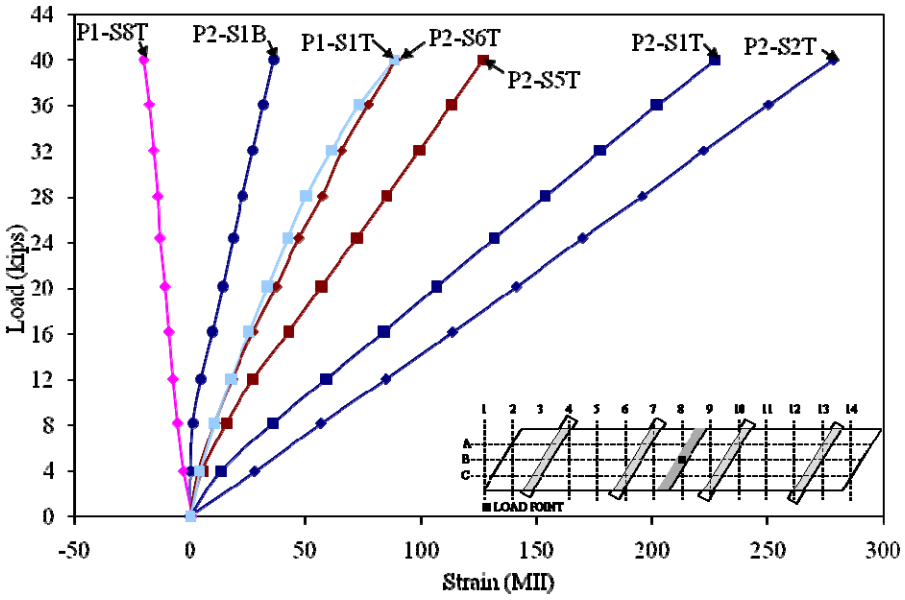

Figure 3.13. Steel strain versus load, load at B8, closure pour in place

A plot of concrete strains versus load for a 40 kip load applied at B8 is shown in Figure 3.14. Locations of each strain can be seen in Figure 2.6. The largest strains occurred in the closure pour concrete; strains in the top surface of the closure pour were compressive and strains in the top surface of the deck panels were tensile. Deck panel strains were less than 16 MII. Location CP-C2T experienced the largest strain (286 MII). All of the strains were less than 3000 MII, which is the maximum useable strain at the extreme concrete compression fiber specified by the American Concrete Institute (ACI) Building Code Requirements for Structural Concrete (2005). Greater strains were experienced at CP-C2T than CP-C1T even though the gages were the same distance from the load because of the skew of the deck panels.

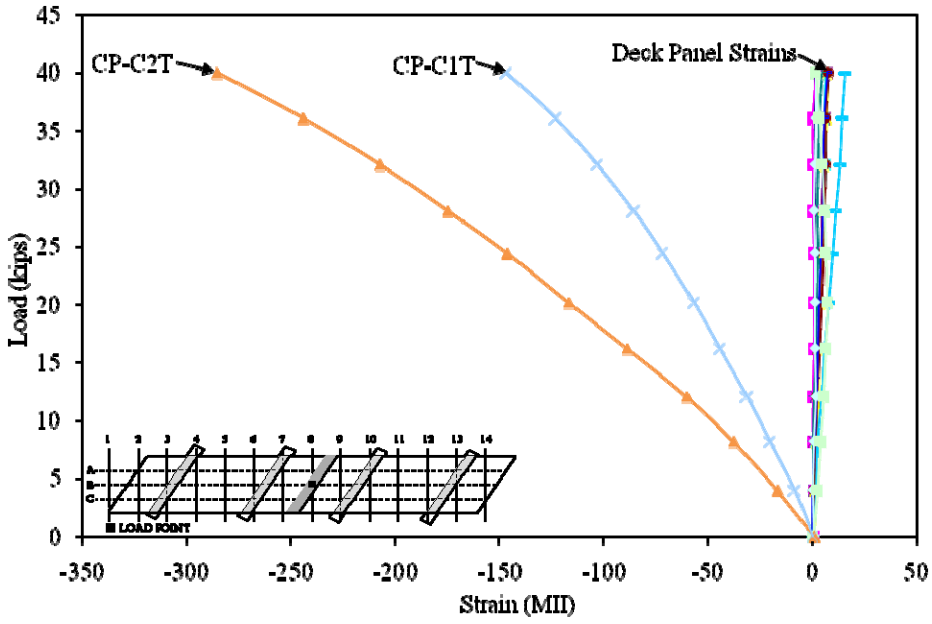

Figure 3.14. Concrete strains versus load, load at B8, closure pour in place

Deflections due to a 40 kip load at B8 are plotted in Figure 3.15; the locations of the deflections are given in Figure 2.8. Deck panel deflections were less than 0.002 in. and not included in the plot for clarity. CP-2 was at the applied load and underwent the largest deflection, 0.051 in. AASHTO specifies a maximum deflection equal to L/800 for a span supported at both ends, which results in a maximum deflection of 0.125 in. for a span length of 8 ft – 4 in. The applied load of 40 kips was greater than the wheel load of a HS 20-44 design truck, and the maximum deflection was less than limits specified by AASHTO; therefore the deck panel meets deflection requirements.

Graphs of the change in deflection as a 16 kip load moved along Line B are presented in Figure 3.16. Results for a 16 kip load are plotted because this load is equivalent to a HS 20-44 wheel load. Changes in deflection near the load were the largest; deflection changes of unloaded spans were less than 0.005 in. For example, from Figure 3.16a one can see that as the load moved from Panel 1 to Panel 2 (B1 to B14) the deflection of points on Panel 1 changed 0.002 in. or less.

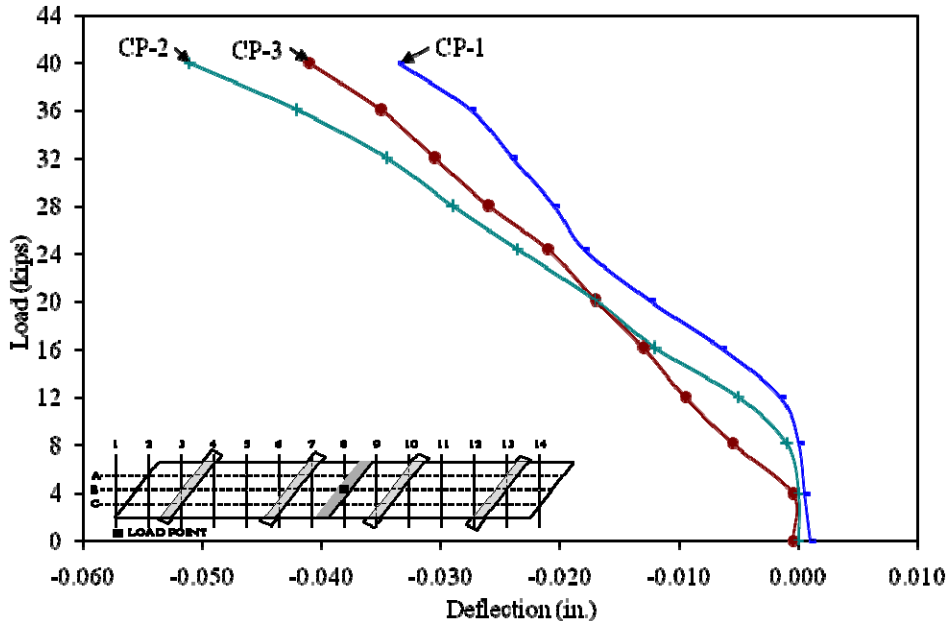

Figure 3.15. Deflection versus load, load at B8, closure pour in place

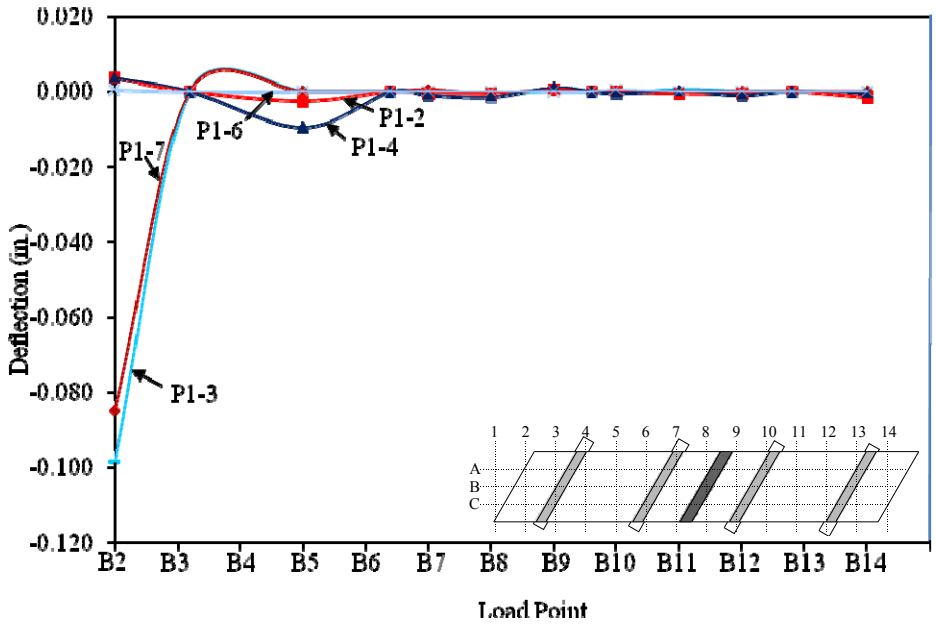

a) Panel 1 deflections

Figure 3.16. Deflection of the deck panels as a 16 kip load moved across grid Line B

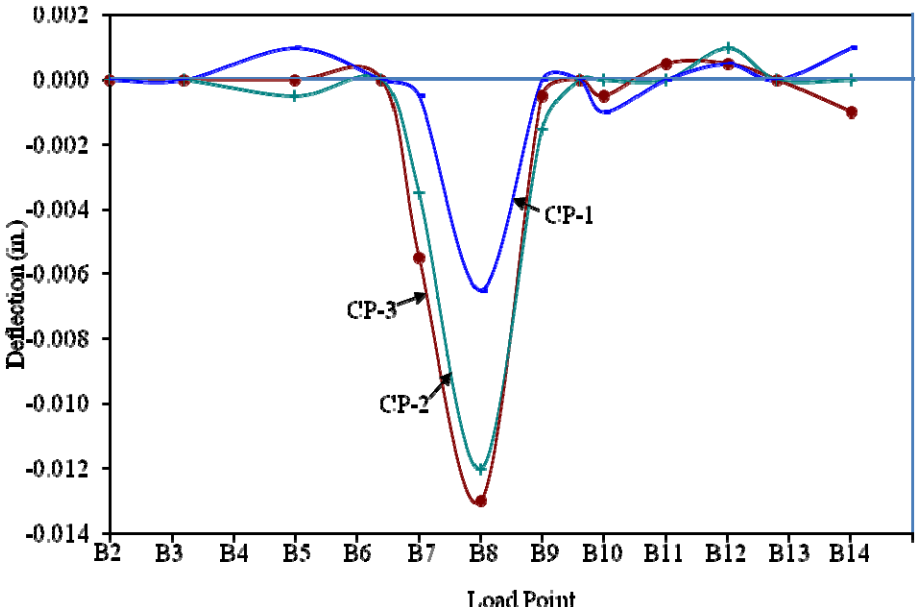

b) Closure pour deflections

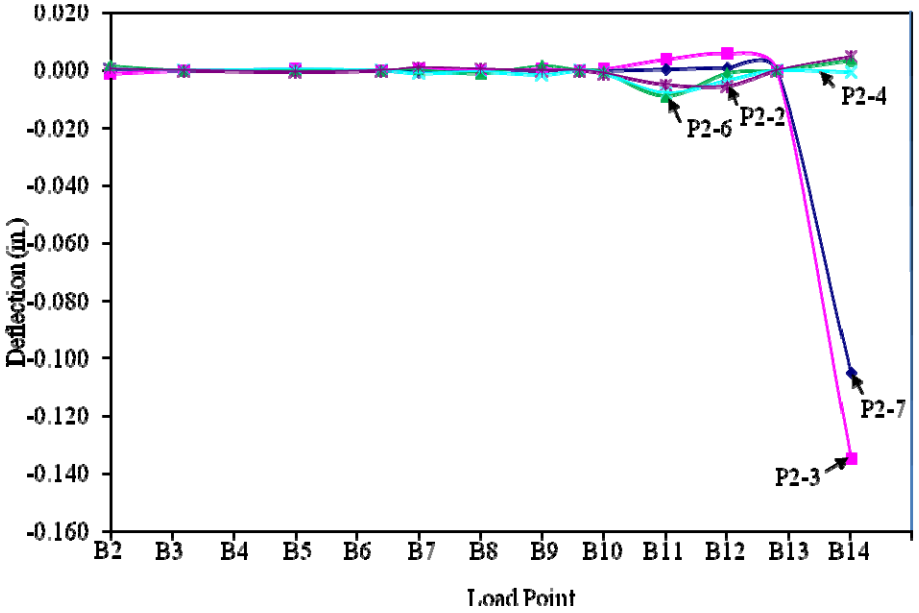

c) Panel 2 deflections

Figure 3.16. Deflection of the deck panels as a 16 kip load moved across grid Line B

The largest change in deflection occurred when the cantilever section was loaded. These are load points B2 and B14. Point P2-3 underwent the largest deflection change, 0.135 in. (see Figure 3.16c). This deflection was within the AASHTO deflection limit of L/300 equal to 0.163 in. for a cantilevered span length of 4 ft – 1 in. Deflections for the deck panel spanning between the support beams had a maximum value of 0.017 in., which is less than the AASHTO deflection limit of L/800 equal to 0.125 in for a span with length equal to 8 ft – 4 in.

Presented in Figure 3.17 are the deflection changes experienced as a 40 kip load moved from load point A11 to C11 along grid Line 11. Locations of load points can be seen in Figure 2.24 and locations of deflection are shown in Figure 2.8. Changes in deflection of Panel 1 were less than 0.002 in. and excluded from the plot for clarity. As one would expect, the cantilevered section of the deck panel (P2-3 and P2-7) deflected upward (positive) and the loaded portion of the deck panel (P2-2, P2-4, P2-6) deflected downward (negative). Deflections for the cantilevered section were independent of the location of the load, as the deflection changed 0.002 in. among the three load points. The stiffness of the closure pour was apparent in this test, as deflection changes of the closure pour were a maximum of 0.002 in.

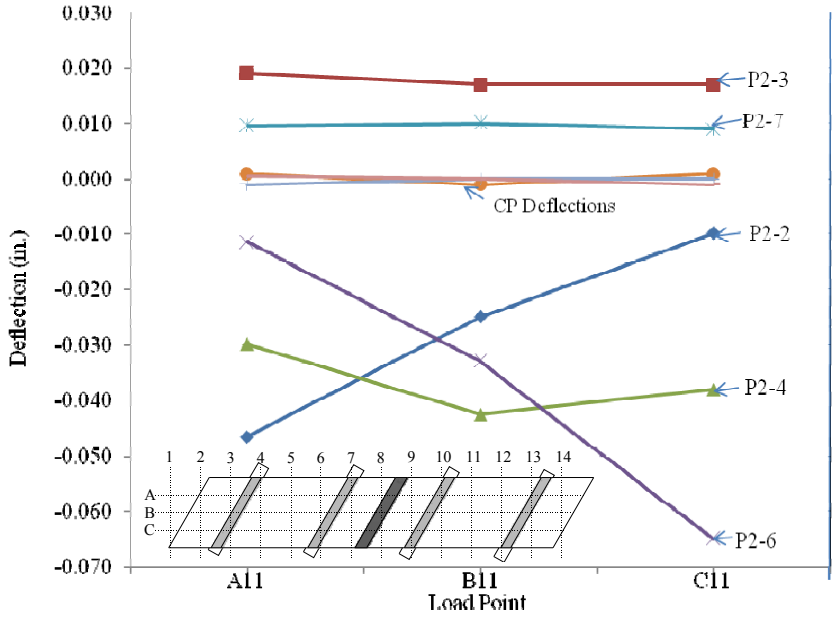

Figure 3.17. Deflection of the deck panels as a 40 kip load moved along grid line 11

Another observation from Figure 3.17 is the loaded span responded as expected. When the load was at A11, P2-2 experienced the greatest deflection, and the deflection at this point decreased as the load moved to C11. P2-4 deflected the most when the load was above this point (at B11) and deflected approximately the average of the P2-2 and P2-6 deflections for load points A11 and C11. Point P2-6 deflected the least of P2-2, P2-4, and P2-6 when the load was at A11, and the deflection increased as the load moved along Line 11.

A plot of deflections for a load at point B11 for the individual and connected panels is shown in Figure 3.18. From these plots, one can see the effect the closure pour had on the system. Every deflection decreased after the closure pour was cast, with the greatest changes occurring at the cantilevered sections of the deck panel. Deflections at P2-7, located at a corner of the cantilevered deck panel, decreased by 0.02 in. after the closure pour was cast. In Figure 3.18, deflections CP-1 and P2-5, along with CP-3 and P2-7, are at approximately the same location and can be compared. Casting the closure pour resulted in a decrease of 0.025 in. in deflections at the locations.

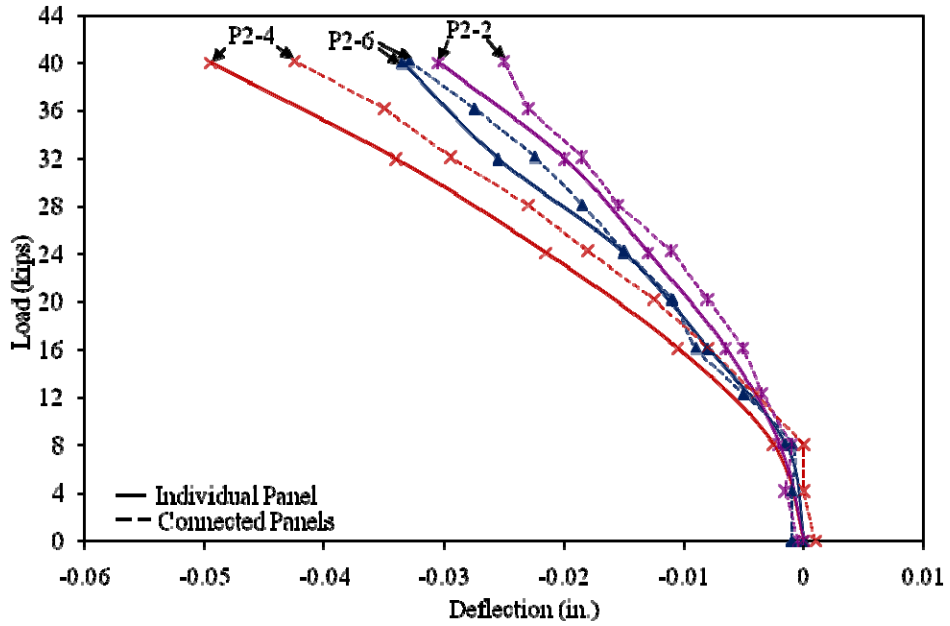

a) Deflections P2-2, P2-4, and P2-6

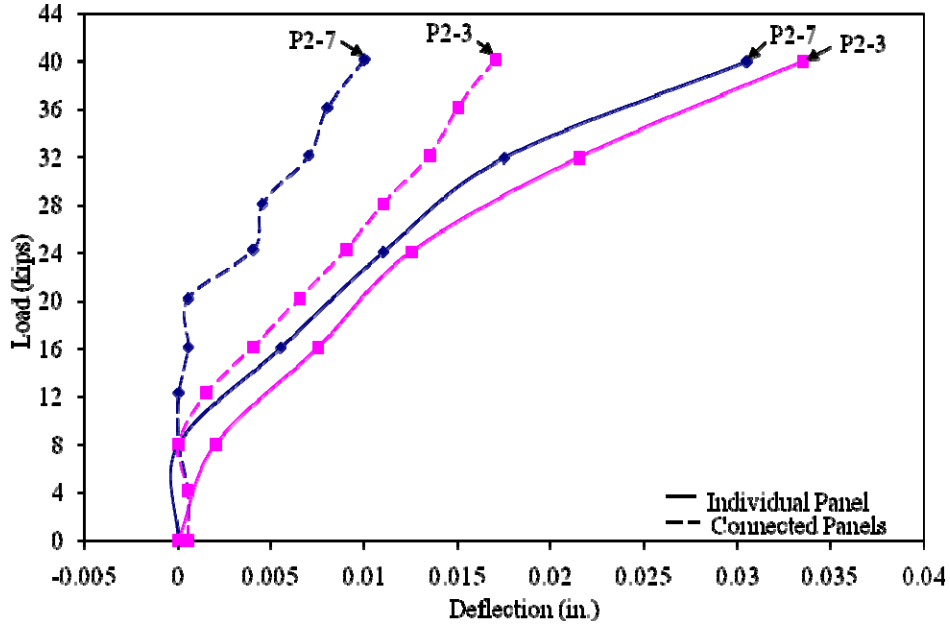

b) Deflections P2-3 and P2-7

Figure 3.18. Deflections for load point B11 before and after casting the closure pour

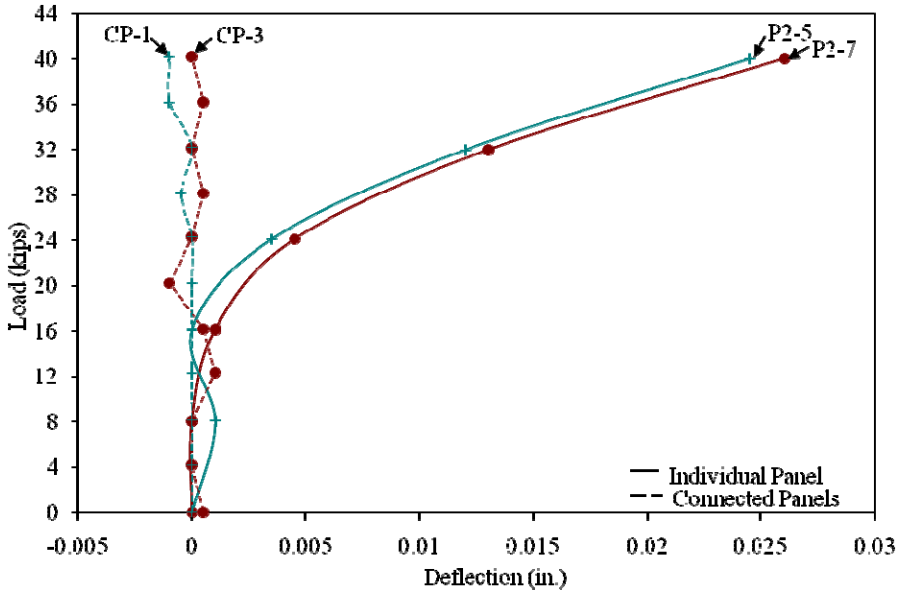

c) Deflections P2-5, P2-7, CP-1, and CP-3

Figure 3.18. Deflections for load point B11 before and after casting the closure pour

3.7 Ultimate Strength Results

Results for the ultimate strength tests are presented in the following sections. A single panel was tested to its ultimate flexural strength. Strength testing on connected panels included testing to the following failures: punching shear; combined punching shear and flexure; and flexure.

3.7.1 Single Panel Ultimate Test Results

Photographs of a single panel tested to failure are presented in Figure 3.19. A line load was applied to the deck panel, and a flexural failure occurred at a load of 153 kips. Concrete that spalled from the deck panel surface is visible in Figure 3.19a. In Figure 3.19b one can see flexure cracks propagating up the side of the deck panel.

Two values for the experimental moment due to the line load were calculated; this was done because the fixity provided by the supports was unknown. The first value assumes the support beams acted as pinned supports and the second value assumes fixed supports. The experimental moment was 368 ft-kips when the supports were treated as pinned and 184 ft-kips when fixed. These values bracket the theoretical strength of 263 ft-kips, calculated using strain compatibility equations. Because the theoretical strength lies between the pinned moment and fixed moment, the support beams provided a fixity between pinned and fully fixed. Theoretical and experimental flexural strengths for a single deck panel are presented in Table 3.7.

The largest concrete strains occurred along the axis of bending. Concrete strains are plotted in Figure 3.20 for a load to 150 kips, and the location of each strain is shown in Figure 2.6. Point P3-C8T experienced the largest strain (-3919 MII). This strain exceeds the strain value of -3000

MII specified by ACI as the maximum useable strain at the extreme concrete compression fiber. P3-C3T experienced -2969 MII of strain, and all other strains were less than -700 MII.

a) Deck panel after loading

b) Flexure cracks

Figure 3.19. Flexural failure of the single deck panel tested

Table 3.7. Single panel flexural strengths

Flexural Capacity	Capacity (ft-kips)
Theoretical	263
Experimental (for pinned supports)	368
Experimental (for fixed supports)	184

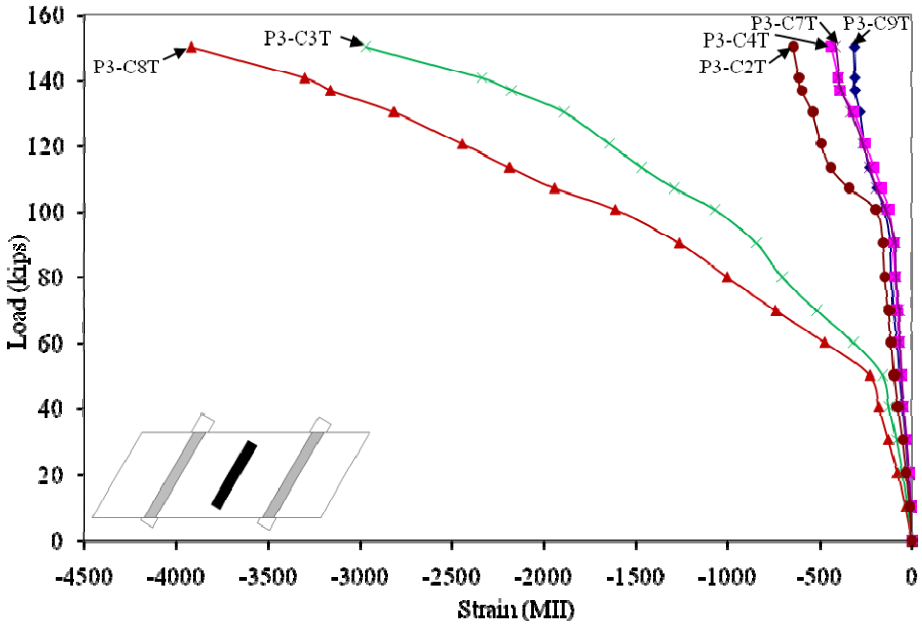

Figure 3.20. Concrete strain versus load for single panel ultimate load test

Deflections experienced during the test for a load up to 150 kips are plotted in Figure 3.21, and locations of each deflection are shown in Figure 2.8. Deflections of the loaded span of the panel were downward (negative), and deflections of the cantilevered sections were upward (positive). P3-4 was at midspan at the location of the applied load and therefore experienced the largest deflection, 0.95 in. at failure. Location P3-6 had a greater deflection change than P3-2 because of the skew of the deck panel. Point P3-3 deflected 1.24 in. upward and experienced the largest deflection during the test.

3.7.2 Nine Inch Square Footprint Results

A punching shear failure of the deck panel occurred at a load of 150 kips; photographs of the deck panel from above after failing in punching shear are presented in Figure 3.22. The failed concrete has been removed to show the reinforcing steel in Figure 3.22b. Inspection of the deck panel after failure occurred showed the reinforcing steel had been pushed downward and caused strips of the concrete to spall from the underside of the deck panel (Figure 3.22c).

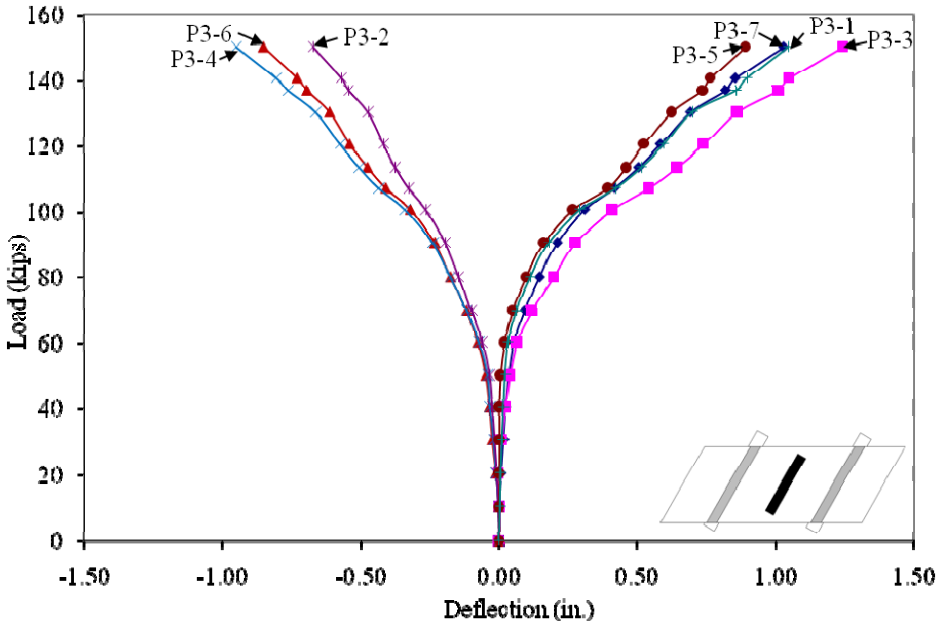

Figure 3.21. Deflection versus load for single panel ultimate load test

a) Top view of punching shear failure footprint

Figure 3.22. Photographs of the deck panel after a punching shear failure

b) Top view after concrete removal

c) Underside of the deck panel

Figure 3.22. Photographs of the deck panel after a punching shear failure

The theoretical punching shear was calculated using concrete shear strength equations published by ACI (2005). A concrete compressive strength equal to 7,600 psi (from the concrete strength testing) was used to determine the theoretical punching shear strength. The experimental shear force was 146 kips, which exceeded the theoretical strength of 135 kips by 8%. Theoretical and experimental punching shear capacities are presented in Table 3.8.

Table 3.8. Punching shear capacity

Capacity	Shear Force (kips)
Theoretical	135
Experimental	146

Concrete strains experienced during loading were measured for loading up to 140 kips and are plotted in Figure 3.23; locations for each strain are shown in Figure 2.6. Strains were recorded only to 140 kips because failure occurred prior to the next automated reading by the DAS. Strain gages at concrete strain locations on Panel 1 did not measure the strain accurately and are excluded from the plot. Strains were the largest in the closure pour, reaching -1101 MII prior to failure. This value was less than -3000 MII, which is specified by ACI as the maximum useable strain at the extreme concrete compression fiber. The maximum strain measured in Panel 2 was 118 MII.

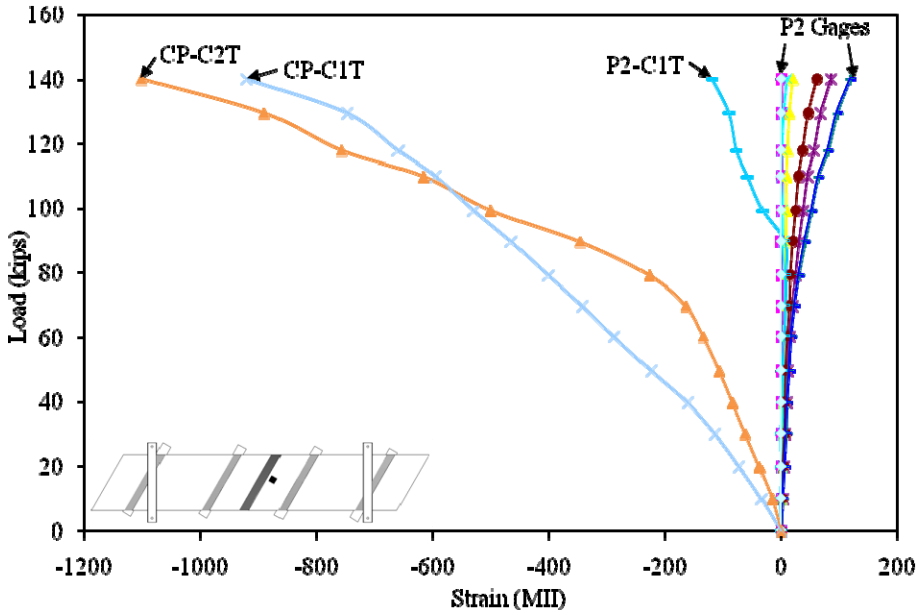

Figure 3.23. Concrete strain versus load for 9 in. square footprint loading

A maximum steel strain experienced during testing was a tensile strain of 1740 MII. This strain is equivalent to a stress of 50 ksi, which is less than the bar yield stress of 60 ksi. Steel strains for the closure pour hooked bars are presented in Figure 3.24 for loading to 140 kips. Locations for each strain are shown in Figure 2.7. As expected, the bottom bars of each hook were in tension throughout the test. Half of the top bars started as compression reinforcement and carried tension by the end of the test as a result of the concrete cracking and the depth of the compression zone in the concrete decreasing.

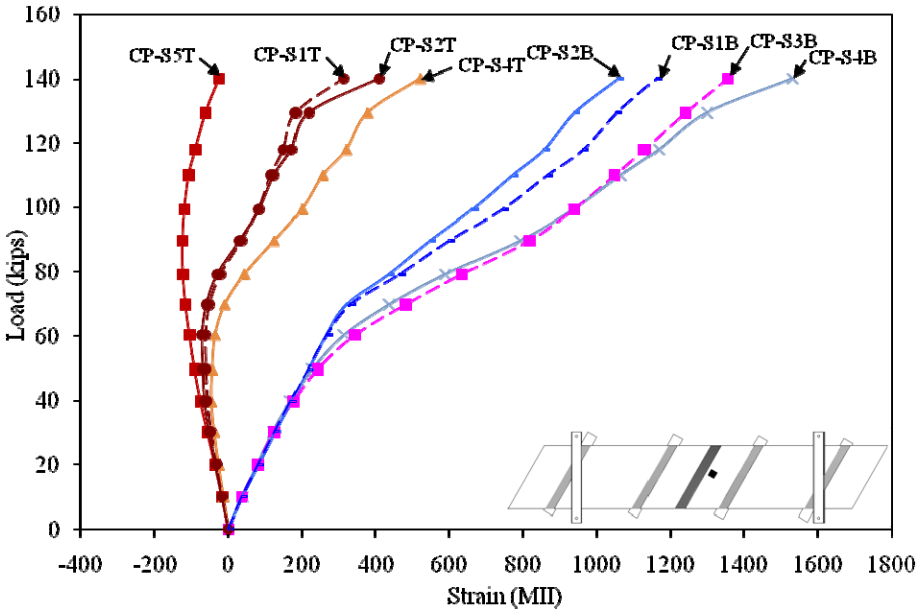

a) Strains CP-S1 through CP-S5, top and bottom bars

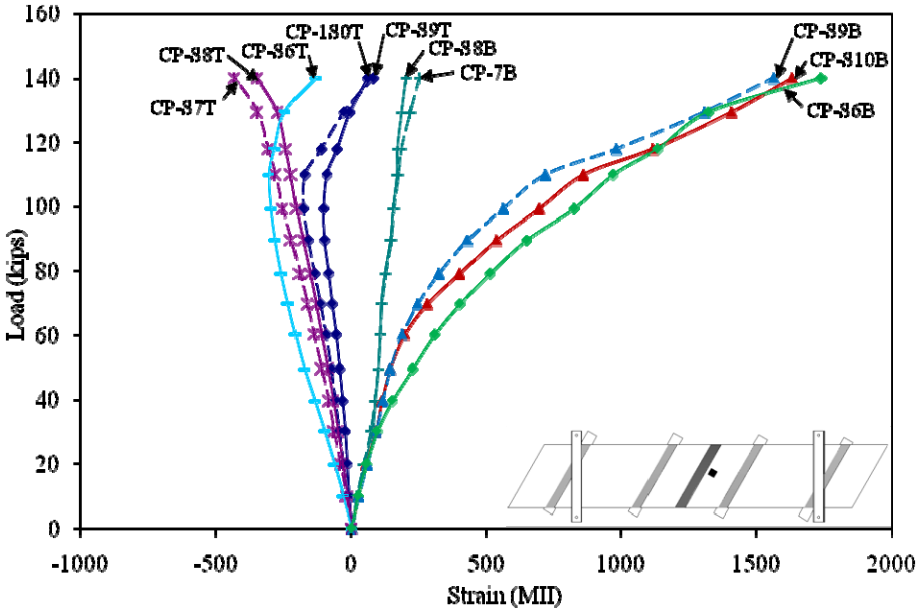

b) Strains CP-S6 through CP-S10, top and bottom bars

Figure 3.24. Closure pour steel strain versus load for 9 in. square footprint loading

Strains in the reinforcing steel of the longitudinal channels are plotted in Figure 3.25 for loading to 140 kips. Strains less than 140 MII were excluded from the graph for clarity, and the location of each plotted strain is shown in Figure 2.7. From the figure, one can see the Panel 2 reinforcement carried more load than the Panel 1 reinforcement, as only one instrumented bar on Panel 1 experienced over 140 MII. This load distribution would be expected because the load was closer to the Panel 2 bars. All of the bars were in tension as the panel underwent negative

bending about the support, and the top bars experienced the largest strains. The largest strain was 1158 MII in Bar P2-S2T.

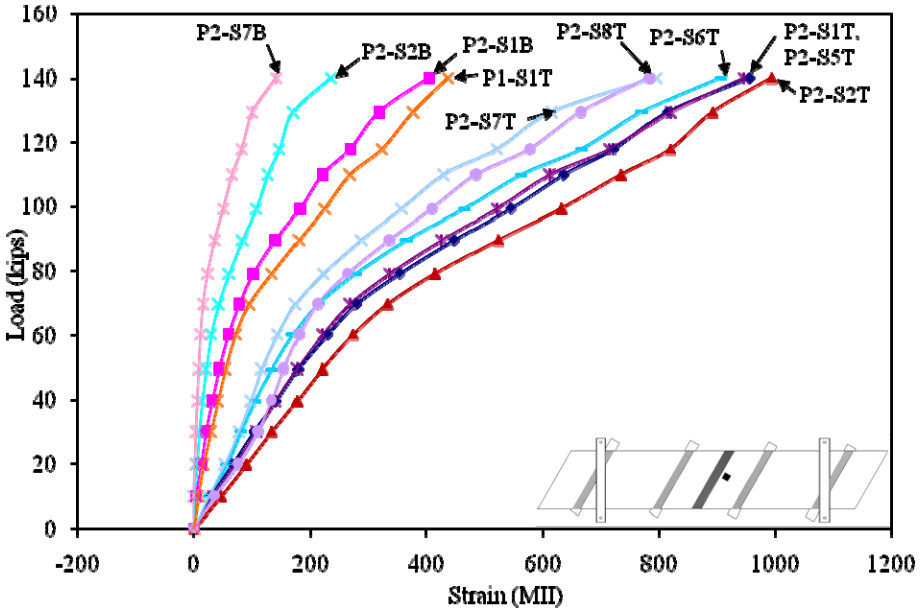

Figure 3.25. Steel strain versus load for 9 in. square footprint loading

Deflections for the 9 in. square footprint test show the closure pour was stiffer than the rest of the deck panels. The maximum deflection measured for the closure pour was 0.02 in. and was 0.032 in. for a non-cantilevered section of the deck panels, even though the load was applied next to the closure pour. Plotted in Figure 3.26 are deflections experienced for loading up to 140 kips at the locations shown in Figure 2.8. Changes in deflection at P1-2 and P2-2 were less than 0.002 in. and were not plotted for clarity. These deflections were less than anticipated due to the nearby restraining beam limiting the positive deflection of the deck panels. When observing the data, one will notice the deflections had a sudden increase in the positive direction for loads between 80 kips and 100 kips. This sudden change in the deflections could not be explained by the researchers, as nothing abnormal was observed during testing and the strain data for the concrete and reinforcing bars does not exhibit a similar response.

3.7.3 Tandem Wheel Footprint Results

Failure occurred at a load of 157 kips do to a combination of punching shear and flexure. Figure 3.27 is a photograph of the deck panel failure caused by the tandem wheel footprint. In this figure, the concrete that failed around the footprint due to punching shear can be seen, along with the concrete that spalled from the surface due to bending.

Provided in Table 3.9 are the theoretical and experimental flexure and shear capacities of a deck panel for loading by a tandem wheel footprint. Experimental values were calculated with statics, theoretical flexure strength from strain compatibility equations, and punching shear strength

from equations in ACI Building Code Requirements for Structural Concrete (2005). A comparison of the values shows the applied moment (298 ft-kips) exceeded the theoretical flexural strength (263 ft-kips) by 14%. One reason for this is the support beams provided some restraint, reducing the applied moment by providing additional fixity. Also of note is the applied shear (150 kips) was 80% of the theoretical punching shear capacity (188 kips), yet a punching shear failure occurred. The punching shear capacity may have been reduced because of the flexural cracks reduced the depth of concrete available to resist punching shear.

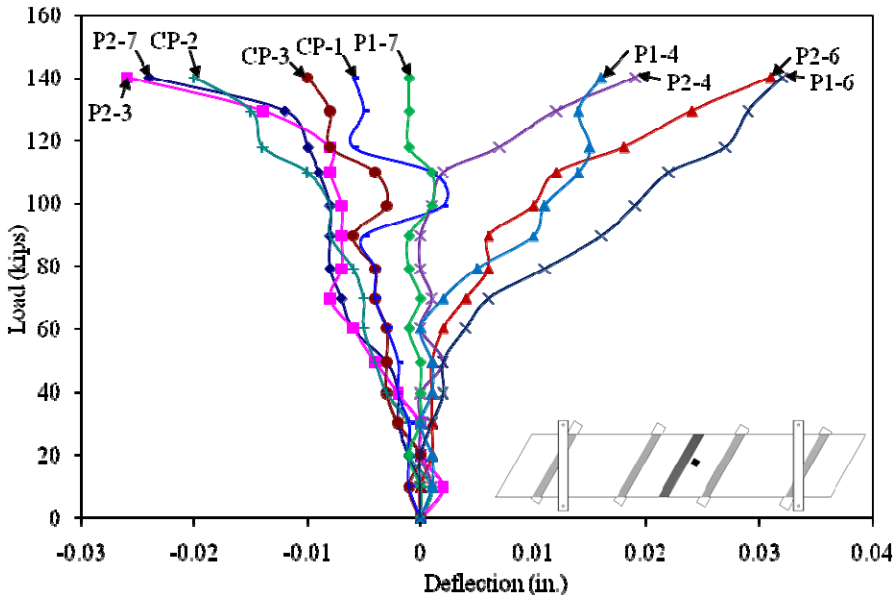

Figure 3.26. Deflection versus load for 9 in. square footprint loading

Figure 3.27. Punching shear and flexure failure due to tandem wheel footprint

Table 3.9. Theoretical and experimental capacities for the tandem wheel footprint test

Failure Mode	Strength
Theoretical Punching Shear	188 kips
Applied Punching Shear	150 kips
Theoretical Flexural	263 ft-kips
Applied Moment	298 ft-kips

Closure pour hooked bar steel strain values were low, with the maximum strain being 342 MII. This strain is equivalent to a stress of 10 ksi, which is significantly below the yielding stress of 60 ksi for the hooked bars. Steel strains experienced in the closure pour hooked bars are plotted in Figure 3.28 for loads up to 149 kips; refer to Figure 2.7 for the location of each strain. Strains are only plotted to a load of 149 kips because failure occurred prior to the next automated DAS recording. Any strain less than 30 MII was excluded from the plot for clarity. The plot also shows the top bars were in tension and the bottom bars in compression, meaning negative bending occurred at the closure pour.

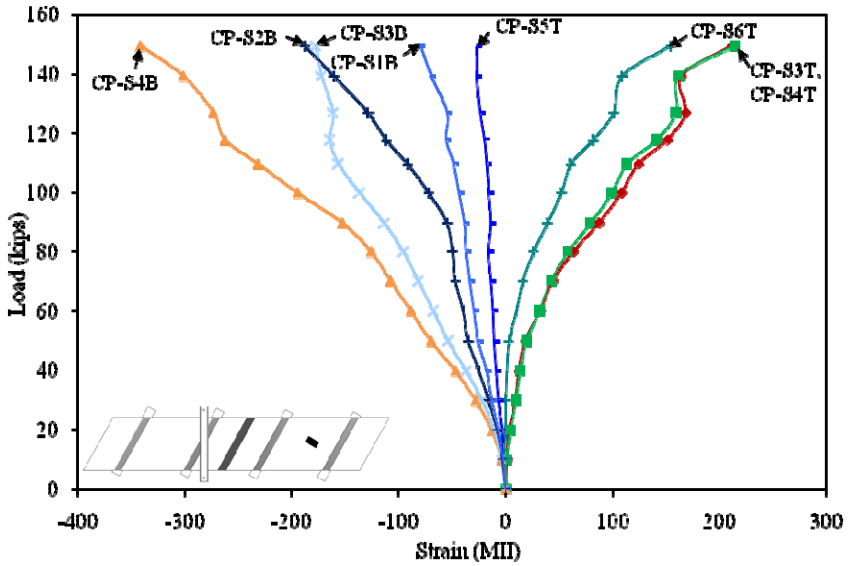

Figure 3.28. Closure pour steel strain versus load for tandem wheel footprint

Mild reinforcement bar strains for loading to 149 kips are shown in Figure 3.29, and the locations of each strain are presented in Figure 2.7. Excluded from the figure for clarity were the strains in the Panel 1 bars, which all were less than -100 MII. Panel 2 strains were tensile, with the top bar strains greater than the bottom bar strains by 800 MII on average. The strain in the top bars of Panel 2 was similar in magnitude, showing load was distributed equally throughout the deck panel. Bottom bar strains were less than 200 MII of strain. Point P2-S6T experienced the largest strain (1054 MII) which is equivalent to a stress of 31 ksi.

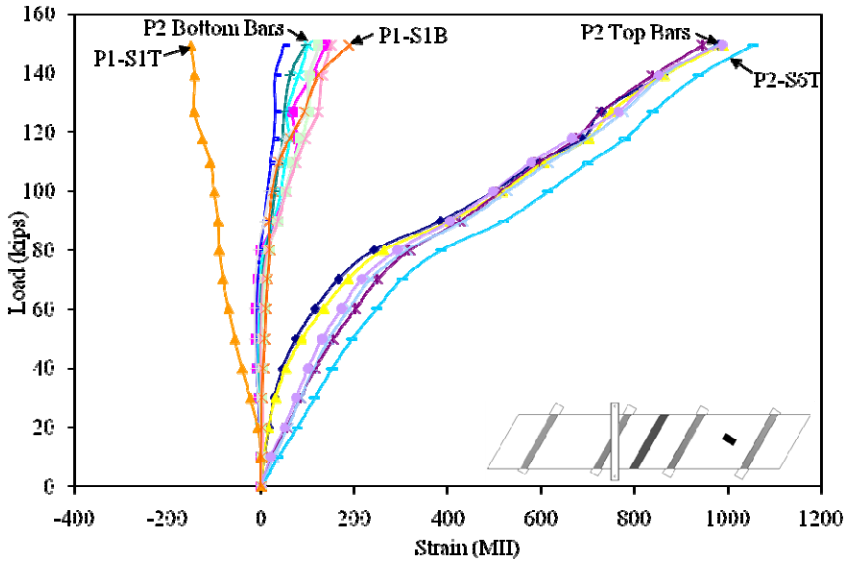

Figure 3.29. Steel strain versus load for tandem wheel footprint test

The highest concrete strain (-2163 MII) was at P2-C3T, which was closest to the applied load. P2C8T was located on the axis of bending for the deck panel, which explains why the strain experienced at this point was the second largest even though P2-C9T was located closer to the load. The low strains in the closure pour verify the steel strains previously discussed and that a low portion of the load was transferred to that section of the deck panel system. All the concrete strains experienced during the tandem wheel footprint test for loading to 149 kips are plotted in Figure 3.30, and locations for each strain plotted are given in Figure 2.6. Strains in Panel 1 were not plotted because the gages malfunctioned, and strains in Panel 2 and the closure pour that were less than -165 MII were excluded for clarity.

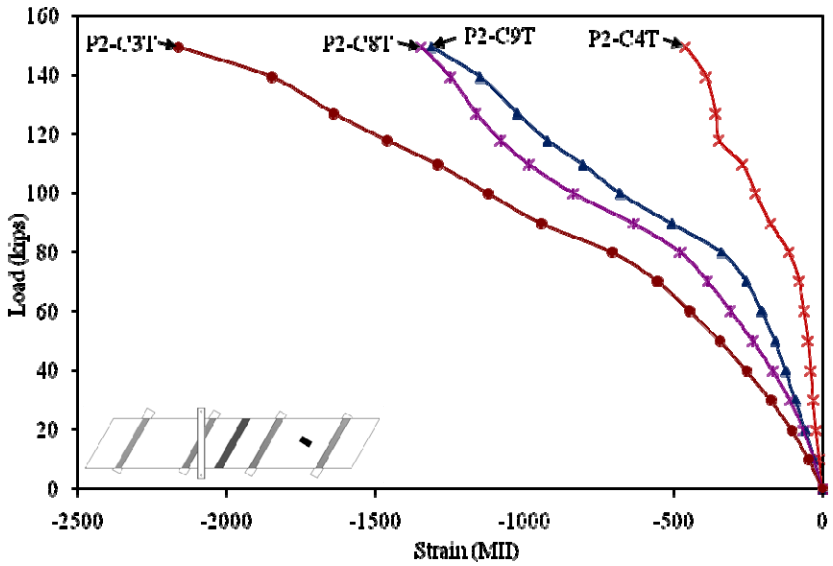

Figure 3.30. Concrete strain versus load for tandem wheel footprint loading

Deflections at the locations shown in Figure 2.8 are plotted versus loading to 149 kips in Figure 3.31. Panel 1 deflections were less than 0.007 in. and were not included in the plot for clarity, along with the deflection at CP-2, which had the transducer removed after the 9 in. footprint test. The cantilevered section adjacent to the loaded span deflected upward 1.11 in., and the loaded span deflected downward 0.078 in. Point P2-2 had a greater deflection change than P2-6, a result due to the skew of the deck panels.

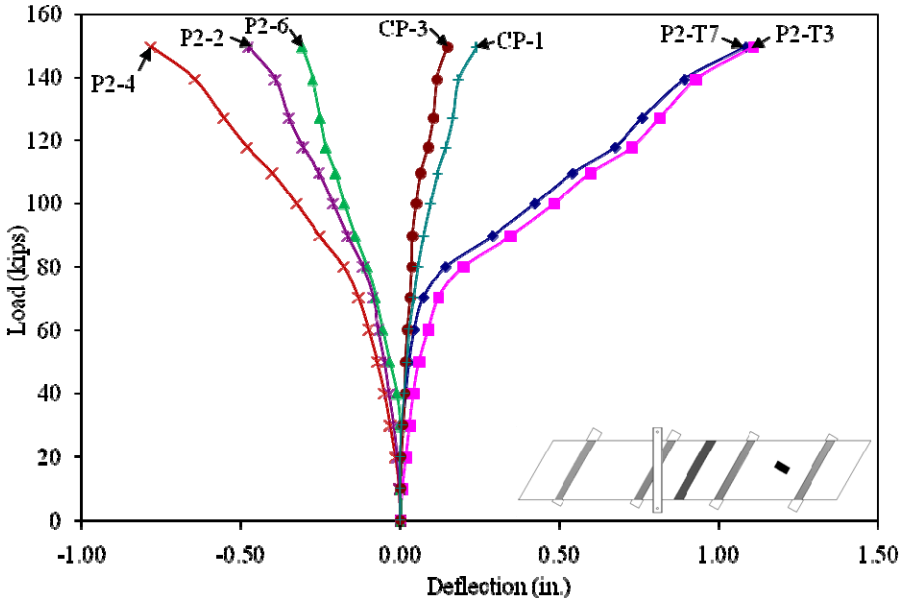

Figure 3.31. Deflection versus load for tandem wheel footprint loading

3.7.4 Line Load Results

A photograph of the deck panel failure due to an applied line load is shown in Figure 3.32; Figure 2.29 presents the location of the applied load. The deck panel failed due to flexure at an applied load of 196 kips. This load is equivalent to a moment of 372 ft-kips, which exceeds the theoretical flexural strength of 263 ft-kips. These values are given in Table 3.10. The applied moment value was calculated by using statics and treating the deck panel system as a simply supported continuous beam. However, the support beams supply some restraint against rotation, which was shown in the single panel test. Strain compatibility was used to calculate the theoretical flexural strength of the deck panel.

Tensile strains in the closure pour steel were less than 310 MII, and compressive strains were less than -100 MII. Every top bar was in tension, while half the bottom bars were in compression and half in tension. The maximum strain experienced was 303 MII, which is equivalent to a stress of 9 ksi. Closure pour steel strains are plotted in Figure 3.33 for loading to 189 kips, and locations for each strain are shown in Figure 2.7.

Figure 3.32. Flexural cracking in deck panel due to applied line load

Table 3.10. Deck panel moment capacities

Failure Type	Capacity (ft-kips)
Theoretical Flexure	263
Applied Moment	372

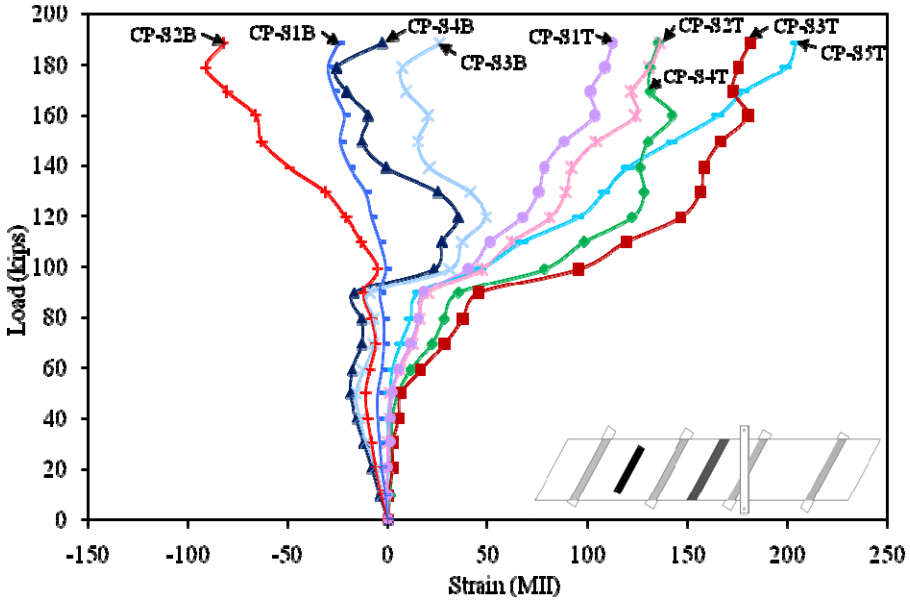

a) CP-S1 through CP-S5, top and bottom bars

Figure 3.33. Closure pour steel strain versus load for applied line load

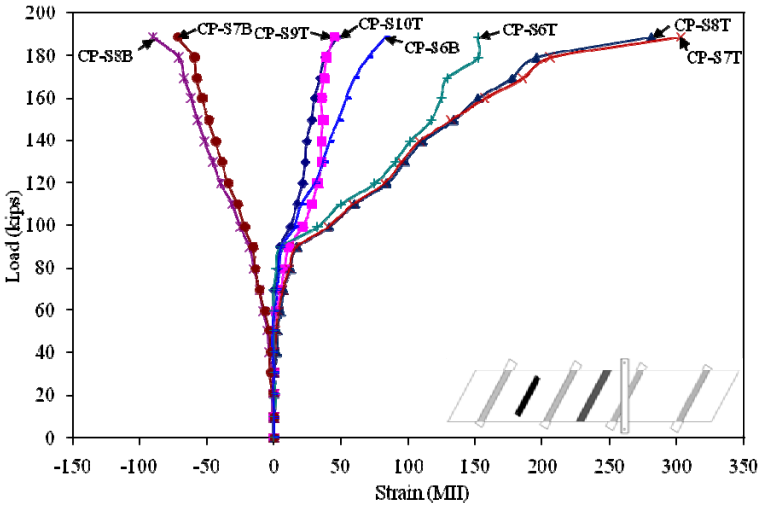

b) CP-S6 throught CP-S10, top and bottom bars

Figure 3.33. Closure pour steel strain versus load for applied line load

Plots of concrete strains and steel strains for the post-tensioning channel reinforcement are not provided for this test. Concrete strain gages on Panel 1 malfunctioned, and strains for Panel 2 and the closure pour were less than 100 MII. Panel 1 steel strains also were not measured correctly, so these strains were discarded.

Deflections experienced during this test are plotted for loading up to 189 kips in Figure 3.34, and locations of each deflection are given in Figure 2.8. Deflections along the closure pour and Panel 2 were less than 0.08 in. and were excluded from the plot for clarity. As one would expect, the loaded span deflected the most, with the panel deflecting 0.808 in. at midspan. Points P1-2 and P1-6 deflected different amounts because of the skew of the deck panels. The cantilevered portion of the deck panel deflected upward, with P1-3 deflecting 0.139 in.

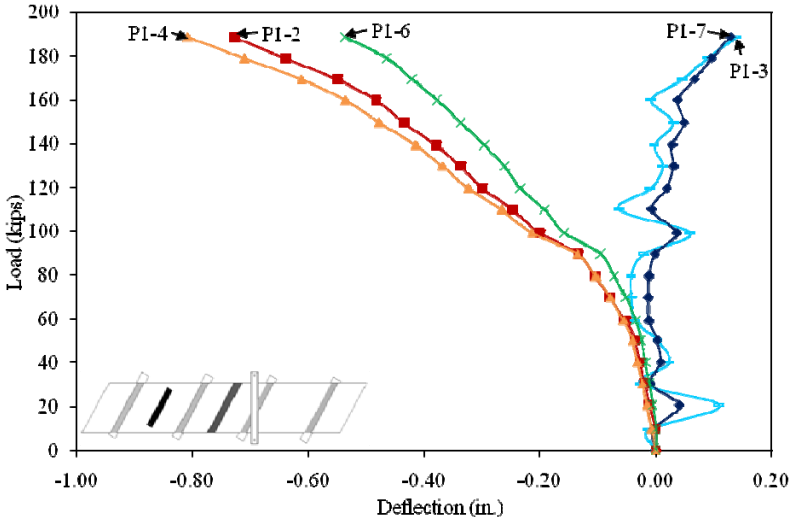

Figure 3.34. Deflection versus load for applied line load

4. SUMMARY, CONCLUSIONS, AND RECOMMENDATIONS

4.1 Summary

Three deck panels were obtained from Andrews Prestressed Concrete, Inc. for laboratory testing. Testing included determining the concrete strength of the deck panels, determination of the stress in the mild reinforcing due to the prestressing force, determining strains in the panels while lifting them with a crane, determining the strains in the panels while leveling them, observation of the concrete flow through a model of the longitudinal post-tensioning channel, service load testing of individual panels and two panels with the closure pour in place, and ultimate strength testing of a single panel and connected panels.

4.1.1 Concrete Strength Testing Summary

Three concrete cores were removed from one deck panel after the conclusion of testing and tested to determine the compressive strength of the concrete. The strength of the cores was assumed to be representative of the three deck panels. Cores were found to have an average strength of 7,600 psi, which exceeds the specified compressive strength of 5,000 psi by 27%.

4.1.2 Stresses in Mild Reinforcing Due to Prestressing

Strains in six mild reinforcing bars were measured while the prestressing strands in one longitudinal channel were cut. Stresses in five of the six bars were less than the theoretical compressive stress with prestressing losses considered of 20.7 ksi. Bar 2B had the largest stress (21.5 ksi), exceeding the theoretical compressive stress minus losses by 4%. The lowest stress was found in Bar 2T (13.0 ksi), 37% less than the theoretical compressive stress considering losses.

The average stress in the top and bottom bars was calculated and compared. Top bars were found to be under an average compressive stress of 14.2 ksi. Bottom bars experienced an average compressive stress of 17.9 ksi. Both of these values were less than the theoretical compressive stress minus prestressing force losses which was 20.7 ksi.

4.1.3 Lifting Panel Strain Summary

Temporary strains induced in the mild reinforcement in the longitudinal post-tensioning channels were measured during the crane lifting tests. Two different strap configurations were used to lift a deck panel, and the panel was lifted twice for each setup. The first configuration used four straps, with each strap wrapped around two groups of bars (see Figure 2.12). Bar 1T experienced a strain of 251 MII, the largest strain during this test. This strain is equivalent to a moment of 0.48 in.-kips (a stress of 7.3 ksi). Using the calculated moment, the theoretical compressive force in the bar due to prestressing (15.5 kips), and Equation H1-1a in the 13th Edition of the AISC Steel Construction Manual (Equation 2 in this report), the percentage of the bar strength used was 60%.

Lifting configuration two used two straps to lift a deck panel, with one strap wrapped around all the bars in the bottom layer of a post-tensioning channel (see Figure 2.13). Bar 2B experienced the largest strain during this test, 231 MII. This strain is equivalent to a moment of 0.44 in.-kips (a stress of 6.7 ksi), and resulted in 60% of the bar strength being used when combined with the compressive force present due to prestressing.

The utilization of bars for the four lifting strap test ranged from 54% to 61%; utilization for the two lifting strap configuration ranged from 54% to 60%. These results show the strains in the bars essentially did not vary with the two strap configurations tested.

4.1.4 Leveling Test Summary

A deck panel was leveled in the laboratory to the slope required in the field bridge. Eight additional tests were conducted to determine the deck panel's response to various slopes, with strains experienced in the mild reinforcing bars recorded during the testing. A strain of -595 MII (a stress of 17.3 ksi) was experienced in Bar 2T, and was the largest strain in any bar during testing. Using a compressive force of 15.5 kips and the AISC interaction equation, Bar 2T used 70% of the available capacity.

4.1.5 Longitudinal Post-Tensioning Channel Concrete Placement Test Summary

A model of the post-tensioning channel was created to observe the flow of concrete through the channel in a laboratory setting. The model provided a worse-case scenario for flow, as the stirrups and mild reinforcement were at a lower height than would be encountered in the field due to panel leveling. Concrete was observed to flow around all of the steel in the channel and leave no void spaces.

4.1.6 Service Load Test Summary

Service load testing was conducted on an individual panel and on two connected panels. Loads on the individual panels ranged from 20 kips on cantilevered portions to 48 kips on the interior span. A 9 in. square footprint was used to apply the load. Load was applied at eight points on Panel 1 and 14 points on Panel 2 (see Figure 2.21). Application of load to eight of the same points on the two panels allowed for comparison of results. Deflections at the same locations for the same load points on the two panels were found to be within 0.005 in.

Concrete strains, steel strains, and deflection data were recorded during testing. Steel strains induced by the cantilevered portions of the deck panel bending over the support girders resulted in a maximum strain of 101 MII. Concrete strains were less than -253 MII. All deflections were within the AASHTO limits for the respective span lengths, with the maximum interior deflection equaling 0.067 in. The maximum cantilever deflection for a 16 kip load, a load equivalent to a HS 20-44 wheel load, was 0.146 in.

Load was applied at 19 different location in the connected panel service load tests; applied loads were limited to 20 kips on cantilevers and 40 kips on interior spans. Steel strains for the closure

pour hooked bars reached a maximum strain of 307 MII during service load testing, which is significantly less than the yield strain of 2069 MII for Grade 60 reinforcement. The maximum strain experienced in a mild reinforcing bar was a tensile strain of 278 MII. Concrete strains did not approach ACI limits for the maximum useable compressive strain of -3000 MII, having a maximum value of -286 MII. As one would expect, deck panel deflections decreased after casting the closure pour. Changes in deflection decreased 0.025 in. for a 40 kip load at B11 after the closure pour was cast.

4.1.7 Ultimate Strength Test Summary.

Four ultimate strength tests were conducted on the deck panels. An individual panel was tested to flexural failure, and three tests were conducted on two connected deck panels. The single panel failed in flexure at a load of 153 kips, or a moment equal to 368 ft-kips for pinned supports and 184 ft-kips for fixed supports. These values bracket the theoretical strength of 263 ft-kips, indicating that the laboratory support girders provided a fixity between pinned and fully fixed.

The second ultimate strength test was an attempt to fail the closure pour connecting the panels; however, the deck panel next to the closure pour failed in punching shear instead. A 9 in. square footprint was used in this test, and failure occurred at an applied shear force of 146 kips. The theoretical punching shear capacity for a 9 in. square footprint is 135 kips, which was 8% less than the applied shear.

A tandem wheel footprint was used for the second ultimate strength test conducted on the connected panels. This footprint resulted in a combinations punching shear and flexure failure at a load of 157 kips. For this load, the applied shear was 150 kips and the moment was 298 ft-kips. The theoretical punching shear was 188 kips, and the theoretical flexure strength was 263 ft-kips. Reasons for the discrepancies in the loading are: the restraining beams used to resist the uplift forces caused by loading provided fixity to the system and decreased the applied moment; punching shear capacity was reduced because flexure cracks in the deck panel reduced the depth of concrete available to resist shear stresses.

For the final ultimate strength test, the connected panels were tested to flexure failure. A beam was used to apply a 196 kip load to the panel as a line load. The applied moment of 372 ft-kips exceeded the theoretical flexural strength of 263 ft-kips by 41%; however the restraining beams used to resist the uplift force provided some fixity to the system, reducing the applied moment to a value less than that given.

4.2 Conclusions

4.2.1 Concrete Strength Testing Conclusions

The following conclusions can be drawn from the concrete strength tests:

- The average compressive strength of the concrete cores was 7,600 psi.

- The average strength exceeded the specified strength of 5,000 psi by 27%

4.2.2 Stresses in Mild Reinforcing Due to Prestressing

The following can be concluded about the stresses in the mild reinforcing due to prestressing:

- Stresses in five of the six instrumented bars were less than the theoretical stress minus prestress losses (20.7 ksi).
- Top bars had an average stress of 14.2 ksi.
- Bottom bars had an average stress of 17.9 ksi.

4.2.3 Lifting Panel Strain Conclusions

The following conclusions can be drawn from the crane lifting tests conducted on the deck panels:

- The maximum strain measured when lifting a deck panel with four lifting straps was 251 MII (a stress of 7.3 ksi).
- The utilization of the reinforcing bar capacity due to combined bending and axial stresses when lifted with four straps ranged from 54% to 61%.
- The maximum strain measured when lifting a deck panel with two lifting straps was 231 MII (a stress of 6.7 ksi).
- The utilization of the reinforcing bar capacity due to combined bending and axial stresses when lifted with two straps ranged from 54% to 60%.
- Because bar utilization ranged from 54% to 61% for four strap lifting and 54% to 60% for two strap lifting, the strap configuration used did not have a significant effect on the reinforcing bars.
- Bars were less than 100% utilized for both lifting configurations, showing both are acceptable for use.

4.2.4 Leveling Test Conclusions

The following conclusions can be drawn from the leveling tests conducted on the deck panels:

- The maximum strain measured during the leveling tests was -595 MII (a stress of 17.3 ksi).
- The utilization of the reinforcing bar due to combined bending and axial stresses ranged from 60% to 76% of the capacity.
- Mild reinforcing bars did not exceed the available strength during any of the leveling tests.

4.2.5 Longitudinal Post-Tensioning Channel Concrete Placement Test Conclusions

The following can be concluded from the longitudinal post-tensioning channel concrete placement test results:

- Concrete was observed flowing below the leveling device.
- Concrete was observed flowing between the post-tensioning strands.
- No void spaces were observed in the channel during the tests.

4.2.6 Service Load Test Conclusions

The following conclusions can be drawn from the service load test results:

- Strains induced in the reinforcing bars during tests without the closure pour cast were less than yielding, with 101 MII (a stress of 2.9 ksi) the maximum strain experienced.
- Deflections of the deck panel between the supports reached 0.067 in. prior to casting the closure pour, which was within the AASHTO limit of 0.125 in.
- Strains in the concrete before casting the closure pour reached -253 MII, which is less than the value of -3000 MII recommended by ACI as the maximum useable compressive strain.
- The deflection of the cantilever portion of the deck panel reached 0.146 in. for a 16 kip load prior to casting the closure pour, which is within AASHTO limits.
- Reinforcing steel experienced 278 MII of strain (a stress of 8.1 ksi) in tests after the closure pour was cast.
- Strains in the hooked bars in the closure pour reached 307 MII (a stress of 8.9 ksi), which is less than the yielding strain of 2069 MII.
- The maximum strain measured in the concrete after the closure pour was cast was -286 MII, which is less than the -3000 MII recommended by ACI as the maximum usable compressive strain.
- The maximum deflection of a portion of the deck panels spanning between two support beams after the closure pour was cast was 0.051 in., which was within the AASHTO limit of 0.125 in.
- Deflections of the deck panel spanning between support beams decreased by 18% after the closure pour was cast.
- Cantilever deflections decreased 49% or more after the closure pour was cast.

4.2.7 Ultimate Strength Test Conclusions

The following conclusions can be made from the ultimate strength test results:

- The support beams provided a fixity between pinned and fully fixed. A single panel failed under an applied moment of 368 ft-kips if the supports are pinned or 184 ft-kips if the supports are fixed. The theoretical moment capacity was 263 ft-kips.

- The experimental punching shear capacity of the deck panels for a 9 in. square footprint was 146 kips, which was 8% greater than the theoretical strength of 135 kips.
- A deck panel failed under combined flexure and punching shear for a load applied by a tandem wheel footprint. The applied moment at failure was 298 ft-kips, 13% greater than the theoretical flexural capacity of 263 ft-kips. The shear force at failure was 150 kips, 80% of the theoretical punching shear of 188 kips.
- The moment applied to the two deck panel system was 372 ft-kips, exceeding the theoretical capacity of 263 ft-kips by 41%. The difference in values was due to the fixity provided by the support beams.
- Deck panel failures occurred at loads much greater than those the panels would be exposed to in the actual field bridge.

4.3 Recommendations

The following actions are recommended based on the laboratory testing of the deck panels:

- The mild reinforcement and prestressing force should be evaluated to produce a more efficient deck panel section.
- Additional testing should be conducted if panel lifting configurations other than those tested are to be used.
- Testing should be conducted to determine the strength benefit of having adjacent panels in the longitudinal direction.
- Strains should be measured during panel leveling and subsequent placement of concrete in the longitudinal channels to determine if concrete placement has an effect on the strains in the bars (i.e. if strains are permanent or temporary).

REFERENCES

AASHTO. 2002. *Standard Specifications for Highway Bridges.* Washington, DC: American Association of State Highway and Transportation Officials.

American Concrete Institute. 2005. *ACI 318-05 Building Code Requirements for Structural Concrete*. American Concrete Institute.

American Institute of Steel Construction. 2005. *Steel Construction Manual*. Thirteenth Edition. American Institute of Steel Construction Inc.

Badie, Sameh S., Mantu C. Baishya, Maher K. Tadros. 1998. *NUDECK-An Efficient and Economical Precast Prestressed Bridge Deck System.* PCI Journal, Vol. 43, No. 5: 56-71.

Badie, Sameh S., Mounir R. Kamel, and Maher K. Tadros. 1999. *Precast Pretensioned Trapezoidal Box Beam for Short Span Bridges*. PCI Journal, Vol. 44, No. 1: 48-59.

Bell III, Charles, Carol K. Shield, and Catherine French. 2006. *Application of Precast Decks and Other Elements to Bridge Structures*. Report No. 2006-37. Minnesota Department of Transportation.

Ehmke, Forrest Gregory. 2006. Analysis of a Bridge Deck Built on Interstate Highway 39/90 with Full-Depth, Precast, Prestressed Concrete Deck Panels. Master's thesis, University of Wisconsin-Madison.

Fallaha, Sam, Chuanbing Sun, Mark D. Lafferty, and Maher K. Tadros. 2004. *High Performance Precast Concrete NUDECK Panel System for Nebraska's Skyline Bridge*. PCI Journal, Vol. 49, No. 5: 40-50.

Hawkins, N. M., and J. B. Fuentes. 2002. *Test to Failure of a 54 ft. Deteriorated Pretensioned Precast Concrete Deck Beam.* Illinois Cooperative Highway and Transportation Series No. 281. University of Illinois: Urbana-Champaign.

Hawkins, N. M., and J. B. Fuentes. 2003. *Structural Condition Assessment and Service Load Performance of Deteriorated Pretensioned Deck Beam Bridges.* Illinois Cooperative Highway and Transportation Series No. 285. University of Illinois: Urbana-Champaign.

Hieber, D.G., J.M. Wacker, M.O. Eberhard, and J.F. Stanton. 2005. *State-of-the-Art Report on Precast Concrete Systems for Rapid Construction of Bridges*. Final Technical Report, Contract T2695, Task 53. Washington State Department of Transportation and Federal Highway Administration.

Huckelbridge Jr., Arthur A., Hassan El-Esnawi, and Fred Moses. 1995. *Shear Key Performance*

in Multibeam Box Girder Bridges. Journal of Performance of Constructed Facilities, Vol. 9, No. 4: 271-285.

Issa, Mohsen A., Ahmad-Talal Idriss, Iraj I. Kaspar, and Salah Y. Khayyat. 1995. *Full Depth Precast and Precast, Prestressed Concrete Bridge Deck Panels*. PCI Journal, Vol. 40, No. 1: 59-69.

Issa, Mohsen A., Alfred A. Yousif, Mahmoud A. Issa, Iraj I. Kaspar, and Salah Y. Khayyat. 1998. *Analysis of Full Depth Precast Concrete Bridge Deck Panels*. PCI Journal, Vol. 43, No. 1: 74-85.

Issa, Mohsen A., Cyro L. Ribeiro do Valle, Hiba A. Abdalla, Shahid Islam, Mahmoud A. Issa. 2003. *Performance of Transverse Joint Grout Materials in Full-Depth Precast Concrete Bridge Deck Systems*. PCI Journal Vol. 48, No. 4: 92-103.

Menkulasi, Fatmir, and Carin L. Roberts-Wollman. 2005. *Behavior of Horizontal Shear Connections for Full-Depth Precast Concrete Bridge Decks on Prestressed I-Girders*. PCI Journal, Vol. 50, No. 3: 60-73.

Naaman, Antoine E. 2004. *Prestressed Concrete Analysis and Design: Fundamentals*. Second Edition. Techno Press.

Poston, Randall W., Karl H. Frank, and Jeffery S. West. 2003. *Enduring Strength*. Civil Engineering, Vol. 73, No. 9: 58-63.

Russell, Henry G., Mary Lou Ralls, and Benjamin M. Tang. 2005. *Prefabricated Bridge Elements and Systems in Japan and Europe*. Transportation Research Record: Journal of the Transportation Research Board, No. 1928: 103-109.

Slavis, C. 1982. *Precast Concrete Deck Modules for Bridge Deck Reconstruction*. Transportation
Research Record 871, Transportation Research Board: 30-33.

Tokerud, Roy. 1979. *Precast Prestressed Concrete Bridges for Low-Volume Roads*. PCI Journal, Vol. 24, No. 4: 42-55.

VanGeem, Martha. 2006. *Achieving Sustainability with Precast Concrete*. PCI Journal, Vol. 51, No. 1: 42-55.

Volume 1-3. Field Testing of a Precast Concrete Bridge: Boone County Bridge

Technical Report Documentation Page

1. Report No. IHRB Project TR-561	2. Government Accession No.	3. Recipient's Catalog No.	
4. Title and Subtitle Precast Concrete Elements for Accelerated Bridge Construction: Field Testing of a Precast Concrete Bridge, Boone County Bridge		5. Report Date January 2009 6. Performing Organization Code	
7. Author(s) Terry J. Wipf, F. Wayne Klaiber, Brent Phares, and Matthew Becker		8. Performing Organization Report No. CTRE Project 06-262	
9. Performing Organization Name and Address Bridge Engineering Center Iowa State University 2711 South Loop Drive, Suite 4700 Ames, IA 50010-8664		10. Work Unit No. (TRAIS) 11. Contract or Grant No.	
12. Sponsoring Organization Name and Address Iowa Highway Research Board Iowa Department of Transportation 800 Lincoln Way Ames, IA 50010		13. Type of Report and Period Covered Final Report 14. Sponsoring Agency Code	
15. Supplementary Notes Visit www.ctre.iastate.edu for color PDF files of this and other research reports.			

16. Abstract

A full-depth precast deck bridge was built in Boone County in 2006 as a replacement for an existing bridge. The bridge was constructed in an accelerated manner using precast concrete components. A series of laboratory tests were completed by Iowa State University on individual segments of the bridge. Detailed description and analysis of these tests can be found in sections 1 and 2 of Volume 1.

This third and final section of Volume 1 documents the field testing portion of this project. Two field tests were carried out on the Boone County bridge. The first took place the summer following construction and the second took place one year later. A summary of the testing process, instrumentation plan, and analysis of data are located in this report.

17. Key Words accelerated bridge construction—Boone County, Iowa—field testing—laboratory strength testing—precast concrete abutments, pier caps, deck panels—prestressed concrete girders		18. Distribution Statement No restrictions.	
19. Security Classification (of this report) Unclassified.	20. Security Classification (of this page) Unclassified.	21. No. of Pages 41	22. Price NA

Form DOT F 1700.7 (8-72) **Reproduction of completed page authorized**

PRECAST CONCRETE ELEMENTS FOR ACCELERATED BRIDGE CONSTRUCTION:
FIELD TESTING OF A PRECAST CONCRETE BRIDGE, BOONE COUNTY BRIDGE

Final Report
January 2009

Principal Investigator
Terry J. Wipf, Director, Bridge Engineering Center
Center for Transportation Research and Education, Iowa State University

Co-Principal Investigators
F. Wayne Klaiber, Professor, Department of Civil, Construction, and Environmental Engineering
Iowa State University

Brent M. Phares, Associate Director, Bridge Engineering Center
Center for Transportation Research and Education, Iowa State University

Mike D. LaViolette, Former Bridge Engineer
Iowa State University

Research Assistant
Matthew Becker

Authors
Terry J. Wipf, F. Wayne Klaiber, Brent Phares, and Matthew Becker

Sponsored by
the Iowa Highway Research Board (IHRB Project TR-561)
and Boone County, Iowa, through the Federal Highway Administration's
Innovative Bridge Research and Construction Program

Preparation of this report was financed in part through funds provided by
the Iowa Department of Transportation through its research management agreement with
the Center for Transportation Research and Education (CTRE Project 06-262).

A report from
Center for Transportation Research and Education
Iowa State University
2711 South Loop Drive, Suite 4700
Ames, IA 50010-8664
Phone: 515-294-8103
Fax: 515-294-0467
www.ctre.iastate.edu

TABLE OF CONTENTS

LIST OF FIGURES

LIST OF TABLES

ACKNOWLEDGMENTS

The authors would like to thank the Iowa Highway Research Board, the Iowa Department of Transportation, Boone County and the Federal Highway Administration for providing funding, design expertise, and research collaboration for this project. Special recognition is give to the following individuals for their significant contributions to the research: Ahmad Abu-Hawash, Jim Nelson, Stuart Nielsen, and many other staff from the Office of Bridges and Structures at the Iowa Department of Transportation; Curtis Monk, Iowa Division, Federal Highway Administration; Dave Anthoney (recently retired), Bob Kieffer and Scott Kruse, Boone County; and Doug Wood, Iowa State University along with numerous graduate and undergraduate students, including Ryan Bowers, Matt Goliber, Dustin Gardner and Nathan Hardisty.

EXECUTIVE SUMMARY

A full-depth precast deck bridge was built in Boone County in 2006 as a replacement for an existing bridge. The bridge was constructed in an accelerated manner using precast concrete components. A series of laboratory tests were completed by Iowa State University on individual segments of the bridge. Detailed description and analysis of these tests can be found in sections 1 and 2 of Volume 1.

This third and final section of Volume 1 documents the field testing portion of this project. Two field tests were carried out on the Boone County Bridge. The first took place the summer following construction and the second took place one year later. A summary of the testing process, instrumentation plan, and analysis of data are located in this report.

1. BACKGROUND

The world moves at a constantly increasing pace. Traffic volumes rise along with the number of bridge construction projects. In this fast-paced world, it can be difficult for construction crews to keep up. It also is critical to keep impact on transportation at a minimum. This means getting construction crews in and out of a job as quickly as possible. Much work has been done to find a way to speed up the construction process of bridges in Iowa. A variety of rapid construction techniques can be used to accelerate the construction of bridges and minimize disruption to traffic.

The importance of rapid construction technologies has been recognized by the Federal Highway Administration (FHWA) and the Iowa Department of Transportation (DOT). It was decided that a bridge would be built in Boone County, Iowa to test accelerated bridge construction techniques. Construction began on July 17, 2006 and concluded December 28, 2006. This bridge underwent extensive tests during construction, in the laboratory, and in the field. Funding for the design, construction, and evaluation of this project was provided by the FHWA-sponsored Innovative Bridge Research and Construction (IBRC) Program. Funding for the laboratory testing was provided by the Iowa DOT and the Iowa Highway Research Board; funding for the documentation and the post-tensioning monitoring and verification was provided by the FHWA and Boone County.

In the Boone County Bridge project, construction was accelerated using precast bridge elements. Precast bridge components are cast off-site, allowed to cure, and transported to the site. Once at the scene of construction, individual pieces of the bridge can be put together in a quick and efficient manner. This process has advantages for the public, the owner, and the environment.

The most obvious advantage of rapid construction is time saved. Highways have higher daily traffic volumes than ever before. It is important to shorten the length of construction in order to reduce the impact on traffic flow. Traditional bridge construction processes require time to set up forms, pour concrete, and allow concrete to cure. By using precast bridge elements, time on the site is greatly reduced. Rapid construction is also less harmful to the environment than traditional methods. This is especially apparent on bridges that cross bodies of water. Less time on the site means fewer occurrences of pollution.

One disadvantage of rapid construction is that the initial cost of precast elements is more costly than traditional construction methods. This extra cost can be offset by a reduction in labor costs. Less time on the job site corresponds with a lower cost for labor.

The location selected for this bridge is in the northern part of Boone County. The bridge crosses Squaw Creek on 120th Street. The original bridge on this site was called the Marsh Arch Bridge. The Marsh Arch Bridge is shown in Figure 1.1. The new bridge is a continuous, four-girder, three-span bridge with a full-depth, precast deck and can be seen in Figure 1.2. The bridge is 151 ft - 4 in long with a width of 33 ft - 2 in. Deck panels are 8-inches thick, half the width of the bridge, and pre-stressed in the transverse direction. Each panel had two full-depth channels, located over the pre-stressed girders, for post-tensioning. Once the panels were erected, the

entire bridge deck was post-tensioned in the longitudinal direction, after which the post-tensioning channels were grouted. Precast pier caps and precast abutments were also used in the bridge substructure.

Figure 1.1 Marsh Arch Bridge originally on 120th St

Figure 1.2 Completed replacement bridge on 120th St

Extensive testing was performed on this bridge. Three stages of testing took place: construction, laboratory, and field testing. During construction, strain gages were attached to the post-tensioning bars in the bridge deck panels. These gages were monitored during the post-tensioning process. The gages remain in the bridge deck and can be monitored at any time. The laboratory portion of testing took place at the Iowa State University Structures lab. The individual bridge elements that were tested in the lab were the precast abutments, pier caps, and bridge deck panels. Finally, two field tests were performed using strain and deflection gages. The tests were conducted in the summers of 2007 and 2008. The field tests consisted of static and rolling cases using standard tandem-axle gravel trucks. These trucks were provided by Boone County.

2. FIELD TEST

2.1 Introduction

The initial field test was performed on June 28, 2007. A combination of static and rolling loads were used to create critical load cases on the bridge. These loads were simulated by typical tandem-axle gravel trucks. During the test, strains and deflections were measured by transducers located at critical sections of the bridge. Installation of the instrumentation and all runs of the test vehicles were completed in one day. For descriptive purposes, the three spans are numbered 1 through 3 from east to west. This makes Span 1 the first span crossed by the truck and Span 3 the last span crossed by the truck. The four girders are numbered 1 through 4 from south to north and the two piers are described as east and west piers.

In addition to the strain and displacement transducers, vibrating wire gages were also monitored. These vibrating wire gages were originally installed during construction to measure strains during the post-tensioning process. The gages remain in the bridge and can be used to monitor strains in bridge during field tests. The gages were monitored during the static test by a switch-and-balance system.

2.2 Strain and Displacement Instrumentation Description

Instrumentation was installed on the bridge in order to determine maximum loading stresses and deflections on the bridge. Flexural strains in the concrete girders and guardrail were measured by strain transducers while string potentiometers measured deflections along the mid-span of the central span. A total of 36 strain transducers and 9 deflection transducers were used during the test. The instrumentation layout of these gages can be seen in Figure 2.1.

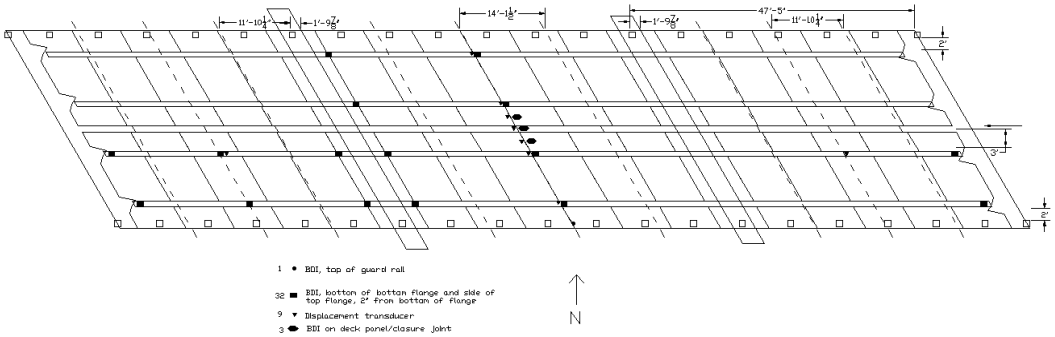

Figure 2.1 Final instrumentation layout used for first field test

Gage installation was completed on the morning of the test. Strain transducers were applied to top and bottom flanges of specific girders or on the bottom of the bridge deck. The locations of the strain gages on top and bottom flanges are shown in Figure 2.2. Deflection transducers were secured to a level platform near ground level and connected to the bridge superstructure with

piano wire. A tripod system was set up below the bridge to provide a level surface for the string potentiometers. This tripod system can be seen in Figure 2.3.

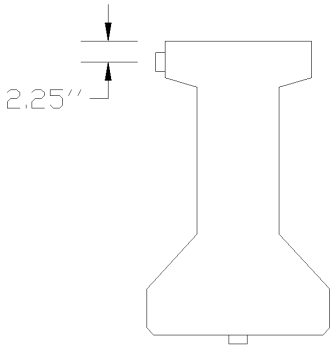

Figure 2.2 Typical strain gage locations on concrete girders

Figure 2.3 Tripod system used to support displacement transducers

The mid-span of Span 2 was a heavily instrumented area due to the potential for maximum deflections and strains. At this location, each girder was instrumented with a deflection gage and a top and bottom flange strain gage. In addition to the girders, the closure joint at mid-span was instrumented to check for significant deflection and strain differential between the sides of the joint. The gage configuration at the closure joint is shown in Figure 2.4. Along with the mid-span, the east side of the west pier had strain gages at all four girders. These strain gages were used to analyze negative moment conditions at this pier.

Figure 2.4 Instrumentation layout at closure joint

Span 3 also contained a significant amount of instrumentation. At this span, Girders 1 and 2 had strain gages at the west abutment, mid-span and west side of the west pier. All strain gages located at abutments and piers are installed a distance of 32" (girder depth) from the abutment or pier. In addition to the strain gages, one deflection transducer was installed on Girder 2 at mid-span. A tripod system was not needed for the transducer at this location. Instead, the string potentiometer was fixed to a board and secured to the rip-rap below on the ground.

Instrumentation was less concentrated at Span 1. At this location, strain gages were installed on Girders 1 and 2 at the east abutment. These strain gages were used to compare behavior of east and west abutments. In addition to the strain gages, a deflection transducer was installed on Girder 2 at mid-span. The location and set up of this gage is identical to the deflection gage at Span 3.

The final element monitored during the test was the guardrail. A single strain transducer was applied directly to the top of the south guardrail at the mid-span of Span 2. This gage was used to determine behavior of the guardrail during rolling tests.

2.3 Vibrating Wire Instrumentation Description

Vibrating wire gages were installed within the deck panels prior to concrete placement in order to monitor strains during the post-tensioning process and additional field tests. Twelve vibrating wire gages were installed in four of the deck panels. The deck panels were labeled A, B, C and D and can be seen highlighted in Figure 2.5. These gages were concentrated near the southern-most post-tensioning channel. A different number of gages were located at each panel. Each deck panel consisted of four gage locations as shown in Figure 2.6. A gage located at deck panel C and location 2 is therefore designated as Gage C2. Each panel contained gages at different locations. The gage locations at each panel can be seen in Table 2.1.

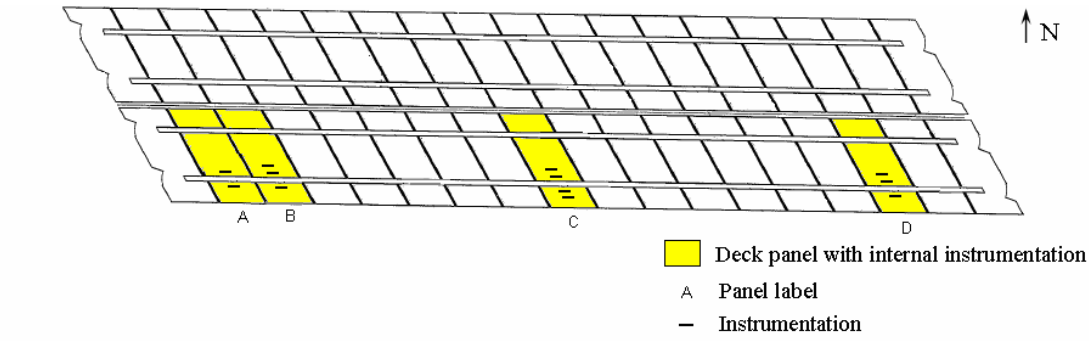

Figure 2.5 Deck panels instrumented with vibrating wire gages

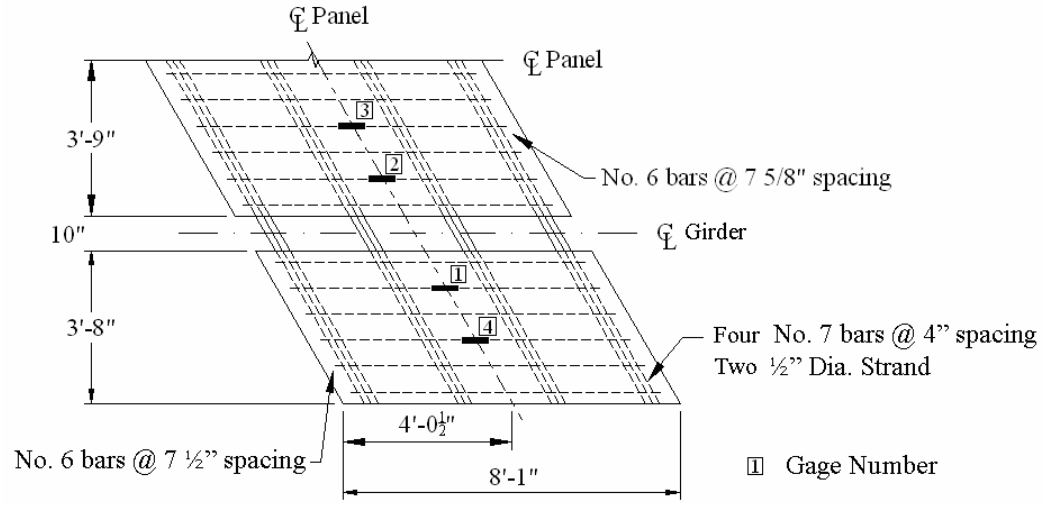

Figure 2.6 Typical VWG locations in deck panels

Table 2.1 Gage numbers and locations in each deck panel

Deck Panel	No. of Gages	Gage Location
A	2	A1, A2
B	3	B1, B2, B3
C	4	C1, C2, C3, C4
D	3	D1, D2, D3

An additional seven vibrating wire gages were installed on post-tensioning strands throughout the bridge. These gages were labeled 1 through 7 and their locations can be seen in Figure 2.7. All seven gages were monitored during the post-tensioning process. At the conclusion of this procedure, gages 1, 2 and 4 were removed. The remaining four gages were left in place for use during field tests. As a result, strains in each of the four longitudinal joints can therefore be monitored at the middle of the bridge.

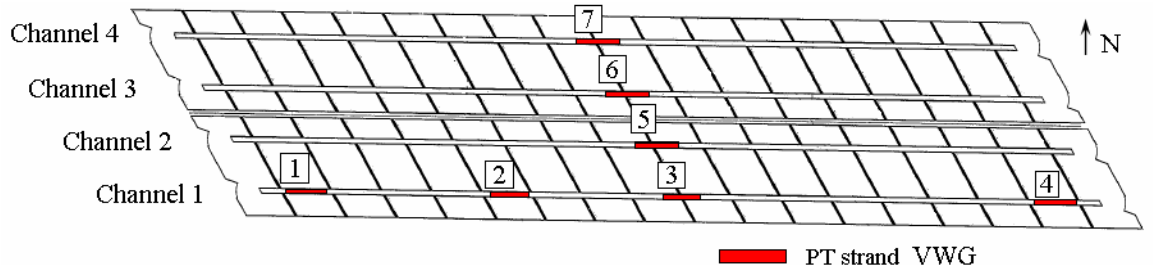

Figure 2.7 Post-tensioning vibrating wire gage locations

Some issues with the vibrating wire gages prevented the monitoring of a few of the gages during the field test. Gages B1 and B2 were not recorded because they did not read on the switch-and-balance system. Also, gages in Deck Panel C were not recorded because their wires were too short to reach the switch-and-balance machine.

2.4 Load Vehicles

The two test vehicles used to simulate traffic loads were standard tandem-axle gravel trucks, which were provided by Boone County. The trucks were loaded and axle weights and gross weights were recorded as shown in Table 2.2. An assumption has been made that the rear axle load is split evenly between the two axles. The critical lengths of each vehicle were recorded prior to the test. The two trucks had identical dimensions which are shown in Figure 2.8.

Table 2.2 Test vehicle loads

Truck #	Front Axle (kips)	Rear Axle (kips)	Gross Weight
29	17.46	18.16	53.76
31	17.22	18..16	53.52

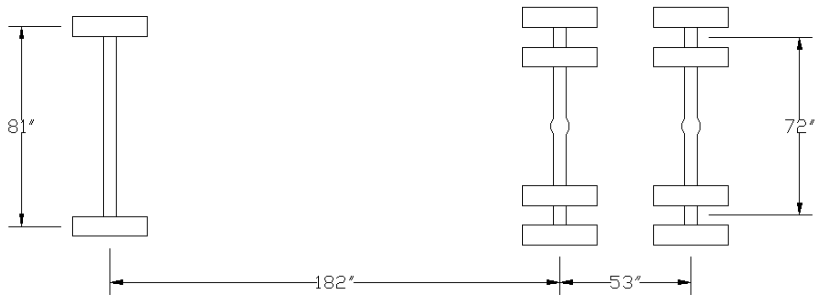

Figure 2.8 Test vehicle dimensions

2.5 Test Lanes

The field test was run on five different traffic lanes as shown in Figure 2.9. These lanes were chosen to produce maximum effects on the bridge. The trucks followed the lane line with the left tire for Lane 1 and the right tire for Lanes 2 through 5. Lane 1 is located 2 feet north of the south guardrail. Lane 2 is positioned 3 feet south of the centerline. Lane 3 is directly on the centerline. Lane 4 is 3 feet north of the centerline and Lane 5 is two feet south of the north guardrail. Lanes 1 and 5 are used to evaluate exterior loads and can be used in comparison of symmetry. Lane 4 is use to place the truck over the center of the bridge. Lanes 2 and 3 are used to evaluate load transfer as the truck is shifted across the bridge width. The test vehicle can be seen driving on Lane 3 in Figure 2.10.

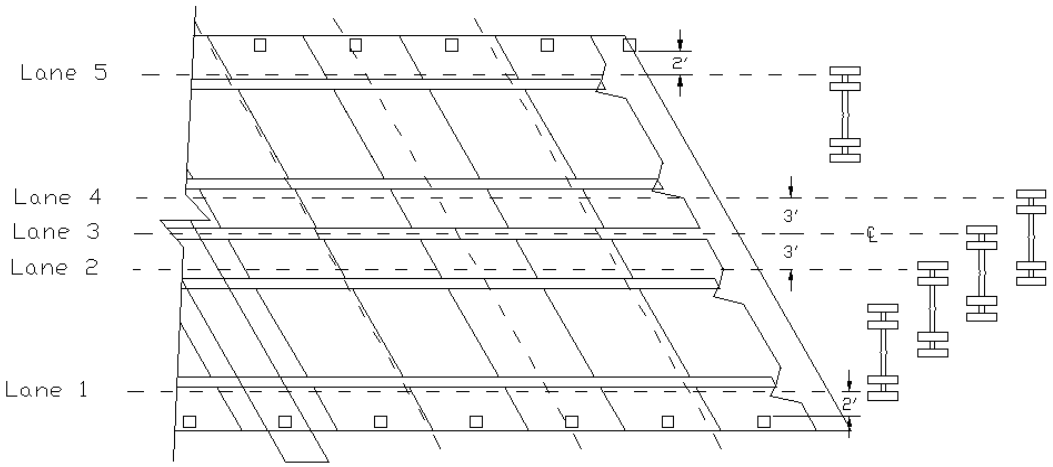

Figure 2.9 Lane configurations for static and rolling tests

Figure 2.10 Test vehicle in Lane 3 position

2.6 Static Tests

Static load tests were conducted on the bridge to evaluate maximum load cases on the bridge. Three different load cases were devised to produce maximum effects at a certain point of interest. Each of these three load cases was performed on Lanes 1, 2 and 4. Load Case 1 was made up of Truck 31 at the mid-span of Span 2 and Truck 29 at the mid-span of Span 1 as shown in Figure 2.11. This load case produced a maximum negative moment at the east pier. Load Case 2 was made up of Truck 31 at the mid-span of Span 3 and Truck 29 at the mid-span of Span 1 as shown in Figure 2.12. This produced the greatest maximum moment in Span 2. Load Case 3 was made up of Truck 29 at the mid-span of Span 2 as shown in Figure 2.13. This produced a maximum moment at Span 2. The center of the rear tandem axles was used as the position point on the truck. The truck layout for each load case can be seen in Figure 2.14. The traffic lanes used in these tests are shown in Figure 2.9.

Figure 2.11 Static test (Load Case 1)

Figure 2.12 Static test (Load Case 2)

Figure 2.13 Static test (Load Case 3)

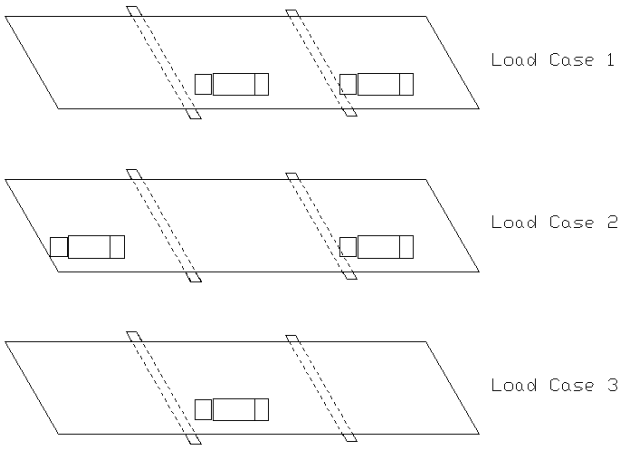

Figure 2.14 Load cases for static tests

The static test procedure was as follows. The data acquisition system was activated and Truck 31 was led to the mid-span of Span 2. As soon as Truck 31 was set, Truck 29 was placed at the mid-span of Span 1 to make Load Case 1. After a significant amount of data was taken, Truck 29 was brought to the mid-span of Span 3. Truck 31 remained in its position at the mid-span of Span 1 to make Load Case 2 complete. For Load Case 3, Truck 31 continued off of the bridge and Truck 29 moved to the mid-span of Span 2. The static tests for Lanes 2 and 4 were a repetition of this procedure.

2.7 Rolling Tests

Rolling tests were conducted after the static tests. A rolling test consists of one single truck slowly moving across the bridge along a single lane. The truck speed in maintained at approximately 5 mph. A rolling test was performed twice on each of the five traffic lanes. Three

trials were done on Lane 1 because of a communication error on test 1.1. Duplicate tests were performed in order to compare tests and account for any irregularities. A drawing of the five driving lanes used for the rolling tests can be reviewed in Figure 2.10.

A total of fifteen marks were drawn across the bridge at certain positions. These marks are used to allow the position of the truck to be found in relation to the data. A mark was made at all abutments, quarter spans, mid spans, third-quarter spans, and piers. In addition to these bridge marks, a beginning mark was made 10 feet before the east abutment and an ending mark was made 20 feet beyond the west abutment. The positions of the first and last mark ensure that data is taken before the truck on the bridge until it is completely off. During the test, the operator of the data acquisition system made a note each time the rear axle of the testing vehicle crossed a mark. This allows the researcher to approximate where the truck was at any specific moment during the test.

The rolling test data was acquired using the same equipment as in the static tests. The truck was lined up with the appropriate lane and brought to a halt at about 20 feet before the east abutment. The data acquisition system was then switched on and the truck began across the bridge at a constant crawling speed. Marks were taken as the rear axle of the testing vehicle passed each mark on the bridge. When the truck passed the last mark, the data acquisition system was turned off.

3. DATA ANALYSIS

Strain and displacement data were analyzed bridge performance. Several graphs from the field test data are presented. These graphs were chosen because they best describe the behavior of the bridge. The bridge experienced very little displacement or strain during the test. Upon examination of the data, it was determined that two of the displacement gages were not operational. Later in the report, these two gages are pointed out and values are assumed for these locations. Errors in the test can be attributed to the small values, gage malfunctions, and gage vibrations. Marks were taken each time the right rear axle reached a quarter-span line.

3.1 MS 2 Analysis

Strains and displacements at MS 2 were recorded as the truck moved across the bridge. This process was replicated for all five lanes. Figure 3.1a and Figure 3.1b show the displacement and strain profiles, respectively, at MS 2 when the right rear axle of the truck was located at MS 2.

MS 2 Deflection Profiles

The deflection profiles shown in Figure 3.1a portray the movements of the girders due to the weight of the truck. It is important to note that the displacement gage located on Girder 3 was not operating during the test. Values have been assumed to complete the profiles on the graph. Trend lines to and from this point have been dashed to indicate this assumption. Lanes 1 and 5 illustrate the activity at the midspan when the truck is at each guardrail. Both profiles are most displaced at the nearest girder and go to zero at the far girder in a fairly straight line. As expected, the profiles created by Lanes 1 and 5 are nearly symmetric. Lane 4 gives the deflection profiles with the truck is on the bridge centerline. The displacement profile in this traffic lane is symmetric about the centerline as anticipated. The profiles of Lanes 2 and 3 are almost identical. The greatest deflection occurred on Girder 2 when the truck was in Lane 3.

MS 2 Strain Profiles

The strain profiles shown in Figure 3.1b reveal forces in the girders at MS 2 when the rear axle was located at MS 2. Lane 1 shows the high tension forces in the girder nearest the truck with a straight line trend to zero at the other side. Lane 5 is symmetric to Lane 1 except for the gage at Girder 4. It is possible that this gage also was not working at the time. Lane 4 depicts the strain profile when the truck is on the bridge centerline. The profile is symmetric about the centerline. Lanes 2 and 3, as with the deflection profiles, are quite similar. Lane 3 once again has the higher value of strain.

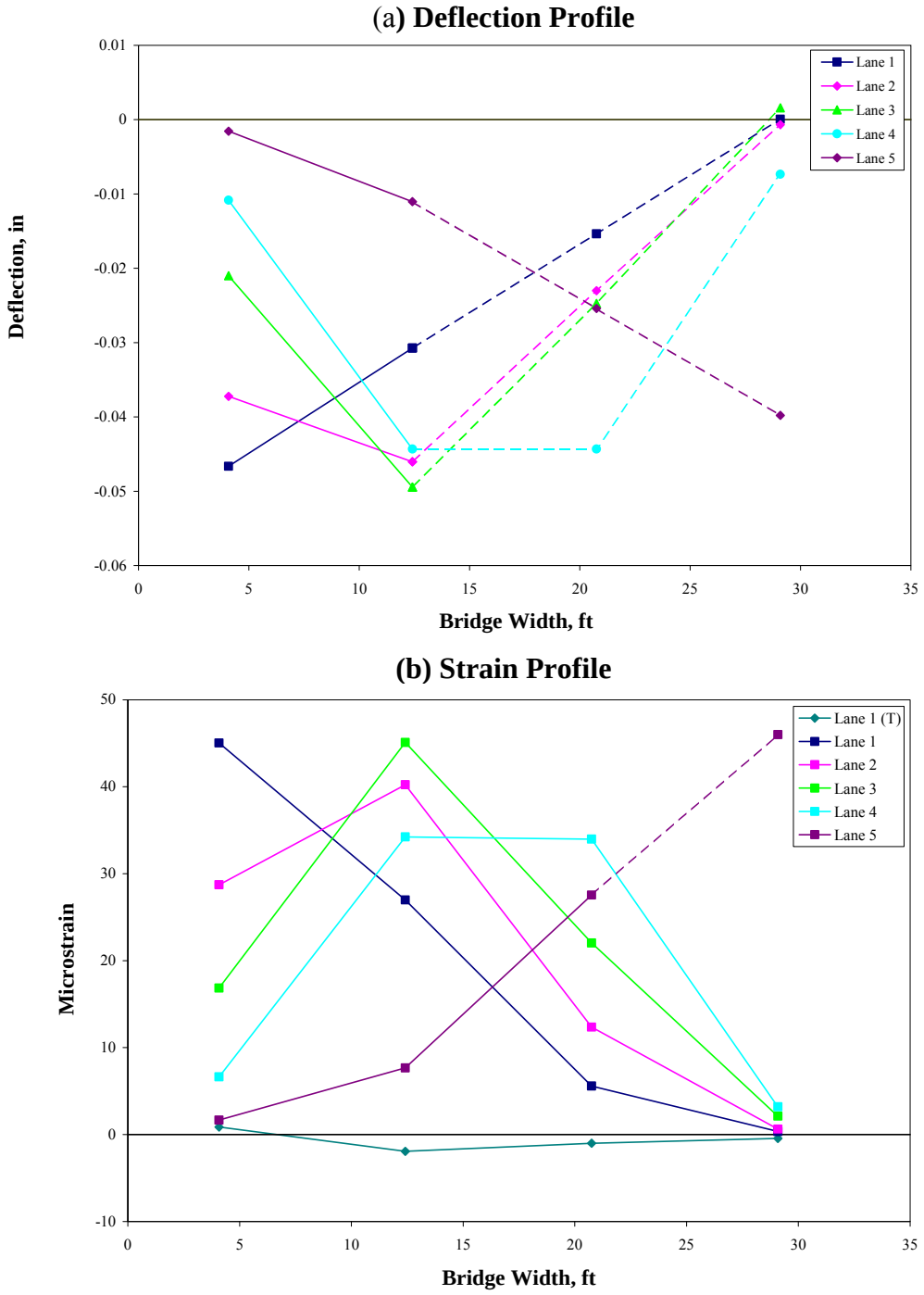

Figure 3.1 MS 2 Deflection and Strain (Lanes 1-5)

MS 2 Profiles from Static Loading

Midspan 2 Profiles were analyzed for both strain and deflection when the trucks were in Load Cases 1 through 3. The deflection profiles are in Figures 3.2a, 3.3a, and 3.4a. The strain profiles are in Figures 3.2b, 3.3b, and 3.4b. The truck loading case is shown above each set of Figures.

MS 2 Deflection Profiles

Load Case 1 and 3 created almost identical deflection profiles at the midspan of Span 2. The load pattern in Lane 1 created a straight-line deflection profile from Girder 1 to Girder 4 with Girder 1 having a maximum deflection of -.05 inches. Lanes 2 and 4 generated the greatest deflection at Girder 2. Loading in Lane 4 did not produce a symmetric profile about the centerline as expected. This unanticipated behavior can be attributed to the problem with the gage on Girder 3. Load Case 2 produced a very small amount of deflection with a maximum deflection of .008 inches. The bridge deflected slightly upward as would be expected.

MS 2 Strain Profiles

Load Cases 1 and 3 produce very similar strain profiles. Lane 1 loading creates a straight-line strain profile from Girder 1 to Girder 4 with Girder one having a maximum strain of approximately 45 microstrains. Lanes 2 and 4 produce very similar strain profiles. Maximum strain occurs in Girder 2 in these cases. Load Case 3 creates very little strain in the Midspan 2 profile. Maximum strain in this case is approximately -8 microstrains.

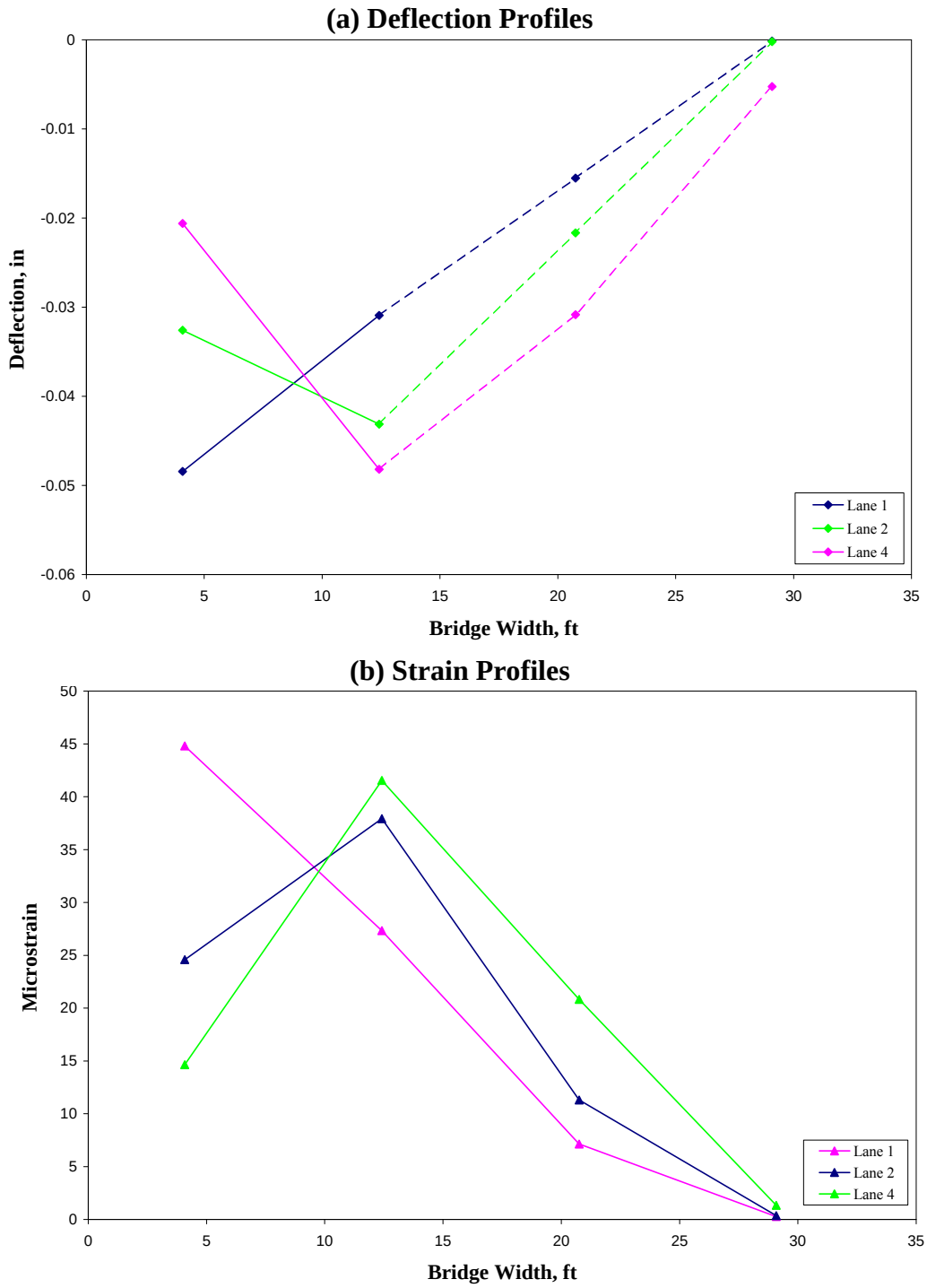

Figure 3.2 MS 2 Strain and Deflection Profiles (Load Case 1)

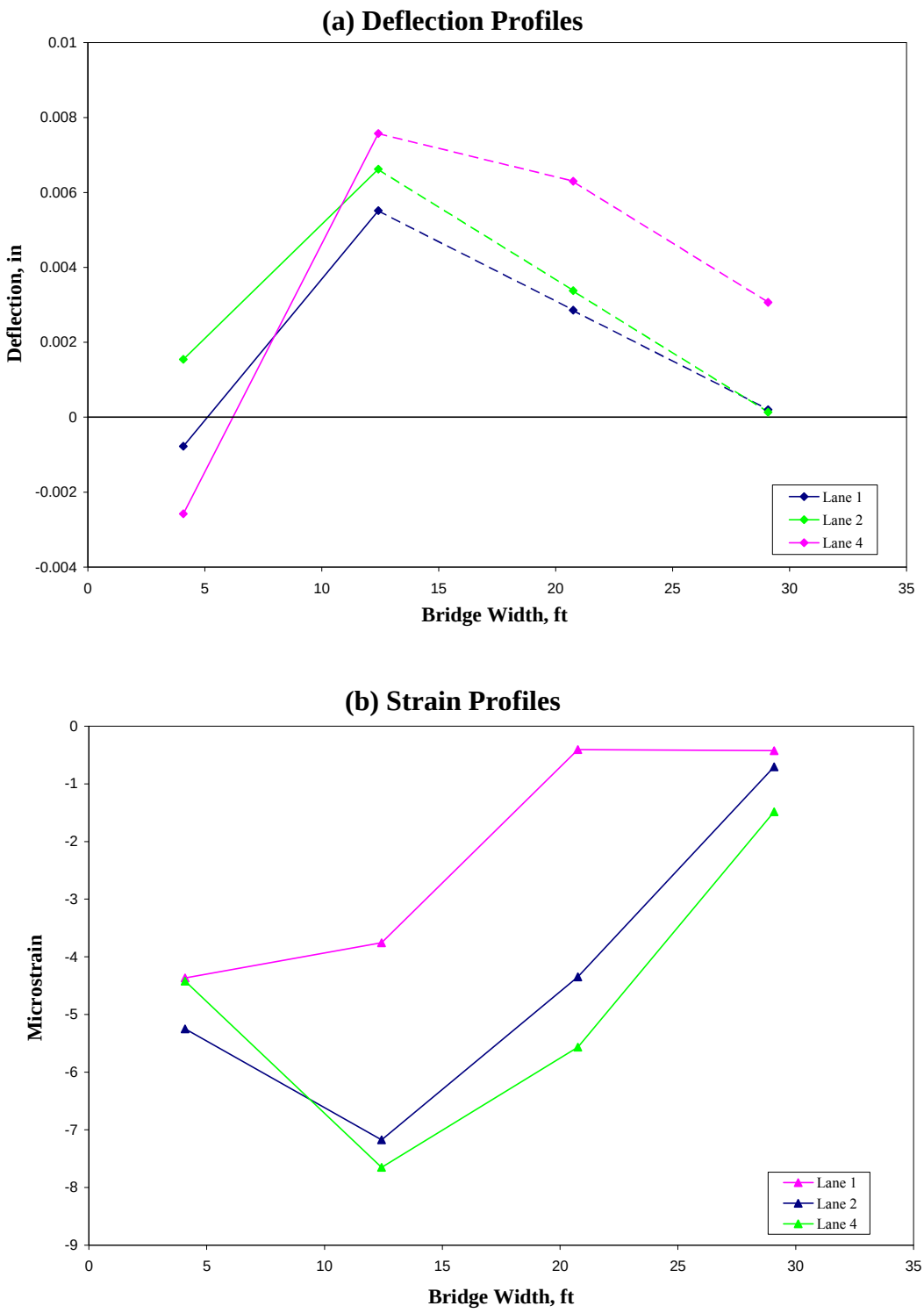

Figure 3.3 MS 2 Strain and Deflection Profiles (Load Case 2)

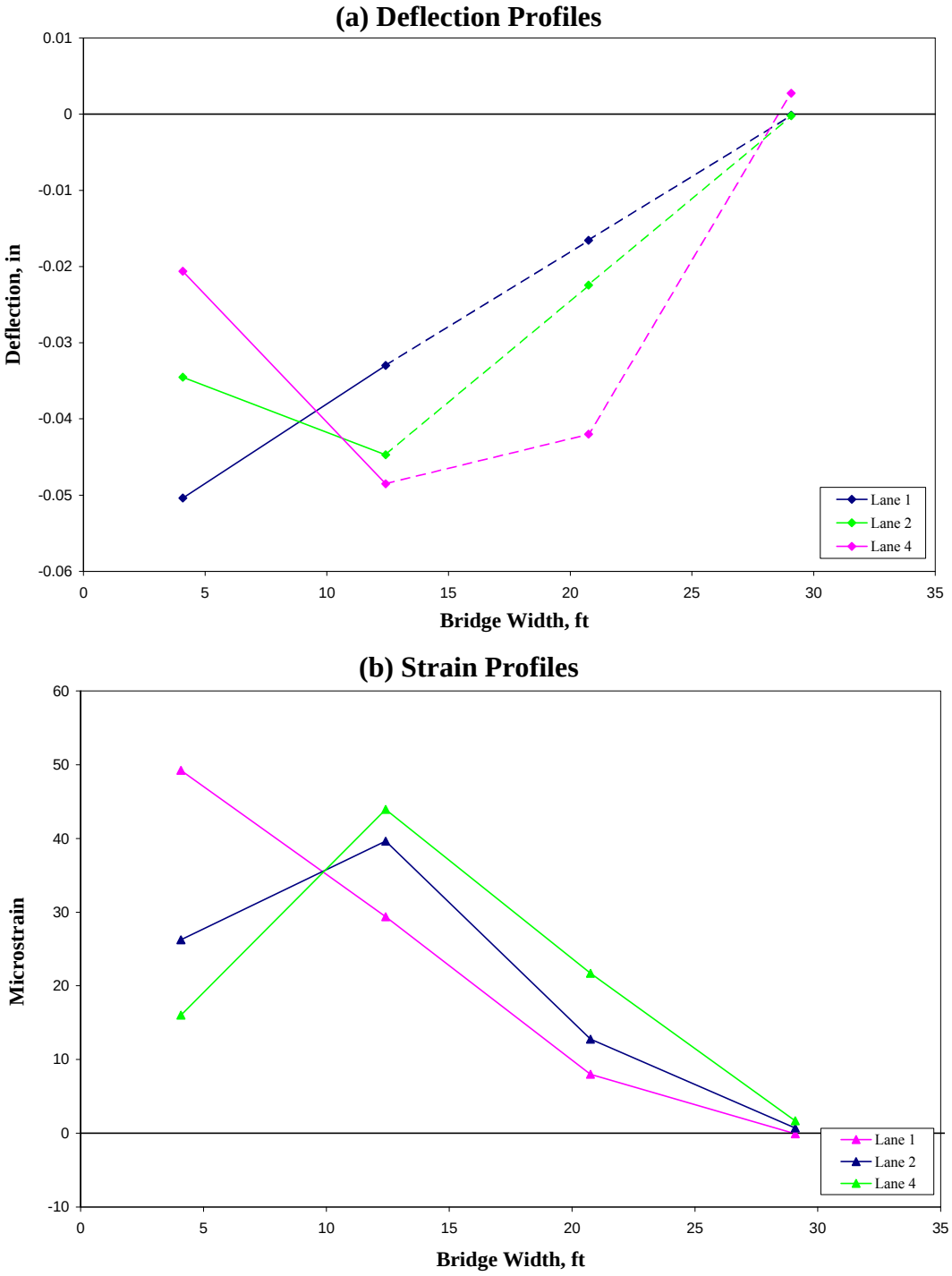

Figure 3.4 MS 2 Strain and Deflection Profiles (Load Case 3)

3.2 Girder 2 Analysis

The behavior of Girder 2 was also analyzed. Girder 2 is a full-length precast concrete girder. Deflection gages were applied on the midspans of each span in order to get a general idea of the deflection profile. These deflections are the main focus of analysis for this element of the bridge.

Girder 2 Deflection Profiles

The Girder 2 deflection profile is shown below in Figure 3.5. This profile corresponds with the rear axle positioned over MS2. All five traffic lane conditions are included. A maximum deflection of -.05 inches was found when the truck was in Lane 3. Lanes 2 and 4 were very similar with slightly less deflection than Lane 3. As expected, the Lane 5 condition created the least amount of deflection. The transducer at MS 1 was not working correctly, so it was assumed that MS 1 values were equal to MS 3 values.

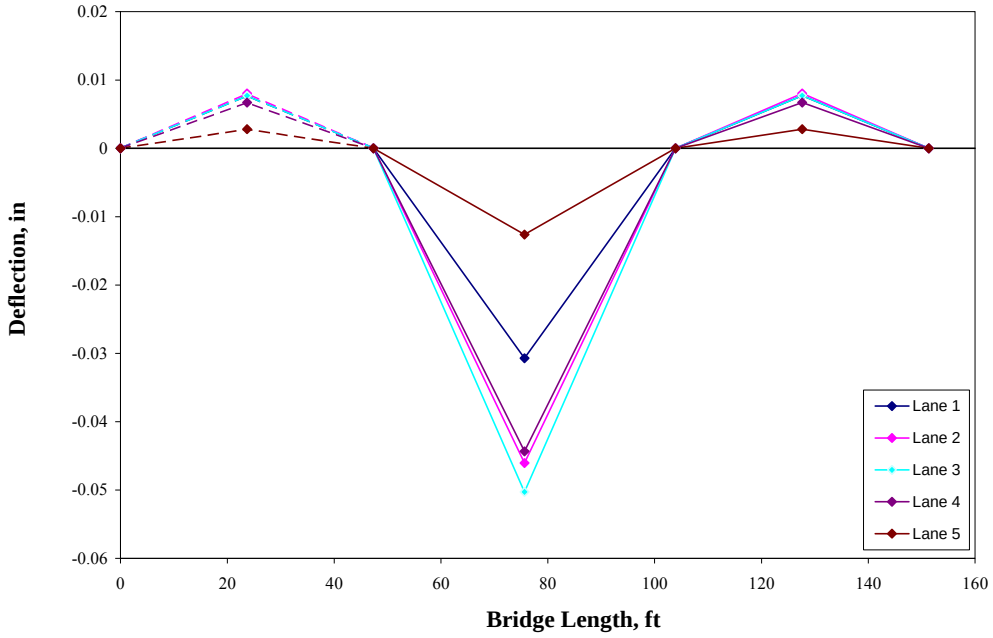

Figure 3.5 Girder 2 Deflection Profile (Lanes 1-5)

Girder 2 deflection profiles were also monitored during each static load test. The data is presented in Figures 3.6a through 3.6c. Load Case 1 and 3 produce the greatest deflection at MS 2. Very small displacements were recorded at MS 1 and MS 3. This can be attributed to the fact that they are end spans and have shorter span lengths. As stated above, MS 1 was assumed due to faulty testing equipment.

Load Case 1

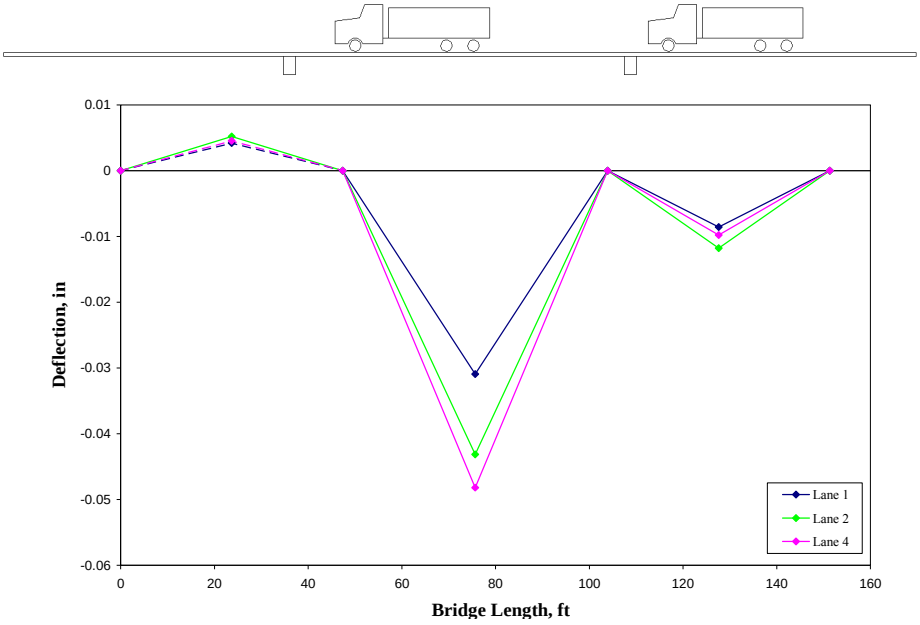

Load Case 2

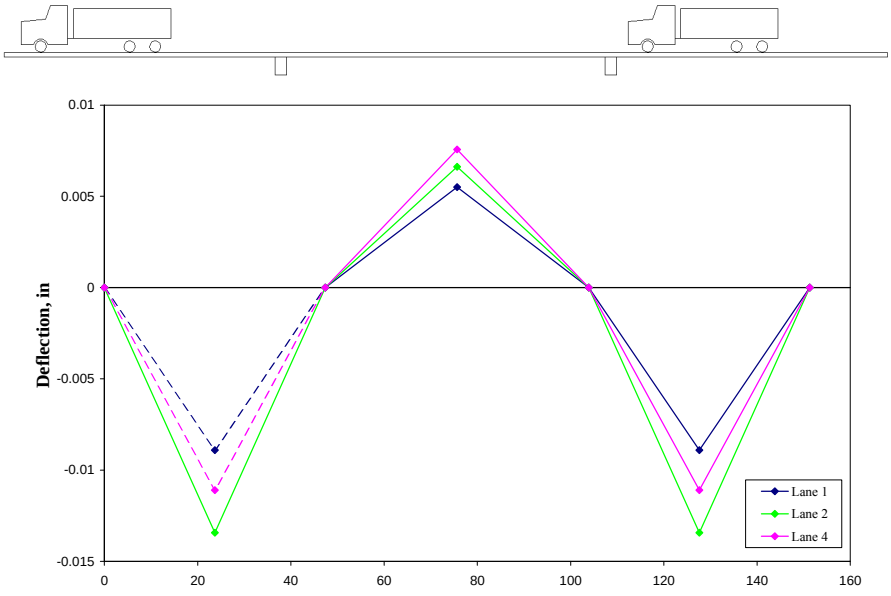

Figure 3.6 Girder 2 Deflection Profiles (Load Cases 1-3)

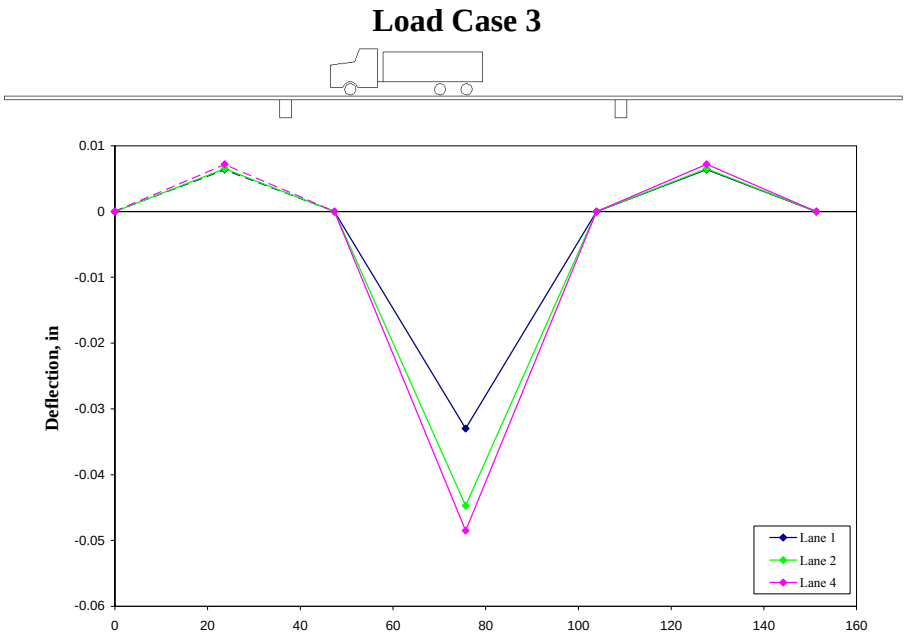

Figure 3.6 Girder 2 Deflection Profiles (Load Cases 1-3)

Girder 2 Deflection History

Deflection gages were recorded as the truck traversed the bridge. Figures 3.7a - 3.7e show data from the gages along Girder 2 during this time. Gages were located at the MS of each span. The graphs show that MS 2 consistently deflected more than MS 1 and MS 3. These graphs verify earlier graphs by showing greatest deflection occurring when the truck was in Lane 3. Once again, Lanes 2 and 4 produced slightly less deflection than Lane 3 and Lane 5 produces the smallest amount of deflection. MS 1 and MS 3 deflected a maximum distance approximately equal to 80% of the maximum deflection experienced at MS 2.

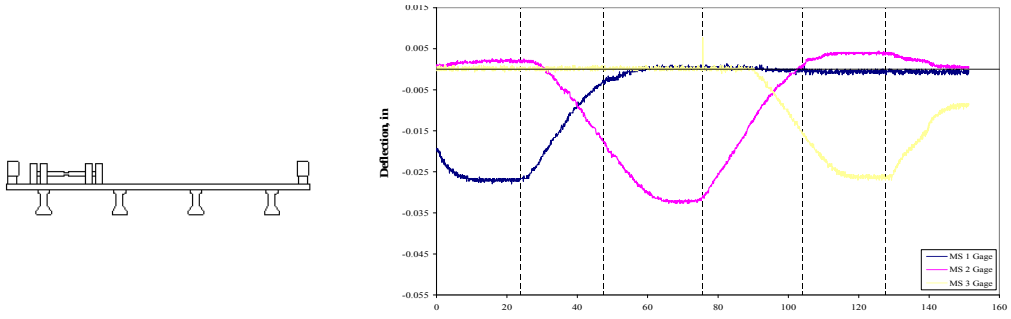

Figure 3.7 Girder 2 Deflection History (MS Gages)

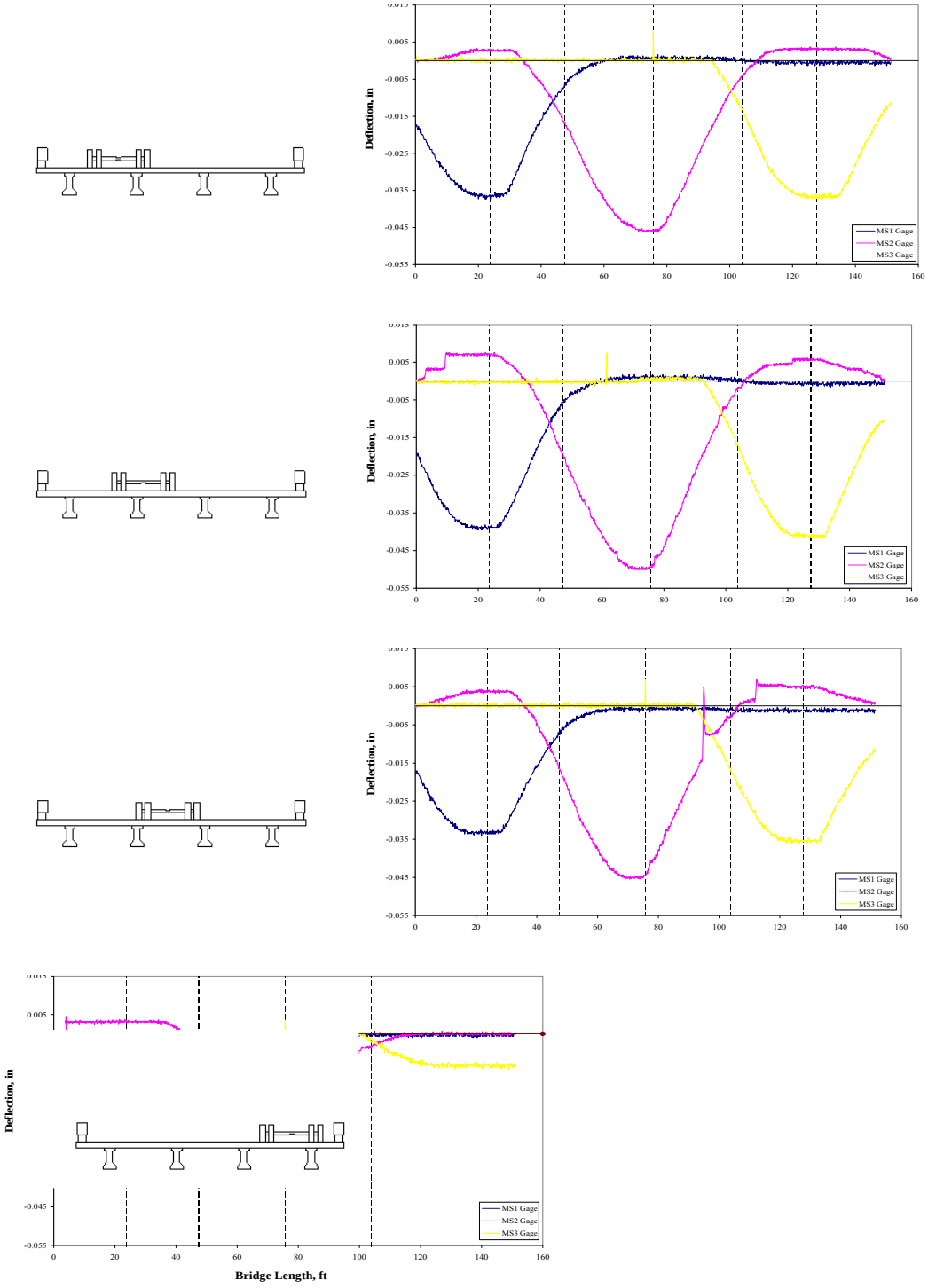

Figure 3.7 Girder 2 Deflection History (MS Gages)

3.3 East Side of West Pier Strain Profiles

Strain gages were installed at the east side of the west pier in order to evaluate strain at this location. It was possible to investigate the strain profile at this location at anytime during each of the five traffic lane tests. Figure 3.8 shows the strain profiles at the east side of the west pier for each traffic lane when the rear axle was at MS 1. A maximum compression of 15 με occurred when the truck was in Lane 2. The maximum negative condition could be attained by placing a truck at MS 1 and MS 2. The maximum negative strain condition at the pier can therefore be assumed to be twice the maximum strain from one truck, or 30 με. Virtually no strains were generated when the truck was in Lane 4.

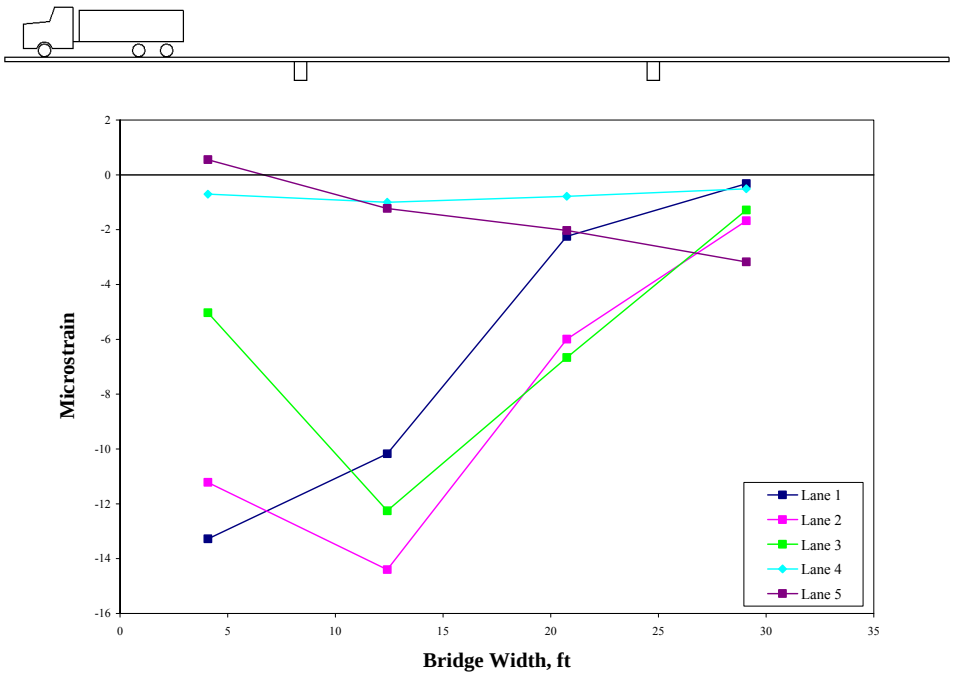

Figure 3.8 East Side of West Pier Strain Profile (Rear Axle at MS 1)

3.4 South Guardrail Strain History

A strain gage was located on the top of the south guardrail at MS 2. This strain gage was monitored as the truck traversed the bridge in each of the five traffic lanes. Figure 3.9 illustrates the strain in this guardrail relative to the position of the truck on the bridge. A maximum negative strain of 32 με occurred in the guardrail while the truck was in Lane 1. This significant amount of strain establishes the fact that the guardrail contributes to the stiffness of the bridge. Strain in the guardrail lessens as the truck passes further from the south side of the bridge. Strain in the south guardrail is virtually zero when the truck is in Lanes 4 and 5.

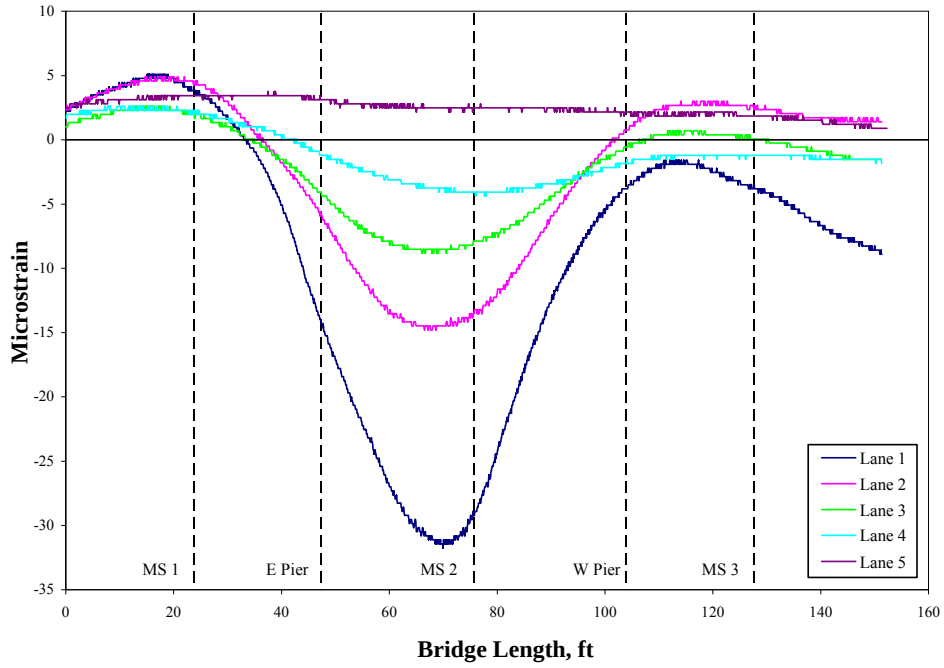

Figure 3.9 South Guardrail Strain History

3.5 Abutment Strains

Strain transducers at both abutments were monitored during each of the five traffic lanes. Data from the west abutment and east abutment are shown in Figures 3.10a and 3.10b, respectively. The Lane 2 loading condition was used for these graphs because it was the maximum strain condition for the abutments. Strains on the graphs are shown relative to the position of the truck on the bridge.

(a) West Abutment

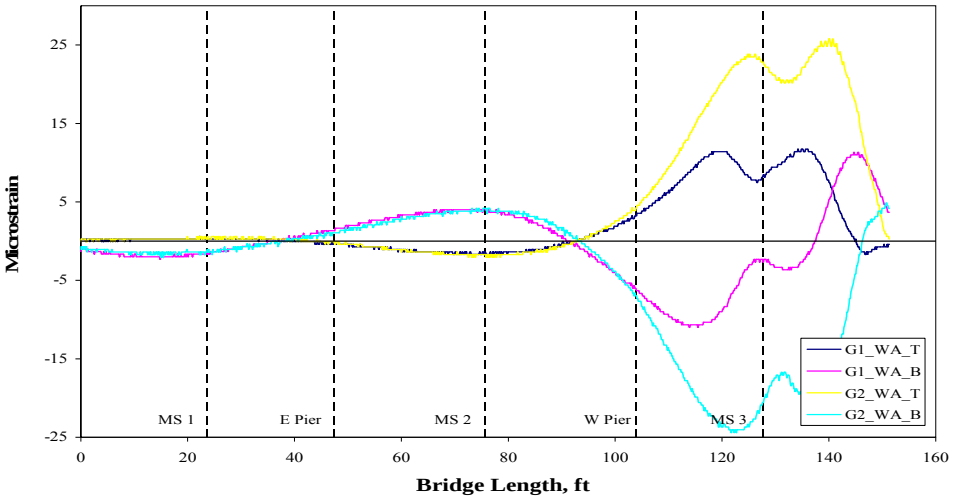

(b) East Abutment

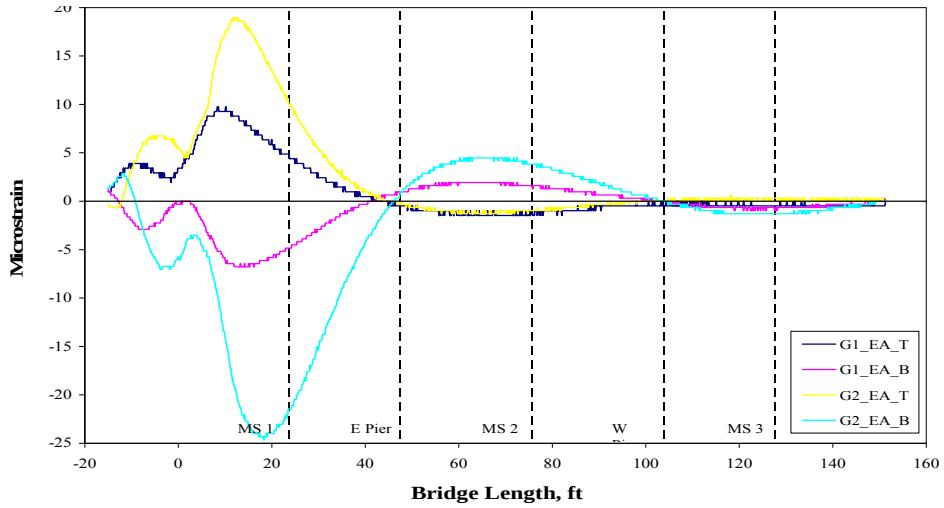

Figure 3.10 Abutment Strain History

3.6 Girder 1 Strain History

Strain transducers were located on the bottom flange of Girder 1 at the midspan of spans 2 and 3. Strains in these locations relative to the position of the truck can be seen in Figures 3.11a-3.11e. The five graphs each represent data from a different traffic lane loading condition. As expected, the greatest strains occurred when the truck was in Lane 1. Strains decreased with each successive lane. Lane 5 is not included in the report due to the lack of significant strain values. Strain gages were not located at the MS 1 location. MS 3 had a maximum strain equal to approximately 80% of the maximum strain of MS 2. This was determined using Lanes 1, 2 and 3. Lane 4 data was too insignificant to compare.

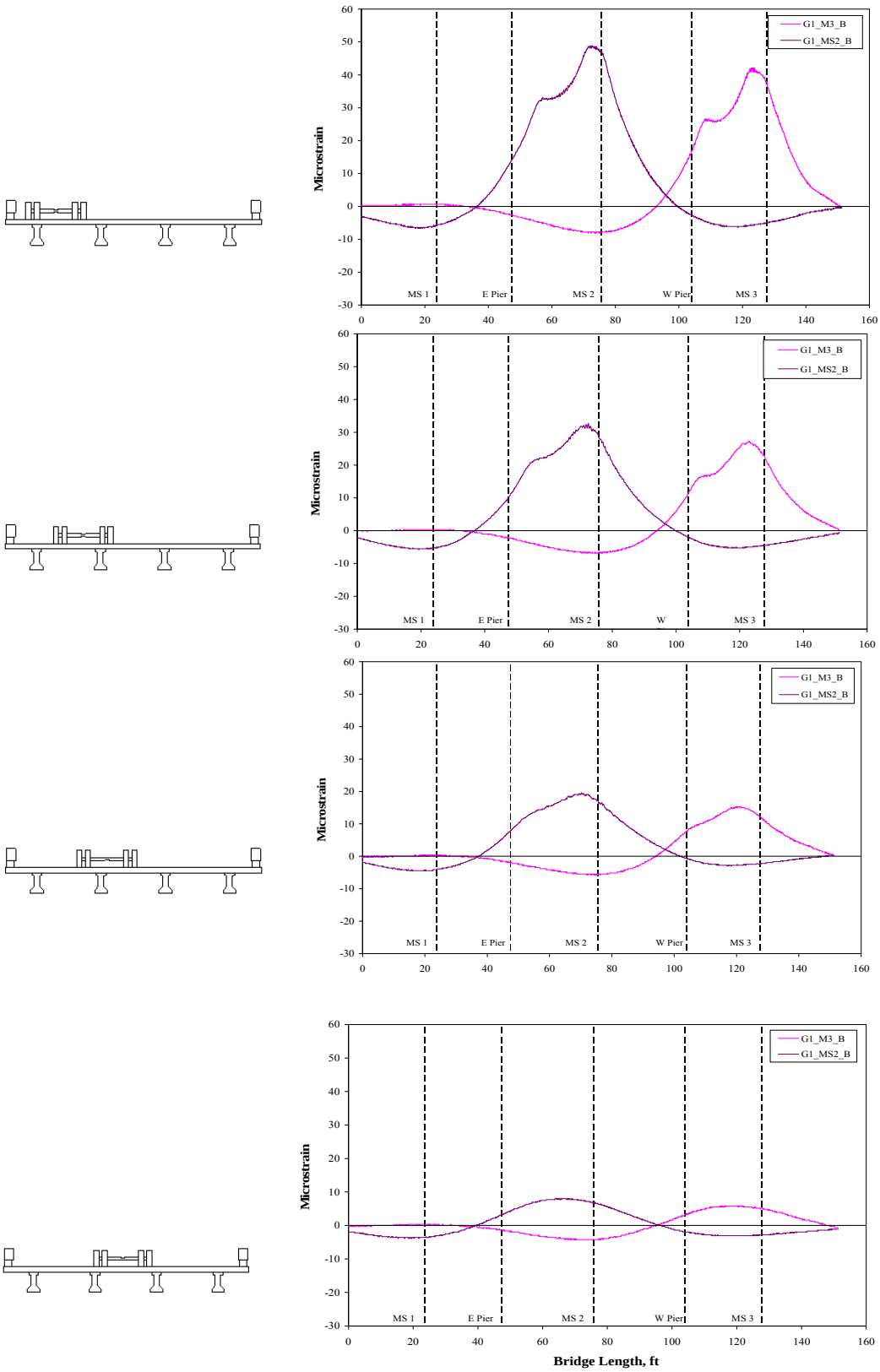

Figure 3.11 Girder 2 Strain History (Lanes 1-4)

3.7 Composite Behavior Analysis

Composite behavior was analyzed at each girder location of MS 2. Three strain locations were used: top flange, bottom flange and post-tensioning strand. Strains at the top and bottom flange of each girder were grouped with the strains from the corresponding post-tensioned strand to make a strain depth profile. Strain depth profiles for each girder during LC 1.1 are shown in Figures 3.12a through 3.12d. A structure experiencing composite behavior should exhibit a straight-line strain profile along its depth. It was found that Girders 2 and 3 consistently demonstrate straight-line strain depth profiles throughout each load case. Girders 1 and 4, however, do not show evidence of straight-line strain behavior. This is most likely due to defective instrumentation on the bridge. It is believed that the VWG at Girders 1 and 4 are damaged. This may be due to over straining of the gages during the post-tensioning process. In addition, the strain BDI gage at the bottom flange of Girder 4 is assumed to be faulty.

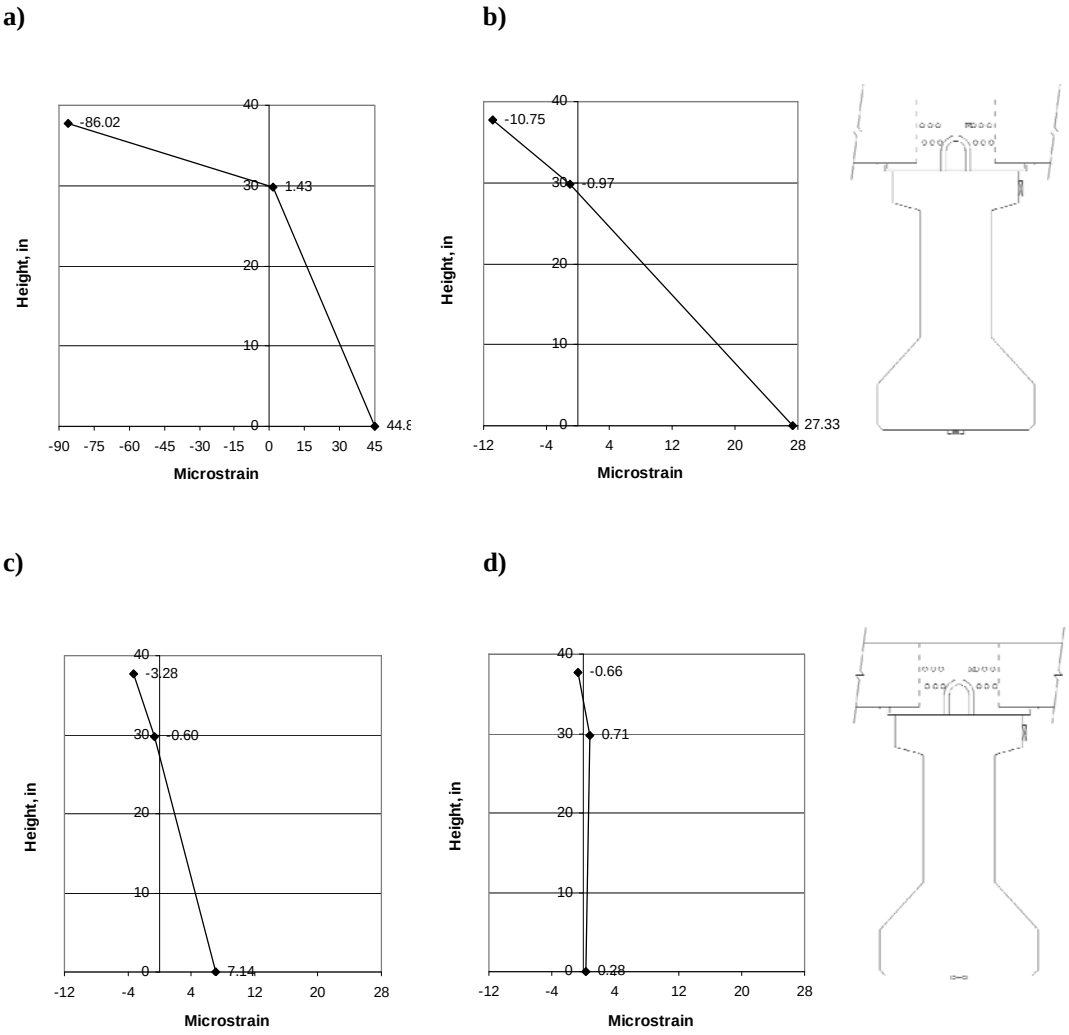

Figure 3.12 Strain Depth Profile (Girders 1-4)

The top and bottom flange strains were used to calculate a theoretical strain at the level of the post-tensioned strand. The actual strains were then compared to the theoretical strains. The theoretical strains calculated further enforce the possibility that VWG at Girders 1 and 4 are not working. Data for LC 1.1 can be seen in Table 3.1. PT_C and PT_A correspond to the calculated theoretical post-tensioning strain and the actual post-tensioning strain during the test. The difference between these two values is given as ΔPT. Theoretical strain was calculated using a straight line interpretation along the girder-deck cross section.

Table 1.1 Strain Depth Data

	G1	G2	G3	G4
ΔPT	76	2	1	1
PT_C	-10.24	-8.58	-2.68	0.83
PT_A	-86.02	-10.75	-3.28	-0.66
TF	1.43	-0.97	-0.60	0.71
BF	44.80	27.33	7.14	0.28

3.8 Girder Distribution Factor

Load distribution across the bridge was determined using a girder distribution method. Distribution of the load to each girder can be found by calculating the moment in each girder. This can be done using the relationship $\sigma = \frac{Mc}{I_x}$. In this equation, σ is stress, M is moment, c is the distance from the x axis, and I_x is the moment of inertia about the x axis. It was assumed that I_x and *c* were identical at each girder location. This simplifies the equation to $\sigma = M$. Furthermore, using the equation $\sigma = \varepsilon E$, and for a constant E, it can be assumed that the strain is proportional to the moment in the girder. The load distribution was then evaluated using the strain at the bottom flange of each girder.

Load distribution at each girder was then calculated by taking the strain at each individual girder divided by the total strain of all four girders. This data was plotted for Lanes 1 through 5 for the case when the truck was positioned at MS 2. These graphs are shown in Figures 3.13. The AASHTO design load distribution factor, S/14, was added to the graphs for comparison. In all cases, load distribution at each girder stays below this design value. As stated earlier, the strain BDI at Girder 4 was not working. This caused the data for Lanes 4 and 5 to be incorrect.

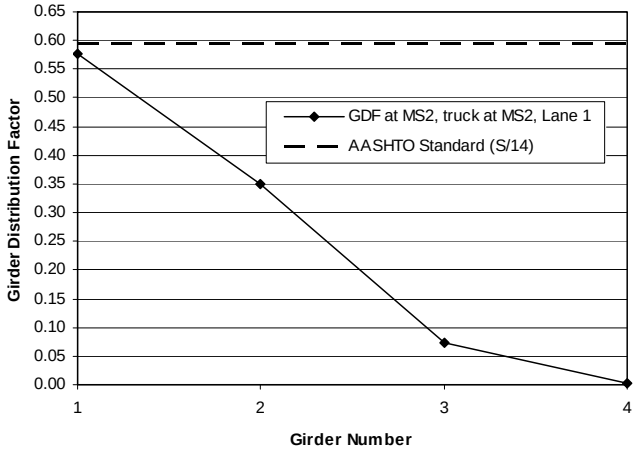

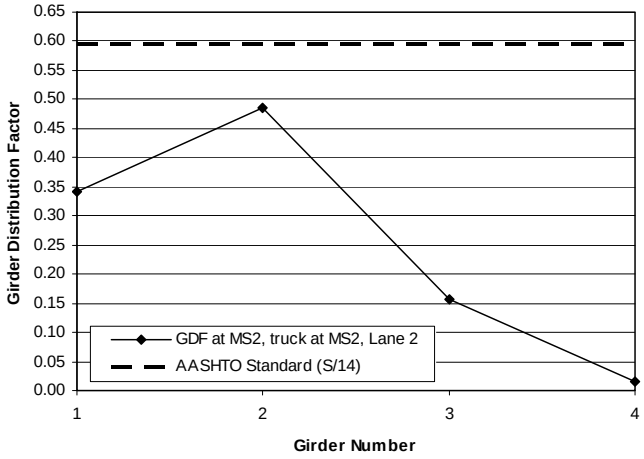

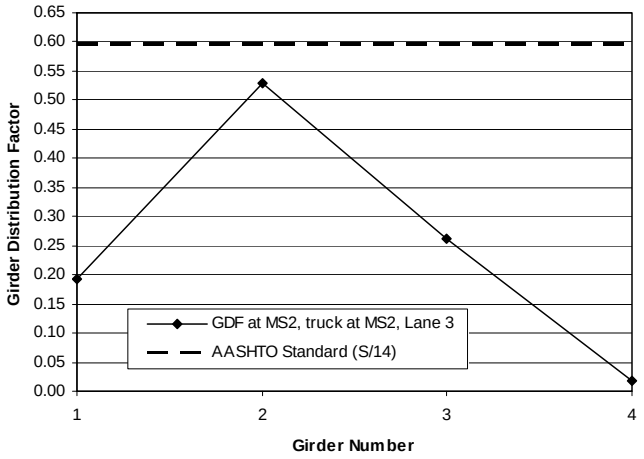

Figure 3.13 Load Distribution at MS 2 (Lanes 1-5)

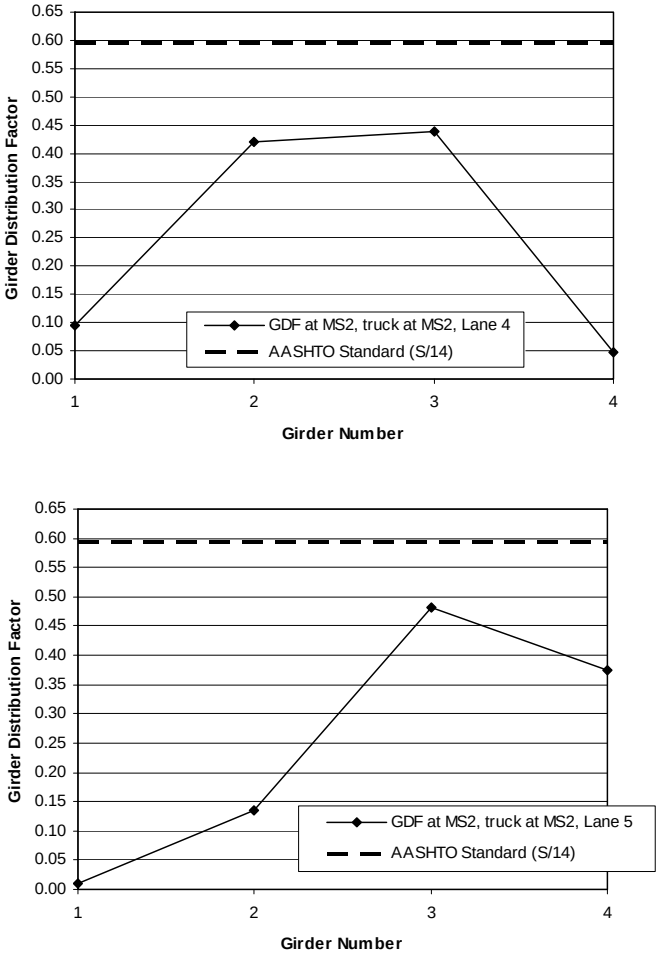

Figure 3.13 Load Distribution at MS 2 (Lanes 1-5)